

Universität
Rostock



Traditio et Innovatio

Beiträge zur Chemie der
Pniktogene:
Pnictanylidenphosphorane und
Cyclotripnictane

Habilitationsschrift

zur Erlangung des akademischen Grades
doctor rerum naturalium habitatus / habitata (Dr. rer. nat. habil.)
der Mathematisch-Naturwissenschaftlichen Fakultät
der Universität Rostock

vorgelegt von Christian Hering-Junghans, geboren am 15.03.1986 in Güstrow
Rostock, 12.05.2022

Die vorliegende Arbeit wurde in der Zeit von Februar 2017 bis März 2022 am Leibniz Institut für Katalyse e.V. eigenständig angefertigt.

1. Gutachter: Prof. Dr. Axel Schulz, Universität Rostock
2. Gutachter: Prof. Dr. Thomas Baumgartner, York University, Kanada
3. Gutachter: Prof. Dr. Christian Müller, Freie Universität Berlin

Datum der Verteidigung: Rostock, 06.04.2023

Erklärung

Ich versichere hiermit an Eides statt, dass ich die vorliegende Arbeit selbstständig angefertigt und ohne fremde Hilfe verfasst habe. Dazu habe ich keine außer den von mir angegebenen Hilfsmitteln und Quellen verwendet und die den benutzten Werken inhaltlich und wörtlich entnommenen Stellen habe ich als solche kenntlich gemacht.

Rostock, 12.05.2022

Dr. Christian Hering-Junghans

Zusammenfassung

Im Rahmen dieser kumulativen Habilitationsschrift wird zunächst die Chemie der Phosphanlydenphosphorane, Spezies mit der generellen Formel $R-P(PR'_3)$, genauer betrachtet. Neben optimierten Synthesen für stabile Aryl-substituierte Phosphanlyden- σ^4 -phosphorane, auch als Phospha-Wittig-Reagenzien bezeichnet, wurde deren Reaktivität gegenüber Lewis-Basen untersucht und so ein effektiver formaler Transfer der Phosphiniden-Einheit ($R-P$), auf N-heterocyclische Carbene, N-heterocyclische Olefine mit anschließender $C(sp^2)-H$ -Aktivierung, auf Isonitrile und auf Titanocen realisiert. Das Phosphinidentransfer-Potential der Phospha-Wittig-Reagenzien wurde darüber hinaus ausgenutzt, um erstmals Phosphaalumene, Verbindungen mit einer formalen $P=Al$ -Doppelbindung, zu synthetisieren. In Abhängigkeit der Aluminium-Vorstufe und der Gruppe R am Phosphiniden konnten ebenso 2π -aromatische PAI_2 -Dreiringsysteme erhalten werden. Die Syntheseroute zu Phospha-Wittig-Reagenzien wurde genutzt, um ein stabiles Arsa-Wittig-Reagenz darzustellen und in Analogie zu $R-P(PR'_3)$ gelang der Arsiniden-Transfer und somit die Darstellung der ersten Arsaalumene und eines terminalen Arsiniden-Titanocen-Komplexes.

In einem weiteren Kapitel wird die Chemie der Triphosphirane und von cyclischen Oligophosphanen im Allgemeinen betrachtet, welche in Analogie zu Phospha-Wittig-Reagenzien als Oligomere der freien Phosphinidene aufgefasst werden können. Neben der selektiven Synthese von Aryl-substituierten Triphosphiranen mit Hilfe von PMe_3 und Zn , wurde deren Reaktivität gegenüber Titanocen-Vorstufen untersucht und neuartige Titanocen-Diphosphenkomplexe synthetisiert. Dieses Konzept konnte erfolgreich auf die korrespondierenden Arsensysteme übertragen werden. Versuche die Triphosphiran-Synthese katalytisch in Bezug auf PMe_3 zu gestalten, resultierten in Phosphin-katalysierten Protokollen zur selektiven Darstellung von Diphosphenen bzw. Diaryldihalodiphosphanen, welche klassisch nicht zugänglich sind. Gegenüber niedervalenten Aluminiumspezies fungieren Triphosphirane als Phosphiniden-Überträger und ermöglichten die Synthese von Basen-freien cyclischen Diphosphadialanen, welche je nach sterischem Anspruch der Gruppe am P-Atom unterschiedlich verknüpft sind und die Dimere der entsprechenden Phosphaalumene darstellen.

Summary

In the context of this cumulative habilitation thesis, the chemistry of phosphanylidene phosphoranes, species with the general formula $R-P(PR'_3)$, is discussed first. In addition to optimized syntheses for stable aryl-substituted phosphanylidene- σ^4 -phosphoranes, also known as phospho-Wittig reagents, their reactivity towards Lewis bases was investigated. An effective formal transfer of the phosphinidene moiety ($R-P$), to N-heterocyclic carbenes, N-heterocyclic olefins with subsequent $C(sp^2)-H$ activation, to isonitriles and to titanocenes was synthetically realized. The phosphinidene transfer potential of the phospho-Wittig reagents was also exploited to synthesize phosphaalumenes, compounds with a formal $P=Al$ double bond, for the first time. Depending on the aluminium precursor and the group R on the phosphinidene, 2π -aromatic PAI_2 three-membered ring systems could also be obtained. The synthetic route to phospho-Wittig reagents was used to prepare a stable Arsa-Wittig reagent and, in analogy to $R-P(PR'_3)$, facile arsinidene transfer and thus the preparation of the first arsaalumene and a terminal arsinidene-titanocene complex were achieved.

In a further chapter, the chemistry of triphosphiranes and cyclic oligophosphanes in general is discussed, which can be understood as oligomers of free phosphinidenes in analogy to phospho-Wittig reagents. Besides the selective synthesis of aryl-substituted triphosphiranes using PMe_3 and Zn , their reactivity towards titanocene precursors was investigated and novel titanocene-diphosphene complexes were synthesized. This concept was successfully transferred to the corresponding arsenic systems. Attempts to render the triphosphirane synthesis catalytic with respect to PMe_3 resulted in phosphine-catalyzed protocols for the selective preparation of diphosphenes or diaryldihalodiphosphanes, which are accessible using classic routes. Towards low-valent aluminium species, triphosphiranes act as phosphinidene transfer reagents and enable the synthesis of base-free cyclic diphosphadialanes, which are linked differently depending on the steric requirement of the group at the P atom and represent the dimers of the corresponding phosphaalumenes.

Für Rudolf

Inhaltsverzeichnis

1	Zielstellung	1
2	Einleitung	3
2.1	Phosphinidene	8
2.2	Phosphanylidenphosphorane	13
2.2.1	Geschichte und Synthesen von Phosphanylidenphosphoranen	14
2.2.2	Strukturelle- und ^{31}P -NMR-Daten sowie Bindungssituation	19
2.2.3	Reaktivität gegenüber Elektrophilen	24
2.2.4	Phosphan-Substitution – Phosphinidin-Transfer mit $\text{R-P}(\text{PR}'_3)$	28
2.2.5	Synthese von Phosphaalkenen – Die Phospha-Wittig-Reaktion	35
2.3	Phosphiniden-Oligomere – Cyclooligophosphane	37
2.3.1	Synthese von Cyclophosphanen	38
2.3.2	Ringerweiterungsreaktionen von Cyclotriphosphanen	43
2.3.3	Fragmentierung von Cyclophosphanen	46
2.3.4	Bildung von NHC-Phosphiniden-Addukten	50
2.3.5	Arsen-analoge Dreiringe – Cyclotriarsane	52
2.4	Mehrfachbindungen zwischen Elementen der Gruppe 13 und 15	56
2.4.1	Phosphaborene	58
2.4.2	Mehrfachbindungen zwischen Al und N	63
2.4.3	Mehrfachbindungen zwischen Al und P, As	68
2.4.4	Mehrfachbindungen zwischen Ga und P, As, Sb	71
3	Zusammenfassung	77
4	Referenzen	79
5	Originalpublikationen	87

5.1	Terphenyl(bisamino)phosphines: electron-rich ligands for gold-catalysis.....	89
5.2	Reactivity of phospho–Wittig reagents towards NHCs and NHOs	101
5.3	On 1,3-phosphaazaallenes and their diverse reactivity.....	111
5.4	Titanocene pnictinidene complexes.....	125
5.5	A selective route to aryl-triphosphiranes and their titanocene-induced fragmentation.	131
5.6	Phosphine-catalysed reductive coupling of dihalophosphanes.....	143
5.7	Aryl-substituted triarsiranes: synthesis and reactivity	153
5.8	Isolable Phospha- and Arsaalumenes	159
5.9	Cyclo-Dipnictadialanes.....	167
6	Appendix.....	Fehler! Textmarke nicht definiert.
6.1	Akademischer Lebenslauf.....	Fehler! Textmarke nicht definiert.
6.2	Publikationsliste.....	Fehler! Textmarke nicht definiert.
6.3	Einladungsvorträge	Fehler! Textmarke nicht definiert.
6.4	Konferenzbeiträge.....	Fehler! Textmarke nicht definiert.

Abkürzungsverzeichnis

Ad	Adamantyl	^{Mes} Ter	2,6-Dimesitylphenyl
Äq.	Äquivalent(e)	Mes*	Supermesityl (2,4,6-tri-tert-butylphenyl)
Ar	Aryl	MS	Messenspektrometrie
CAAC	Cyclisches Alkylaminocarben	MO	Molekülorbital
COD	1,5-Cyclooctadien	NBD	Norbornadien
Cov.	kovalent	NBO	natürliches Bindungorbital
DFT	Dichtefunktionaltheorie	NHC	<i>N</i> -heterocyclisches Carben
Dip	2,6-Di-iso-propylphenyl	NHO	<i>N</i> -heterocyclisches Olefin
^{Dip} Ter	2,6-Di-(iso-propylphenyl)phenyl)	NLMO	natürliches lokalisiertes MO
DMAP	4-dimethylaminopyridine	NMR	<i>nuclear magnetic resonance</i> (Kernresonanz)
<i>et al.</i>	<i>et alii/aliae</i> (und andere)	NPA	Natürliche Populationsanalyse
ESR	Elektronenspinresonanz- Spektroskopie	<i>o</i>	ortho
FLP	Frustriertes Lewis-Säure-Base Paar	<i>p</i>	para
HOMO	höchstes besetztes MO	RT	Raumtemperatur
IBO	<i>intrinsic bond orbital</i>	SC-XRD	<i>Single crystal X-Ray diffraction</i> (Einkristallröntgenstruktur- analyse)
<i>i</i> Pr	Isopropyl	<i>t</i> Bu	<i>tert</i> -Butyl
IR	Infrarot	^{Mes} Ter	Terphenyl (2,6-dimesitylphenyl)
kov.	kovalent	Tf	Triflyl (CF ₃ SO ₂)
LB	Lewis-Base	Tip	2,4,6-Tri-iso-propylphenyl
LP	<i>lone pair of electrons</i> (freies Elektronenpaar)	TGA	Thermogravimetrische Analyse
LS	Lewis-Säure	THF	Tetrahydrofuran
LUMO	tiefstes unbesetztes MO	THT	Tetrahydrothiophen
<i>m</i>	meta	vdW	van der Waals
μ -	verbrückend (in Formeln)		
Mes	Mesityl (2,4,6-trimethylphenyl)		

Maßeinheiten

In dieser Arbeit werden die im Internationalen Einheitensystem (SI) gültigen Maßeinheiten verwendet. Alle davon abweichenden Einheiten und deren Umrechnung in SI-Einheiten sind im Folgenden aufgeführt:

Größe	Einheit	Bezeichnung	Umrechnung in SI-Einheiten
Frequenz	MHz	Megahertz	$1 \text{ MHz} = 1 \times 10^6 \text{ s}^{-1}$
	Hz	Hertz	$1 \text{ Hz} = 1 \text{ s}^{-1}$
Länge	Å	Ångström	$1 \text{ Å} = 1 \times 10^{-10} \text{ m}$
Temperatur	°C	Grad Celsius	$\vartheta/^\circ\text{C} = T/\text{K} - 273.15$
Volumen	mL	Milliliter	$1 \text{ mL} = 1 \text{ cm}^3 = 1 \times 10^{-6} \text{ m}^3$
Wärmemenge	kJ	Kilojoule	$1 \text{ kJ} = 1 \times 10^3 \text{ m}^2 \text{ kg s}^{-2}$
Wellenzahl	cm ⁻¹	reziproke Zentimeter	$1 \text{ cm}^{-1} = 100 \text{ m}^{-1}$
	d	Tag	$1 \text{ d} = 8.64 \times 10^4 \text{ s}$
	h	Stunde	$1 \text{ h} = 3.6 \times 10^3 \text{ s}$
Zeit	min	Minute	$1 \text{ min} = 60 \text{ s}$

Verzeichnis von Substituenten

Name	Strukturformel
Mes [*]	
MesTer	
DipTer	
TipTer	

Name	Strukturformel
Dip	
DipNacnac	
^P Nacnac	
[^s PDip]	
[^s PAr [*]]	

1 Zielstellung

Die Phosphorchemie ist ein wichtiger Bestandteil zeitgenössischer anorganischer Molekülchemie. Insbesondere die Chemie niedervalenter Phosphorverbindungen hat sich in den vergangenen 40 Jahren zu einem diversen Feld in Bezug auf deren Anwendung in der Materialchemie und der Katalyse entwickelt.

Im Rahmen meiner Habilitation sollten neuartige Wege des Phosphiniden-Transfers entwickelt werden. Das bedeutet, dass Synthesewege für den Transfer einer R–P-Einheit, ein sogenanntes Phosphiniden, etabliert werden. Dabei wurden zunächst Phosphanylidenphosphorane des Typs Ar–P(PMe₃) näher untersucht, da diese in Analogie zu organischen Aziden in Entropiegetriebenen PMe₃-Austauschreaktionen das Ar–P-Fragment übertragen sollten. Zum einen sollte der Austausch gegen stärkere Nucleophile, wie z.B. NHCs oder Isonitrile im Detail untersucht werden. Darüber hinaus stellte sich die Frage, ob die Kombination mit niedervalenten Aluminiumspezies erstmals einen synthetischen Zugang zu Phosphaalumenen ermöglichen könnte. Diese Systeme mit einer Phosphor-Aluminium Mehrfachbindung neigen zur Oligomerisierung und konnten bisher nicht dargestellt werden. Die analogen Arsanylidenphosphorane des Typs Ar–As(PMe₃) sind zwar bekannt, konnten bisher jedoch nicht reiner Form dargestellt und deren Reaktivität nicht untersucht werden. Ein Ziel war es solche Verbindungen durch die gezielte Modifikation des sterischen Anspruchs der Arylgruppe (Ar) synthetisch zu realisieren und deren Potential in Arsiniden-Transferreaktionen zu untersuchen.

Der Einsatz von Phosphanylidenphosphoranen in der Synthese von Phosphaalkenen, Systeme mit einer Phosphor-Kohlenstoff-Doppelbindung, wurde bereits beschrieben. Jedoch sind die bekannten Protokolle auf den Einsatz von sterisch anspruchsvollen Gruppen am Phosphor beschränkt. In diesem Zusammenhang sollte untersucht werden, ob es möglich ist Phosphaalkene mit sterisch weniger anspruchsvollen Gruppen am Phosphor mit Hilfe der sogenannten Phospha-Wittig Reaktion herzustellen.

2 Einleitung



Abbildung 1. „Der Alchemist“ auf der Suche nach dem „Stein der Weisen“. Künstlerische Darstellung der Destillation von Urin durch Henning Brandt 1669 von Joseph Wright of Derby. © Public Domain, Bild von [The Alchemist Discovering Phosphorus - Wikipedia](#).

Phosphor ist ein essenzielles Element für unsere moderne Gesellschaft und vielmehr für alle Organismen auf unserem Planeten. Im späten Mittelalter begaben sich Alchemisten auf die Suche nach dem „Stein der Weisen“, eine sagenumwobene Substanz, die in der Lage sein sollte, jegliche Materie in pures Gold zu verwandeln. 1669 etablierte Henning Brandt ein einfaches, jedoch höchst effektives Protokoll bei dem Urin zunächst zu einem Sirup reduziert wurde und durch Erhitzen ein rotes Öl herausdestilliert wurde, wobei ein schwammartiges schwarzes Material über einer Salzfraktion zurückblieb. Im Anschluss vereinigte er die schwarze Masse

wieder mit dem roten Öl und nach starkem Erhitzen über einen Zeitraum von 16 h wurde letztendlich weißer Phosphor erhalten, der in kaltem Wasser erstarrte.^[1] Obwohl Brandt nicht einen magischen Stein gefunden hatte der Materie verwandeln konnte, entdeckte er das Element Phosphor, welches im Dunklen leuchtete (Abbildung 1). Diese Eigenschaft des Phosphors ist untrennbar mit dessen Namen verbunden, der sich aus dem Griechischen „*Phôs*“ (Licht) und „*phoros*“ (Träger, Überbringer) ableitet. Urin beinhaltet neben Phosphaten Kohlenstoffverbindungen und somit kann Brandts Rezept als Vorstufe für die auch heute noch angewendete industrielle Synthese von weißem Phosphor, ausgehend von Phosphat-haltigen Erzen und Koks in elektrischen Lichtbogenöfen, angesehen werden.^[2]

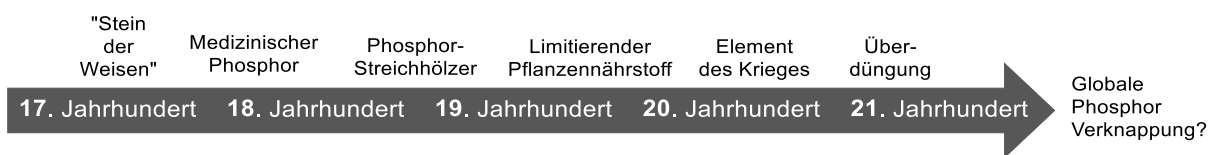


Abbildung 2. Schematische Darstellung der Verwendung und „Verschwendung“ von Phosphor von der ursprünglichen Entdeckung Brandt's im 17. Jahrhundert bis zur Überdüngung im 21. Jahrhundert.

Nach der Entdeckung des Elements wurde es im 17. Und 18. Jahrhundert hauptsächlich für fragwürdige medizinische Anwendungen eingesetzt. Die Erkenntnis das Knochen eine bessere Phosphatquelle als Urin darstellten, resultierte in der „Massenproduktion“ von Phosphor-Streichhölzern. Jedoch litten Fabrikarbeiter unter einer Berufskrankheit, die als „*Phossy Jaw*“ bezeichnet wurde und auf Dämpfe von weißem Phosphor zurückgeht, wobei insbesondere die Struktur der Kieferknochen zerstört wird.^[3] Weißer Phosphor ist bereits in geringen Dosen ein tödliches Gift und wurde daher schnell als „*Devils Element*“ (das teuflische Element) bezeichnet,^[2] auch aufgrund der Anwendung in militärischen Produkten (z.B. Brandbomben) oder als Organophosphor-Biozide (z.B. das Nervengas VX ist bereits bei einer Dosis von 0.1 mg/kg Körpergewicht tödlich).^[4]

In elementarer Form ist Phosphor hoch reaktiv und kommt in der Natur nicht in dieser Form vor, da es im Kontakt mit Luft spontan verbrennen kann. Die bekanntesten allotrope Formen des Phosphors sind der weiße (P_4), rote, violette und schwarze Phosphor.^[5] Weißer, roter und violetter Phosphor sind Nichtmetalle und Isolatoren und deren Struktur ist in Abbildung 3 dargestellt. Schwarzer Phosphor wurde ausgehend von P_4 bei extrem hohen Drücken und Temperaturen 1914 erstmals dargestellt^[6] und stellt bei Raumtemperatur das thermodynamisch stabilste Allotrop des Phosphors dar,^[7] welches im Gegensatz zu weißem und roten Phosphor ein Halbleiter ist und ähnlich wie Graphit schichtartig aufgebaut ist (Abbildung 3, links).^[8]

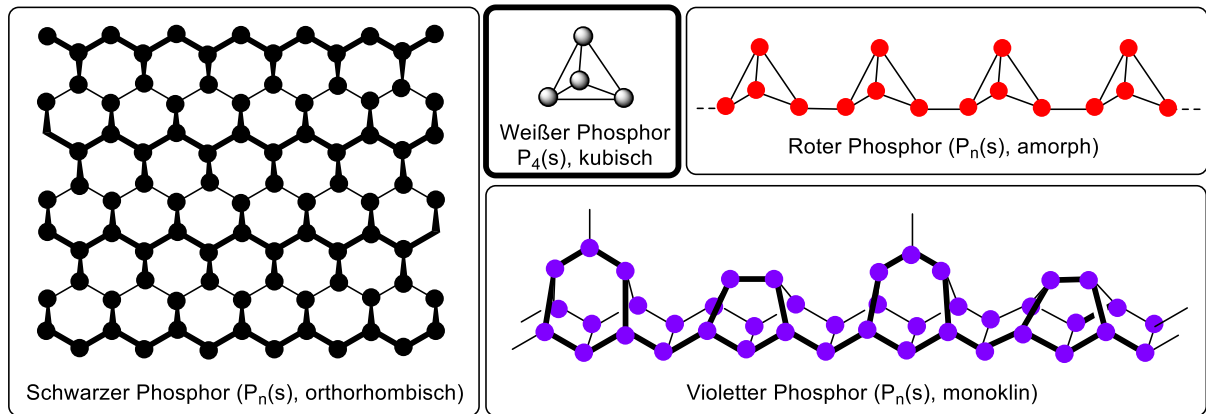
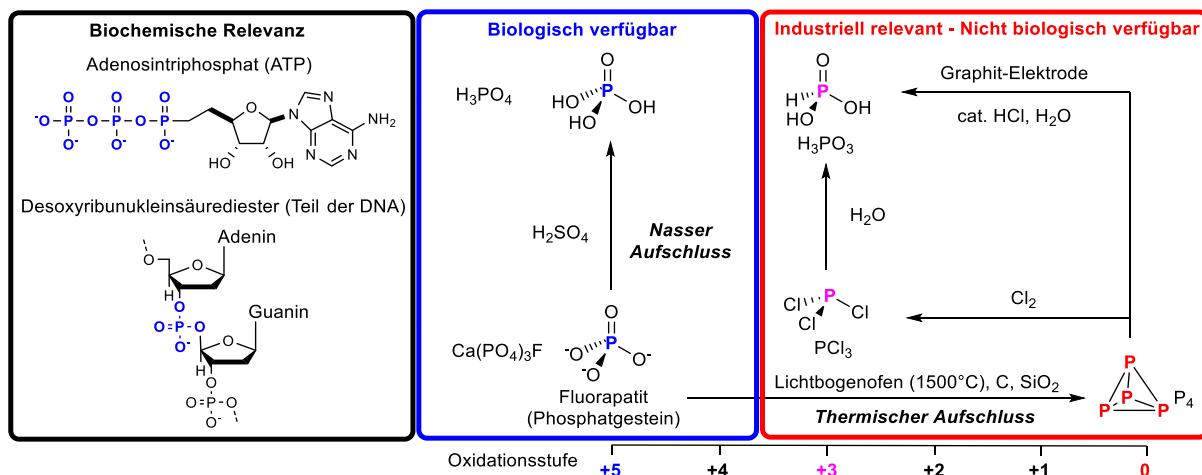


Abbildung 3. Allotrope Formen des Elements Phosphor.

Aus biochemischer Sicht ist Phosphor das Fundament allen Lebens auf der Erde. Ein erwachsener menschlicher Körper trägt ca. 700 g Phosphor in sich, hauptsächlich in der Form von Calciumphosphaten in Knochen und Zähnen. Organismen haben ausgeklügelte Mechanismen entwickelt, um Phosphat aufzunehmen, zu verteilen, zu verwerten, zu speichern und auszuscheiden, um eine ausgewogene Phosphat-Homöostase zu gewährleisten.^[9] Auf molekularer Ebene bilden Phosphatdiester das Rückgrat der DNA und Phosphoranhydride im Adenosintriphosphat stellen die universelle „Energiewährung“ auf zellulärer Ebene dar.^[10] Tiere nehmen Phosphor hauptsächlich über die Nahrung auf. Pflanzen hingegen beziehen Phosphor aus dem Boden, wobei der Bodenphosphor im Wesentlichen aus Phosphor-reichen Apatiten stammt, deren Bildung sich auf einen Zeitraum von ca. 10-15 Mio. Jahren erstreckt. Ein Phosphor-Mangel in Pflanzen kann zu signifikanten Defiziten in deren Wachstum und zu Defiziten bei der Ernte von Nutzpflanzen führen, sodass heutzutage in großem Umfang Phosphatdünger eingesetzt werden.^[11]

Bis zum Ende des 19. Jahrhunderts wurde meist Guano, die Exkremate von Vögeln und Fledermäusen, als Phosphorquelle eingesetzt. Bauern vertrauten über Jahrhunderte auf die Wiederverwendung von Phosphat-haltigen Rohstoffen, wie zum Beispiel Flussschlamm, in dem sich Phosphor anreichert. Die Entwicklung des „Nassprozesses“ zur großindustriellen Herstellung von Phosphorsäure (Aufschlussphosphorsäure) aus Phosphat-haltigen Gesteinen und Schwefelsäure hat dazu geführt, dass der natürliche Phosphorkreislauf durch anthropogene Einflüsse gebrochen wurde^[12] und Phosphoratome nun von Vorkommen mit einer hohen Konzentration zu niederkonzentrierten Regionen in Meeren und Böden getragen werden.^[13] Ungefähr 95% des abgebauten Phosphatgesteins wird im „Nassprozess“ in Phosphorsäure umgewandelt.^[11] Die dafür benötigte Schwefelsäure wird hauptsächlich für diesen Prozess hergestellt und es wird deutlich wie die industrielle Nutzung von Phosphor und Schwefel

untrennbar miteinander verbunden sind.^[14] Mit einem Rückgang der Raffination fossiler Brennstoffe und somit der Verfügbarkeit von Schwefelsäure, sind Methoden zur Gewinnung nützlicher Produkte direkt aus Phosphatgestein oder unter Verwendung anderer Säuren als Schwefelsäure wünschenswert.^[15]

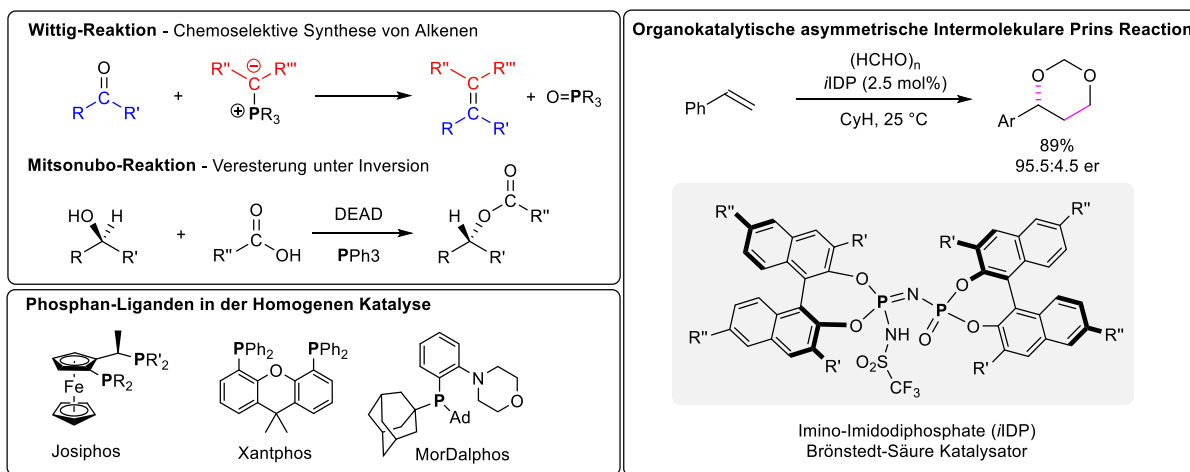


Schema 1. Biochemisch relevante Phosphormoleküle (links) und die Verwertung von Phosphat-haltigen Gesteinen zu biologisch verfügbarer Phosphorsäure und industriell relevanten Verbindungen wie P_4 und PCl_3 .

Die moderne Phosphorchemie basiert auf P_4 der thermisch in elektrischen Bogenöfen aus den verbleibenden 5% des abgebauten Phosphat-haltigen Gesteins in der Reduktion mit Kohlenstoff erhalten wird. Im Moment ist P_4 das wichtigste Basismaterial, um Phosphor-haltige Feinchemikalien industriell herzustellen. Dabei werden Intermediate wie Phosphortrichlorid (PCl_3) verwendet, welches P–Cl Bindungen besitzt, die durch Salz-Metathese-Reaktionen oder reduktive Prozesse funktionalisiert werden können.^[16] Sowohl P_4 als auch PCl_3 passen nicht in das moderne Mantra „Grüner Chemie“^[17] und da sie außer als industrielle Intermediate von geringer Bedeutung sind, sollte zukünftig versucht werden diese Zwischenstufen bei der Herstellung P-haltiger Verbindungen zu umgehen.

Moderne Synthesemethoden der anorganischen und organischen Chemie sind ohne das Element Phosphor nicht mehr vorstellbar. So werden Phosphor-Ylide in der sogenannten Wittig-Reaktion für die chemoselektive Synthese von Alkenen^[18] oder Arylphosphane in der Mitsunobu-Reaktion für die stereoselektive Synthese von Estern eingesetzt (Schema 2).^[19] Erst kürzlich erhielten List und MacMillan den Chemie-Nobelpreis für Ihre Arbeiten an Organokatalysatoren, die in vielen Fällen Phosphor-basiert sind.^[20] So werden zum Beispiel Imino-Imidodiphosphate als Brönstedt-Säure Katalysatoren in der asymmetrischen Prins-Reaktion zur Darstellung von 1,3-Dioxanen eingesetzt (Schema 2).^[21] Darüber hinaus sind

Phosphan-Liganden integraler Bestandteil Übergangsmetall-katalysierter Prozesse (Schema 2).^[22] Aber auch im Bereich der Materialwissenschaften ist Phosphor ein wichtiges Element, z.B. in Leuchtdioden oder Stählen.^[23] In letzter Zeit hat das Phosphoren (in Analogie zum Graphen) als 2-dimensionales Material viel Aufmerksamkeit erhalten^[24] und zeigt eindrucksvoll die unerschöpflichen Anwendungen der Phosphorchemie auf.

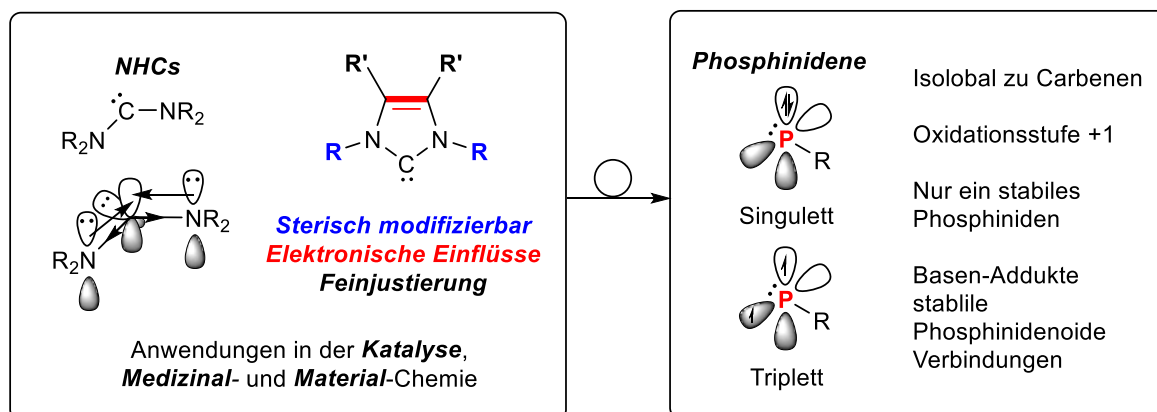


Schema 2. Biochemisch relevante Phosphormoleküle (links) und die Verwertung von Phosphat-haltigen Gesteinen zu biologisch verfügbarer Phosphorsäure und industriell relevanten Verbindungen wie P₄ und PCl₃.

Die vorliegende Habilitationsschrift befasst sich mit Aspekten der Chemie niedervalenter Phosphorverbindungen, in denen Phosphor nicht in den klassischen Oxidationsstufen +III (vgl. PCl₃) bzw. +V (vgl. Phosphate) vorliegt (Schema 1). Es werden neuartige Wege des Phosphiniden- und Arsiniden-Transfers aufgezeigt und Synthesewege zu Cyclotriphosphanen, Ringsysteme des Typs (PnAr)₃ (Pn = P, As) beschrieben, die als Erweiterung bestehender Syntheseprotokolle aufzufassen sind und neuartige Reaktivitäten ermöglichen.

2.1 Phosphinidene

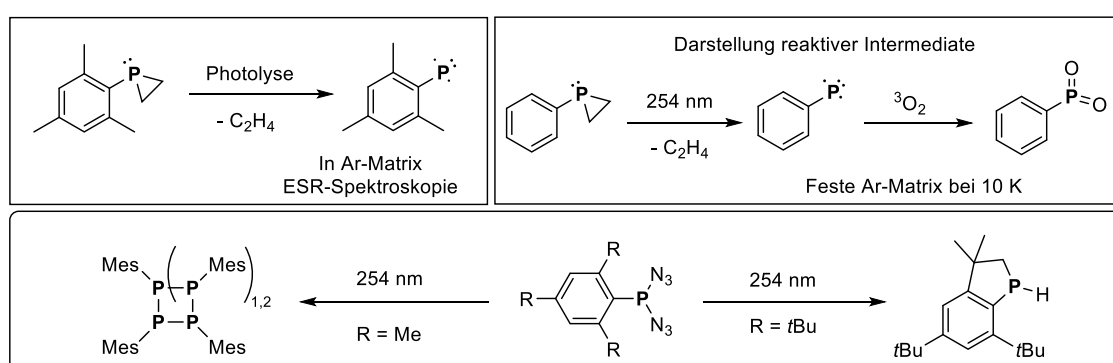
Carbene sind Neutralverbindungen mit einem divalenten Kohlenstoffatom, das in seiner Valenzhülle nur 6 Elektronen trägt.^[25] Solche Moleküle wurden lange Zeit als schwer zugänglich erachtet und erst im späten 20. Jahrhundert gelang Bertrand und Mitarbeitern erstmalig die Isolation eines hoch reaktiven acyclischen Phosphinosilylcarbens.^[26] Nur wenige Zeit später zeigten Arduengo *et al.*, dass es durch den Einsatz sterisch anspruchsvoller Substituenten an beiden Stickstoffatomen eines Imidazoliumsalzes und anschließende Deprotonierung gelingt, stabile Imidazolidene darzustellen (Schema 3, links),^[27] welche in der Literatur als N-Heterocyclische Carbene (NHCs) bezeichnet werden.^[28] Nur zwei Jahrzehnte später wird die Entdeckung von stabilen Carbenen als Ausgangspunkt für die Anwendung dieser Spezies in verschiedensten Feldern, wie der synthetischen Chemie, der Katalyse,^[29] der Materialchemie^[30] und in der Medizinalchemie,^[31] angesehen. Darüber hinaus hat diese Entdeckung auch die Chemie analoger Verbindungen, in denen das Kohlenstoff-Atom durch ein anderes Element ersetzt wurde, vorangetrieben.



Schema 3. Isobal-Beziehung^[32] zwischen N-heterozyklischen Carbenen (NHCs) und Phosphinidenen.

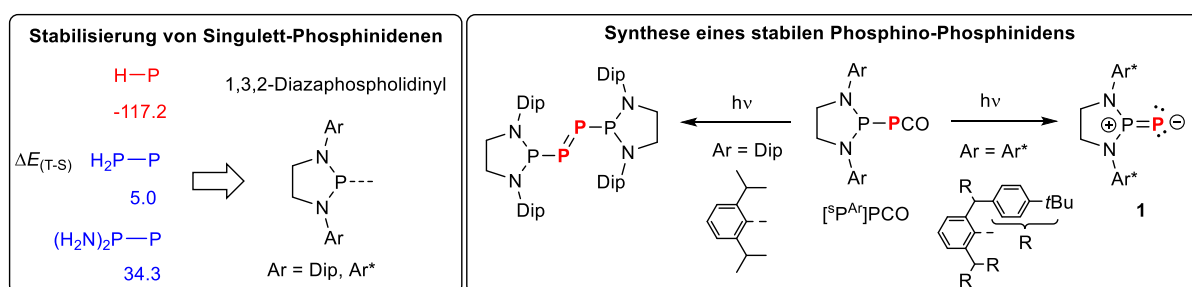
Die Phosphor-analogen Verbindungen der Carbene werden als Phosphinidene bezeichnet und besitzen ein einfach substituiertes P-Atom mit zwei einsamen Elektronenpaaren (LP) und einem leeren Orbital (Schema 3, rechts). Wie bei den Kohlenstoff- und Stickstoff-analogen Verbindungen (Carbene bzw. Nitrene) können sich zwei der nichtbindenden Elektronen in zwei unterschiedlichen Orbitalen mit parallelem Spin aufhalten (Triplet-Phosphiniden) oder gepaart in einem Orbital (Singulett Phosphiniden).^[33] Triplet-Phosphinidene wurden bisher nur in der Gasphase mit Hilfe der Massenspektrometrie und in Tieftemperaturmatrizes durch ESR-, IR- oder UV/VIS-Spektroskopie nachgewiesen.^[34] Erst kürzlich wurde das Triplet-

Phenylphosphiniden Ph-P in einer Argon-Matrix bei 10 K durch die Bestrahlung von Phenylphosphiran Ph-P(C₂H₄) bei 254 nm erzeugt und mit Hilfe der IR-Spektroskopie nachgewiesen (Schema 4, oben rechts).^[35] Mesitylphosphiniden Mes-P wurde zum Beispiel durch die Photolyse von Mesitylphosphiran erzeugt und in einer Argon-Matrix stabilisiert (Schema 4, oben links).^[36] Alan Cowley und Mitarbeiter nutzten Diazidophosphane zur Generierung von Triplett-Phosphinidenen. Unter Bestrahlung spalten diese drei Äquivalente N₂ ab und in Abhängigkeit des Substituenten am Phosphor oligomerisieren die R-P-Einheiten (R = Mes) zu Oligophosphanen des Typs (R-P)_n (n = 4, 5) oder greifen den Substituenten am Phosphor unter C(sp³)-H-Aktivierung an (R = Mes*) (Schema 4, unten).^[37]



Schema 4. Photolyse von Phosphiranan zur Generierung der Triplett-Phosphinidene Mes-P^[36] und Ph-P^[35]. Alternativ können Diazidophosphane unter Bestrahlung N₂ abspalten und intermediär Phosphinidene generiert werden.^[37]

Ihre elektronische Struktur macht Phosphinidene von Natur aus reaktiv und instabil. Im Gegensatz zu den Triplett-Phosphinidenen konnten Singulett-Phosphinidene bis vor Kurzem nicht einmal spektroskopisch nachgewiesen werden. Im Gegensatz dazu sind Singulett-Carbene und -Nitrene^[38] durch die richtige Wahl der Substituenten stabil und somit synthetisch relevant. Das Stammphosphiniden H-P besitzt einen Triplett-Grundzustand der 117.2 kJ·mol⁻¹ unterhalb des Singulett-Zustandes liegt (Schema 5).^[39]

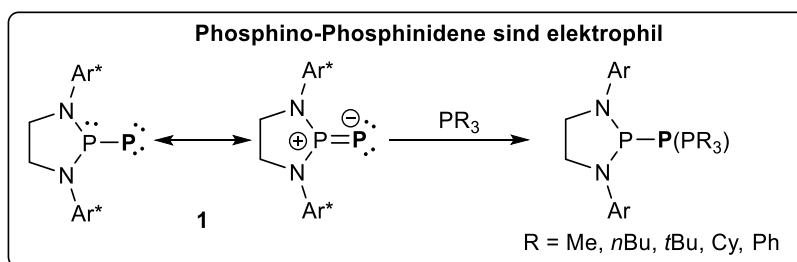


Schema 5. Modulierung der Singulett-Triplett-Lücke (in kJ·mol⁻¹) von Phosphinidenen durch gezielte Substituenten-Wahl (links). Synthese eines stabilen Phosphino-Phosphinidens (rechts).

Systematische theoretische Studien von Nguyen und Mitarbeitern haben gezeigt, dass die Implementierung von Aminogruppen in der β -Position von Phosphinophosphinidenen R_2P-P den Singulett-Zustand durch LP-Abstoßung gegenüber dem Triplett-Zustand stabilisiert.^[40] Ausgehend von dieser theoretischen Studie identifizierten Bertrand *et al.* die starre 1,3,2-Diazapholidin-Einheit ($[^sP^{Ar}] = (H_2CNAr)_2P-X$; Ar = modifizierbare Aryl-Gruppe) um Singulett-Phosphinidene synthetisch zu realisieren.^[41] Zusätzlich wurden sterisch anspruchsvolle Substituenten an den Stickstoffatomen der Diazaphospholidin-Gruppe installiert, um so eine Pyramidalisierung des Ring-Phosphoratoms zu verhindern,^[42] und die Wechselwirkungen der N- und P-LPs zu maximieren. P-P-Bindungen sind in der Regel empfindlich gegenüber Säuren und wenig stabil gegenüber Reduktionsmitteln. In Analogie zur Erzeugung von Nitrenen, welche aus Aziden, aber auch ausgehend von Isocyanaten dargestellt werden können,^[43] wurden zur Phosphiniden-Generierung Phosphaketene des Typs $R-PCO$ eingesetzt. So wurde eine Phosphiniden-artige Reaktivität für das erste isolierbare Phosphaketene Mes^*-PCO beobachtet.^[37, 44] Phosphanylphosphaketene werden ausgehend von den Chlorodiazaphospholidinen $[^sP^{Ar}]Cl$ in der Reaktion mit Natriumphosphaethynolat $[Na(dioxane)_x]PCO$ erhalten.^[45] Die Bestrahlung (200-400 nm) von $[^sP^{Dip}]PCO$ (Dip = 2,6-*i*Pr₂C₆H₃) in der Abwesenheit eines Abfang-Reagenzes ergab das Dimerisierungsprodukt des freien Phosphinidens $[^sP^{Dip}]P=P[^sP^{Dip}]$, ein Diphosphen (Schema 5, rechts).^[46]

Wird die Bestrahlung in Gegenwart von Ad-NC durchgeführt, so wird das 1,3-Phosphaazaallen $[^sP^{Dip}]PCN-Ad$ erhalten. Es ist also erforderlich das niedervalente P-Atom sterisch so abzuschirmen, dass es nicht mehr mit einem zweiten Phosphiniden eine Dimerisierung eingehen kann. Diese sterische Überfrachtung gelang durch die Einführung der $[^sP^{Ar^*}]$ -Einheit und die Bestrahlung von $[^sP^{Ar^*}]PCO$ ergab das erste isolierbare Phosphiniden $[^sP^{Ar^*}]P$ (**1**) unter CO-Abspaltung (Schema 5, rechts).^[41] Die Autoren zeigten, dass **1** im Festkörper über mehrere Wochen stabil ist und mit Isonitrilen unter der Bildung von Phosphaazaallen und mit Malonsäureanhydrid unter der Bildung eines Phosphirans reagiert. Elektronisch wird **1** am besten durch eine zwitterionische Resonanz mit negativer Formalladung am terminalen P-Atom, einer positiven am Ring-P-Atom und einer P-P-Doppelbindung beschrieben. Diese Interpretation wird auch durch die ³¹P-NMR-Daten belegt; mit einer sehr großen ¹J_{PP}-Kopplungskonstante von 884 Hz und einem abgeschirmten Signal für das terminale P-Atom ($\delta(^{31}P) = -200.4$ ppm). Darüber hinaus zeigen DFT-Rechnungen den Doppelbindungscharakter mit einer P-P π -Bindung im HOMO und einem LUMO, welches das π^* -Orbital der P-P-Bindung darstellt. In Folgearbeiten untersuchten Bertrand und Mitarbeiter die Reaktivität von **1** im Detail und konnten zeigen, dass in der Reaktion mit CO-Gas (und

^{13}CO) das ursprüngliche Phosphanylphosphaketene $[\text{sP}^{\text{Ar}^*}]\text{PCO}$ zurückgebildet wird. Die Elektrophilie von **1** erinnert an die Reaktion von CAACs bzw. DACs mit CO unter Bildung von Ketenen. Ebenso konnte gezeigt werden, dass verschiedene Carbene mit **1** unter der Bildung von Carben-Phosphiniden-Addukten reagieren. Der elektrophile Charakter von **1** konnte ebenso durch die Zugabe von Phosphanen belegt werden, wobei unterschiedliche Phosphanylidenphosphorane gebildet wurden (Schema 6). Theoretische Analysen der Fukui-Funktionen zeigten, dass das terminale P-Atom in **1** einen ambiphilen Charakter aufweist.

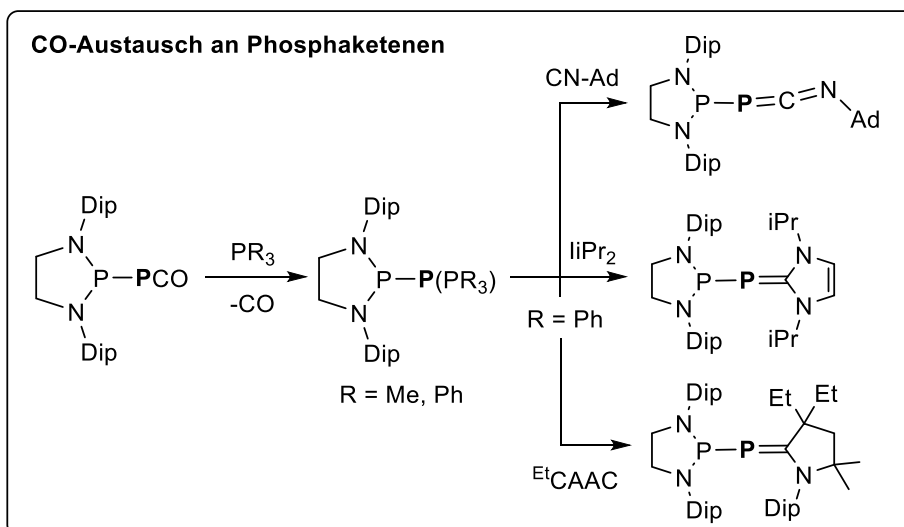


Schema 6. Elektrophile Addition verschiedener Phosphane an **1**.

Aus diesen beiden Studien lassen sich wichtige Rückschlüsse für die Modellierung von Phosphiniden-Transferreagenzien ableiten:

1. Phosphaketene ermöglichen die Generierung eines Singulett-Phosphinidens durch Bestrahlung.
2. Nucleophile binden an das einfach koordinierte P-Atom und es werden Lewis-Basen-stabilisierte Phosphinide erhalten.

Wird der sterische Anspruch der Phosphanylgruppe reduziert, so gelingt es ausgehend von $[\text{sP}^{\text{Dip}}]\text{PCO}$ in der Reaktion mit Phosphanen, die korrespondierenden Phosphanylidenphosphorane $[\text{sP}^{\text{Dip}}]\text{P}(\text{PR}_3)$ unter Decarbonylierung zu erhalten. Interessanterweise, wurde dieser Austausch nicht beobachtet wenn $[\text{sP}^{\text{Ar}^*}]\text{PCO}$ mit PPh_3 umgesetzt wurde. Dies deutet auf einen assoziativen Mechanismus des CO für PR_3 Austausches hin und DFT-Studien suggerieren einen $\text{S}_{\text{N}}2$ -artigen T-förmigen Übergangszustand. Daher kann der Austausch beim sterisch überfrachteten **1** nicht stattfinden. Wird $[\text{sP}^{\text{Dip}}]\text{P}(\text{PR}_3)$ mit Isonitrilen umgesetzt so werden Phosphaazaallene unter PR_3 -Abspaltung gebildet (Schema 7) und die Autoren leiteten den folgenden Stabilitätstrend für die Ligand-Phosphiniden Wechselwirkung ab: $\text{CO} < \text{PR}_3 < \text{CN-R} < \text{NHC} < \text{CAAC}$.



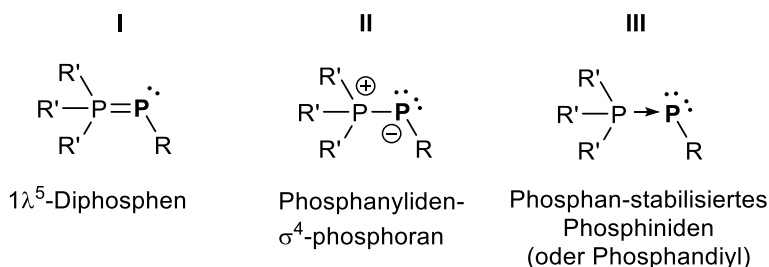
Schema 7. Initialer CO-Austausch in Phosphanylphosphaketenen und anschließende Phosphan-Substitution mit verschiedenen Nucleophilen.

Ausgehend von dieser Darstellung werden im folgenden Phosphanylidphosphorane des generellen Typs $\text{R-P}(\text{PR}_3)$ genauer betrachtet, da diese als Phosphan-stabilisierte Phosphinidene aufgefasst werden können und so ein großes Potential als Phosphiniden-Transferreagenzien besitzen.

2.2 Phosphanylidenphosphorane

In Analogie zu Übergangsmetallzentren reagiert das freie Phosphiniden **1** mit einer Vielzahl von Lewis-Basen (LB) zu den formalen Koordinationsverbindungen R–P(LB) (LB = PR₃, CN–R, CO etc.) (Schema 6 und 7), wie im vorherigen Unterkapitel gezeigt wurde. Aus dieser Reaktivität wird deutlich, dass Verbindungen der allgemeinen Formel R–P(PR'₃), so genannte Phosphanylidenphosphorane, als basenstabilisierte Phosphinidene verstanden werden können und daher eine wertvolle Klasse von R–P-Transferreagenzien darstellen. Die Nomenklatur dieser Systeme ist vielfältig. Unter anderem wird der Begriff Phosphanyliden-σ⁴-phosphoran verwendet, um zu verdeutlichen, dass die Phosphoran-Einheit vier σ-Bindungen trägt (Schema 8, **II**). In einigen Fällen wurde die λ-Konvention angewandt,^[47] und Phosphanylidenphosphorane als 1λ⁵-Diphosphene R'₃P=PR bezeichnet, mit einer P–P-Doppelbindung und insgesamt 5 Bindungen am vierfach-koordinierten P-Atom (Schema 8, **I**). Im Folgenden wird gezeigt, dass in einigen Fällen das Phosphan thermisch oder photochemisch extrudiert oder durch stärkere Lewis-Basen ausgetauscht werden kann, weshalb diese Systeme oft als Phosphan-stabilisierte Phosphinidene (oder Phosphandiyle) bezeichnet werden (Schema 8, **III**). Diese drei Formen werden oft als Resonanzformen beschrieben. Jedoch wird hier auf die Verwendung der Resonanzschreibweise verzichtet, da die Oxidationsstufen der P-Atome in jeder Form unterschiedlich sind und die Verwendung von Resonanzpfeilen in diesem Fall unangebracht ist. Um zu zeigen, dass die Phosphoran-Einheit (oder das koordinierende Phosphan) wann immer möglich substituiert oder extrudiert werden kann, wird die folgende Notation verwendet: R–P(PR'₃).

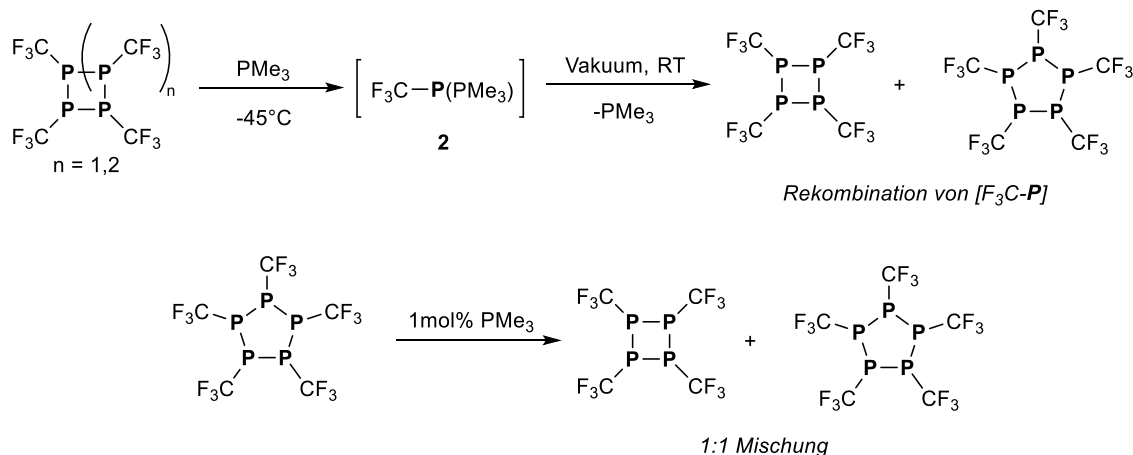
Nomenklatur der Phosphanylidenphosphorane



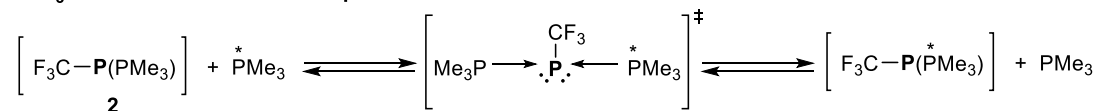
Schema 8. Verschiedene Nomenklaturen für Spezies des generellen Typs R–P(PR'₃).

2.2.1 Geschichte und Synthesen von Phosphanylidenphosphoranen

Die ersten Berichte über die Koordination von Phosphanen an ein niedervalentes Phosphoratom gehen auf Reaktivitätsstudien von Burg und Mahler an den Oligophosphanen $(PCF_3)_n$ ($n = 4, 5$), die als Tetramere und Pentamere des Phosphinidens F_3C-P beschrieben werden können, zurück.^[48] Bei der Kombination von $(PCF_3)_4$ mit PMe_3 im Verhältnis 1:4 stellten die Autoren die Bildung von $F_3C-P(PMe_3)$ (**2**) fest.^[49] **2** ist eine thermisch labile Substanz, die oberhalb von -45 °C PMe_3 freisetzt, wobei sich gleichzeitig $(PCF_3)_4$ und $(PCF_3)_5$ in einem Verhältnis von 6:1 bilden (Schema 9, oben). Die Existenz von $F_3C-P(PMe_3)$ wurde durch ^{19}F -NMR-Experimente mit einem abgeschirmten Signal bei -51.5 ppm (relativ zu CF_3COOH) und deutlicher Kopplung zu zwei chemisch unterschiedlichen P-Zentren nachgewiesen. Werden katalytische Mengen PMe_3 zu reinem $(PCF_3)_5$ gegeben, so wird eine schnelle Redistribution beobachtet und eine 1:1-Mischung der Vier- und Fünfringsysteme wurde erhalten (Schema 9, Mitte).



PMe₃-Austausch an einem Phosphiniden

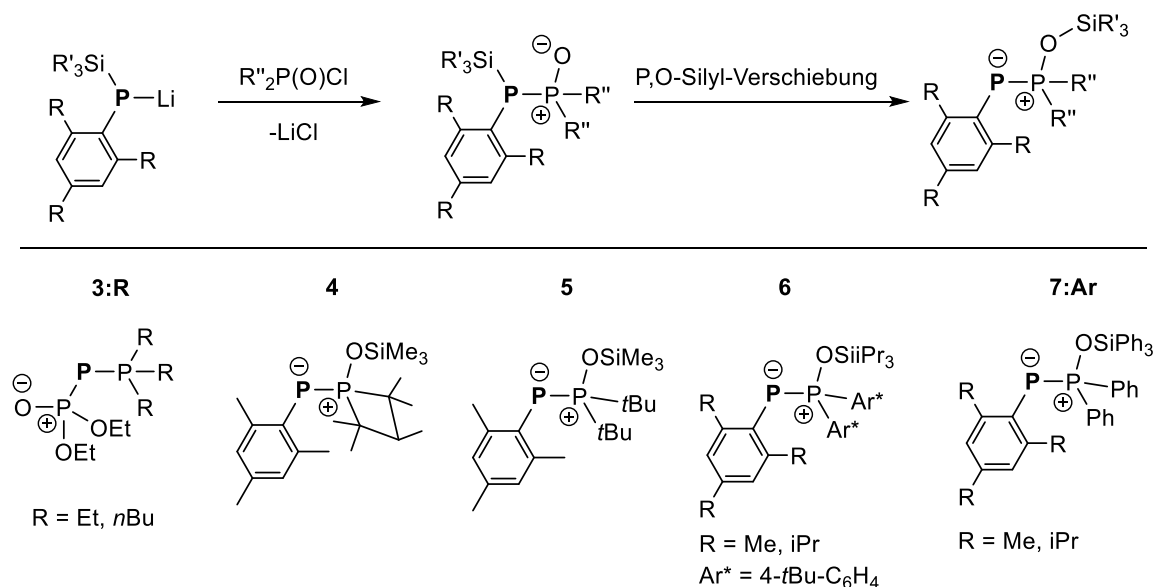


Schema 9. Entdeckung des Phosphanylidenphosphorans $F_3C-P(PMe_3)$ und dessen thermische Zersetzung (oben). Einfluss von katalytischen Mengen PMe_3 auf $(PCF_3)_5$, das die Bildung einer 1:1-Mischung von $(PCF_3)_n$ ($n = 4, 5$) bewirkt (Mitte).^[49] PMe_3 -Austausch in $F_3C-P(PMe_3)$ gemäß ^{31}P -NMR-Experimenten (unten).^[50]

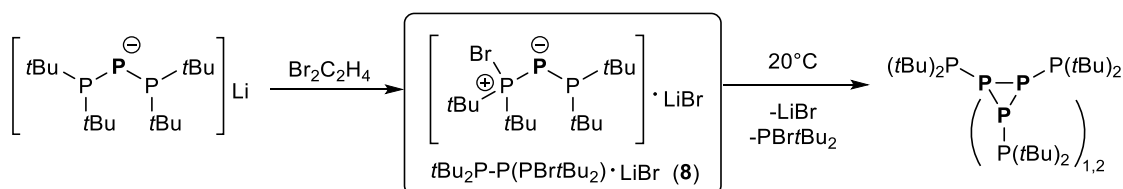
Die Ähnlichkeit von $F_3C-P(PMe_3)$ mit klassischen Wittig-Reagenzien wurde von Cowley *et al.* festgestellt, und das Verhalten von **2** in Gegenwart von PMe_3 wurde mittels ^{31}P -NMR-Spektroskopie eingehend untersucht.^[50] Nach der Koordination erfährt die ^{31}P -NMR-

Verschiebung von PMe_3 eine signifikante Entschirmung auf +12.7 ppm, was auf ein vierfach koordiniertes P-Atom hinweist, ähnlich wie bei Phosphoniumsalzen. Das zweifach koordinierte P-Atom zeigt ein Dublett-Signal bei -81.0 ppm mit einer großen negativen P-P-Kopplungskonstante von $^1J_{\text{PP}} = -436.5$ Hz. Außerdem stellten die Autoren eine Abhängigkeit der $^1\text{H-NMR}$ -Spektren sowohl von der PMe_3 -Konzentration als auch von der Temperatur fest. Die experimentellen Untersuchungen zur Konzentrationsabhängigkeit sprechen eindeutig für einen assoziativen, geschwindigkeitsbestimmenden Schritt, bei dem eine T-förmige, dreifach koordinierte P-CF₃-Einheit vorliegt (Schema 9, unten). Dieser assoziative Phosphan-Austausch ist entscheidend für die weitere Funktionalisierung des R-P-Fragments.

In ähnlicher Weise stellten Fluck und Weber die Verbindungen $(\text{EtO})_2\text{P}(\text{O})-\text{P}(\text{PR}_3)$ (**3:R**) (R = Et, *n*Bu) her.^[51] In diesem Zusammenhang beschreibt ein Bericht von Regitz einen Weg, bei dem Lithiumsilylphosphide in der Reaktion mit einem cyclischen Phosphorylchlorid in einem 1,3-Silylmigrationsprozess zu $\text{Mes}-\text{P}(\text{P}(\text{OSiMe}_3)(\text{C}_3\text{HMe}_5))$ (**4**) reagiert (Schema 10, oben).^[52] Im Gegensatz zu **2** weisen **3** und **4** laut $^{31}\text{P-NMR}$ -Spektroskopie deutlich stärker abgeschirmte (elektronenreichere) zweifach koordinierte P-Atome auf ($\delta(^{31}\text{P}) = -217.5$ (**3**); -209 (**4**) ppm). In diesem Zusammenhang berichtete Regitz auch über $\text{Mes}-\text{P}(\text{P}(\text{OSiMe}_3)t\text{Bu}_2)$ (**5**),^[53] und kürzlich wurde die Synthese von $\text{Mes}-\text{P}(\text{P}(\text{OSiPr}_3)(4-t\text{Bu-C}_6\text{H}_4)_2)$ (**6**),^[54] und $\text{Ar}-\text{P}(\text{P}(\text{OSiPh}_3)\text{Ph}_2)$ (**7:Ar**, Ar = Mes, *Tip*) beschrieben (Schema 10, unten).^[55]



Schema 10. Synthese von Phosphanylidenphosphoranen mit Silylphosphiniten als Donor.

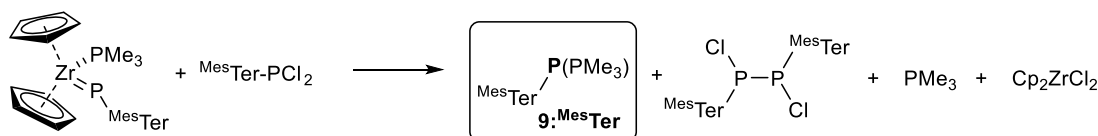


Schema 11. Synthese Phosphanyl-substituierter Phosphanylidenphosphorane nach Fritz et al.^[56]

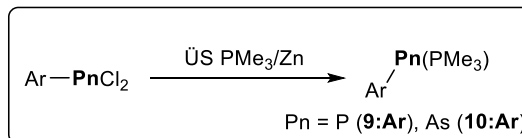
Eine weitere wichtige Klasse von Phosphan-stabilisierten Phosphinidenen wurde erstmals 1989 von Fritz *et al.* beschrieben. Phosphanyl-substituierte Phosphanylidenphosphorane $(t\text{Bu})_2\text{P}-\text{P}(\text{P}(\text{Br})t\text{Bu}_2)\cdot\text{LiBr}$ (**8**) wurden bei der Behandlung des Lithiumphosphids $\text{Li}[\text{P}(\text{P}t\text{Bu}_2)_2]$ mit Dibromethan gewonnen.^[56] Diese Verbindungen sind sehr reaktiv und neigen dazu in Lösung bei Raumtemperatur die Trimere $[(t\text{Bu}_2\text{P})\text{P}]_3$ und Tetramere $[(t\text{Bu}_2\text{P})\text{P}]_4$ von $t\text{Bu}_2\text{P}-\text{P}$ zu bilden (Schema 11). Die Chemie von $(t\text{Bu})_2\text{P}-\text{P}(\text{X})t\text{Bu}_2$ hat sich zu einem wichtigen Teilgebiet moderner Phosphorchemie entwickelt.^[57] Vor kurzem wurde gezeigt, dass $t\text{Bu}_2\text{P}-\text{P}(\text{P}t\text{Bu}_2\text{CH}_3)$ an der Methylgruppe metalliert werden kann, und eine anschließende Behandlung mit einem halben Äquivalent eines Dichlorphosphans $\text{R}\text{P}\text{Cl}_2$ führte in einer Salzmetathese-Reaktion zur Bildung von Kettenspezies mit zwei Phosphanylidenphosphoran-Einheiten des Typs $t\text{Bu}_2\text{P}-\text{P}(\text{P}t\text{Bu}_2\text{CH}_2\text{P}(\text{R})\text{CH}_2t\text{Bu}_2\text{P})\text{P}-\text{P}t\text{Bu}_2$.^[58]

Am häufigsten werden heute Aryl-substituierte Phosphanylidenphosphorane des Typs $\text{Ar}-\text{P}(\text{P}\text{R}'_3)$ (**9:Ar**) verwendet. Die Bildung von $^{\text{Mes}}\text{Ter}-\text{P}(\text{P}\text{Me}_3)$ (**9:MesTer**) wurde erstmals von Protasiewicz *et al.* beobachtet, als sie versuchten Diphosphene aus $\text{Cp}_2\text{Zr}(\text{P}\text{Me}_3)\text{P}^{\text{Mes}}\text{Ter}$ (in Analogie zu Stephans $\text{Cp}_2\text{Zr}(\text{P}\text{Me}_3)\text{P}^{\text{Mes}*}$)^[59] unter Verwendung von $^{\text{Mes}}\text{Ter}\text{P}\text{Cl}_2$ zu synthetisieren (Schema 12, oben). Statt der erwarteten Bildung von $(^{\text{Mes}}\text{Ter}-\text{P})_2$ und $\text{Cp}_2\text{Zr}\text{Cl}_2$ ergab diese Reaktion ein komplexes Gemisch, aus dem $^{\text{Mes}}\text{Ter}-\text{P}(\text{P}\text{Me}_3)$ isoliert wurde.^[60] Später wurde eine rationale Synthese unter Verwendung von sterisch anspruchsvollen Aryldichlorphosphanen in Gegenwart eines Überschusses an PMe_3 und Zn entwickelt.^[61] Verbindungen des Typs $\text{Ar}-\text{P}(\text{P}\text{Me}_3)$ ($\text{R} = \text{Mes}^*$, EIND , $^{\text{Cl}}\text{Ter}$,^[62] $^{\text{Mes}}\text{Ter}$,^[61, 63] DipTer ,^[64] TipTer ^[65]) reagieren leicht mit Aldehyden. In einer Wittig-artigen Reaktion werden Phosphaalkene bei gleichzeitiger Bildung von $\text{O}=\text{P}\text{Me}_3$ erhalten. Daher werden diese Phosphanylidenphosphorane oft als Phospha-Wittig-Reagenzien bezeichnet. Protasiewicz und Mitarbeiter waren auch die ersten, die die Bildung des verwandten Arsanylidene phosphorans $\text{TipTer}-\text{As}(\text{P}\text{Me}_3)$ (**10:TipTer**, Arsa-Wittig-Reagenz) beschrieben (Schema 12),^[66] das strukturell charakterisiert wurde, aber aufgrund der Verunreinigung mit dem Diarsen $(^{\text{Tip}}\text{Ter}-\text{As})_2$ nicht in reiner Form isoliert werden konnte.

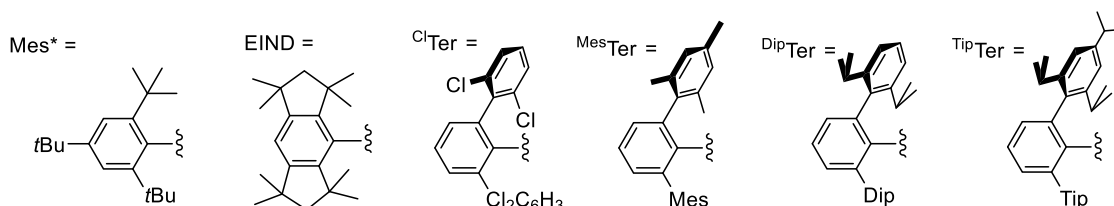
Stabile Aryl-substituierte Phosphanylidenphosphorane



Rationale Synthese



Verschiedene Ar-Gruppen zur Stabilisierung von ArPn(PMe₃)

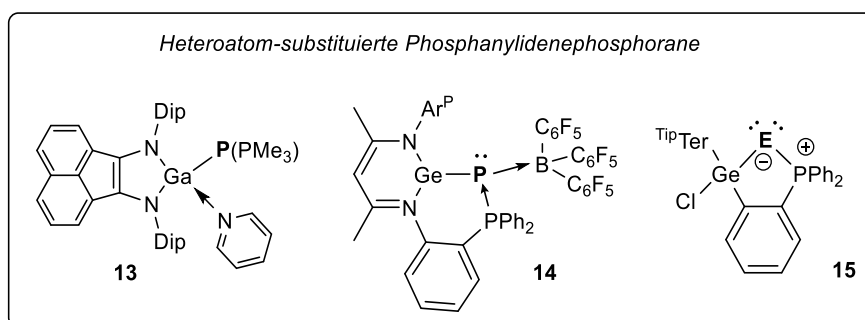


Schema 12. Zufällige Entdeckung von **9:MesTer** (oben) und rationale Synthese von Ar-P(PMe₃) zusammen mit den eingesetzten Aryl-Substituenten (unten, **10** nur mit ^{Dip}Ter und ^{Tip}Ter).

Überraschenderweise konnte im Rahmen dieser Arbeit das stabile Arsa-Wittig-Reagenz **10:^{Dip}Ter** synthetisiert werden. Die Synthese gelang ausgehend von ^{Dip}TerAsCl₂ und einem Überschuss von PMe₃ und Zink in THF.^[67] Dabei muss die Reaktion nach ca. 2 h abgebrochen werden und nach dem Waschen mit *n*-Pentan wurde **10:^{Dip}Ter** in guter Ausbeute als thermisch stabiler gelber Feststoff erhalten. Auch in C₆D₆-Lösung ist **10:^{Dip}Ter** erstaunlich stabil und das Diarsen (^{Dip}Ter-As)₂ wird nur nach mehrtägigem Erhitzen auf 105 °C in Toluol erhalten.^[68] Daraus ergeben sich neuartige Möglichkeiten für den Arsiniden-Transfer unter der Verwendung von Arsa-Wittig-Reagenzien. Einen weiteren wichtigen Beitrag unserer Gruppe stellt die verbesserte Synthese von ^{Mes}Ter-P(PMe₃) dar, welches wir ausgehend von ^{Mes}Ter-PCl₂ darstellten.^[64] Wir konnten zeigen, dass ^{Mes}Ter-PCl₂ ausgehend von dem Bisaminoterphenylphosphan ^{Mes}Ter-P(NEt₂)₂ in der Umsetzung mit wasserfreier HCl erhalten wird. Zusätzlich zeigten wir, dass Systeme des Typs ^{Mes}Ter-P(NR₂)₂ (R = Me, Et) elektronenreiche Phosphan-Liganden darstellen und in der Au(I)-katalysierten Hydroaminierung von terminalen Alkinen hin zu Iminen eingesetzt werden können. Dabei identifizierten wir auch Ag(I)-Komplexe, die entstehen, wenn nicht alles AgCl bei der Generierung der kationischen Au(I)-Katalysatorkomplexe entfernt wird und die Katalyse inhibieren.^[69]

Neben den zuvor beschriebenen acyclischen Derivaten sind auch Phosphanylidenphosphorane bekannt, bei denen die R-P(PR'₃)-Einheit Teil eines Ringsystemes ist. *Peri*-substituierte

umgewandelt wurde.^[75] Die Zugabe der starken Lewis-Säure $B(C_6F_5)_3$ induzierte dann die Abspaltung von CO und die Bildung des *Push-Pull*-substituierten Phosphinidens $(^P\text{Nacnac})\text{GeP}(B(C_6F_5)_3)$ (**14**). Kürzlich verwendete die Gruppe um Wesemann ein intramolekular Phosphan-stabilisiertes Germylen, um in einem ersten Schritt ECl_3 oxidativ an das niedervalente Ge-Atom zu addieren. Dabei entstanden die durch den Phosphan-Donor stabilisierten $\text{Ge}(\text{Cl})\text{ECl}_2$ -Verbindungen. Nach der Reduktion mit Natrium ($\text{E} = \text{P}, \text{Sb}$) oder LiHBEt_3 ($\text{E} = \text{As}$) wurden die entsprechenden cyclischen Pniktiniden-Phosphan-Addukte **15** (Schema 14), ebenfalls intramolekulare Pniktanylidenphosphorane, erhalten.^[76]



Schema 14. Verschiedene kürzlich beschriebene acyclische (**13**) und cyclische (**14**, **15**) Heteroatom-substituierte Phosphanyliden- und Pniktanylidenphosphorane.

2.2.2 Strukturelle- und ^{31}P -NMR-Daten sowie Bindungssituation

Spezies der allgemeinen Formel $\text{R}-\text{P}(\text{PR}'_3)$ zeichnen sich durch elektronenreiche zweifach koordinierte P-Atome aus, deren ^{31}P -NMR-Signale je nach Art des Substituenten deutlich abgeschirmt sind. Die Phosphoran-Einheit zeigt ein Signal in der für Phosphonium-P-Atome typischen Region zwischen ca. -10 und 80 ppm im ^{31}P -NMR-Spektrum. Außerdem deutet eine recht große $^1J_{\text{PP}}$ -Kopplungskonstante zwischen 400 und 700 Hz auf eine Bindungssituation hin, die der von Diphosphenen ähnelt (vgl. $(\text{Mes}^*-\text{P})_2$ $^1J_{\text{PP}} = 574$ Hz).^[77] Tabelle 1 fasst die ^{31}P -NMR-Daten einer Reihe unterschiedlich substituierter $\text{R}-\text{P}(\text{PR}'_3)$ -Spezies zusammen.

Außerdem ist in den strukturell charakterisierten Beispielen die P–P-Bindung zwischen den zweifach- und vierfach-koordinierten P-Atomen mit Werten von ca. 2.06 bis 2.15 Å deutlich kürzer als der theoretisch vorhergesagte Wert für eine P–P-Einfachbindung (vgl. $\Sigma r_{\text{cov}}(\text{P}-\text{P}) = 2.22$ Å) und näher am Wert einer Doppelbindung (vgl. $\Sigma r_{\text{cov}}(\text{P}=\text{P}) = 2.04$ Å).^[78] Alle diese experimentellen Beobachtungen deuten auf ein gewisses Maß an Mehrfachbindungscharakter in Phosphanylidenphosphoranen hin (Schema 8, I). Die wichtigsten strukturellen Parameter für eine Reihe von strukturell charakterisierten Phosphanylidenphosphoranen sind in Tabelle 2 zusammengefasst.

Tabelle 1: ³¹P-NMR-Verschiebungen der Phosphanyliden- (P1) und Phosphoran- (P2) P-Atome in ausgewählten Beispielen von Phosphanyliden-σ⁴-Phosphoranen, zusammen mit den Werten für die ¹J_{P1-P2}-Kopplungskonstante.

Verbindung	δ(³¹ P) P1 [ppm]	δ(³¹ P) P2 [ppm]	¹ J _{P1-P2} [Hz]
F ₃ C-P(PMe ₃) ^[50]	-81.0	12.7	436.5
(EtO) ₂ (O)P-P(P <i>n</i> Bu ₃) ^[51]	-217.5	38.7	456
Mes-P(P(OSiMe ₃)(C ₃ Me ₅ H) ^[52]	-209.0	78.0	433
TipTer-P(PMe ₃) ^[65]	-113.4	-1.6	564
MesTer-P(PMe ₃) ^[61]	-114.7	-2.8	582
DipTer-P(PMe ₃) ^[64]	-116.5	-3.1	560
ClTer-P(PMe ₃) ^[62]	-121.1	6.7	573
Mes*-P(PMe ₃) ^[61]	-134.0	4.7	581
MesTer-P(P <i>n</i> Bu ₃) ^[61]	-151.3	24.1	589
Mes*-P(P <i>n</i> Bu ₃) ^[61]	-153.7	19.9	612
(<i>t</i> Bu ₂ P-P) ₂ ((<i>Pt</i> Bu ₂ CH ₂) ₂ PMe)	-173.7	63.2	616
(<i>t</i> Bu ₂ P-P) ₂ ((<i>Pt</i> Bu ₂ CH ₂) ₂ PPh)	-172.5	67.5	608
<i>t</i> Bu ₂ P-P(P(Me) <i>t</i> Bu ₂)	-204.73	57.5	597
<i>t</i> Bu(Me ₃ Si)P-P(P(Me) <i>t</i> Bu ₂)	-212.88	57.3	604
<i>t</i> Bu ₂ P-P(P(Br) <i>t</i> Bu ₂)	-89	172.3	682
<i>t</i> Bu(Me ₃ Si)P-P(P(Br) <i>t</i> Bu ₂)	-98.6	168.6	706
<i>t</i> Bu ₂ P-P(P(Cl) <i>t</i> Bu ₂)	-124.35	157.51	697
<i>t</i> Bu ₂ P-P(P(I) <i>t</i> Bu ₂)	-42.74	173.34	651
BIANGa(py)-P(PMe ₃) ^[74]	-263	14.7	527
Mes-P(P(OSiPh ₃)Ph ₂) ^[55]	-119.8	74.8	628
Tip-P(P(OSiPh ₃)Ph ₂) ^[55]	-134.1	74.6	632
[P]-P(PMe ₃) ^[79]	-103	12.1	493
[P]-P(P <i>n</i> Bu ₃) ^[79]	-141.1	32.6	512
[P]-P(<i>Pt</i> Bu ₃) ^[79]	-110.5	77.3	609
[P]-P(PCy ₃) ^[79]	-154.2	46	548
[P]-P(PPh ₃) ^[79]	-113.5	38.2	561
[^s P ^{Dip}]-P(PMe ₃) ^[80]	-100.5	12.1	496
[^s P ^{Dip}]-P(PPh ₃) ^[80]	-107.3	39.9	555
TipTerGe(Cl)-P(PPh ₂) ^[76]	-244	56.7	531
A(<i>i</i> Pr ₂ P)P-A ^[71]	-157.7	76.7	480
^P NacnacGeP(B(C ₆ F ₅) ₃) ^[75]	-123.8	22.1	532

Tabelle 2: Charakteristische Strukturparameter, $d(\text{Pn-P})$ ($\text{Pn} = \text{P}, \text{As}$) und Winkel am zweifach koordinierten Pn-Atom ausgewählter, strukturell charakterisierter Phosphanlyden- und Arsanylidenphosphorane.

Verbindung	$d(\text{Pn-P})$ [Å]	P-Pn-R [°]
$t\text{Bu}_2\text{P-P}(\text{P}(\text{Br})t\text{Bu}_2)$ (8) ^[81]	2.077	105.77(7)
$t\text{Bu}_2\text{P-P}(\text{P}(\text{Me})t\text{Bu}_2)$ ^[81]	2.1263(4)	100.95(1)
$t\text{Bu}(\text{Me}_3\text{Si})\text{P-P}(\text{P}(\text{Me})t\text{Bu}_2)$ ^[81]	2.1358(5)	100.29(2)
$t\text{Bu}_2\text{P-P}(\text{P}t\text{Bu}_2\text{CH}_2\text{P}(\text{Ph})\text{CH}_2t\text{Bu}_2\text{P})\text{P-P}t\text{Bu}_2$ ^[58]	2.1332(8); 2.1320(9)	102.83(4); 100.63(4)
9:MesTer ^[63]	2.084(2)	106.79(13)
9:DipTer ^[64]	2.0955(7)	108.47(5)
$\text{Tip-P}(\text{P}(\text{OSiPh}_3)\text{Ph}_2)$ ^[55]	2.0647(6)	97.16(6)
11 ^[71]	2.148(5)	90.4(5)
$[\text{sPA}^*]\text{P}-(\text{PnBu}_3)$ ^[79]	2.1064(11)	91.19(4)
13 ^[74]	2.084(1)	100.9(1)
14 ^[75]	2.132(1)	94.52(2)
15 ^[76]	2.103(1)	90.1(2)
$\text{TipTer-As}(\text{PMe}_3)$ ^[66]	2.2190(17)	101.53(17)
$\text{DipTer-As}(\text{PMe}_3)$ ^[66]	2.2224(5)	107.26(5)

Ein genauerer Blick auf die ylidische Struktur **II** (Schema 8) zeigt, dass Phosphanlydenphosphorane mit den Alkylidenphosphoranen, den klassischen Wittig-Reagenzien vom Typ $\text{R}_2\text{C}=\text{PR}'_3$, verwandt sind.^[18] Zum besseren Verständnis der Bindungssituation wurden unterschiedlich substituierte Modellverbindungen mit Hilfe von DFT-Rechnungen auf dem PBE0-D3/def2-TZVP-Niveau theoretisch untersucht. Dabei wurden insbesondere die Kohn-Sham-Orbitale, sowie die natürlichen lokalisierten Molekülorbitale (NLMOs) für die Modellverbindungen $\text{H-P}(\text{PH}_3)$, $\text{H}_2\text{P-P}(\text{PH}_3)$, $(\text{H}_2\text{N})_2\text{P-P}(\text{PMe}_3)$, $\text{H}_2\text{N-P}(\text{PH}_3)$, $\text{H}_3\text{C-P}(\text{PH}_3)$ und $\text{Ph-P}(\text{PH}_3)$ genauer betrachtet. Das HOMO in all diesen Spezies lässt sich am besten durch ein einsames p-artiges LP am zweifach-koordinierten P-Atom beschreiben, das teilweise in die $\text{P-H-}\sigma^*$ -Orbitale der Phosphoran-Einheit delokalisiert ist (Abbildung 4). Das HOMO-1 zeigt Beiträge eines freien s-artigen LPs am niedervalenten P-Atom (zusätzliches LP am Phosphanlyl-P in Phosphanlyl-substituierten Varianten). Das LUMO hat einen signifikanten σ^* -Charakter mit einem großen Orbitallappen am Phosphanlyden-P-Atom, welcher von der P-P -Bindungsachse wegorientiert ist. Dies weist auf das Potenzial für eine PH_3 -Substitution durch einen nucleophilen Angriff von der Rückseite hin. Es ist anzumerken, dass sich das LUMO in der Phenyl-substituierten Modellverbindung $\text{Ph-P}(\text{PH}_3)$

hauptsächlich auf dem Phenyling befindet und nur das LUMO+1 einen signifikanten σ^* -Charakter aufweist. Das Energieniveau des HOMOs wird direkt durch den Substituenten am P-Atom der Phosphanlyden-Einheit beeinflusst. Elektronegative Substituenten wie Aminogruppen erhöhen die HOMO-Energie, während eine Phosphanly-Substitution das HOMO in Bezug auf $\text{H-P}(\text{PH}_3)$ energetisch stabilisiert. Die Einführung von Aminogruppen an den Phosphanly-Gruppen erhöht wiederum die HOMO-Energie. Interessanterweise zeigt die Phenyl-substituierte Variante eine mittlere HOMO-Energie, während das LUMO erheblich stabilisiert ist.

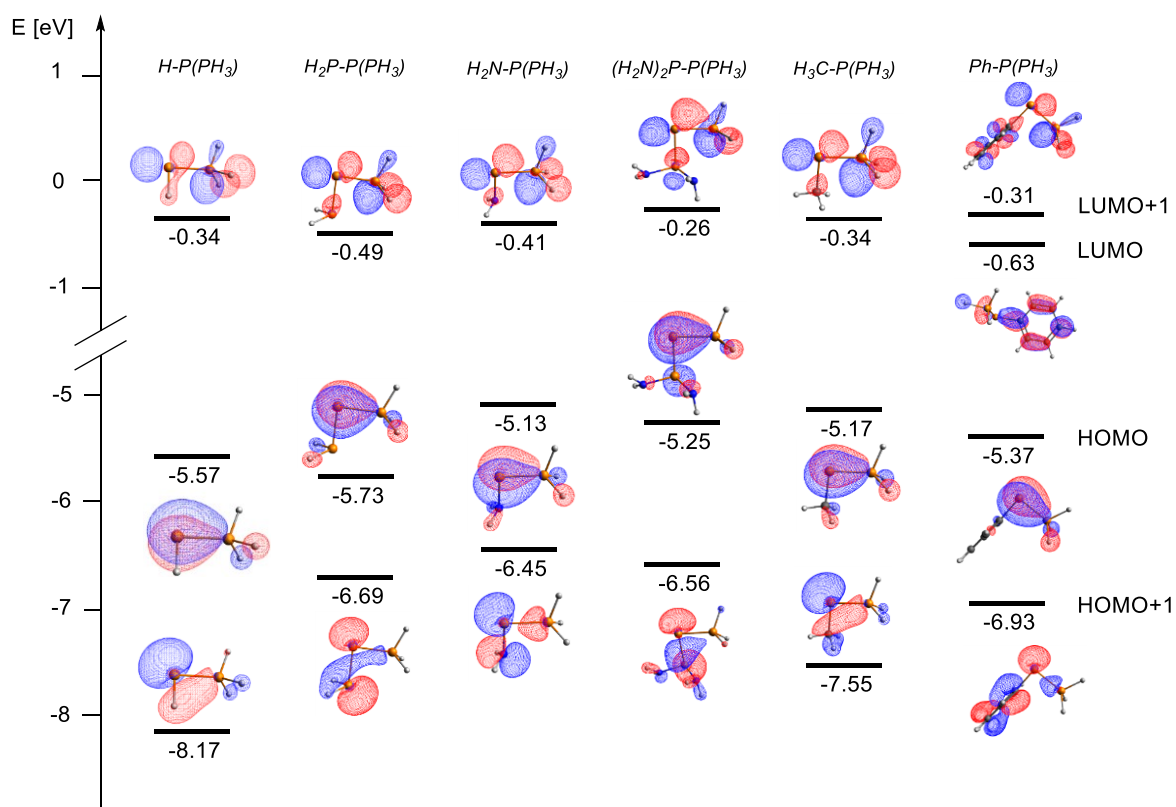


Abbildung 4. KS-Orbitale von Modell-Phosphanlyden- σ^4 -phosphoranen (PBE0-D3/def2-TZVP).

NBO-Analysen auf dem Theorieniveau PBE0-D3/def2-TZVP ergeben ein ähnliches Bild wie die Untersuchung der Kohn-Sham-Orbitale (Abbildung 5). Die Hauptresonanzstruktur für $\text{H-P}(\text{PH}_3)$ zeigt eine P-P-Einfachbindung, die in Richtung des Phosphoran-P-Atoms polarisiert ist; mit einer negativen Partialladung an P1 (-0.381 e) und einer positiven Ladung an P2 (0.406 e). Außerdem befinden sich zwei LPs am zweifach-koordinierten P-Atom P1. Eines besitzt reinen p-Orbitalcharakter (LP2), während das andere zu 75 % s-Charakter aufweist (LP1), was mit dem HOMO und HOMO-1 in den KS-Orbitalen gut übereinstimmt. Das energetisch am niedrigsten liegende NLMO lässt sich am besten als das P-P σ^* -Orbital

beschreiben, das zu ca. 63 % am zweifach koordinierten P-Atom lokalisiert ist. Mit Hilfe der NBO-Analyse kann die Stabilisierungsenergie durch negative Hyperkonjugation unter Verwendung einer Störungsrechnung zweiter Ordnung abgeschätzt werden. Dies zeigt deutlich, dass das p-artige LP an P1 in zwei der drei P-H σ^* -Orbitale mit einer Stabilisierungsenergie von jeweils $59.8 \text{ kJ}\cdot\text{mol}^{-1}$ delokalisiert ist. Der Wiberg-Bindungsindex (WBI) für die P-P-Bindung in H-P(PH₃) beträgt 1.29, was die negative Hyperkonjugation einmal mehr verdeutlicht. Mit Hilfe der natürlichen Resonanztheorie (NRT) kann der Anteil verschiedener Lewis-Strukturen in einem Resonanzschema abgeschätzt werden. Wie bereits erwähnt, sind die Darstellungen als $1\lambda^5$ -Diphosphen oder als Phosphan-stabilisiertes Phosphiniden keine Resonanzformen des Phosphanyliden- σ^4 -phosphorans. Die NRT-Analyse zeigt eindeutig, dass die Darstellung als ylidisches Phosphanyliden- σ^4 -phosphoran die bestimmende Resonanzstruktur (82 %) ist, mit zwei zusätzlichen Resonanzen, die die negative Hyperkonjugation von LP1 durch eine formale P-P-Doppelbindung und ein Hydrid durch P-H-Bindungsspaltung berücksichtigen.

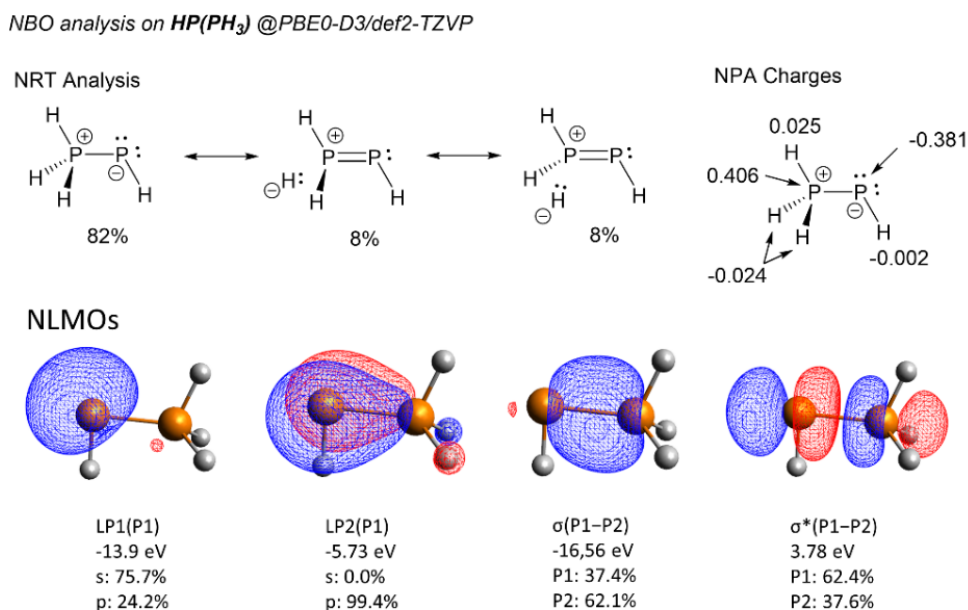
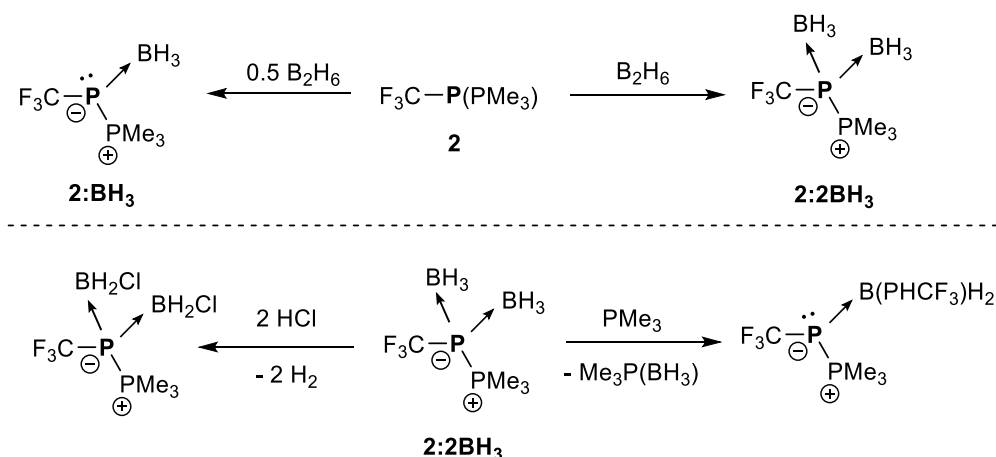


Abbildung 5. Ergebnisse der NBO-Analyse von H-P(PH₃) (PBE0-D3/def2-TZVP).

Aus diesen theoretischen Überlegungen lassen sich zwei Hauptreaktivitätswege von Phosphanyliden- σ^4 -phosphoranen ableiten: Die beiden freien Elektronenpaare an P1 sollten zu einer ausgeprägten Reaktivität gegenüber Elektrophilen führen und andererseits sollte das zugängliche σ^* P-P-Orbital Substitutionsreaktionen der PR₃ Gruppe gegen geeignete Nucleophile in assoziativer Weise ermöglichen.

2.2.3 Reaktivität gegenüber Elektrophilen

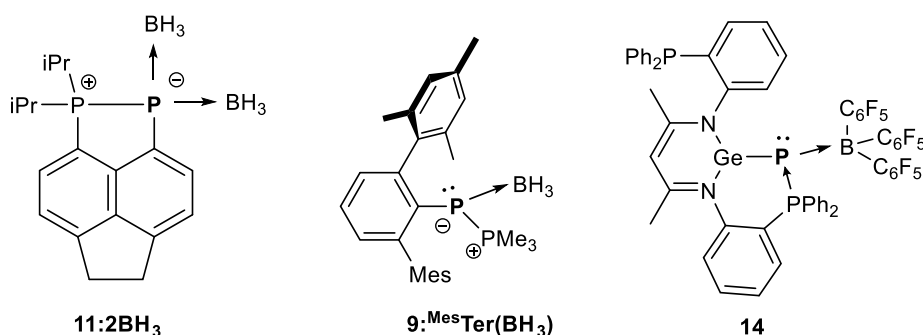
Im Folgenden soll die Reaktivität von $R-P(PR'_3)$ gegenüber Elektrophilen kurz umrissen werden. Die ersten diesbezüglichen Untersuchungen wurden von Burg und Mahler an $F_3C-P(PMe_3)$ (**2**) durchgeführt. Die Behandlung einer THF-Lösung von **2** mit einem leichten Überschuss an Diboran B_2H_6 ergab das thermisch stabile (bis zu $60\text{ }^\circ\text{C}$) Bis-Boran-Addukt $F_3C-P(BH_3)_2(PMe_3)$ (**2:2BH₃**) (Schema 15, oben).^[82] Unter Verwendung eines halben Äquivalents B_2H_6 wurde das einfache Addukt $F_3C-P(BH_3)(PMe_3)$ hergestellt, das sich im festen Zustand bis $56\text{ }^\circ\text{C}$ als stabil und in THF-Lösung bei Raumtemperatur als instabil erwies. Um BH_3 wieder aus **2:2BH₃** zu entfernen, wurde es mit PMe_3 behandelt und neben $Me_3P \cdot BH_3$ entstand $F_3C-P(BH_2P(H)CF_3)$, das durch Insertion des freien Phosphinidens F_3C-P in die B–H-Bindung des koordinierten BH_3 gebildet wurde. Die Reaktion von **2:2BH₃** mit trockener HCl ergab das H_2 -Eliminierungsprodukt $F_3C-P(BH_2Cl)_2(PMe_3)$ als Hauptspezies (Schema 15, unten).



Schema 15. Bildung der Mono- und Bis-Boran-Addukte von **2** (oben) und Untersuchungen zu dessen Reaktivität (unten).

Die Synthese des cyclischen Phosphanyliden- σ^4 -phosphorans **11** erfolgte durch die Reduktion des Phosphan-Phosphan-Donor-Akzeptor-Komplexes $iPr_2(A)P \rightarrow P(A)Cl_2$ ($A =$ Acenaphten-Grundgerüst, P-Atome an den *peri*-Positionen) mit einem Überschuss an $H_3B \cdot SME_2$ zum entsprechenden Bis-Boran-Addukt $iPr_2(A)P \rightarrow P(A)(BH_3)_2$ (**11:2BH₃**, Schema 16, links).^[71] Dieses wurde kristallographisch charakterisiert und stellte den ersten strukturellen Nachweis für ein Bis-Boran-Addukt von Phosphanyliden- σ^4 -phosphoranen dar. Der P–P-Atomabstand von $2.2208(11)\text{ \AA}$ entspricht hier einer typischen Einfachbindung (vgl. $\Sigma r_{kov}(P-P) = 2.22\text{ \AA}$).^[78] Die Entfernung von BH_3 wurde durch die Zugabe von $HNMe_2$ erreicht (Schema 13), was quantitativ **11** ergab und zu einer Kontraktion der P–P-Bindung um ca. 0.08 \AA führte.

Es ist interessant festzustellen, dass nur das einfache Addukt **9**:^{Mes}Ter(BH₃) erhalten werden konnte, wenn ^{Mes}Ter–P(PMe₃) entweder mit H₃B·THF oder H₃B·SMe₂ behandelt wurde (Schema 16, Mitte). Diese Neigung, bei der Addukt-Bildung nur eines der LPs zu binden, lässt sich auf das sterische Profil des Substituenten zurückführen.^[63] In ähnlicher Weise wurde ein intramolekulares Phosphanlydenphosphoran als B(C₆F₅)₃-Addukt erhalten, als das Gesubstituierte Phosphaketon [^PNacnac]GePCO mit B(C₆F₅)₃ behandelt wurde und CO-Eliminierung bewirkte die Bildung des Boran-Adduktes **14** (Schema 16, rechts).^[75]



Schema 16. Strukturen von BH₃-Addukten von cyclischen (**11:2BH₃**, **14**) und acyclischen (**9**:^{Mes}Ter(BH₃)) Phosphanlydenphosphoranen.

Mit zwei verfügbaren freien Elektronenpaaren am Phosphanlyden P-Atom, sollten Phosphanlyden-σ⁴-phosphorane exzellente Liganden für Übergangsmetallfragmente darstellen. Der erste Bericht über die Koordinationschemie von Ar–P(PMe₃) (Ar = Mes*, ^{Mes}Ter) von Protasiewicz *et al.* beschreibt die Umsetzung von Ar–P(PMe₃) mit zwei Äquivalenten [Au(tht)Cl] in Toluol. Dabei wurden die Bis-AuCl-Komplexe [^{Mes}TerP(AuCl)₂(PMe₃)] (**I**, Abbildung 6) oder die dimeren Spezies [Mes*P(AuCl)₂(PMe₃)]₂ (**II**, Abbildung 6) erhalten, die durch aurophile Wechselwirkungen zusammengehalten werden und einen zentralen P₂Au₄-Sechsring mit einer sesselartigen Konformation aufweisen.^[83] In beiden Spezies ist der P–P-Atomabstand (**I**: 2.205(1) Å; **II**: 2.174(3) Å) länger als im freien Ar–P(PMe₃). Diese Verlängerung ist auf die Bindung beider LPs an das AuCl-Fragment zurückzuführen, wodurch der Mehrfachbindungscharakter aufgehoben wird. Mit AgOTf (OTf[–] = [O₃S–CF₃][–]) wurden Komplexe mit der allgemeinen Formel [ArP(AgOTf)₂(PMe₃)] erhalten. Die Bestimmung der Molekülstruktur zeigte jedoch die Bildung der dimeren Spezies [^{Mes}TerP(AgOTf)₂(PMe₃)]₂, in der zwei Triflat-Anionen die beiden Monomer-Einheiten überbrücken (**III**, Abbildung 6).

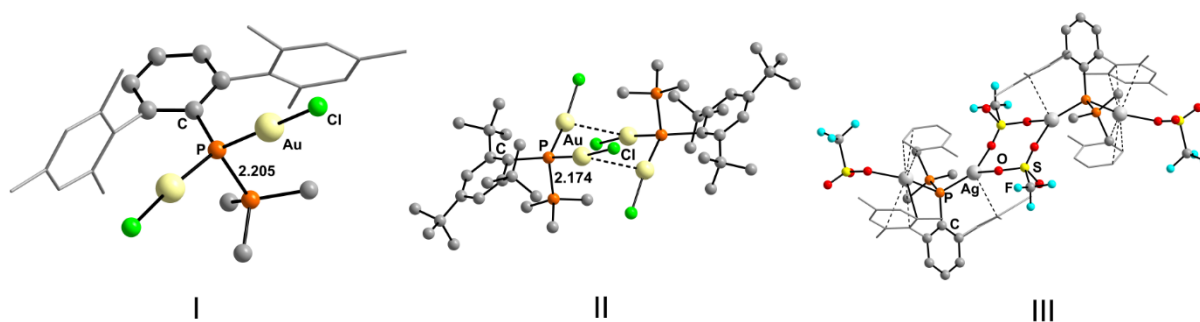
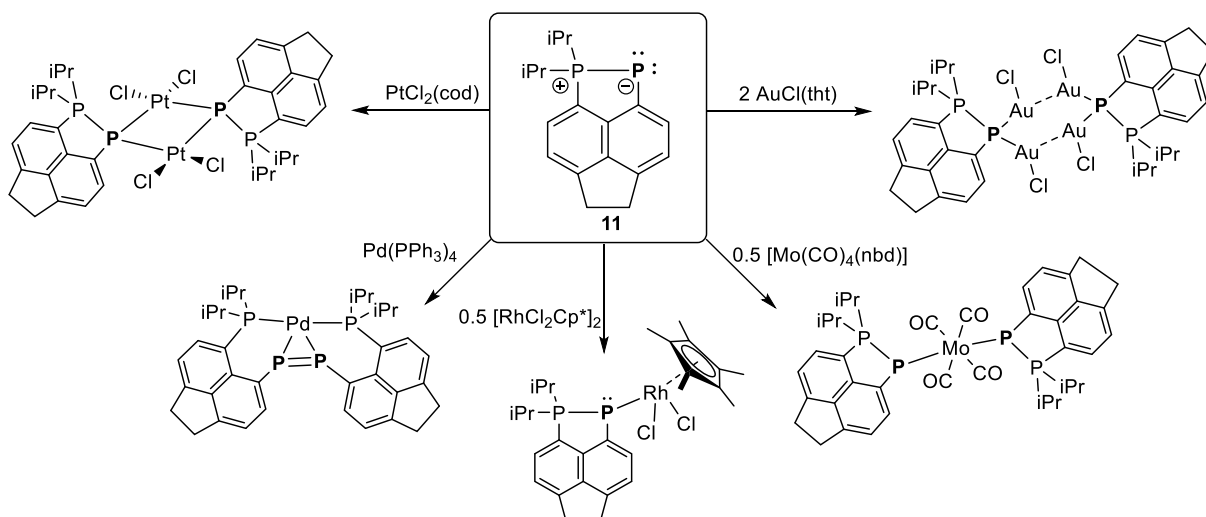


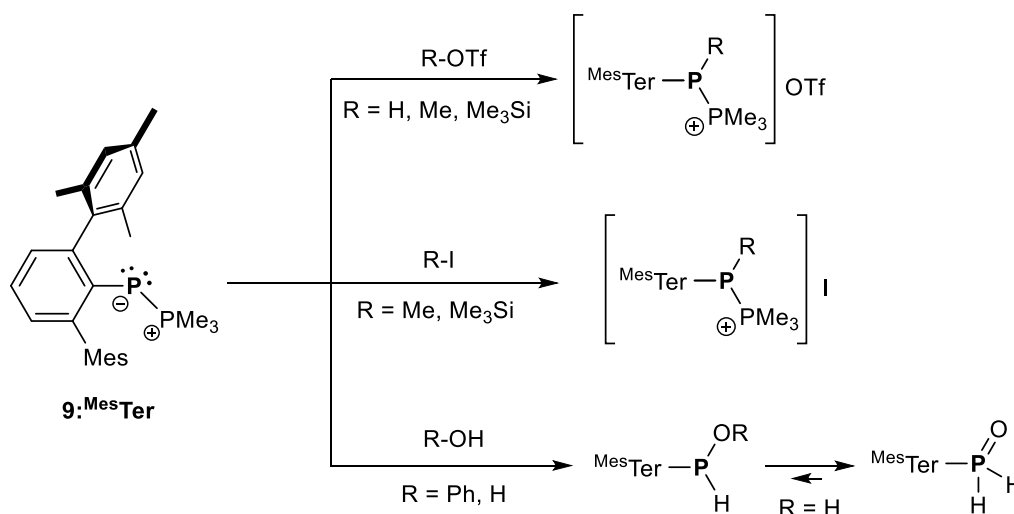
Abbildung 6. Molekülstrukturen von $[\text{Mes}^*\text{TerP}(\text{AuCl})_2(\text{PMe}_3)]$ (links), $[\text{Mes}^*\text{P}(\text{AuCl})_2(\text{PMe}_3)]_2$ (Mitte) und $[\text{Mes}^*\text{TerP}(\text{AgOTf})(\text{PMe}_3)]_2$ (rechts) im Kristall.^[83] Kugel- und Stabmodell und Drahtgitterdarstellung, Atomradien sind willkürlich gewählt.

Ähnliche Beobachtungen machten Kilian und Mitarbeiter für die Acenaphthen-basierte Spezies **11**. Mit $[\text{AuCl}(\text{tht})]$ wurde die Koordination von zwei AuCl -Fragmenten an eine Phosphanlydenphosphoran-Einheit und die Dimerisierung durch aurophile Wechselwirkungen mit einem zentralen P_2Au_4 -Strukturmotiv in einer *Twist-Boat*-Konformation nachgewiesen (Schema 17, oben rechts). Mit $[\text{PtCl}_2(\text{cod})]$ wurde ein inversionssymmetrischer zweikerniger Komplex mit einem zentralen P_2Pt_2 -Ring gebildet (Schema 17, oben links). Die Pt-Atome in diesem Komplex sind *cis*-koordiniert mit zwei μ^2 -Phosphanlyden-Liganden. Einkernige Komplexe wurden erhalten, wenn zwei Äquivalente von **11** mit $[\text{Mo}(\text{CO})_4(\text{nbd})]$ kombiniert wurden, was den $[\text{Mo}(\text{CO})_4]$ -Komplex mit zwei endständigen Phosphanlydenphosphoran-Liganden ergab (Schema 17, unten rechts), in denen die P–P-Bindung nur minimal um ca. 1.5% verlängert ist, was deutlich zeigt, dass die negative Hyperkonjugation in diesen einfach koordinierenden Phosphanlydenphosphoranen erhalten bleibt, was auf eine Koordination über das s-artige LP hinweist. Ähnliche Beobachtungen wurden für Übergangsmetall- η^1 -Komplexe von Diphosphenen gemacht, bei denen die P–P-Doppelbindung unverändert bleibt.^[84] Ein weiterer terminaler η^1 -Komplex von **11** wurde in der Reaktion mit einem halben Äquivalent $[\text{RhCl}_2\text{Cp}^*]_2$ synthetisiert, bei dem die $^1J_{\text{PP}}$ -Kopplungskonstante von 453 Hz auf eine typische Phosphanlydenphosphoran-Einheit hinweist, bei der das s-artige LP an der Koordination beteiligt ist (Schema 17, Mitte). Im Gegensatz zu den obigen Beispielen führte die Reaktion von **11** mit $[\text{Pd}(\text{PPh}_3)_4]$ zur Bildung eines μ^2 -Diphosphen-Komplexes, bei dem die Phosphoran-Einheit mit Pd wechselwirkt und ein endständiges Phosphiniden freisetzt, welches dann dimerisiert und den beobachteten Diphosphen-Liganden ergibt (Schema 17, unten links).^[71, 85]



Schema 17. Vielfältige Koordinationschemie der cyclischen Verbindung **11**.

Neben den Reaktionen mit BH_3 , $\text{B}(\text{C}_6\text{F}_5)_3$ oder Lewis-sauren Übergangsmetallzentren wurde auch die Reaktivität von **9**:^{Mes}Ter gegenüber Me_3SiOTf , HOTf und MeOTf beschrieben. Bemerkenswert ist das Tieffeld-verschobene Phosphanyliden-P-Atom-Signal im ^{31}P NMR-Spektrum bei der Bildung von $[\text{MesTerP}(\text{X})\text{PMe}_3]\text{OTf}$ ($\text{X} = \text{SiMe}_3, \text{H}, \text{Me}$) und eine Abnahme der $^1J_{\text{PP}}$ -Kopplungskonstante (Schema 18, oben), was auf eine Phosphinophosphonium-Spezies hinweist. Die Reaktionen werden weniger selektiv, wenn das Anion des Elektrophils nucleophiler wird, wie dies bei MeI und Me_3SiI der Fall ist. In diesen Fällen wurden Mischungen der Phosphane $\text{MesTerP}(\text{X})\text{I}$, PMe_3 und der Phosphinophosphonium-Spezies $[\text{MesTerP}(\text{X})\text{PMe}_3]\text{I}$ gebildet (Schema 18, Mitte).^[63] Die Reaktionen mit Protonenquellen wie HCl, HO-Ph oder Wasser verlaufen ausgesprochen selektiv.



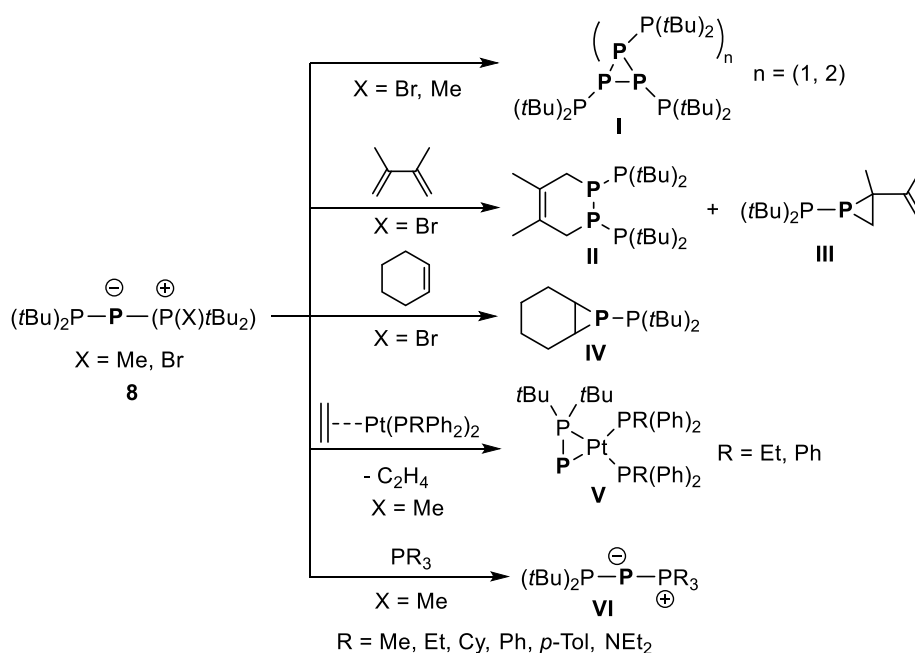
Schema 18. Reaktivität von **9**:^{Mes}Ter gegenüber verschiedenen Elektrophilen.

Mit HCl wird das sekundäre Phosphan $^{\text{Mes}}\text{TerP(H)Cl}$ unter gleichzeitiger Eliminierung von $[\text{HPMe}_3]\text{Cl}$ gebildet. Mit Phenol wurde das sekundäre Phosphan $^{\text{Mes}}\text{TerP(H)OPh}$ durch formale oxidative Addition am Phosphanyliden-P-Atom erhalten. Mit Wasser tautomerisiert das erwartete Produkt $^{\text{Mes}}\text{TerP(H)OH}$ schnell zum korrespondierenden Phosphinoxid $^{\text{Mes}}\text{TerP(O)H}_2$ (Schema 18, unten). In ähnlicher Weise wurde berichtet, dass **2** nach der anfänglichen Behandlung mit MeI und anschließender Zugabe von HCl in $\text{F}_3\text{C(H}_3\text{C)PCl}$ umgewandelt wird, um PMe_3 in Form von $[\text{HPMe}_3]\text{I}$ zu entfernen.^[86]

2.2.4 Phosphan-Substitution – Phosphinidin-Transfer mit $\text{R-P(PR}'_3)$

Bereits in der Publikation zu $\text{F}_3\text{C-P(PMe}_3)$ (**2**) findet sich der erste Nachweis für Phosphiniden-Transferreaktionen. Es wurde gezeigt, dass die Erwärmung einer Lösung von **2** auf Raumtemperatur PMe_3 und eine 6:1-Mischung von $(\text{F}_3\text{C-P})_4$ und $(\text{F}_3\text{C-P})_5$ ergab. Das Potenzial für eine einfache Freisetzung von Phosphinidenen wurde außerdem durch die Tatsache unterstrichen, dass 1 Mol% PMe_3 die Umlagerung von reinem $(\text{F}_3\text{C-P})_5$ bei Raumtemperatur katalysierte (Schema 8).^[49]

In ähnlicher Weise zersetzt sich die Phosphanyl-substituierte Variante $(t\text{Bu})_2\text{P-P(P(Br)tBu}_2)\cdot\text{LiBr}$ (**8**) beim Erwärmen auf $20\text{ }^\circ\text{C}$ zu einem Gemisch von $[(t\text{Bu})_2\text{P-P}]_n$ ($n = 3, 4$) (**I**, Schema 19). In Gegenwart von 2,3-Dimethylbutadien (DMB) wurde diese Zersetzungsreaktion unterdrückt und stattdessen die sechsgliedrige Ringspezies **II** zusammen mit dem Phosphiran **III** gebildet (**II** und **III**, Schema 19). Mit Cyclohexen wurde das [2+1]-Cycloadditionsprodukt **IV** erhalten (Schema 19). Da sich der Halogenid-Substituent in der Phosphoran-Einheit von **8** bei dem Versuch, die Phosphiniden-Einheit auf Übergangsmetallfragmente zu übertragen, als problematisch erwies, kann die halogenidfreie Variante $(t\text{Bu})_2\text{P-P(P(Me)tBu}_2)$ durch Behandlung von **8** mit Methylolithium erhalten werden.^[81, 87] In Analogie zu **8** werden $[(t\text{Bu})_2\text{P-P}]$ und $t\text{Bu}_2\text{PMe}$ bei thermischer P-P-Bindungsspaltung gebildet.^[88] Die Reaktion von $(t\text{Bu})_2\text{P-P(P(Me)tBu}_2)$ mit den Platinkomplexen $[\eta^2\text{-(H}_2\text{C=CH}_2)\text{Pt(PRPh}_2)_2]$ ($\text{R} = \text{Et, Ph}$) in Toluol ergab die Komplexe $[\eta^2\text{-(tBu}_2\text{P-P)Pt(PRPh}_2)_2]$ ($\text{R} = \text{Et, Ph}$) als rote kristalline Feststoffe, mit einer seitlich koordinierten Phosphanylphosphiniden-Einheit im strukturell charakterisierten verzerrt quadratisch-planaren Komplex $[\eta^2\text{-(tBu}_2\text{P-P)Pt(PEtPh}_2)_2]$ (**V**, Schema 19).^[89] Der kurze P-P-Atomabstand in diesem Komplex ist ein gutes Beispiel dafür, dass Phosphinophosphinidene am besten mit einer Mehrfachbindung und einem zwitterionischen Charakter, ähnlich dem von **1**, beschrieben werden.

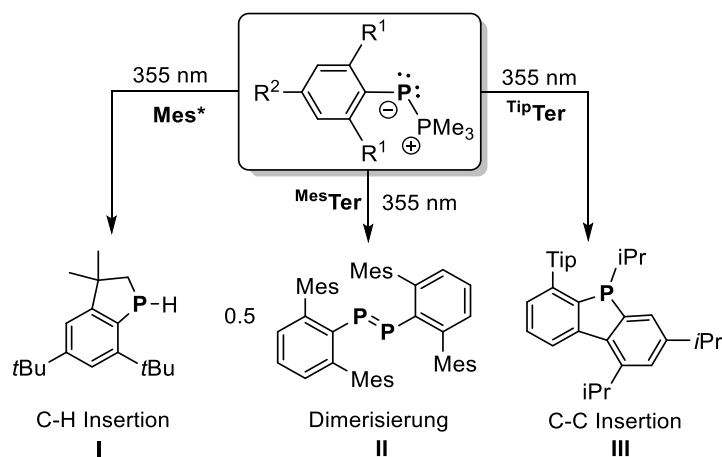


Schema 19. Vielseitige Reaktivität des Phosphanyl-substituierten Phosphanylidenephosphorans **8**.

Der leichte Austausch von $t\text{Bu}_2\text{PMe}$ in $(t\text{Bu})_2\text{P}=\text{P}(\text{Me})t\text{Bu}_2$ wurde für PMe_3 (sogar bei $-70\text{ }^\circ\text{C}$) und PEt_3 (vollständiger Austausch bei $20\text{ }^\circ\text{C}$) gezeigt (**VI**, Schema 19). Die Produkte sind bei Raumtemperatur nicht unbegrenzt stabil und zersetzen sich zu phosphorreichen Materialien. Bei PPhEt_2 , PPh_2Et , PPh_2iPr , PPh_2Me , PCy_3 , PPh_3 , $\text{P}(p\text{-Tol})_3$ und $\text{P}(\text{NEt}_2)_3$ wurde keine vollständige Umsetzung beobachtet und es wurden Mischungen aus dem Ausgangsmaterial und dem Austauschprodukt identifiziert.^[90]

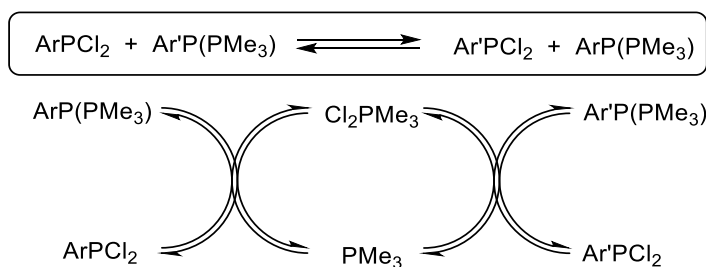
Aus den vorherigen theoretischen Betrachtungen geht hervor, dass das LUMO der Phosphanylidene phosphorane einen signifikanten σ^* -Charakter aufweist, so dass die Photolyse die Spaltung der P–P-Bindung und die Erzeugung des Phosphinidens erleichtern sollte. Sogenannte „Phospha-Wittig“-Reagenzien vom Typ $\text{Ar}-\text{P}(\text{PMe}_3)$ mit sperrigen Substituenten am Phosphanylidene-P-Atom, bilden unter Laserbestrahlung bei 355 nm in einer C_6D_6 -Lösung das Phosphiniden $\text{Ar}-\text{P}$.^[65] Neben dem visuellen Verblässen der gelben Farbe von $\text{Mes}^*\text{-P}(\text{PMe}_3)$ wurde durch ^{31}P -NMR-Spektroskopie freies PMe_3 und das bekannte 3,3-Dimethyl-5,7-di-tert-butylphosphorindan **I** nachgewiesen (Schema 20, links). Dieses Phosphorindan ist ein bekanntes Zersetzungsprodukt von $\text{Mes}^*\text{-P}$, das durch Insertion des Phosphiniden-P-Atoms in eine benachbarte $\text{C}(\text{sp}^3)\text{-H}$ -Bindung der *o*- $t\text{Bu}$ -Gruppe entsteht.^[91] $\text{Mes}^*\text{Ter}-\text{P}(\text{PMe}_3)$ ergibt bei der Bestrahlung unter Freisetzung von PMe_3 das Diphosphen $(\text{Mes}^*\text{Ter}-\text{P})_2$ **II**, dessen photolytische Stabilität einen weiteren photochemischen Abbau verhindert (Schema 20, Mitte). Power und Mitarbeiter berichteten über Versuche das Diphosphen $(\text{Tip}^*\text{Ter}-\text{P})_2$ durch eine Reduktion von $\text{Tip}^*\text{TerPCl}_2$ mit Magnesium zu erhalten, bei

der jedoch nur die Bildung des Phosphafluorens **III** beobachtet wurde (Schema 19, rechts).^[92] Dieses entsteht durch die Insertion des Phosphinidens TipTer-P in eine der C-*iPr*-Bindungen des Tip-Substituenten. Mit dem Phospha-Wittig-Reagenz $\text{TipTer-P(PMe}_3\text{)}$ wurde das gleiche Phosphafluoren **III** als Hauptprodukt der photolytischen P-P-Bindungsspaltung beobachtet. Die Photolyse in Anwesenheit eines Überschusses von PMe_3 zeigte, dass die Aktivierung der C-H- oder C-C-Bindung zu **I** bzw. **III** schneller erfolgt als eine Rekombination des freien Phosphinidens mit PMe_3 . Im Falle von $\text{Mes}^*\text{Ter-P(PMe}_3\text{)}$ wird die Diphosphen-Bildung in Gegenwart von überschüssigem PMe_3 verlangsamt, und die längere Lebensdauer des freien Phosphinidens wurde durch Zugabe von $\text{Mes}^*\text{-P(PMe}_3\text{)}$ nachgewiesen, wobei das unsymmetrische Diphosphen $\text{Mes}^*\text{P=P}^{\text{Mes}^*}\text{Ter}$ gebildet wurde.



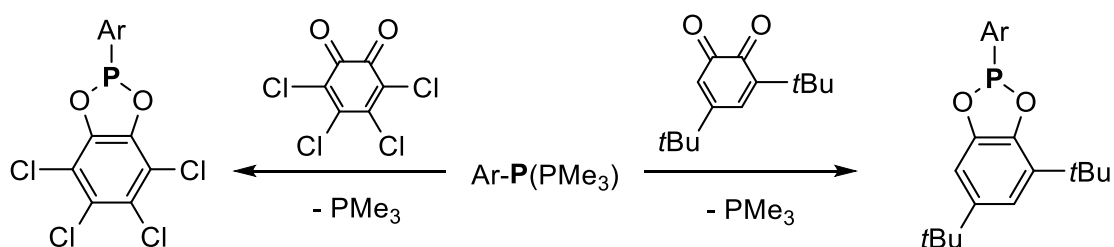
Schema 20. Drei verschiedene Ergebnisse der Bestrahlung von $\text{Ar-P(PMe}_3\text{)}$, die zur intermediären Bildung von freien Phosphiniden führt.

Später wurde festgestellt, dass das Mischen von Mes^*PCl_2 und $\text{Mes}^*\text{Ter-P(PMe}_3\text{)}$ bei Raumtemperatur in C_6D_6 zu einem raschen Gleichgewicht führt. Es wird eine Mischung aus $\text{Mes}^*\text{-P(PMe}_3\text{)}$, $\text{Mes}^*\text{TerPCl}_2$ und Mes^*PCl_2 erhalten, wobei eine Gleichgewichtskonstante $K \geq 190$ mit Hilfe von $^1\text{H-NMR}$ -Spektroskopie abgeschätzt wurde.^[93] Beim Testen verschiedener Kombinationen von Dichlorphosphanen und Phospha-Wittig-Reagenzien wurde festgestellt, dass Verbindungen mit einer Mes^* -Gruppe die größte Tendenz haben, ihre Chloratome zu übertragen, wohingegen bei ähnlichen Gruppen K nahe bei 1 liegt. Die Zugabe von 2 Äq. PMe_3 zu Mischungen von ArPCl_2 und $\text{Ar}'\text{-P(PMe}_3\text{)}$ führte zu einer schnellen Gleichgewichtseinstellung, ohne die endgültige Gleichgewichtskonstante zu beeinflussen, was PMe_3 zu einem Katalysator für diesen Austausch macht. Bei der Verwendung von $n\text{Bu}_3\text{PCl}_2$ wurde eine effiziente Katalyse festgestellt, und der in Schema 21 dargestellte katalytische Zyklus wurde für den Chloratom-Transfer vorgeschlagen.



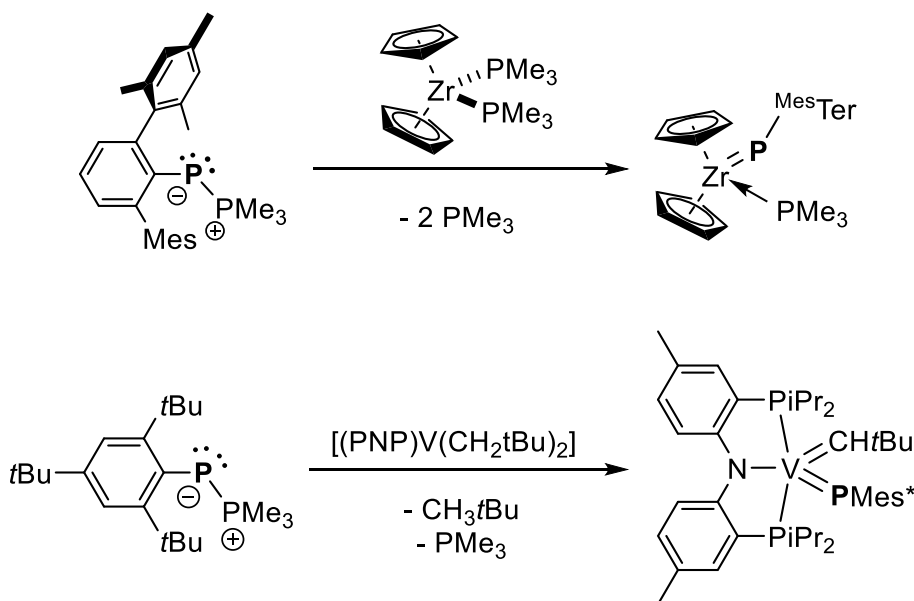
Schema 21. Ein ungewöhnlicher Chloratom-Austausch-Prozess zwischen ArPCl_2 und $\text{Ar}'\text{-P}(\text{PMe}_3)$.

Die Reaktion von $\text{Ar-P}(\text{PMe}_3)$ mit Aldehyden bietet einen effizienten Zugang zu Phosphaalkenen, während Ketone nicht umgesetzt werden können.^[61] Protasiewicz *et al.* postulierten, dass die $\text{C}=\text{O}$ -Gruppen in *o*-Chinonen reaktiver sind und in einer Phospha-Wittig-Reaktion 1,2-Diphosphaalkene erhalten werden sollten. Die Reaktion von $\text{Ar-P}(\text{PMe}_3)$ ($\text{Ar} = \text{Mes}^*$, Mes^*Ter) mit Tetrachloro- oder 3,5-Di-*tert*-butyl-*o*-benzochinon ergab nur freies PMe_3 und ein Verhältnis von Chinon zu Ar-P von 1:1. Es stellte sich heraus, dass das Ar-P -Fragment oxidativ addiert, um die entsprechenden 1,3,2-Dioxaphospholane in ausgezeichneten Ausbeuten unter Verwendung von 3,5-Di-*tert*-butyl-*o*-benzochinon (Schema 22, rechts) und in geringen Ausbeuten unter Verwendung von Tetrachlor-*o*-benzochinon (Schema 22, links) zu erhalten.^[94]



Schema 22. Oxidative Additionen von Phosphiniden-Fragmenten an *ortho*-Chinone, die 1,3,2-Dioxaphospholan-Derivate ergeben.

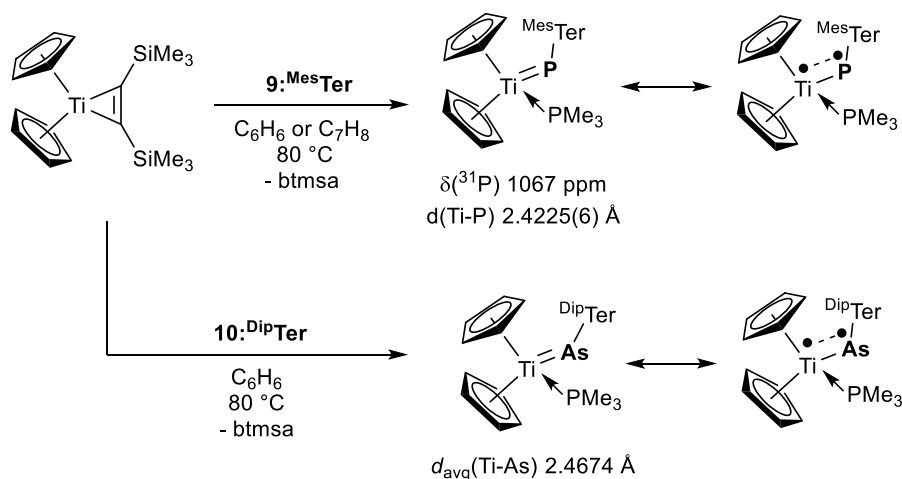
Darüber hinaus konnte gezeigt werden, dass die Phosphiniden-Einheit auf Übergangsmetall-Fragmente übertragen werden kann. Die Kombination des $\text{Zr}(\text{II})$ -Vorstufenkomplexes $[\text{Cp}_2\text{Zr}(\text{PMe}_3)_2]$ und $\mathbf{9}:\text{Mes}^*\text{Ter}$ führte zur Bildung des Zirconocen-Phosphiniden-Komplexes $[\text{Cp}_2(\text{PMe}_3)\text{ZrP}^{\text{Mes}^*\text{Ter}}]$ mit einem charakteristischen entschirmten Phosphiniden-P-Atom mit einem ^{31}P -NMR-Signal bei 762 ppm (Schema 23, oben). Außerdem wurde der Vanadium-Vorstufenkomplex $[(\text{PNP})\text{V}(\text{CH}_2t\text{Bu})_2]$ ($\text{PNP} = \text{N}[2\text{-P}(\text{CHMe}_2)_2\text{-4-Methylphenyl}]_2$) mit $\mathbf{9}:\text{Mes}^*$ umgesetzt und bei 50 °C für 12 h gerührt, was zur Bildung des zu diesem Zeitpunkt ersten Vanadium(V)-Phosphinidenkomplexes $[(\text{PNP})\text{V}=\text{PMes}^*(\text{CH}t\text{Bu})]$ zusammen mit PMe_3 und $\text{H}_3\text{C}t\text{Bu}$ führte (Schema 23, unten).^[95]



Schema 23. Phospha-Wittig-Reagenzien als Phosphinidenquellen für die Synthese von terminalen Phosphiniden-Komplexen des Zirconiums und Vanadiums.

Im Rahmen dieser Arbeit wurde 9^{MesTer} mit dem Titanocen-Äquivalent $\text{Cp}_2\text{Ti}(\text{btmsa})$ ($\text{btmsa} = \text{C}_2(\text{SiMe}_3)_2$) umgesetzt und das Gemisch auf $80\text{ }^\circ\text{C}$ erhitzt, wobei eine neue Spezies mit einem signifikant entschirmten P-Atom ($\delta(^{31}\text{P}) = 1068\text{ ppm}$) erhalten wurde. SC-XRD-Experimente zeigten die Bildung des ersten endständigen Titanocen-Phosphiniden-Komplexes $[\text{Cp}_2(\text{PMe}_3)\text{TiP}^{\text{MesTer}}]$.^[68] Theoretische Untersuchungen legen nahe, dass dieser Komplex einen signifikanten Singulett-Biradikalcharakter aufweist und daher am besten durch zwei Resonanzen zwischen einer klassischen $\text{Ti}=\text{P}$ -Doppelbindung und antiferromagnetisch gekoppelten Elektronen an Ti und P beschrieben wird (Schema 24, oben). Mit dem Arsa-Wittig-Reagenz $\text{DipTer}-\text{As}(\text{PMe}_3)$ konnte der analoge terminale Titanocen-Arsiniden-Komplex $[\text{Cp}_2(\text{PMe}_3)\text{TiAs}^{\text{DipTer}}]$ erfolgreich synthetisiert werden (Schema 24, unten), wobei ein formaler Arsiniden-Transfer mit 10^{DipTer} realisiert wurde. Auch diese Spezies weist einen signifikanten Singulett-Biradikalcharakter auf.

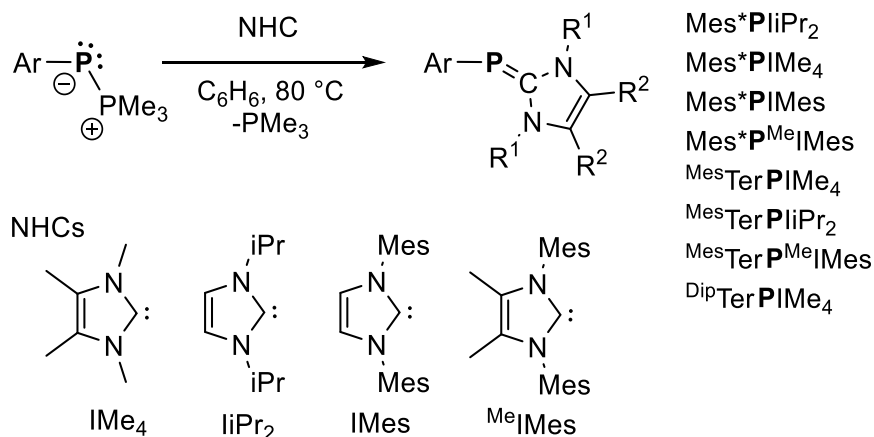
Wie bereits aus der für $[\text{P}^{\text{Dip}}]\text{P}(\text{PMe}_3)$ beschriebenen Reaktivität ersichtlich war, sollte die Zugabe von stärkeren Lewis-Basen zu **9** zu einem leichten Austausch von PMe_3 gegen die jeweilige Lewis-Base führen. Diese Möglichkeit wurde im Rahmen dieser Arbeit genauer untersucht. Obwohl Reaktionen zwischen einer Vielzahl von NHCs ($\text{NHC} = \text{IMe}_4, \text{IiPr}_2, \text{IMes}, \text{Me}^e\text{IMes}$) und 9^{Ar} ($\text{Ar} = \text{Mes}^*, \text{MesTer}, \text{DipTer}$) in C_6D_6 -Lösung bei Raumtemperatur nicht beobachtet wurden, erfolgte die selektive Umwandlung in die entsprechenden NHC-Phosphiniden-Addukte ($\text{NHC}=\text{PAr}$) bei längerem Erhitzen auf $80\text{ }^\circ\text{C}$ oder $105\text{ }^\circ\text{C}$ ($\text{Ar} = \text{Mes}^*$; $\text{NHC} = \text{IMes}, \text{Me}^e\text{IMes}$) (Schema 25).^[64]



Schema 24. Synthese terminaler Titanocen-Phosphiniden und -Arsiniden-Komplexe.^[68]

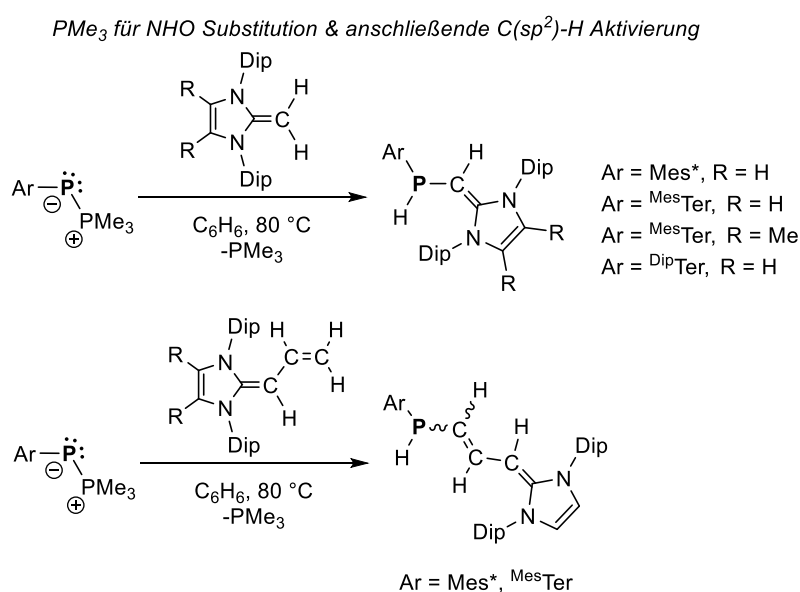
DFT-Studien ergaben einen T-förmigen Übergangszustand mit einer Energiebarriere von 99.5 kJ·mol⁻¹ für die Reaktion von Mes*-P(PMe₃) mit IiPr₂ und einen insgesamt exergonischen Prozess ($\Delta_R G^\circ = -74.8$ kJ·mol⁻¹) für die Bildung von (IiPr₂)=PMes* unter Freisetzung von PMe₃. Die Untersuchung der intrinsischen Bindungsorbitale (IBOs) entlang der Reaktionskoordinate zeigte, dass das IBO, welches das LP am NHC repräsentiert, sich in das C-P σ -Bindungsorbital in (IiPr₂)=PMes* umwandelt, und das IBO der P-P-Bindung in Mes*-P(PMe₃) in das LP des PMe₃ umgewandelt wird. Dieses Bild stimmt mit einem anfänglichen nukleophilen Angriff des NHC am σ^* -Orbital der P-P-Bindung überein, so dass eine Beschreibung als S_N2-artige Substitution gerechtfertigt ist. Der Umfang dieser Substitutionsreaktion ist in Schema 25 skizziert und ergänzt bereits etablierte Syntheserouten zu NHC-Phosphiniden-Addukten,^[96] die vielseitige Liganden in der ÜM-Chemie darstellen.^[97]

PMe₃ / NHC Substitution



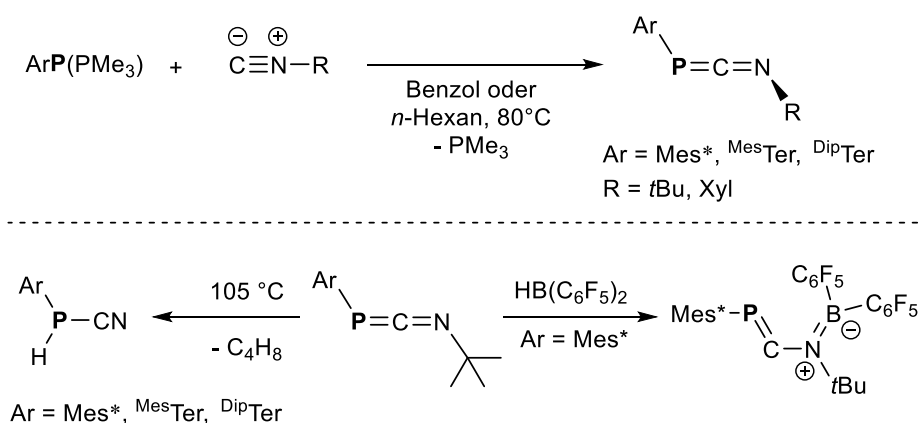
Schema 25. Synthese verschiedener NHC-Phosphiniden-Addukte ausgehend von **9:Ar**.

N-heterocyclische Olefine (NHOs) sind elektronenreiche Alkene mit einer stark polarisierten C=C-Bindung und einer beträchtlichen Elektronendichte an der endständigen =CH₂-Einheit.^[98] Obwohl NHOs starke σ -Donoren darstellen, sind ihre π -Akzeptor-Eigenschaften im Vergleich zu den NHCs vernachlässigbar. Bei der Kombination von IDipCH₂ (IDip = (HCNDip)₂C) mit **9:Mes*** wurde im ¹H-NMR-Spektrum eine neue Spezies mit einer PH-Einheit nachgewiesen, was auf die Bildung des P-substituierten NHO IDipC(H)P(H)Mes* hinweist (Schema 26, oben). Dies wurde durch SC-XRD-Experimente bestätigt, mit einem exocyclischen C–C-Atomabstand von 1.360(2) Å.^[64] Dieser Austausch von PMe₃ gegen ein NHO, gefolgt von einer anschließenden Aktivierung der C(sp²)–H-Bindung, wurde theoretisch untersucht, und es konnte eine hohe Barriere für den anfänglichen Austausch von IDipCH₂ gegen PMe₃ (ca. 163 kJ·mol⁻¹) gefunden werden. Das NHO-Phosphiniden-Addukt stellt ein energiereiches Zwischenprodukt dar, das in einem zweiten Schritt mit einer niedrigeren Barriere eine H-Verschiebung von IDipCH₂ zu P-Mes* eingeht, wodurch in einer insgesamt exergonischen Reaktion die beobachteten P-substituierten NHOs entstehen. Dieses Konzept wurde auf das Endiamin IDipC₃H₄ mit zwei nucleophilen Zentren am α - und γ -Kohlenstoff ausgedehnt:^[99] Die Behandlung von IDipC₃H₄ mit **9:Ar** (Ar = Mes*, ^{Mes}Ter) resultierte in Endiaminspezies des Typs IDipC₃H₃P(H)Ar, bei denen das endständige Kohlenstoffatom (γ -C-Atom) nun P-substituiert ist (Schema 26, unten). In Lösung liegen IDipC₃H₃P(H)Ar hauptsächlich als E-konfigurierte 1,3-Diene vor, während im Kristall das Z-konfigurierte Dien IDipC₃H₃P(H)Mes* beobachtet wurde. NRT-Analysen und eine Betrachtung der KS-Orbitale zeigen stark delokalisierte π -Bindungssysteme.



Schema 26. Synthese verschiedener P-substituierter NHOs und Endiamine ausgehend von **9:Ar**.

Wir haben auch gezeigt, dass PMe_3 gegen Isonitrile (CN-R) ausgetauscht werden kann und so 1,3-Phosphaazaallene erhalten werden.^[100] Die Umsetzung von **9:Ar** ($\text{Ar} = \text{Mes}^*, \text{Mes}^*\text{Ter}, \text{Dip}^*\text{Ter}$) mit den Isonitrilen $\text{CN}t\text{Bu}$ und CNXyl ($\text{Xyl} = 2,6\text{-Me}_2\text{C}_6\text{H}_3$) ergab sechs Beispiele für Spezies des Typs ArPCNR nach Erhitzen von 1:1-Gemischen auf $80\text{ }^\circ\text{C}$ für 16 h in Benzol- oder *n*-Hexan-Lösung (Schema 27, oben). Die *t*Bu-substituierten Phosphaazaallene wurden bei längerem Erhitzen auf $105\text{ }^\circ\text{C}$ unter gleichzeitiger Abspaltung von *iso*-Buten in die Cyanophosphine ArP(H)CN überführt (Schema 27, unten). Darüber hinaus wurde festgestellt, dass $\text{Mes}^*\text{PCN}t\text{Bu}$ mit Hilfe von Pier's Boran $\text{HB}(\text{C}_6\text{F}_5)_2$ über die C=N -Bindung hydroboriert werden kann, was zur Bildung des Heterobutadien-Systems $\text{Mes}^*\text{P=C(H)-N}(\text{B}(\text{C}_6\text{F}_5)_2)t\text{Bu}$ führt (Schema 27, unten).

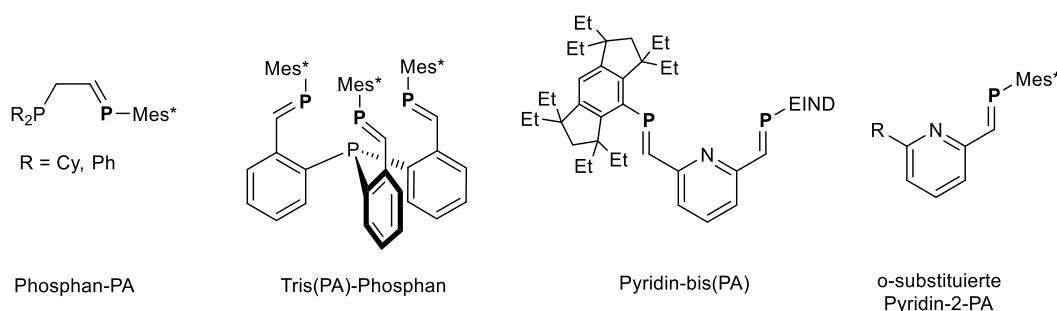


Schema 27. Synthese von 1,3-Phosphaazaallenen ausgehend von **9:Ar** (oben). Thermische Zersetzung hin zu Cyanophosphanen und Hydroborierungs-Reaktionen (unten).

2.2.5 Synthese von Phosphaalkenen – Die Phospha-Wittig-Reaktion

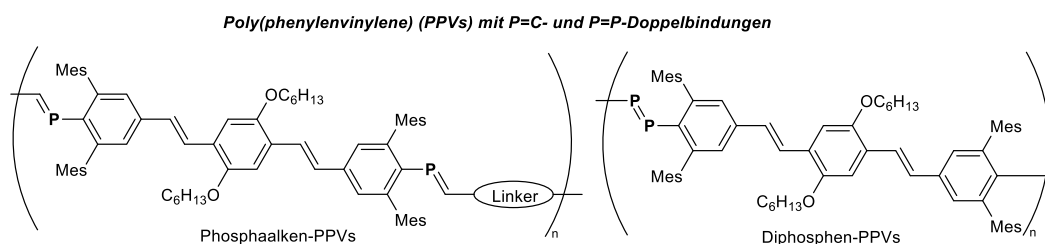
Bereits Marinetti und Mathey führten den Begriff "Phospha-Wittig-Reaktion" für die Reaktion von $(\text{RO})_2\text{P}(\text{O})\text{-P}^{(-)}[\text{W}(\text{CO})_5]\text{R}'$ mit Ketonen zu $(\text{CO})_5\text{W}$ -koordinierten Phosphaalkenen (PAs) ein.^[101] Heutzutage wird der Begriff Phospha-Wittig-Reaktion zumeist für die Umsetzung von $\text{Ar-P}(\text{PMe}_3)$ mit Aldehyden verwendet.^[61] Unabhängig der elektronischen Situation am Aldehyden ergibt die Umsetzung mit $\text{Ar-P}(\text{PMe}_3)$ die Phosphaalkene in zumeist exzellenten Ausbeuten, wobei selektiv die *E*-Phosphaalkene gebildet werden und O=PMe_3 als Nebenprodukt anfällt. Diese Route zu Phosphaalkenen stellt eine signifikante Verbesserung gegenüber der Phospha-Peterson-Route dar. So wurde $\text{Mes}^*\text{P=C(H)Ph}$ ausgehend von Mes^*PH_2 in einer sequentiellen Reaktion zunächst mit *n*-BuLi, dann mit $\text{Me}_2t\text{BuSiCl}$ und dann wiederum mit *n*-BuLi und Benzaldehyd umgesetzt, wobei $\text{Mes}^*\text{P=C(H)Ph}$ nach säulenchromatografischer Aufarbeitung in 80% Ausbeute erhalten werden konnte.^[102] Der

Vorteil der Phospha-Wittig-Reaktion ist der direkte Einsatz des leicht zugänglichen Mes^*PCl_2 , welches direkt mit Zn und Benzaldehyd in Toluol, Benzol oder THF zusammengegeben werden kann. $\text{Mes}^*\text{P}=\text{C}(\text{H})\text{Ph}$ wird dann durch das Zutropfen von PMe_3 mit einer Ausbeute von 87% erhalten. Zumeist wird die Phospha-Wittig-Reaktion beim Design neuartiger PA-basierter Ligandensysteme eingesetzt (Schema 28).^[103] Beim Anwenden der Phospha-Wittig-Methodik ist darauf zu achten, dass OPMe_3 aus dem Produkt entfernt werden muss. Dies gelingt durch Extraktion des Phosphaalkens mit aliphatischen Lösemitteln^[103a] oder durch eine Sublimation, wenn das Produkt thermisch stabil ist.



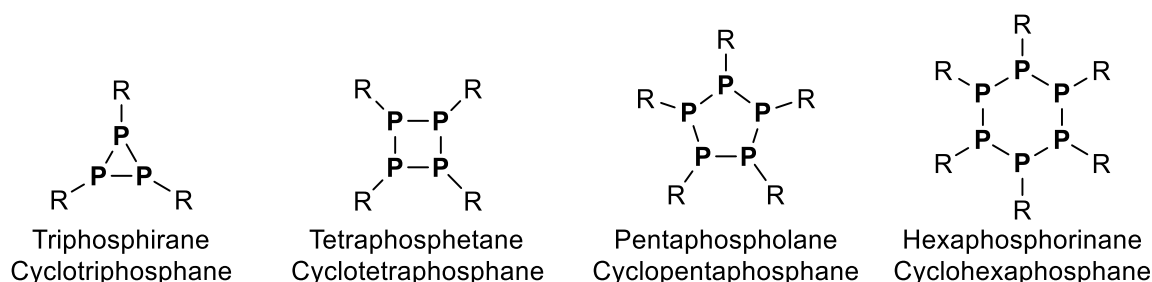
Schema 28. Verschiedene Ligandensysteme, die in einer Phospha-Wittig-Reaktion erhalten wurden.

Darüber hinaus wurde gezeigt, dass das bifunktionelle Phospha-Wittig-Material *E,E*-1,4-Bis-($\text{Me}_3\text{P}=\text{P}$)-(3,5-Dimesitylstyryl)-2,5-di-*n*-hexyloxybenzol, in der Reaktion mit konjugierten Aldehyden konjugierte Poly(phenylenvinyl)-Polymere (PPVs) mit $\text{P}=\text{C}$ -Einheiten in der Hauptkette bildet (Schema 29, links).^[104] In der Abwesenheit von Aldehyden werden durch Photo- oder Thermolyse Diphosphen-haltige PPVs gebildet (Schema 29, rechts). Die Phospha-Wittig-Methodik kann nur angewendet werden, wenn das intermediär gebildete Phosphanylidenphosphoran stabil ist. Bei dem Versuch anstatt Mes^*PCl_2 TipPCl_2 in der Phospha-Wittig-Reaktion einzusetzen entsteht nicht wie erwartet ein Phosphaalken, sondern es wird viel mehr das Cyclotriphosphan (Tip-P)₃ gebildet,^[77] welches auf die intermediäre Bildung von $\text{Tip-P}(\text{PMe}_3)$ hindeutet. Jedoch ist der thermische Zerfall, ähnlich wie bei $\text{F}_3\text{C-P}(\text{PMe}_3)$, schneller als die Reaktion mit den Aldehyden.



Schema 29. Phosphaalken- (links) und Diphosphen-basierte (rechts) Poly(phenylenvinylene).

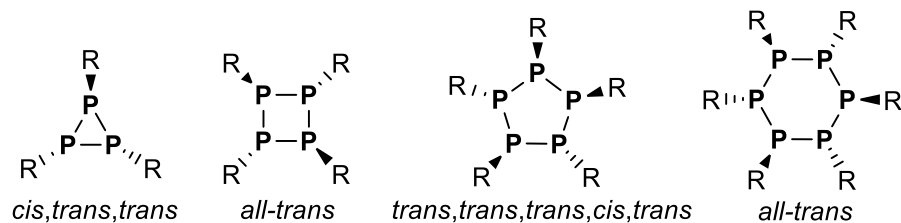
2.3 Phosphiniden-Oligomere – Cyclooligophosphane



Schema 30. Generelle Nomenklatur von Cyclooligophosphanen des Typs $(R-P)_n$ ($n = 3, 4, 5, 6$).

1877 berichteten Köhler und Michaelis über die Reaktion von $PhPH_2$ mit $PhPCl_2$ unter einem Strom von trockenem Wasserstoff, wobei ein hellgelbes Pulver entstand, das sie aufgrund der Elementaranalyse als das sogenannte Phosphobenzol $PhP=PPh$ identifizierten.^[105] Fast 100 Jahre später im Jahr 1964 bestimmten Daly und Maier die Kristallstruktur des vermeintlichen Phosphobenzols als das Cyclophosphan $(PPh)_5$ (**16**).^[106] Das erste echte Phosphabenzol-Derivat $(Mes^*-P)_2$ wurde dann 1981 von Yoshifuji *et al.* durch die Reduktion von Mes^*PCl_2 mit Mg als luftstabiler, orangefarbener Feststoff dargestellt.^[107] Die anfänglichen Kontroversen um monocyclische Phosphane wurden 1969 von Haiduc zusammengefasst und bis 1993 wurde die Chemie der cyclischen Oligophosphane mehrfach in Übersichtsartikeln diskutiert.^[108] An dieser Stelle sollen die jüngsten Erkenntnisse über die Synthesewege zu homoleptischen monocyclischen Phosphanen des Typs $(R-P)_n$ ($n = 3, 4, 5, 6$) und deren vielfältige Reaktivität beschrieben werden. Die Schreibweise $(R-P)_n$ soll dabei andeuten, dass Cyclophosphane als Oligomere der korrespondierenden Phosphinidene aufgefasst werden können. Außerdem können Cyclooligophosphane als isolobale Verwandte der Cycloalkane aufgefasst werden. So wäre zum Beispiel das Cyclohexaphosphan $(Ph-P)_6$ ein Analogon von Cyclohexan,^[109] was durch die Sesselkonformation von $(Ph-P)_6$ verdeutlicht wird.^[110]

Monocyclische Oligophosphane $(R-P)_n$ ($n = 3, 4, 5, 6$) weisen die in Schema 30 dargestellten Strukturen auf und die akzeptierte Nomenklatur ist unter jeder Struktur angegeben. Im Folgenden wird die Terminologie Cyclotriphosphan usw. verwendet. Die Ringgröße von Cyclophosphanen hängt von der Größe der P-Substituenten ab. Je nach den angewandten Synthesestrategien können unter kinetischer Kontrolle verschiedene Ringgrößen isoliert werden. Cyclophosphane $(R-P)_n$ besitzen n freie Elektronenpaare am Phosphor, was sie zu einer interessanten Liganden-Klasse mit mehreren Donorstellen und verschiedenen Überbrückungsmöglichkeiten macht.

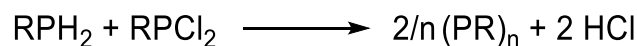


Schema 31. Konfiguration der R-Substituenten in $(\text{R-P})_n$ in Bezug auf den zentralen P_n -Ring.

In Cyclophosphanen sind die Substituenten am zentralen Ring in der Regel so angeordnet, dass diesen ein Maximum an Platz zur Verfügung steht (Schema 31). Bei Cyclotriphosphanen $(\text{R-P})_3$ wird eine charakteristische *cis,trans,trans*-Anordnung beobachtet, die im ^{31}P -NMR-Spektrum ein charakteristisches AB_2 -Spinsystem ergibt und die Reaktivität wird dominiert von Insertionsreaktionen in die P-P -Bindung mit beiden Substituenten auf der gleichen Seite der Ringebene. Bei Cyclotetraphosphanen sind alle Substituenten in *trans*-Stellung angeordnet, was zu einem Singulett im ^{31}P -NMR-Spektrum und weniger abgeschirmten P-Atomen im Vergleich zu den entsprechenden Cyclotriphosphanen führt. Cyclopentaphosphane weisen eine Konformation auf, in der das Maximum an *trans*-Orientierungen realisiert ist, was zu komplexen Multipllett-Signalen im ^{31}P -NMR-Spektrum führt. Cyclohexaphosphane sind selten, aber wie bei $(\text{R-P})_4$ ordnen sich alle Substituenten in einer *trans*-Orientierung an, was kürzlich durch die Bestimmung der Molekülstruktur von $((o\text{-Tol})\text{-P})_6$ gezeigt wurde.^[111]

2.3.1 Synthese von Cyclophosphanen

Im Allgemeinen gibt es zwei Synthesestrategien für Cyclophosphane: (1) unspezifische Protokolle, die das thermodynamisch stabilste Oligomer bevorzugen; (2) Methoden, die eine spezifische Ringgröße ergeben. Im Folgenden beschränkt sich die Diskussion auf solche Protokolle, die die Isolierung der jeweiligen Cyclophosphane in reiner Form ermöglichen. Gleichung 1:



Wie bereits beschrieben, ist die Reaktion von Dihalogen(organo)phosphanen mit primären Phosphanen ein möglicher Syntheseweg (Gleichung 1).^[105] Eine frühe Arbeit von Seichter *et al.* fasste verschiedene Ansätze zur Synthese cyclischer Oligophosphane zusammen. Dieser Artikel wird bis heute als Referenz herangezogen. So wird $(\text{Ph-P})_4$ durch die Dehydrochlorierung in Et_2O in 92 % Ausbeute erhalten. In ähnlicher Weise werden $(n\text{Pr-P})_4$, $(n\text{Bu-P})_4$ und $(\text{Cy-P})_4$ in guten isolierten Ausbeuten bei der Reaktion von RPH_2 und RPCl_2 in

Benzol bzw. Toluol erhalten.^[112] $(C_6F_5-P)_4$ lässt sich bequem aus $C_6F_5PH_2$ und $C_6F_5PCl_2$ bei 40-60 °C in Petrolether in ausgezeichneten Ausbeuten von bis zu 94 % herstellen.^[113] In Fällen, in denen die primären Phosphane RPH_2 schwierig zu handhaben sind, stellt die Reduktion der entsprechenden Dihalogenphosphane mit Metallen, Metallhydriden oder tertiären Phosphanen die bevorzugte Synthesemethode dar.

Für reduktive Ansätze werden Reduktionsmittel wie Alkalimetalle (Li, Na), Erdalkalimetalle und -verbindungen (Mg, $Mg(\text{Anthracen})(\text{thf})_3$), LiH oder PMe_3 verwendet (Tabelle 3). Bei diesen reduktiven Ansätzen ist auf die korrekten stöchiometrischen Verhältnisse zu achten, da mit überschüssigem Reduktionsmittel verwandte anionische Oligophosphanide erhalten werden können. Die Umsetzung von 10 Äq. Na oder K mit vier Äq. PCl_2 in siedendem THF ergab die entsprechenden Alkalimetall-Tetraphosphan-1,4-diide $[M_2(\text{thf})_n(P_4R_4)]$ ($M = \text{Na, K}$; $R = t\text{Bu, Ph, Mes}$; $n = 4-6$).^[114] Diese Oligophosphanid-Dianionen sind eine weitere Klasse interessanter Phosphorbausteine,^[115] und ihre Reaktivität gegenüber kleinen Molekülen,^[116] und Übergangsmetallfragmenten wurde eingehend untersucht.^[117]

Tabelle 3: Reduktive Syntheserouten zu Cyclooligophosphanen.

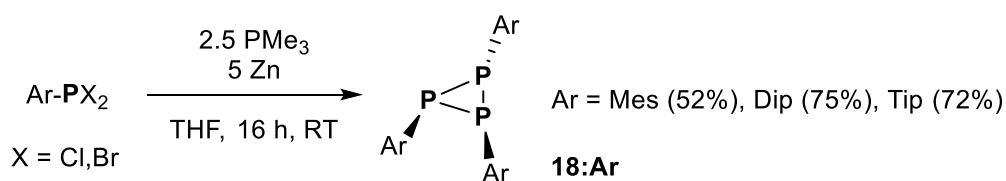
$(R-P)_n$	Edukt	Reduktionsmittel (Lösemittel)	Ausbeute [%]
$(P^t\text{Bu})_3$ (17) ^[118]	$t\text{Bu}PCl_2$	Mg (THF)	57
$(P\text{Ad})_3$ ^[119]	$\text{Ad}PCl_2$	Na (Toluol)	51
$(P\text{Mes})_3$ ^[120]	MesBr, P_4	$[Ti\{N(t\text{Bu})(3,5-C_6H_3Me_2)\}_3]$ (C_6H_6)	67
$(P(N(\text{SiMe}_3)_2))_3$ ^[121]	$(\text{Me}_3\text{Si})_2\text{N}PCl_2$	$Mg(\text{anthracene})(\text{thf})_3$ (Et_2O)	50
$(PC_6F_4-p-H)_4$ ^[122]	$(C_6F_4-p-H)PCl_2$	Mg ($\text{Et}_2\text{O}/\text{CH}_2\text{Cl}_2$)	47
	$(C_6F_4-p-H)PCl_2$	PMe_3 , Zn (CDCl_3)	99
$(P^t\text{Bu})_4$ ^[123]	$t\text{Bu}PCl_2$	Red. Na (1,4-Dioxan)	63
$(P\text{Me})_5$ ^[118]	$\text{Me}PCl_2$	LiH (Toluol)	79
$(P\text{Et})_5$ ^[124]	$\text{Et}PCl_2$	LiH (Toluol)	58
$(P\text{Ph})_5$ (16) ^[125]	$\text{Ph}PCl_2$	Aktiviertes Zn (THF)	92

Das am häufigsten verwendete Cyclotriphosphan $(t\text{Bu}-P)_3$ (**17**) kann durch die Reduktion von $t\text{Bu}PCl_2$ mit Mg-Spänen in siedendem THF hergestellt werden. Die anschließende Extraktion mit *n*-Pentan und eine Vakuumdestillation ergibt **17** als klebrigen, farblosen kristallinen Feststoff, der unter einer Argonatmosphäre bei $T < -30$ °C gelagert werden kann. Als Nebenprodukt wird $(t\text{Bu}-P)_4$ gebildet, das aus dem Rückstand sublimiert werden kann.^[118] $(t\text{Bu}-P)_4$ kann alternativ durch die Reduktion von $t\text{Bu}PCl_2$ mit Na in siedendem 1,4-Dioxan

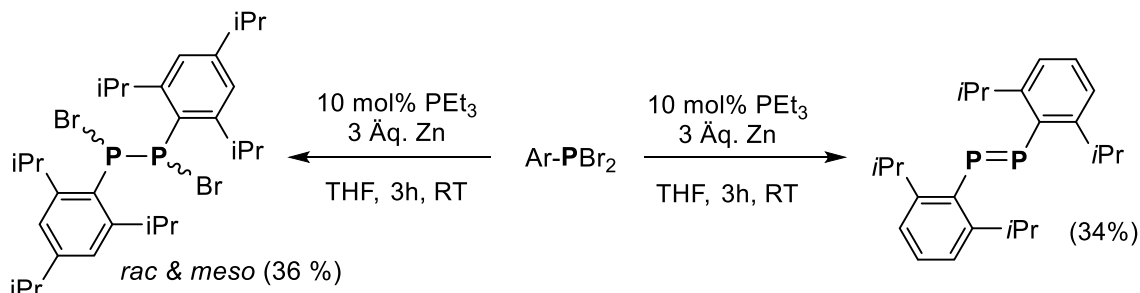
hergestellt werden.^[123] Schmutzler berichtete über die selektive Bildung von (1-Ad-P)₃ aus AdPCl₂ in siedendem Toluol nach Reduktion mit zwei Äquivalenten Natrium, als amorpher, weißer Feststoff mit einem Schmelzpunkt von ca. 250°C.^[119] Der reduktive Abbau von weißem Phosphor P₄ mit Mesityl-Radikalen (generiert aus MesBr und der Ti(III)-Spezies [Ti{N(*t*Bu)(3,5-C₆H₃Me₂)}₃],^[126] zeigte, dass nach der Extraktion mit Et₂O (Mes-P)₃ als Hauptprodukt in guter isolierter Ausbeute entsteht.^[120] (Cy-P)₃ wurde erstmals von Baudler *et al.* durch die Dehalogenierung von CyPCl₂ mit Na in 1,4-Dioxan beschrieben, allerdings vermindert eine abschließende fraktionierte Kristallisation ergiebige Ausbeuten.^[127] Burford und Mitarbeiter beschrieben später ein Protokoll, bei dem [(Cy-P)₃PCyMe]OTf in CH₂Cl₂ mit PMe₃ behandelt wird, was die Isolierung von (Cy-P)₃ in mäßiger Ausbeute, aber in hoher Reinheit ermöglicht.^[128] (*p*-HF₄C₆-P)₄ kann durch die Reduktion von (*p*-HF₄C₆)PCl₂ mit Mg in mäßiger Ausbeute erhalten werden. Durch eine Phospha-Wittig-artige Reaktion mit PMe₃ und Zn-Staub in CDCl₃ kann (*p*-HF₄C₆-P)₄ jedoch quantitativ isoliert werden.^[122]

Unsere Gruppe untersuchte die Möglichkeit Phospha-Wittig-Reagenzien mit sterisch weniger anspruchsvollen Aryl-Gruppen am Phosphanyliden P-Atom darzustellen. Dabei fanden wir eine Möglichkeit die Aryl-substituierten Cyclotriphosphane (Ar-P)₃ (**18:Ar**; Ar = Mes, Dip, Tip) selektiv und in sehr guten Ausbeuten zu synthetisieren. Die Reduktion der gemischten Dihalogenphosphane Ar-PX₂ (X = Cl, Br) mit einem Überschuss PMe₃ und Zinkpulver ergab nach dem Rühren über Nacht und anschließender Extraktion mit Benzol oder Et₂O (Ar = Mes) (Ar-P)₃ als farblose Feststoffe (Schema 32, oben).^[129] Dabei konnte PMe₃ als aktives Reduktionsmittel identifiziert werden, was durch die Reaktion stöchiometrischer Mengen PMe₃Cl₂^[130] in der Gegenwart von Zink in einer THF/MeCN-Mischung mit Tip-PCl₂ unter Bildung von (Tip-P)₃ belegt wurde. Dies gab einen Hinweis darauf, dass die Reduktion auch mit katalytischen Mengen PR₃ stattfinden sollte. Bei der Umsetzung von Tip-PBr₂ mit Zn-Pulver wurde keine Reaktion beobachtet. Werden jedoch 10 mol% PEt₃ als Katalysator zugegeben, so konnte die selektive Bildung des Dihalodiphosphans (TipPBr)₂ als Mischung der *meso*- und *rac*-Verbindung erhalten werden (Schema 32, unten links).^[131] Die Bildung des Triphosphans (Tip-P)₃ wurde nicht beobachtet. Überraschenderweise verläuft die Reduktion von Dip-PBr₂ mit katalytischen Mengen PEt₃ unter der selektiven Bildung des Diphosphans (Dip-P)₂, welches als gelber kristalliner Feststoff isoliert wurde (Schema 32, unten rechts). In C₆D₆-Lösung ist (Dip-P)₂ metastabil und zersetzt sich über einen Zeitraum von 71 Tagen sowohl in (Dip-P)₃ als auch in (Dip-P)₄. Die Bildung von (Dip-P)₂ ist bemerkenswert, denn Diphosphene mit kleinen Gruppen an den Phosphoratomen sind zumeist thermodynamisch instabil in Bezug auf eine Dimerisierung.

Stöchiometrische Reduktion

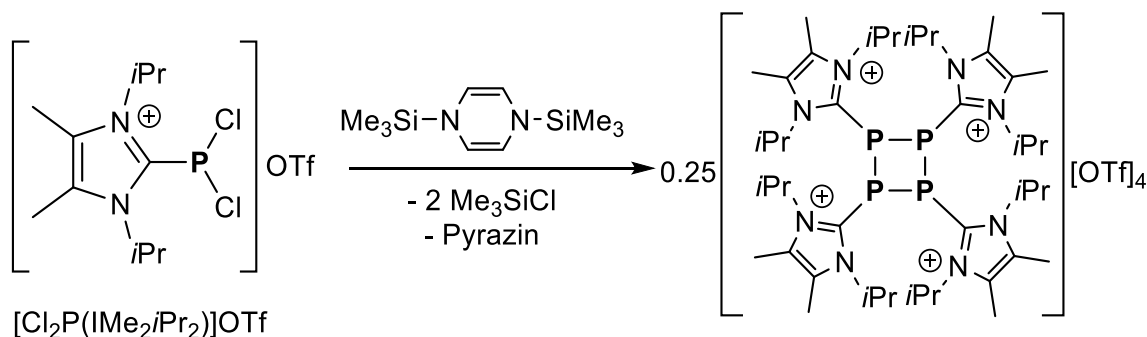


Katalytische Reduktion



Schema 32. Selektive Darstellung von Aryl-substituierten Cyclotriphoshanen (oben). PEt₃-katalysierte reduktive Kupplungsreaktion von Dibromphosphanen (unten).

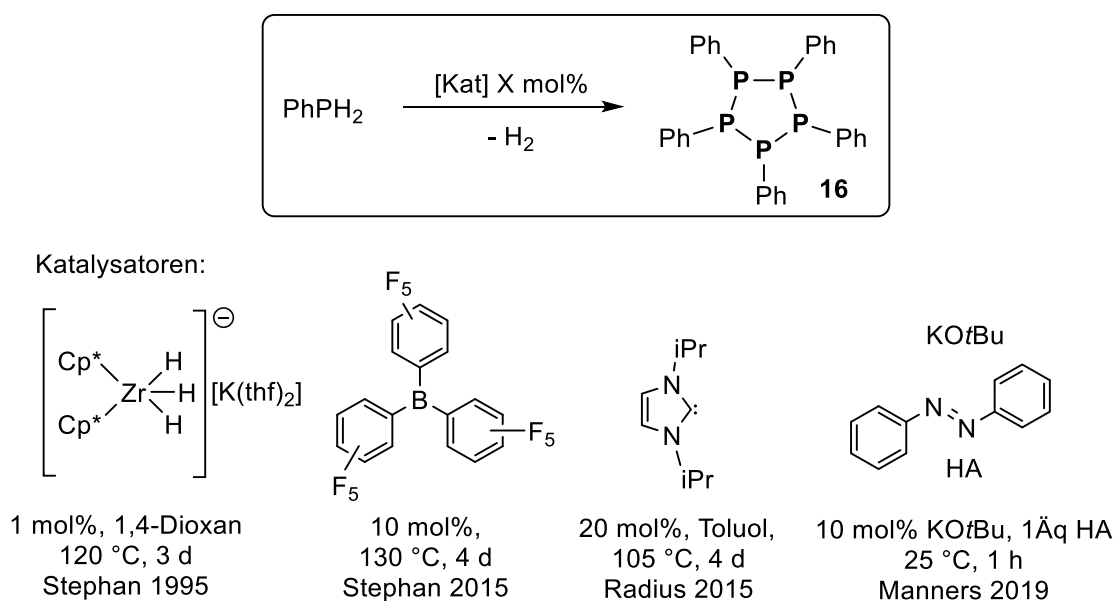
Ein synthetisch einfacher und ertragreicher Weg zu **17** wurde von Grützmaier und Mitarbeitern beschrieben, wobei PhPCl₂ mit thermisch aktiviertem Zinkpulver in THF reduziert wird und die anschließende Umkristallisation aus CH₃CN lieferte reines (Ph-P)₅ in exzellenten Ausbeuten.^[125] Dies verbesserte die bekannten Reduktionen mit Li, Na, K oder Mg, die eine breitere Produktverteilung von (PPh)_n (n = 4, 5, 6) ergeben. Die Reduktion von MePCl₂ in THF mit zwei Äquivalenten LiH ergibt nach einer Destillation (Me-P)₅ als farbloses Öl mit einem charakteristischen starken Geruch.^[118] In ähnlicher Weise lässt sich (Et-P)₅ am besten aus EtPCl₂ mit LiH als Reduktionsmittel herstellen, wobei ein 1:1-Gemisch von (PEt)_n (n = 4,5) entsteht, das durch Vakuumdestillation fraktioniert werden kann.^[124]



Schema 33. 1,4-Bis(trimethylsilyl)-1,4-dihydropyrazin wird für die Reduktion von NHC-stabilisierten Dichlorphosphenium-Ionen verwendet, um ein tetrakationisches Cyclotetraphosphan zu erhalten.

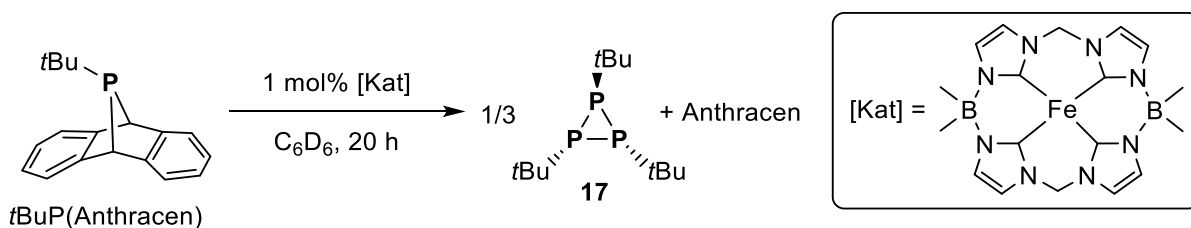
Erst kürzlich stellten Weigand und Mitarbeiter das erste kationische Cyclotetraphosphan $[L-P]_4[OTf]_4$ ($L = IMe_2iPr_2$) vor, das durch die Reduktion von $[LPCl_2]OTf$ mit 1,4-Bis(trimethylsilyl)-1,4-dihydropyrazin hergestellt wurde (Schema 33).^[132] Wird die Reaktionsmischung bei $-35\text{ }^\circ\text{C}$ bis zur beginnenden Kristallisation aufkonzentriert, werden Kristalle des kationischen Cyclotriphosphans $[L-P]_3[OTf]_3$ erhalten. Bei Raumtemperatur wandelt sich $[L-P]_3[OTf]_3$ sauber in $[L-P]_4[OTf]_4$ um, was verdeutlicht, dass das Triphosphan das kinetische, das Tetraphosphan dagegen das thermodynamische Produkt ist.

Neben dem stöchiometrischen Einsatz von Reduktionsmitteln oder der 1:1 Umsetzung von RPH_2 und $RPCl_2$, wurden auch katalytische Protokolle beschrieben. Unter Verwendung von $[Cp^*_2ZrH_3][K(thf)_2]$ (1 mol%) als Katalysator führte die Dehydrokupplung von RPH_2 ($R = Ph, Cy, Mes$) selektiv zu den entsprechenden Cyclopentaphosphanen $(R-P)_5$ (Schema 34).^[133] Mechanistische Studien unter Verwendung von $[CpTi(NP*t*Bu_3)(CH_2)_4]$ mit $PhPH_2$ haben dazu beigetragen, Metallatriphosphane in Anlehnung an $[CpTi(NP*t*Bu_3)(PPh)_3]$ als potenzielle Zwischenprodukte bei der Dehydrokupplung zu identifizieren.^[134] Stephan zeigte später die Dehydrooligomerisierung von $PhPH_2$ zu $(Ph-P)_5$ unter Verwendung von 10 Mol-% $B(C_6F_5)_3$ in Benzol bei $130\text{ }^\circ\text{C}$ (Schema 34).^[135] Manners und Mitarbeiter beschrieben die Verwendung katalytischer Mengen von $KOtBu$ (10 mol%) in Gegenwart stöchiometrischer Mengen von Azobenzol als Wasserstoffakzeptor (HA) zur Dehydrokupplung primärer und sekundärer Phosphane.^[136]



Schema 34. Katalytische Dehydrokupplung von $PhPH_2$. Die Katalysatoren sind zusammen mit den Reaktionsbedingungen dargestellt.

Radius und Mitarbeiter berichteten über die NHC-vermittelte Dehydrokupplung der primären Phosphine (*p*-Tol)PH₂ und PhPH₂.^[111] Die Kombination von PhPH₂ mit IiPr₂ im Verhältnis 5:1 in Toluol und Erhitzen auf 105 °C für 4 Tage lieferte **16** in 36 % isolierter Ausbeute, während (*p*-Tol-P)₆ unter ähnlichen Bedingungen in 20 % Ausbeute erhalten wurde (Schema 34). Wird PhPH₂ mit IiPr₂ in einem exakten Verhältnis von 1:2 umgesetzt, erhält man das NHC-Phosphiniden-Addukt PhP=IiPr₂ in quantitativer Weise mit H₂IiPr₂ als Nebenprodukt.



Schema 35. Eisen(II)-katalysierte Phosphinidentrimerisierung ausgehend von *t*BuP(Anthracen).

Erst kürzlich verwendeten Jenkins und Mitarbeiter einen dianionischen Tetra-NHC-Makrozyklus, um einen quadratisch planaren Fe(II)-Komplex zu erhalten, der den Phosphiniden-Transfer von *t*BuP(Anthracen) unter Freisetzung von Anthracen katalysiert und **17** als einziges Produkt in quantitativer Ausbeute liefert (Schema 35).^[137]

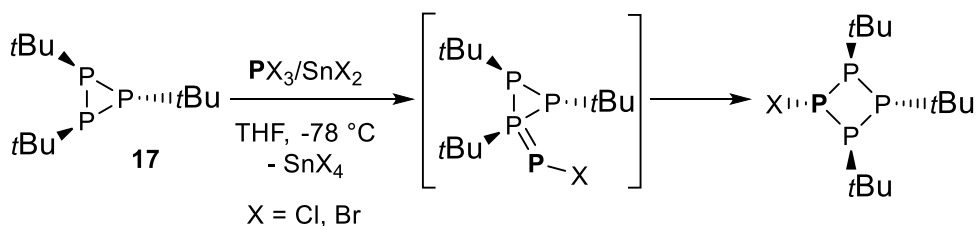
Zusammenfassend lässt sich sagen, dass Phosphine RPH₂ geeignete Ausgangsmaterialien für die katalytische Dehydrokupplung zu Cyclooligophosphanen sind. Zukünftige Studien auf diesem Gebiet sollten sich auf ein breiteres Substratspektrum konzentrieren, da meist Aryl-substituierte Phosphine verwendet werden. Darüber hinaus wird die Entwicklung von Strategien für RPH₂, die die Verwendung von P₄ umgehen,^[15] diesen Ansatz noch attraktiver gestalten.

2.3.2 Ringerweiterungsreaktionen von Cyclotriphosphanen

Bei diesen Reaktionen handelt es sich um Ringerweiterungen, die neue Heterocyclen hervorbringen, bei denen eine der P–P-Bindungen, in der Regel diejenige zwischen den beiden äquivalenten P-Atomen, geöffnet wurde.

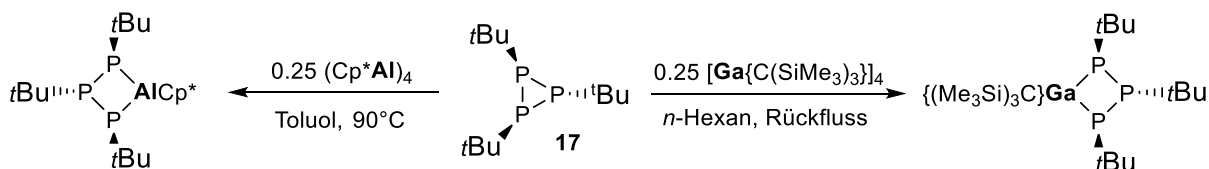
Binder und Mitarbeiter zeigten die Insertion des Halogenphosphandiyls [PCI] in (*t*Bu–P)₃.^[138] [PCI] wurde *in situ* aus einer 1:1-Mischung von PCl₃/SnCl₂ in THF bei –78 °C erzeugt, die dann langsam zu **17** gegeben wurde, wobei [(*t*Bu–P)₃PCI] als thermisch stabiler gelber Feststoff mit einem AB₂C-Spinsystem im ³¹P-NMR-Spektrum entsteht (Schema 36). Die Autoren

vermuten, dass $[(t\text{BuP})_3\text{PCl}]$ durch die anfängliche Bildung eines exocyclischen $1\lambda^5$ -Diphosphens entsteht, welches sich dann in die benachbarte P–P-Bindung einschleibt.



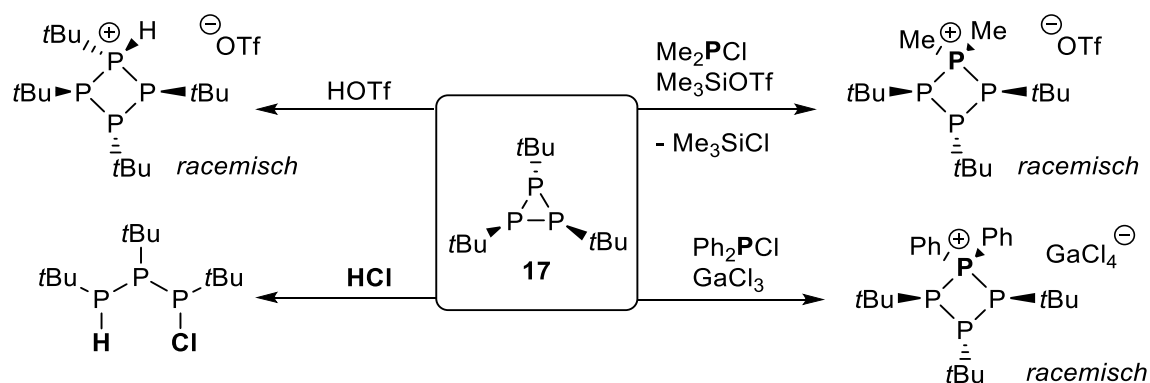
Schema 36. Insertion von $[\text{P}-\text{Cl}]$ in das Cyclotriphosphan **17**.

Eine Ringerweiterung von $(t\text{Bu}-\text{P})_3$ wurde mit den $\text{E}^{13}(\text{I})$ -Verbindungen $(\text{Al}_4\text{Cp}^*)_4$ und $\text{Ga}_4[\text{C}(\text{SiMe}_3)_3]_4$ beobachtet. Die Reaktion von **17** mit $(\text{Al}_4\text{Cp}^*)_4$ in Toluol bei $90\text{ }^\circ\text{C}$ lieferte nach Abkühlung auf $-20\text{ }^\circ\text{C}$ $[\text{Cp}^*\text{Al}(\text{P}t\text{Bu})_3]$ als gelben kristallinen Feststoff in 53% Ausbeute (Schema 37, links).^[139] In ähnlicher Weise berichteten Uhl und Benter über die Synthese von $[\{(\text{Me}_3\text{Si})_3\text{C}\}\text{Ga}(\text{P}t\text{Bu})_3]$ als roten Feststoff, der durch die Kombination von $\text{Ga}_4[\text{C}(\text{SiMe}_3)_3]_4$ mit vier Äquivalenten $(t\text{Bu}-\text{P})_3$ in siedendem *n*-Hexan erhalten wird (Schema 37, rechts).^[140] Sowohl $[\text{Cp}^*\text{Al}(\text{P}t\text{Bu})_3]$ als auch $[\{(\text{Me}_3\text{Si})_3\text{C}\}\text{Ga}(\text{P}t\text{Bu})_3]$ zeigen ein typisches A_2X -Spinsystem im ^{31}P -NMR-Spektrum, was eindeutig die Insertion von $\text{E}^{13}(\text{I})$ in die *cis,cis* P–P-Bindung von **17** anzeigt. Das Al-Atom in $[\text{Cp}^*\text{Al}(\text{P}t\text{Bu})_3]$ ist planar mit einem η^5 -koordinierten Cp^* -Liganden. Der GaP_3 -Ring ist über die transannularen P-Atome minimal gefaltet (15.6°).



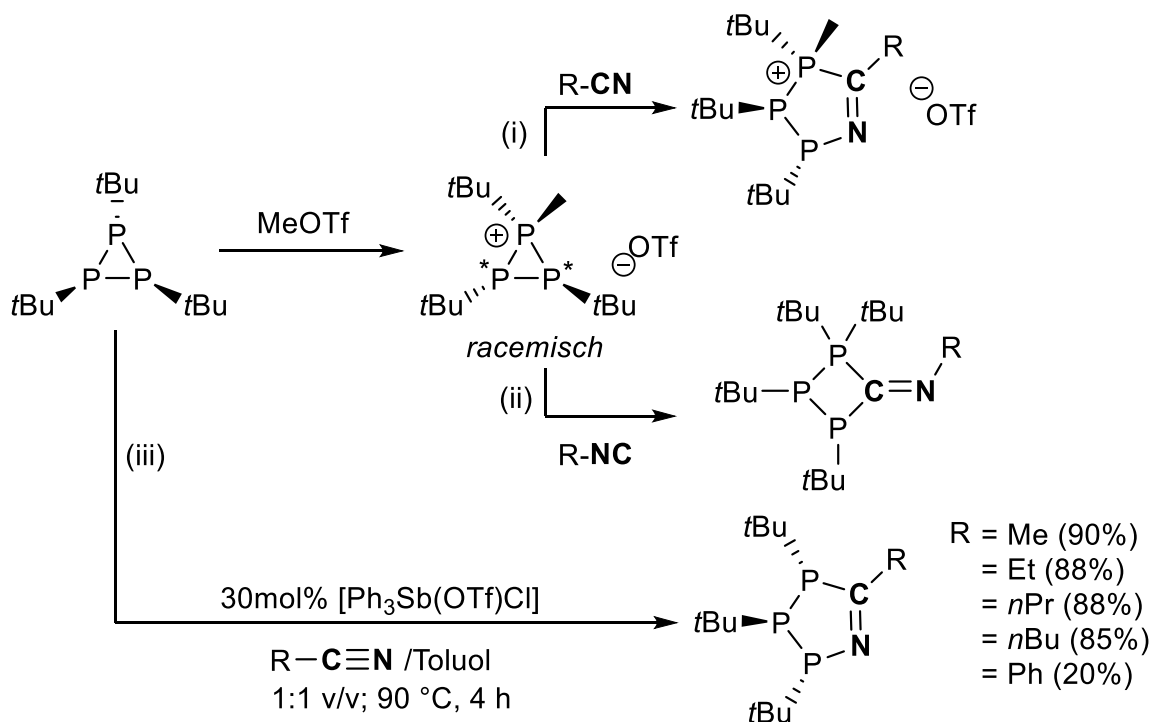
Schema 37. Insertionen von $\text{E}^{13}(\text{I})$ -Verbindungen in das Cyclotriphosphan $(t\text{Bu}-\text{P})_3$.

Die selektive Insertion des Phospheniumions $[\text{Me}_2\text{P}]^+$, erzeugt aus Me_2PCl und Me_3SiOTf , in die *cis,cis*-P–P-Bindung von $(t\text{Bu}-\text{P})_3$ wurde erstmals von Burford *et al.* beschrieben (Schema 38, oben rechts).^[128] Die Addition von HOTf an **17** führt zu einer quantitativen Ringerweiterung und liefert $[\text{HP}t\text{Bu}(\text{P}t\text{Bu})_3]\text{OTf}$ als racemisches Gemisch (Schema 38, oben links), während mit HCl eine Ringöffnung zum linearen $t\text{BuP}(\text{H})-\text{P}t\text{Bu}-\text{P}(\text{Cl})t\text{Bu}$ beobachtet wurde (Schema 38, unten links). Unter Verwendung eines Gemischs aus $\text{Ph}_2\text{PCl}/\text{GaCl}_3$ als Phospheniumionen-Äquivalent wurde über die Insertion in $(t\text{Bu}-\text{P})_3$ und die Bildung des Tetrachlorogallatsalzes $[\text{Ph}_2\text{P}(\text{P}t\text{Bu})_3][\text{GaCl}_4]$ berichtet (Schema 38, unten rechts).^[141]



Schema 38. Ringerweiterung von **17** mit HOTf, während die Behandlung mit HCl zu einer Ring-geöffneten Spezies führt. Phospheniumionen fügen sich in den dreigliedrigen Ring ein und ergeben racemische Mischungen der Ring-erweiterten kationischen viergliedrigen Ringsysteme.

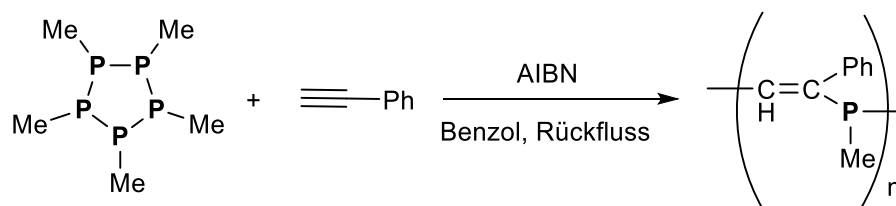
$(t\text{Bu-P})_3$ widersteht wie auch dreigliedrige Kohlenstoffringe nukleophilen, elektrophilen und dipolaren Ringöffnungsreaktionen. Die anfängliche elektrophile Aktivierung von **17** mit MeOTf führt aber zu einer starken Polarisierung der P–P-Bindungen in Richtung des quartären P-Atoms und ermöglicht eine maskierte dipolare Reaktivität wie sie für *Push-Pull*-substituierte Cyclopropane bekannt ist.^[128, 142] Durch solch eine elektrophile Aktivierung kann das eher unreaktive **17** weitere Umwandlungen eingehen. Als Beispiel soll die Reaktivität gegenüber Nitrilen herangezogen werden. Die Reaktion von $[\text{MePtBu}(\text{PtBu})_2]\text{OTf}$ mit verschiedenen Nitrilen ergab kationische P_3CN -Heterocyclen, die formalen [3+2]-Cycloadditions-Produkte (Schema 39, Reaktion i). Mit Isonitrilen wurden kationische P_3C -Ringe erhalten, die durch die Insertion in eine der aktivierten P–P-Bindungen gebildet wurden (Schema 39, Reaktion ii).^[142] Manners und Mitarbeiter zeigten darüber hinaus, dass neutrale Azatriphospholene zugänglich sind, wenn $(t\text{Bu-P})_3$ mit einem Äquivalent HOTf in reinen RCN-Lösungen behandelt und anschließend mit NEt_3 deprotoniert wird.^[143] Die Verwendung von 30 mol% $\text{Ph}_3\text{Sb}(\text{OTf})\text{Cl}$ als Lewis-Säure-Katalysator in einer 1:1 Volumen-Mischung von R-CN/Toluol ermöglichte die katalytische Bildung einer Vielzahl von Azatriphospholenen des Typs $[(\text{PtBu})_3\text{NCR}]$ in Ausbeuten von bis zu 90% für R = Me (Schema 39, iii). Kontrollexperimente mit isoliertem $[\text{Me-C}\equiv\text{N-Me}]\text{OTf}$ oder methyliertem $(\text{PtBu})_3$ zeigten, dass die dipolare Addition sowohl durch die elektrophile Aktivierung des Cyclotriphosphans als auch des Nitrils initiiert werden kann.



Schema 39. Elektrophile Addition von MeOTf an $(t\text{Bu-P})_3$ und anschließende Ringerweiterung (i) mit Nitrilen R-CN ($\text{R} = \text{Me}, \text{Et}, i\text{Pr}, t\text{Bu}$); (ii) Isonitrilen R-NC ($\text{R} = i\text{Pr}, 2,6\text{-Me}_2\text{Ph}, \text{C}_5\text{H}_{11}$) und (iii) Lewis-Säure-katalysierte Ringerweiterung mit Nitrilen zu neutralen Azatriphospholenen.

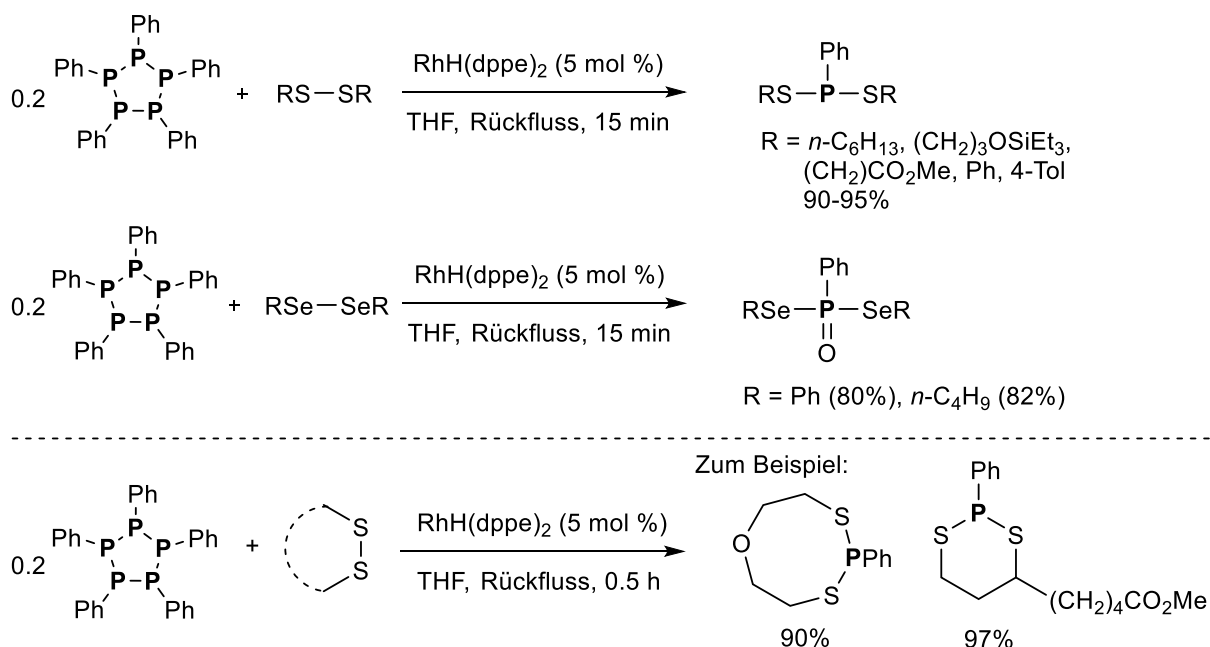
2.3.3 Fragmentierung von Cyclophosphanen

Im Jahr 2007 verwendeten Naka *et al.* $(\text{Me-P})_5$ zur Synthese von Polyvinylphosphanen, in einer Radikal-induzierten alternierenden Co-Polymerisation. Unter einer Stickstoffatmosphäre reagiert $(\text{Me-P})_5$ mit Phenylacetylen in Gegenwart von AIBN (AIBN = Azobis(isobutyronitril); 1.6 Mol-%) bei 78 °C in entgastem Benzol zum korrespondierenden Co-Polymer (Schema 40). In Abwesenheit von AIBN wurde keine Reaktion festgestellt. Im festen Zustand ist das gebildete Poly(vinylphosphan) luft- und feuchtigkeitsstabil, zersetzt sich jedoch in Lösung und zeigt eine charakteristische Fluoreszenz, welche auf einen $n\text{-}\pi^*$ -Übergang in der Hauptkette zurückzuführen ist.^[144]



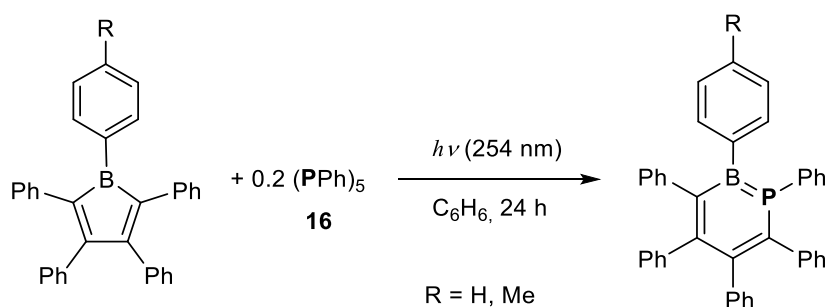
Schema 40. Radikalische, alternierende Co-Polymerisation von $(\text{Ph-P})_5$ mit Phenylacetylen.

Darüber hinaus konnte gezeigt werden, dass $(\text{Ph-P})_5$ bei der Rh-katalysierten Insertion in acyclische und cyclische Disulfide und Diselenide als PPh-Reservoir fungieren kann. Dadurch ist es möglich, lineare und heterocyclische Organophosphorverbindungen mit RS-P(Ph)-SR- und RSe-P(Ph)-SeR-Gruppen zu synthetisieren (Schema 41). Ein möglicher Mechanismus besteht darin, dass zunächst $[\text{RhH}(\text{dppe})_2]$ mit $(\text{Ph-P})_5$ zu einem $\text{LRh}(\text{PPh})_2$ -Komplex ($\text{L} = \text{dppe}$) reagiert, welcher dann oxidativ RS-SR anlagert. In einem nächsten Schritt schiebt sich Ph-P dann in eine Rh-S-Bindung ein, wobei ein Rh-Phosphiniden-Zwischenprodukt entsteht, das dann reaktiv das Produkt RS-P(Ph)-SR eliminiert. Der aktive Katalysator wird dann durch die Reaktion des intermediären Phosphinidenkomplexes mit $(\text{Ph-P})_5$ regeneriert. Diese Methodik ermöglichte die Herstellung verschiedener S-P(Ph)-S-haltiger Heterocyclen in ausgezeichneten Ausbeuten.^[145]



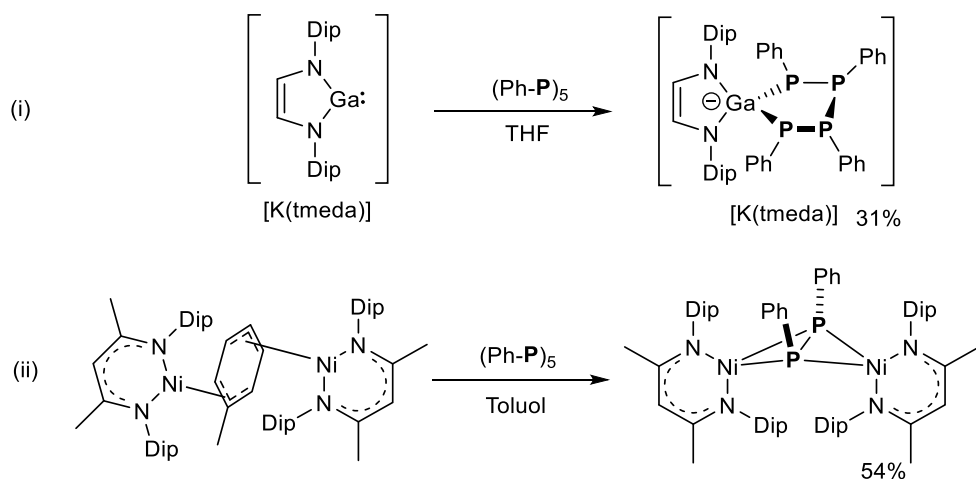
Schema 41. Rh-katalysierte Ph-P-Insertion in verschiedene Disulfide und Diselenide.

Martin *et al.* berichteten über die Insertion des Phenylphosphinidens Ph-P in ein Pentaphenylborol. Die Photolyse (254 nm) einer Benzollösung, die $(\text{Ph-P})_5$ und $\text{PhB}(\text{CPh})_4$ in einem Verhältnis von 1:5 enthält, ergab das erste Beispiel eines 1,2-Phosphaborins mit einer P=B-Doppelbindung im Ring (Schema 42).^[146] Die Verwendung von *p*-TolB(CPh)₄ in Kombination mit **16** ermöglichte eine eindeutige strukturelle Charakterisierung mittels SC-XRD und bestätigte einen planaren sechsgliedrigen Ring mit einer P=B-Doppelbindung [1.795(3) Å] und einem moderaten Grad an Aromatizität.



Schema 42. Insertion des Phenylphosphinidens Ph-P (gebildet aus **16**) in ein Borol.

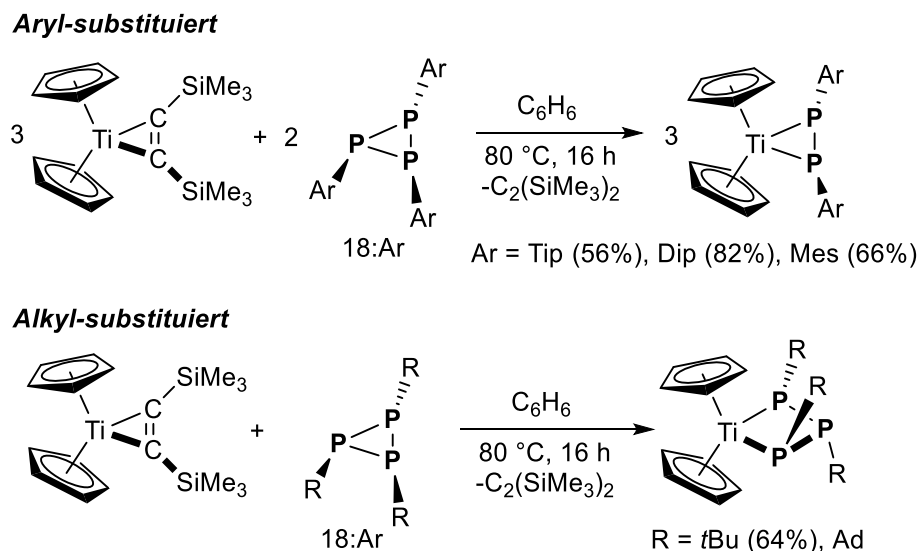
Auf der Suche nach endständigen Galliumphosphinidenen setzten Jones *et al.* den anionischen Gallium(I)-Heterocyclus $[\text{K}(\text{tmeda})][\text{Ga}\{\text{N}(\text{Dip})\text{C}(\text{H})_2\}]$ mit $(\text{Ph-P})_5$ um und stellten eine oxidative Addition einer $(\text{Ph-P})_4$ -Einheit bei gleichzeitigem Verlust eines Ph-P-Fragments fest (Schema 43, i).^[147] Die Ni(I)-Spezies $[(^{\text{Dip}}\text{Nacnac})\text{Ni}]_2(\mu\text{-}\eta^3\text{-}\eta^3\text{-C}_7\text{H}_8)$ reagiert mit $(\text{Ph-P})_5$ unter Bildung des dunkelvioletten bimetallicen Komplexes $[(^{\text{Dip}}\text{Nacnac})\text{Ni}]_2(\mu^4\text{-P}_2\text{Ph}_2)$ in 54% isolierter Ausbeute (Schema 44, ii). Dieses Beispiel zeigt die Analogie zwischen der μ^4 -verbrückenden Diphosphen-Einheit und μ^4 -Acetylen-Liganden.^[148]



Schema 43. (a) Bildung einer spirocyclischen N_2GaP_4 -Verbindung ausgehend von einer anionischen Ga(I)-Quelle mit $(\text{Ph-P})_5$. (b) Ni(I)-induzierte Fragmentierung von $(\text{Ph-P})_5$ und Bildung des Komplexes $[(^{\text{Dip}}\text{Nacnac})\text{Ni}]_2(\mu^4\text{-P}_2\text{Ph}_2)$.

Wir konnten zeigen, dass die Aryl-substituierten Cyclotriphosphane **18:Ar** (Ar = Mes, Dip, Tip) mit $[\text{Cp}_2\text{Ti}(\text{btmsa})]$ in einem Stoffmengen-Verhältnis von 2:3 reagieren und die intensiv farbigen Titanocen-Diphosphen-Komplexe $[\text{Cp}_2\text{Ti}(\text{PAr})_2]$ in mäßigen bis guten isolierten Ausbeuten liefern (Schema 44).^[129] Dass terminale Phosphinidenkomplexe eine potentielle Zwischenstufe darstellen, wurde durch Verwendung einer 1:1-Mischung von $(\text{PTip})_3$ und $(\text{PDip})_3$ nachgewiesen. Wie in diesem Fall zu erwarten, wird eine Mischung der Komplexe $[\text{Cp}_2\text{Ti}(\text{PDip})_2]$, $[\text{Cp}_2\text{Ti}(\text{PTip})_2]$ und $[\text{Cp}_2\text{Ti}(\text{TipPPDip})]$ erhalten. Im Gegensatz zu den Aryl-

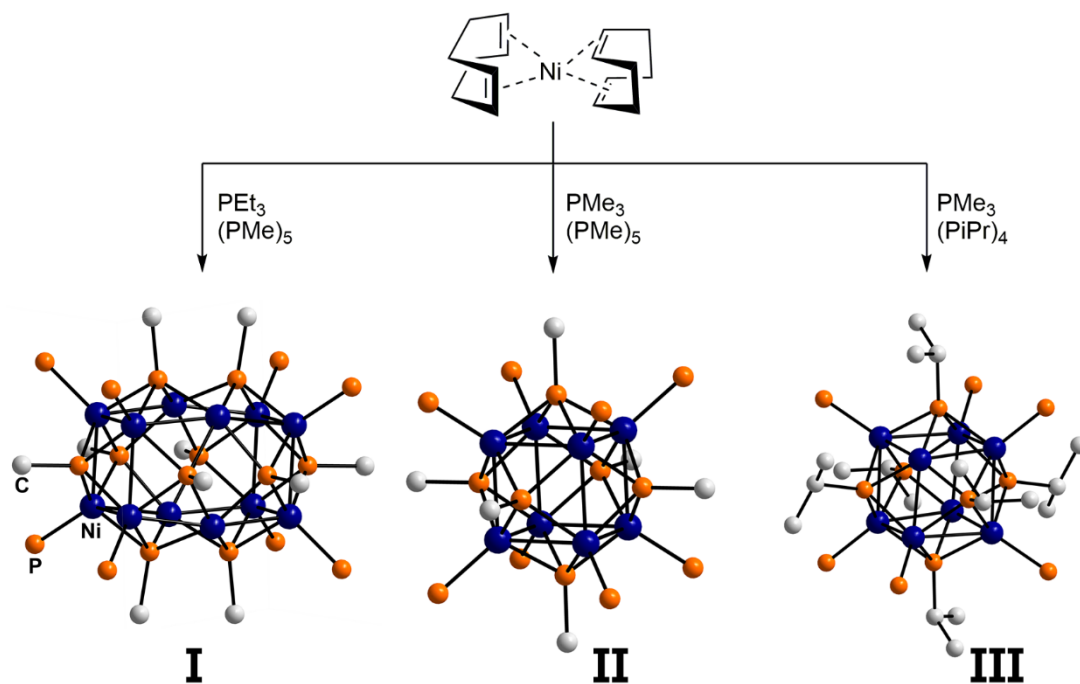
substituierten Triphosphanen konnten wir zeigen, dass Cp_2Ti in die *cis,cis*-P–P-Bindung von $(\text{PR})_3$ ($\text{R} = t\text{Bu}, \text{Ad}$) inseriert, um das entsprechende Cyclotitanatriphosphan $[\text{Cp}_2\text{Ti}(\text{PrBu})_3]$ als tiefrote Verbindung zu erhalten (Schema 44, unten).



Schema 44. Unterschiedliche Reaktivitäten von Aryl- und Alkyl-substituierten Cyclotriphosphanen gegenüber dem maskierten Titanocen-Komplex $\text{Cp}_2\text{Ti}(\text{btmsa})$.

Roy und Mitarbeiter nutzten die Isolobalbeziehung zwischen PR-Einheiten (generiert aus Cyclooligophosphanen) und Chalkogenen um molekulare Nickelphosphid-Cluster darzustellen.^[149] Die Kombination von $(\text{Me-P})_5$, PET_3 (als Kappenligand für Ni-Atome an der Clusteroberfläche) und $\text{Ni}(\text{cod})_2$ in Toluol bei Raumtemperatur resultierte in der Bildung des molekularen Clusters $[\text{Ni}_{12}(\text{PMe})_{10}(\text{PET}_3)_8]$ (Schema 45, **I**) in Form schwarzer Kristalle nach der Überschichtung mit Hexan. Der Clusterkern besteht aus zwei Ni-Würfeln, die sich eine Fläche teilen, wobei jede offene Fläche von einer μ^4 -PMe-Gruppe überbrückt wird, während die Ecken von insgesamt acht PET_3 -Liganden abgesättigt sind. Nach der Kristallisation ist dieser Cluster kaum löslich, aber die Oxidation mit $[\text{Cp}_2\text{Fe}][\text{PF}_6]$ liefert das entsprechende Clusterkation, das nun in THF löslich ist. Wird PMe_3 als Kappenligand anstelle von PET_3 eingeführt, wurde $[\text{Ni}_8(\text{PMe})_6(\text{PMe}_3)_8]$ (Schema 45, **II**) erhalten, wobei jede Fläche des würfelförmigen Nickelkerns von einer μ^4 -PMe-Gruppe überspannt wird, während alle Ecken von PMe_3 koordiniert werden. Unter Verwendung von $(i\text{Pr-P})_4$ in Kombination mit PMe_3 und $\text{Ni}(\text{cod})_2$ entsteht der Cluster $[\text{Ni}_8(\text{PiPr})_6(\text{PMe}_3)_6]$ (Schema 45, **III**) mit zwei freien Koordinationsstellen an gegenüberliegenden Ecken des verzerrten zentralen Ni_8 -Kerns. Der Bildungsmechanismus dieser molekularen NiP-Cluster ist unklar; die Autoren berichten jedoch über die Isolierung des Komplexes $[\text{Ni}_2(\text{PMe}_3)_4(\text{P}_5\text{Me}_5)_2]$ und schließen daraus, dass diese

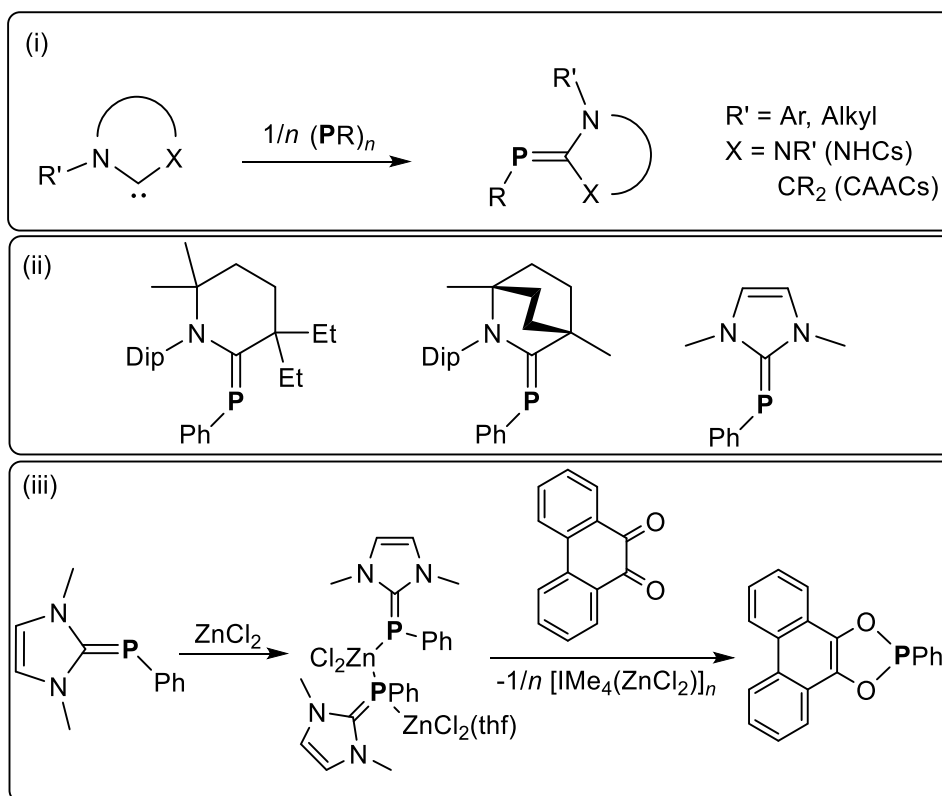
Spezies ein Zwischenprodukt der Clusterbildung sein könnte. Das Abschmelzen von $[\text{Ni}_{12}(\text{PMe})_{10}(\text{PEt}_3)_8]$ unter Vakuum in einem Quarzrohr und anschließendes Erhitzen auf $450\text{ }^\circ\text{C}$ ergibt einen schwarzen Feststoff, der als Ni_2P identifiziert wurde. Dieser zeigt elektrokatalytische Aktivität bei der Wasserstoffentwicklungsreaktion.^[150]



Schema 45. Bildung verschiedener NiP-Cluster (I, II, III) aus $\text{Ni}(\text{COD})_2$, $(\text{R-P})_n$ und Phosphanen als Kappen-Liganden. Die verbrückenden Phosphiniden-Fragmente sind mit C-Substituenten dargestellt, während die an den Ecken koordinierenden Phosphanen nur durch das P-Atom dargestellt sind.^[149]

2.3.4 Bildung von NHC-Phosphiniden-Addukten

Die Kombination von Phosphinidenen mit NHCs ergibt Carben-Phosphiniden-Addukte, die auch als elektronenreiche Phosphaalkene angesehen werden können. Diese Spezies wurden erstmals 1980 von Schmidpeter beschrieben,^[151] und diese Chemie wurde 1997 von Arduengo und Mitarbeitern weiter vorangetrieben.^[152] In den vergangenen Jahren haben sich NHC-Phosphiniden-Addukte von Laborkuriositäten zu einer wichtigen Klasse von Hauptgruppenverbindungen,^[96] und Liganden in der Übergangsmetallchemie entwickelt.^[97] 1997 berichteten Arduengo und Mitarbeiter über die Reaktion des NHC IMes (IMes = 1,3-Dimesitylimidazol-2-yliden) mit den Cyclophosphanen **16** und $(\text{F}_3\text{C-P})_4$.



Scheme 46. (i) Allgemeine Reaktivität von Cyclooligophosphanen gegenüber Carbenen. (ii) Aktuelle Beispiele für CAAC-6, BiCAAC PPh-Addukte und $\text{IMe}_2=\text{PPh}$ (von links nach rechts). (iii) Übertragung von Ph-P auf Chinone mit $\text{IMe}_2=\text{PPh}$ in Gegenwart von ZnCl_2 .

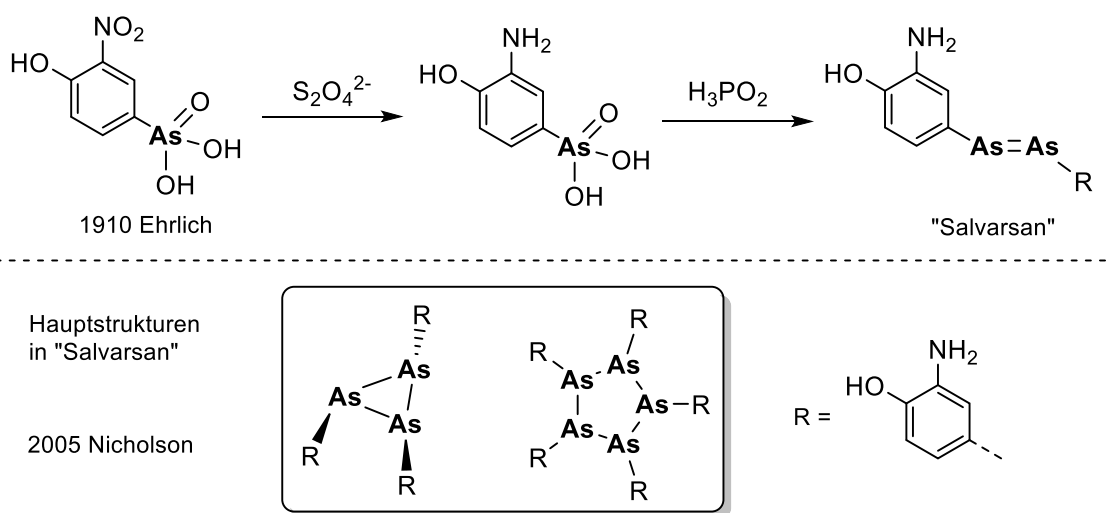
Dabei stellten sie die selektive Bildung der entsprechenden Carben-Phosphiniden-Addukte $\text{IMe}_3=\text{PPh}$ und $\text{IMe}_3=\text{PCF}_3$ fest. Darüber hinaus wurde **16** mit IMe_4 ($\text{IMe}_4 = 1,3,4,5$ -Tetramethylimidazol-2-yliden) behandelt, um $\text{IMe}_4=\text{PPh}$ zu erhalten (Schema 46, i).^[153] Diese Carben-Phosphiniden-Addukte zeigen in Analogie zu den Phosphanylidenphosphoranen elektronenreiche P-Atome, mit abgeschirmten ^{31}P -NMR-Signalen. Diese Eigenschaft und ein gewisser Mehrfachbindungscharakter der P-C-Bindung erlauben eine Interpretation als invers polarisierte Phosphaalkene.^[152] Bertrand und Mitarbeiter zeigten, dass die ^{31}P -NMR-Verschiebungen von Carben-Phosphiniden-Addukten als sensible Sonde für die Bestimmung des π -akzeptierenden Charakters der jeweiligen Carbene verwendet werden können.^[154] Seit dieser Studie wurden Phenylphosphiniden-Carben-Addukte, die sich von **16** und den entsprechenden Carbenen ableiten, verwendet, um die Elektrophilie von BiCAACs (BiCAAC = Bicyclisches Alkylaminocarbon)^[155] und CAAC-6 (CAAC-6 = sechsgliedriges CAAC) zu bestimmen (Schema 24, ii).^[156] Das verwandte NHC-Phosphiniden-Addukt $\text{IMe}_2=\text{PPh}$ wird auf ähnliche Weise aus $(\text{Ph-P})_5$ in Gegenwart von $[\text{HIMe}_2]\text{Cl}$ und $\text{KO}t\text{Bu}$ beim Auftauen einer THF-Lösung von -78°C auf Raumtemperatur hergestellt. $\text{IMe}_2=\text{PPh}$ wurde als Phosphiniden-Transferreagenz unter Verwendung von ZnCl_2 als Abfangreagenz für IMe_2 verwendet, und es

wurde ein effektiver Transfer von Ph–P zu Chinonen, Ketenen und *trans*-Chalcon erreicht (Schema 46, iii).^[157]

Zukünftige Studien auf diesem Gebiet sollten sich auf einen effektiven Phosphinidentransfer konzentrieren. In diesem Zusammenhang könnte die Verwendung sterisch anspruchsvollerer Lewis-Säuren den Zugang zu neuartigen *Push-Pull*-stabilisierten Phosphiniden ermöglichen (in Analogie zu Metallkomplexen der Phosphanylidphosphorane). Strategien eine Addukt-Bildung zwischen dem Carben und der Lewis-Säure zu umgehen (frustriertes Lewis-Paar), könnten zu einem katalytischen Phosphinidentransfer führen.

2.3.5 Arsen-analoge Dreiringe – Cyclotriarsane

Das erste homoleptische Cyclooligoarsan (AsPh)₆ wurde von Michaelis und Schulte entdeckt, als sie Phenylarsenoxid mit kristalliner hypophosphoriger Säure in siedendem Ethanol reduzierten, wobei blassgelbe Kristalle entstanden, von denen man annahm, dass es sich um das Diarsen (Ph–As)₂, das so genannte Arsabenzol, handelte.^[158] Im Gegensatz zu den zuvor beschriebenen Cyclooligophosphanen (R–P)_n (n = 3, 4, 5, 6) sind die schwereren Oligopnictane (R–Pn)_n (Pn = As, Sb, Bi; n = 3, 4, 5, 6) deutlich seltener und für Cyclotriarsane, auch Triarsirane genannt, wurden bisher nur acht Beispiele beschrieben (Abbildung 7).



Schema 47. Ehrlichs "Salvarsan" und dessen dominante Strukturen anhand von MS-Studien.

1910 synthetisierte Ehrlich "Salvarsan" als Heilmittel gegen Syphilis durch die Reduktion von 3-Nitro-4-hydroxyphenyl-arsensäure mit Dithionit und hypophosphoriger Säure, und das Produkt wurde ursprünglich als Diarsen formuliert (Schema 47, oben).^[159] Kürzlich lieferte eine

massenspektrometrische (MS) Studie den ersten Hinweis darauf, dass Salvarsan hauptsächlich aus Cyclooligoarsanen $(R-As)_n$ ($R = 3-H_2N-4-HOC_6H_3$; $n = 3, 5$; Schema 47) besteht.^[160]

Das erste strukturell verifizierte Cyclotriarsan-Derivat war 4-Methyl-1,2,6-triarsatricyclo-[2.2.1.0]-heptan (Abbildung 7, A), eine Käfigverbindung, bei der die organischen Substituenten in eine *all-cis*-Anordnung in Bezug auf den As_3 -Ring gezwungen werden.^[161] Die Behandlung von $K_2[As_2tBu_2]$ mit submolaren Mengen von $tBuAsCl_2$ in unpolaren Lösungsmitteln ergab $(tBu-As)_3$ (Abbildung 7, B), das nach langwieriger Aufarbeitung in ca. 10 % Ausbeute erhalten wurde.^[162] Im Gegensatz dazu ergibt die Reduktion von $FcAsCl_2$ ($Fc = Ferrocenyl$) mit $LiAlH_4$ oder Zn $(Fc-As)_3$ in nahezu quantitativer Ausbeute (Abbildung 7, C).^[163] 1992 beschrieben West und Mitarbeiter ein eher exotisches Beispiel für ein Cyclotriarsan in einer tricyclischen Struktur (Abbildung 7, D), das durch Aktivierung von As_4 mit dem Disilen Si_2Mes_4 synthetisiert wurde.^[164] Darüber hinaus wurde ein Metall-Kohlenstoff-substituiertes Triarsiran $[Tp^*(CO)_2M\equiv C-As]_3$ ($M = Mo, W$; $Tp^* = HB(3,5-Me_2-Pyrazolyl)_3$; Abbildung 7, E) durch die Cyclotrimerisierung von Arсандiolen des Typs $[Tp^*(CO)_2M\equiv C-As]$ hergestellt.^[165]

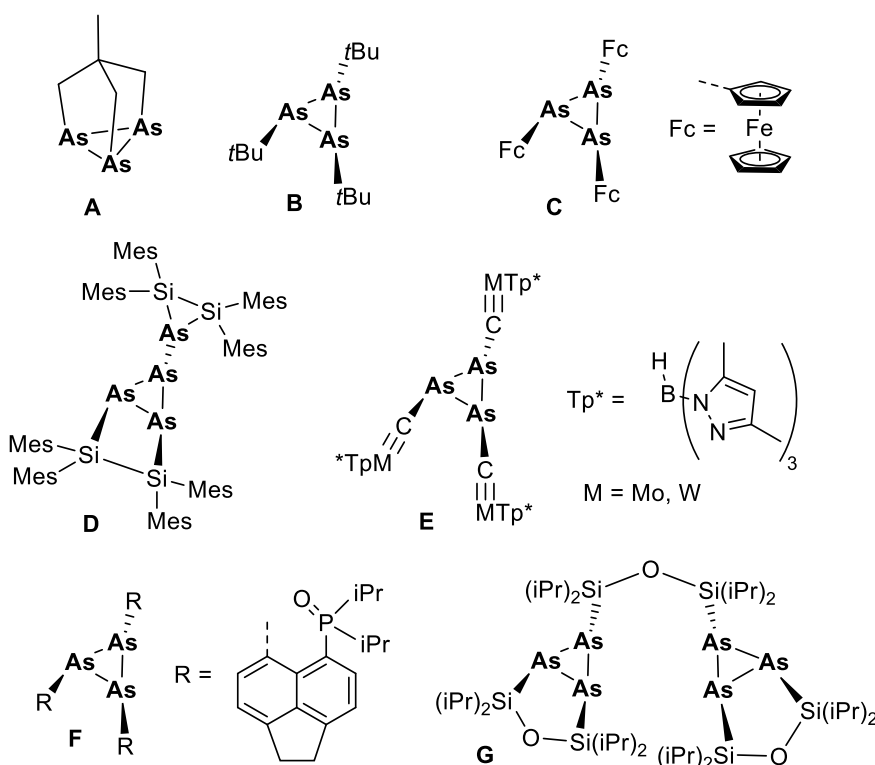
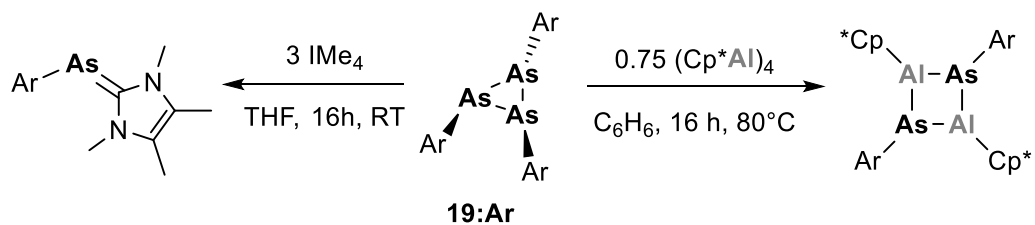
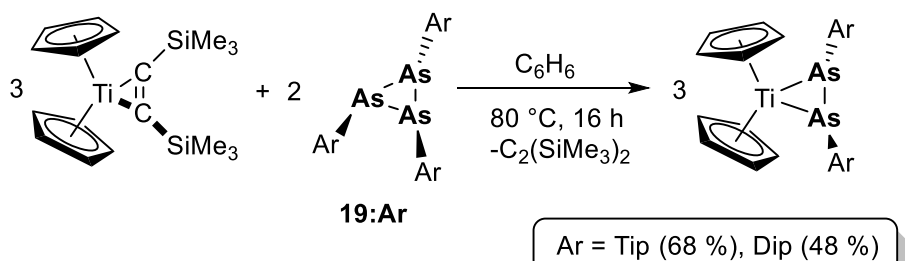
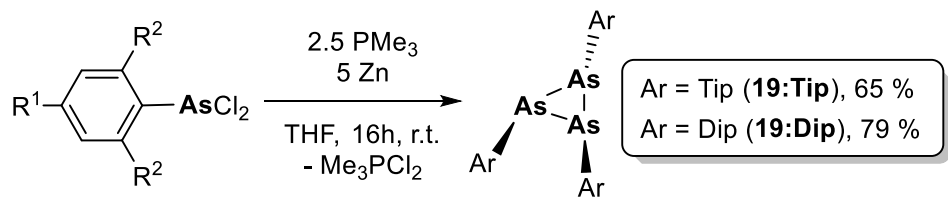


Abbildung 7. Literatur-bekannte Cyclotriarsane (A-G).

Wie in der Chemie der Arsanylidenphosphorane beschrieben, kann das Acenaphthen-basierte System **11** isoliert werden. Bei der Einwirkung von Sauerstoff auf **11** wird die intramolekulare Phosphan-Stabilisierung aufgehoben und das freie Arsiniden oligomerisiert zu den

entsprechenden cyclischen Tri- (Abbildung 1, **F**) und Tetraarsanen.^[72] Die Oxidation von Strontium- und Bariumdiarsanyldisiloxanen ergab eine einzigartige Siloxan-verbrückte tetracyclische Bis-As₃-Verbindung (Abbildung 1, **G**), bei der alle As-Atome Silyl-substituiert sind.^[166] Cyclotriarsane sollten interessante Ausgangsverbindungen in der anorganischen Chemie darstellen, wie die Verwendung von (Me-As)₅ und (Ph-As)₆ in der Arsen-organischen Chemie zeigt.^[167] Wenn (tBu-As)₄ in Gegenwart von (AlCp*)₄ erhitzt wurde, konnte die polyedrische Verbindung (Cp*₃Al₃As₂) erhalten werden.^[168]

In Anlehnung an die selektive Synthese der Cyclotriphosphane **18:Ar** untersuchten wir, ob die Arsen-analogen Systeme in ähnlicher Weise dargestellt werden können. Ausgehend von den Dichlorarsanen Ar-AsCl₂ (Ar = Dip, Tip) gelang die selektive Reduktion zu den Cyclotriarsanen (Ar-As)₃ (**19:Ar**) mit einem Überschuss PMe₃ und Zn in guten Ausbeuten und die Molekülstrukturen der Ringsysteme konnten durch SC-XRD-Experimente bestimmt werden (Schema 48, oben).^[169] Zusätzlich zeigten wir, dass die Umsetzungen von **19:Ar** (Ar = Dip, Tip) mit Cp₂Ti(btmsa) zur selektiven Bildung von tief farbigen Diarsandiid-Komplexen des Typs Cp₂Ti(AsAr)₂ führten (Schema 48, Mitte). Dabei wurden wiederum Diarsene als Zwischenstufen angenommen und dies konnte durch die Umsetzung mit dem Diarsen (^{Mes}Ter-As)₂^[92] mit Cp₂Ti(btmsa) nachgewiesen werden, was zum Komplex Cp₂Ti(As^{Mes}Ter)₂ führte. Die intensive rote Farbe der Diarsandiid-Komplexe ist auf eine breite Absorption im UV-Vis-Spektrum oberhalb von 800 nm zurückzuführen, welche mit Hilfe von TD-DFT-Rechnungen als LMCT-Bande identifiziert wurde. CAS(6,6)-Rechnungen zeigen geschlossen-schalige Systeme, die am besten als Ti(IV)-Spezies mit einem zweifach negativ geladenen Diarsandiid-Liganden [(Ar-As)₂]²⁻ beschrieben werden. Zusätzlich zeigten wir, dass die Cyclotriarsane **19:Dip** und **19:Tip** mit dem NHC IMe₄ reagieren und so NHC-Arsiniden-Addukte des Typs ArAs=IMe₄ erhalten werden (Schema 48, unten links). Die Umsetzung von **19:Ar** mit drei Äquivalenten Cp*Al (generiert aus (Cp*Al)₄) in aromatischen Lösemitteln und anschließendem Erhitzen auf 80 °C für 16 h ergab die ersten Beispiele von Basen-freien Cyclo-1,3-diarsa-2,4-dialanen des Typs [Cp*Al(μ-AsAr)]₂ (Schema 48, unten rechts), welche die formalen Dimere der schwer zugänglichen Arsaalumene Cp*Al=AsAr darstellen.^[170] Auf Systeme mit E¹³-E¹⁵-Mehrfachbindungen soll im Folgenden genauer eingegangen werden.



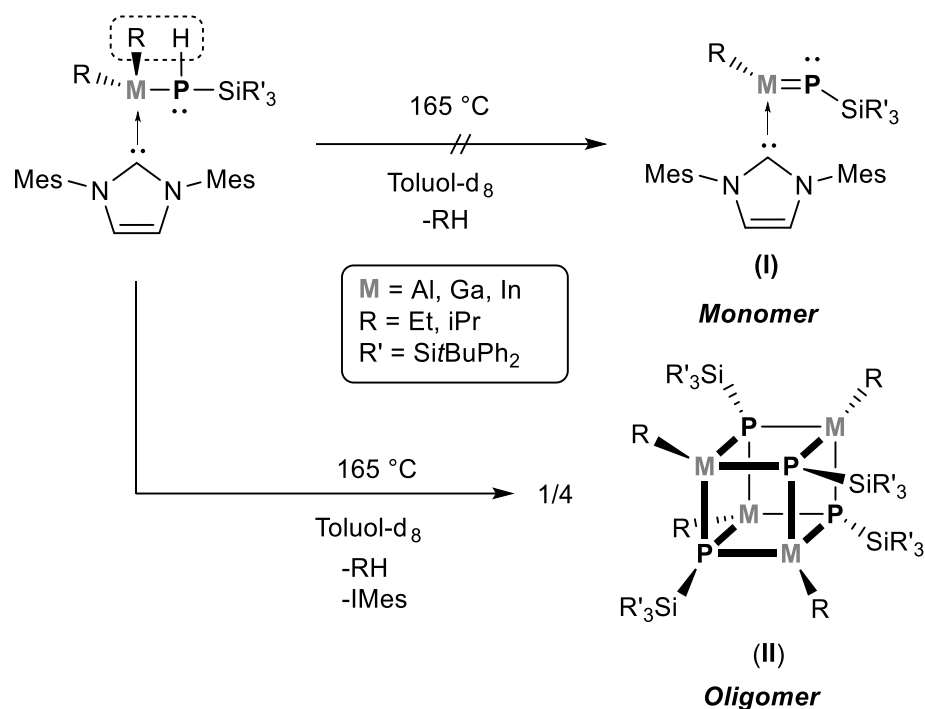
Schema 48. Selektive Bildung der Cyclotriarsane **19:Ar** (oben) und deren Reaktivität gegenüber $\text{Cp}_2\text{Ti}(\text{btmsa})$ (Mitte), sowie NHCs und $(\text{Cp}^*\text{Al})_4$ (unten).

2.4 Mehrfachbindungen zwischen Elementen der Gruppe 13 und 15

Moderne Synthesemethoden haben die Synthese schwer fassbarer, hochempfindlicher Moleküle ermöglicht, die durch ungewöhnliche Bindungssituationen bisher unbekannt Reaktivitäten offenbaren. Auch mehr als 90 Jahre nach Paulings Kommentar zur Natur der chemischen Bindung ist die Suche nach neuartigen chemischen Bindungssituationen immer noch von größtem Interesse.^[171]

Die Doppelbindungsregel besagt, dass Elemente, deren Valenzelektronen eine Hauptquantenzahl größer als 2 besitzen, mit sich selbst oder einem anderen Element keine Mehrfachbindungen eingehen. Daher galten Mehrfachbindungen zwischen schwereren Elementen lange Zeit als nicht darstellbar.^[172] Diese Bindungen haben jedoch längst ihren Status als Laborkuriosität hinter sich gelassen, wie bereits zuvor am Beispiel des Diphosphens (Mes*P)₂ gezeigt wurde,^[107] und die Fortschritte auf diesem Gebiet wurden regelmäßig in Übersichtsartikeln zusammengefasst.^[173] Es hat sich gezeigt, dass Mehrfachbindungen zwischen Hauptgruppenelementen wertvolle Werkzeuge für die Aktivierung von chemischen Bindungen sind. Mehrfachbindungssysteme zwischen E¹³-E¹³, E¹⁴-E¹⁴, E¹⁵-E¹⁵, E¹³-E¹⁵, E¹³-E¹⁶, E¹⁴-E¹⁴, E¹⁴-E¹⁵, E¹⁴-E¹⁶ und E¹⁵-E¹⁶ – sowohl homo- als auch heterodiatomare Mehrfachbindungen – wurden etabliert, und die Zahl der Veröffentlichungen auf diesem Gebiet nimmt weiter zu.

In diesem Kapitel sollen insbesondere E¹³-E¹⁵-Mehrfachbindungen näher betrachtet werden. Diese sind isovalenzelektronisch zu C-C-Mehrfachbindungen. Die Anwendung von Verbindungen mit E¹³-E¹⁵-Bindungen in MOCVD-Prozessen (MOCVD = metallorganische chemische Gasphasenabscheidung) macht sie zu potenziellen Vorstufenmolekülen für Halbleitermaterialien der Gruppe 13/15, wobei Spezies mit Mehrfachbindungen während der Gasphasenabscheidung nicht ausgeschlossen werden können.^[174] Wie im Folgenden gezeigt wird, ist die Synthese von Verbindungen mit Mehrfachbindungen zwischen Elementen der Gruppe 13 und 15 herausfordernd. Eine Ursache dafür ist die intrinsische Schwäche der π -Bindung aufgrund einer ineffektiven Überlappung der p_{π} - p_{π} -Orbitale. Außerdem bedeuten benachbarte Lewis-Säure und -Base-Zentren, dass diese Verbindungen eine ausgeprägte Oligomerisierungstendenz besitzen, was am folgenden Beispiel verdeutlicht werden soll.



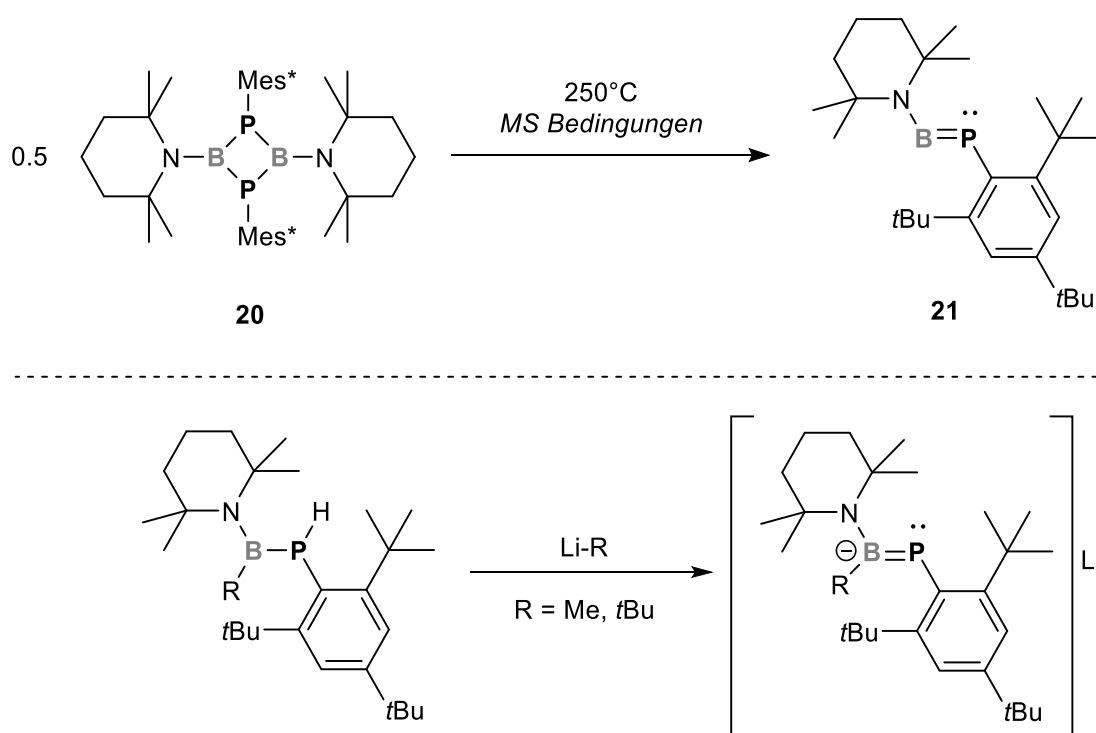
Schema 49. Versuchte Synthese verschiedener Pnictatrielene (neutrale $E^{13}-E^{15}$ -Doppelbindungssysteme) durch eine thermisch induzierte, intramolekulare Alkan-Eliminierung. Erwartete (oben) und beobachtete Reaktivität (unten).^[175]

Von Hänisch und Mitarbeiter verwendeten NHC-stabilisierte monomere Metallsilylphosphanide vom Typ $(\text{IMes})\text{R}_2\text{MP}(\text{H})\text{Si}t\text{BuPh}_2$ ($M = \text{Al-In}$; $R = \text{Et, iPr}$),^[175] von denen man erwartete, dass sie bei thermischer intramolekularer Alkan-Eliminierung (RH) die entsprechenden NHC-stabilisierten Phosphatrielene $(\text{IMes})\text{RM}=\text{PSi}t\text{BuPh}_2$ (**I**) ergeben würden (Schema 49, oben). Jedoch konnten keine NHC-stabilisierten Monomere beobachtet werden und stattdessen wurden Heterocubane (**II**), die formalen Tetramere der entsprechenden Phosphatrielene erhalten (Schema 49, unten).

Doch welche Voraussetzungen müssen erfüllt sein, um diese schwer fassbaren Mehrfachbindungen zu stabilisieren? In DFT-Studien, insbesondere von Su *et al.*,^[176] wurde die Bindungssituation in verschiedenen Pnictatrielen untersucht und für die synthetische Realisierung von $E^{13}-E^{15}$ -Mehrfachbindungen müssen sowohl elektronische als auch sterische Faktoren berücksichtigt werden. Im Folgenden sollen insbesondere B-P, Al-N, Al-P/As und Ga-Pn (Pn = P, As, Sb) Mehrfachbindungssysteme eingehender betrachtet werden.

2.4.1 Phosphaborene

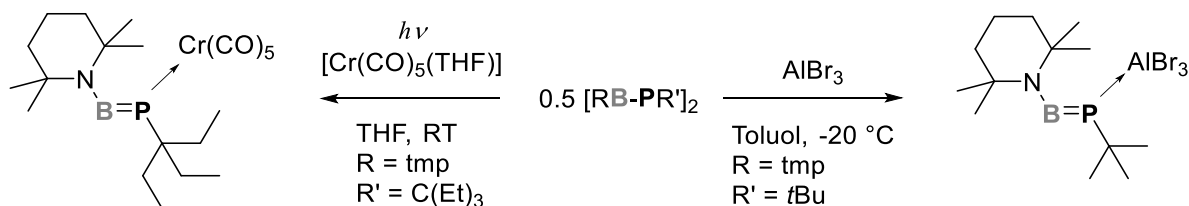
Die ersten Versuche Phosphaborene (oder Boraphosphene), Systeme mit einer P=B-Doppelbindung, zu synthetisieren wurden von Alan Cowley und Mitarbeitern in den späten 80er Jahren beschrieben.^[177] Sie verwendeten eine kombinierte Salzmetathese- und Me_3SiCl -Eliminierungsroute in der Reaktion von $(\text{tmp})\text{BCl}_2$ ($\text{tmp} = 2,2,6,6\text{-Tetramethylpiperidyl}$) mit dem Lithiumphosphid $[\text{Mes}^*\text{P}(\text{SiMe}_3)\text{Li}]$, um das viergliedrige Ringsystem $[(\text{tmp})\text{BPMe}^*]_2$ (**20**) zu erhalten. Dieses sogenannte Diphosphadiboretan fragmentiert bei thermischer Behandlung (ca. $250\text{ }^\circ\text{C}$) zu $[\text{Mes}^*\text{P}=\text{B}(\text{tmp})]$ (**21**), wie MS-Studien zeigten. (Schema 50, oben).



Schema 50. Ein viergliedriger BP-Heterozyklus und dessen Spaltung in ein Phosphaborene bei Thermolyse (oben). Bildung von anionischen Phosphinidenboraten mit formaler BP-Doppelbindung (unten).

Darüber hinaus untersuchten Cowley und Mitarbeiter die Reaktivität von $[(\text{tmp})\text{B}(\text{Cl})\text{P}(\text{H})\text{Me}^*]$ gegenüber MeLi und $t\text{BuLi}$ und erhielten dabei Phosphinidenborat-Anionen vom Typ $[(\text{tmp})\text{RB}=\text{PMe}^*]\text{Li}$ ($\text{R} = \text{Me}, t\text{Bu}$). Die ^{31}P -NMR-Verschiebungen von $+72$ bzw. $+85/+87$ ppm sind im Vergleich zu klassischen Phosphidanionen entschirmt (vgl. $[\text{Mes}^*\text{P}(\text{SiMe}_3)\text{Li}]$ $\delta(^{31}\text{P}\{^1\text{H}\}) = -146.6$ ppm).^[178] Die Autoren führen die erhebliche

Entscheidung auf eine Rückbindung vom besetzten p-Orbital am Phosphor in das freie p-Orbital am Bor zurück.

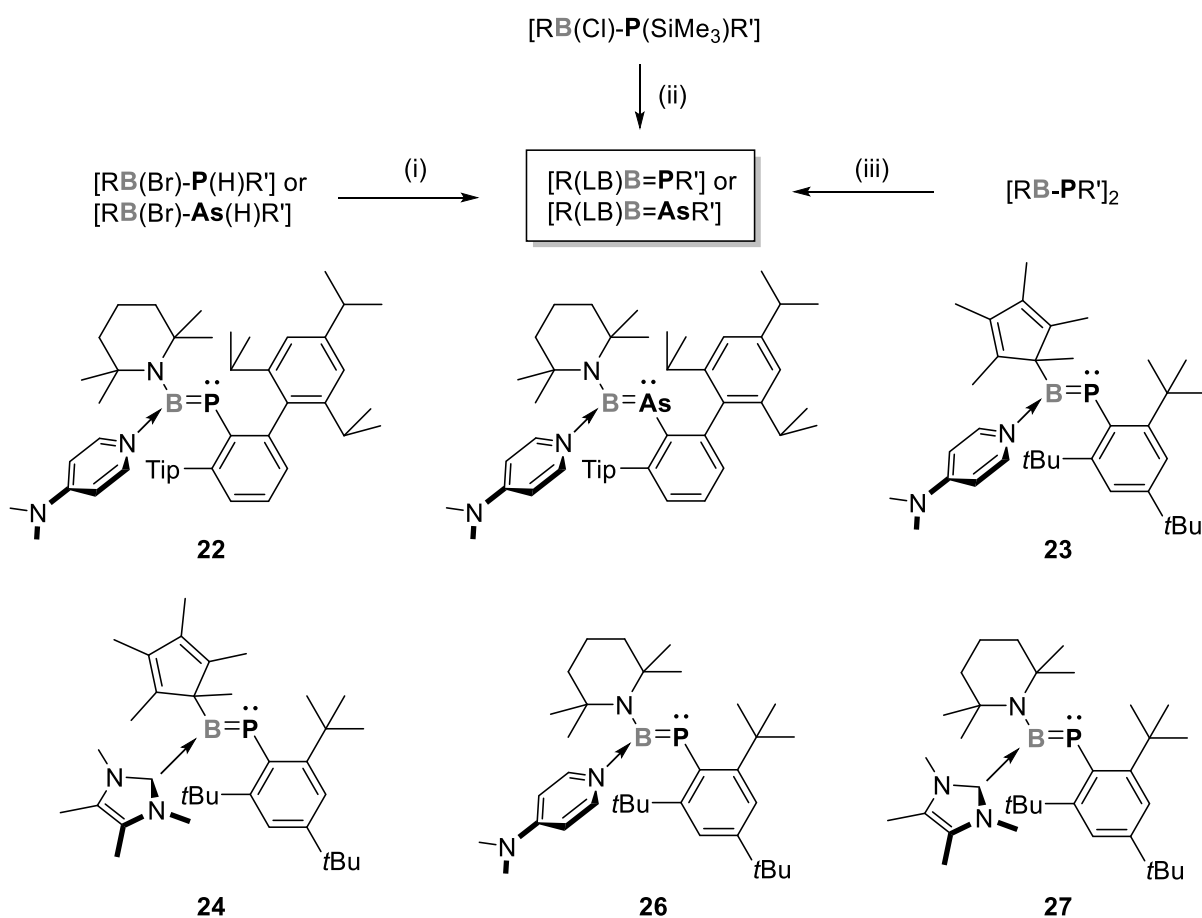


Schema 51. Lewis-Säure induzierte Fragmentierung von Diphosphadiboretanen.

Nöth und Mitarbeitern haben gezeigt, dass bestimmte B_2P_2 -Vierringe in Gegenwart einer Lewis-Säure tatsächlich in die entsprechenden Boraphosphene gespalten werden können (Schema 51).^[179] Die Behandlung von $[(tmp)B-PC(Et)_3]_2$ mit einer frisch hergestellten Lösung von $[Cr(CO)_5(thf)]$ in THF resultierte in der Bildung von $[(CO)_5Cr\{(tmp)B=PC(Et)_3\}]$. In diesem Fall wird das neutrale Boraphosphen durch P-Koordination an das Lewis-saure $[Cr(CO)_5]$ -Übergangsmetallfragment stabilisiert. Bei $[Me_2NBPtBu]_2$ mit weniger sperrigen Substituenten hingegen wurde eine exocyclische Koordination an $Cr(CO)_5$ beobachtet, und der B_2P_2 -Vierring blieb erhalten. Diese Beobachtungen stimmen mit der Detektion von monomerem $[(tmp)B=PC(Et)_3]^+$ unter Gasphasenbedingungen überein, während $[Me_2NB=PtBu]^+$ massenspektrometrisch nicht beobachtet werden konnte. Die Massenspektrometrie stellt somit ein leistungsfähiges Instrument zur Vorhersage stabiler Pnictatrielene dar. Die Molekülstruktur von $[(CO)_5Cr\{(tmp)B=PC(Et)_3\}]$ unterstützt die Bildung einer B=P-Doppelbindung mit einem B–P-Atomabstand von 1.743(5) Å (Tabelle 4). Im Jahr 2005 zeigten Nöth und Mitarbeiter, dass der viergliedrige B_2P_2 -Ring in $[(tmp)B-P(tBu)]_2$ bei niedrigen Temperaturen in Gegenwart von $AlBr_3$ in das korrespondierende Monomer gespalten werden kann.^[180] Die röntgenkristallografische Bestimmung der Molekülstruktur von $[AlBr_3(tmp)B=P(tBu)]$ ergab einen B–P-Atomabstand von 1.787(4) Å.

Das Lewis-saure Bor-Atom in Phosphaborenen sollte auch die Stabilisierung mit Hilfe von Lewis-Basen erlauben. Power und Mitarbeiter nutzten Verbindungen der Art $[(tmp)B(Br)-Pn(H)^{Tip}Ter]$ ($Pn = P, As$) als Vorstufen für nachfolgende Hydrodehalogenierungsreaktionen.^[181] Die Zugabe eines Überschusses an DMAP (DMAP = 4-Dimethylaminopyridin) führte zur Abspaltung von $DMAP \cdot HBr$ sowie zum gleichzeitigen Einfangen der Borapnictene $[(tmp)(DMAP)B=Pn^{Tip}Ter]$ mit DMAP ($Pn = P$ (**22**), As). In Übereinstimmung mit früheren Studien über Phosphinidenborate zeigt $[(tmp)(DMAP)B=P^{Tip}Ter]$ eine ^{31}P -NMR-Verschiebung

von +57.3 ppm, was im Vergleich zum Vorstufenmolekül ins Tieffeld verschoben ist. SC-XRD-Studien ergaben B–Pn-Atomabstände von ($d(\text{B–P}) = 1.8092(17)$ bzw. $d(\text{B–As}) = 1.914(6)$ Å).



Schema 52. Allgemeine Strategien zur Stabilisierung von Boraphosphenen mit Lewis-Basen (oben): (i) 2 Äq. DMAP, Toluol, -78 °C auf RT. (ii) 1 Äq. DMAP oder 2 Äq. ImMe_4 , Benzol, RT. (iii) 2 Äq. DMAP oder 2 Äq. ImMe_4 , Benzol, 80 °C.

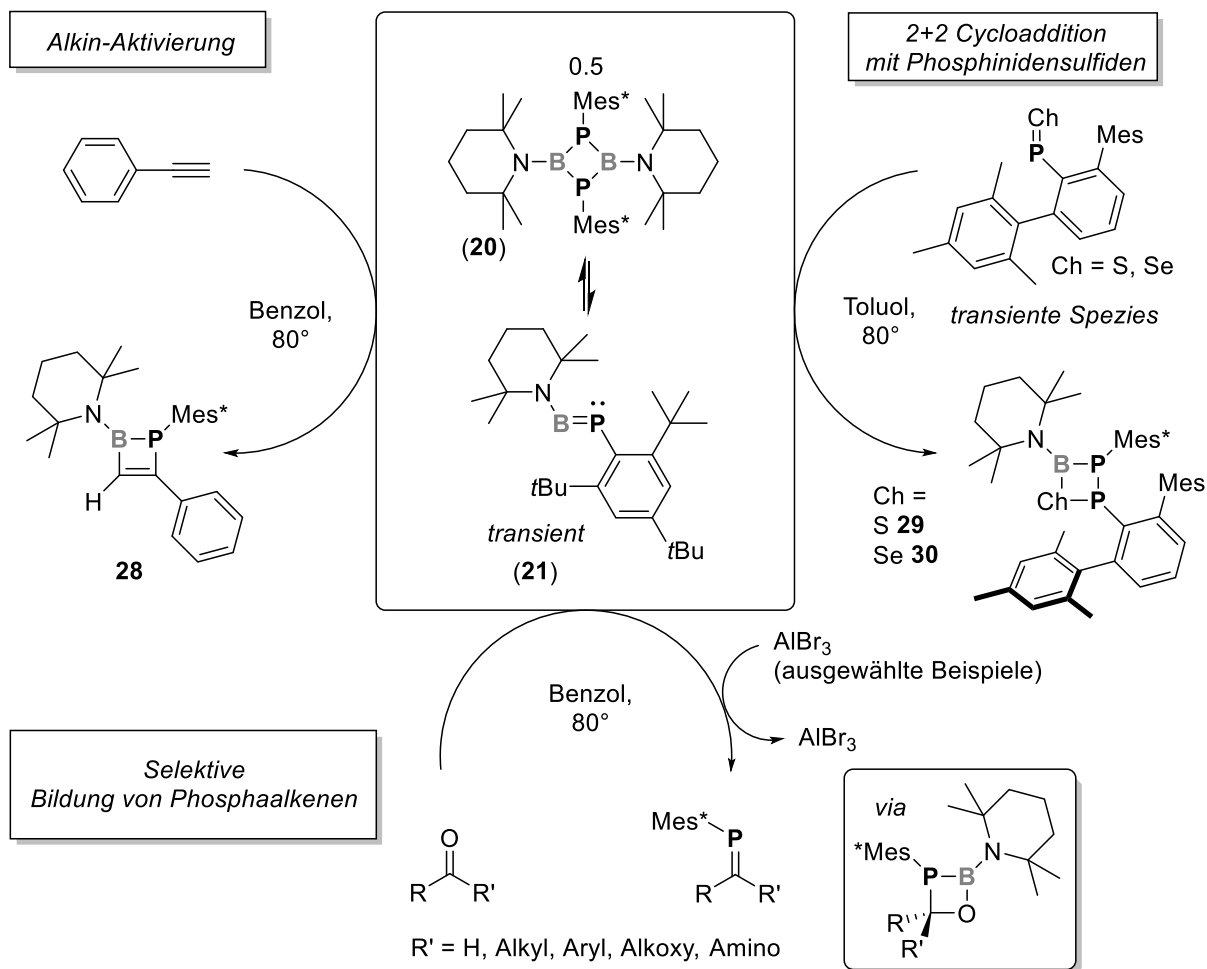
Tabelle 4: Chemische Verschiebungen [ppm] und B–P Atomabstände [Å] von neutralen Lewis-Säure and -Base stabilisierten Verbindungen mit B–P Doppelbindungen.^{72–77}

Verbindung	$^{11}\text{B-NMR}$	$^{31}\text{P-NMR}$	$d(\text{B–P})$
$[\text{Cr}(\text{CO})_5\{(\text{tmp})\text{B}=\text{PC}(\text{Et})_3\}]$	62.9 ^a	-45.3^a	1.743(5)
$[\text{AlBr}_3\{(\text{tmp})\text{BPC}(\text{Et})_3\}]$	68.4 ^a	-59.8^a	1.787(4)
$[(\text{tmp})(\text{DMAP})\text{B}=\text{P}^{\text{Tip}}\text{Ter}]$ (22)	41.2 ^a	57.3^a	1.8092(17)
$[\text{Cp}^*(\text{DMAP})\text{B}=\text{PMes}^*]$ (23)	52.3 ^a	96.7^a	1.795(3)
$[\text{Cp}^*(\text{ImMe}_4)\text{B}=\text{PMes}^*]$ (24)	48.5 ^a	192.9^a	1.8067(15)
$[\text{Cp}^*\text{B}(\text{Br})=\text{PMes}^*][\text{IDipSiMe}_3]$ (25)	54.9 ^b	75.2^b	1.8039(16)
$[(\text{tmp})(\text{DMAP})\text{B}=\text{PMes}^*]$ (26)	44.5 ^b	64.0^b	1.8211(16)
$[(\text{tmp})(\text{ImMe}_4)\text{B}=\text{PMes}^*]$ (27)	43.9 ^b	151.5^b	1.8309(16)

^a 298 K, C₆D₆; ^b 298 K, THF-d₈

Kürzlich zeigte die Gruppe um Michael Cowley, dass die Me₃SiCl-Eliminierung ausgehend von [Cp*B(Cl)-P(SiMe₃)Mes*] mit Hilfe von DMAP oder dem kleinen NHC IMe₄ initiiert werden kann. Auf diesem Wege werden wiederum Basen-stabilisierte Phosphaborene des Typs [Cp*B(L)=PMes*] erhalten (L = DMAP (**23**), IMe₄ (**24**)).^[182] Durch kombinierte ³¹P-NMR-Untersuchungen und SC-XRD-Experimente zeigten die Autoren, dass dieser neuartige Weg zu Boraphosphenen schrittweise abläuft. Im ersten Schritt wird die SiMe₃-Gruppe durch das NHC abstrahiert, wodurch ein anionisches Phosphinidenborat mit einem Me₃Si-substituierten Imidazolium Gegenion entsteht. In einem zweiten Schritt wird dann Me₃SiCl freigesetzt und das gewünschte Basen-stabilisierte Boraphosphen erhalten. Die Isolierung des Phosphinidenborat-Zwischenproduktes gelang unter Verwendung des sterisch anspruchsvolleren NHCs IDip (IDip = (HCNDip)₂C:) und [Cp*B(Br)=PMes*][IDip-SiMe₃] (**25**) konnte strukturell charakterisiert werden. Die ¹¹B- und ³¹P-NMR-Signale sowie die B-P-Atomabstände der jeweiligen Basen-stabilisierten Boraphosphene sowie des Phosphinidenborats **25** sind in Tabelle 4 zusammen mit den zuvor beschriebenen Verbindungen zusammengefasst. Die Analyse der natürlichen Bindungorbitale (NBO) zeigte, dass solche B=P-Doppelbindungen stark in Richtung des Phosphoratoms polarisiert sind (etwa 71 %) mit einem Wiberg-Bindungsindex (WBI) von 1.67. Derselben Gruppe gelang es dann wenig später das Diphosphadiboretan [Mes*PB(tmp)]₂ (**20**) als Syntheseäquivalent für das korrespondierende Phosphaboren zu verwenden.^[183] Zunächst wurden die Basen-Addukte [(tmp)(L)B=PMes*] (L = DMAP (**26**), IMe₄ (**27**)) ausgehend von **20** und der jeweiligen Lewis-Base bei einer Temperatur von 100 °C in Benzollösung dargestellt (Schema 52, iii). Zusätzlich wurde eine Lösung von **20** mit Phenylacetylen bei erhöhten Temperaturen umgesetzt und die Umwandlung in ein cyclisches BP-Analogon von Cyclobuten, ein sogenanntes 1,2-Phosphaboreten (**28**), mit vollständiger Regio-Selektivität beobachtet (Schema 53, links).^[183] Wenig später zeigten Arbeiten von Ragona, Cowley und Mitarbeitern auf, dass **20** mit [Ch-(μ-P^{Mes}Ter)]₂ (Ch = S, Se) zu viergliedrigen BPPCh-Ringen reagiert (Schema 53, rechts; S: **29**, Se: **30**).^[184] Dieses allgemeine Reaktionsverhalten des transienten Phosphaborens **21** zur Bildung viergliedriger Ringe wurde erst kürzlich in der chemischen Synthese zur Herstellung von Phosphaalkenen ausgenutzt (Schema 53, unten). Die Reaktion von intermediär generiertem **21** mit einer Vielzahl von Ketonen, Aldehyden, Estern sowie Carbonsäureamiden ergab verschiedene CPBO Vierringe, sogenannte 1,2,3-Phosphaboraoxetane. In der Gegenwart einer Lewis-Säure wie AlBr₃ erfolgt eine Cyclo-Reversion zu den entsprechenden Phosphaalkenen Mes*P=CRR' und als Nebenprodukte entstehen [(tmp)NBO]_x-Heterocyclen (x = 2, 3). Die

Ähnlichkeit zur Phospha-Wittig-Reaktion ist augenscheinlich und diese Umwandlung wurde als „Phospha-Bora-Wittig“-Reaktion bezeichnet, wobei nun auch Ketone als Substrate eingesetzt werden können.

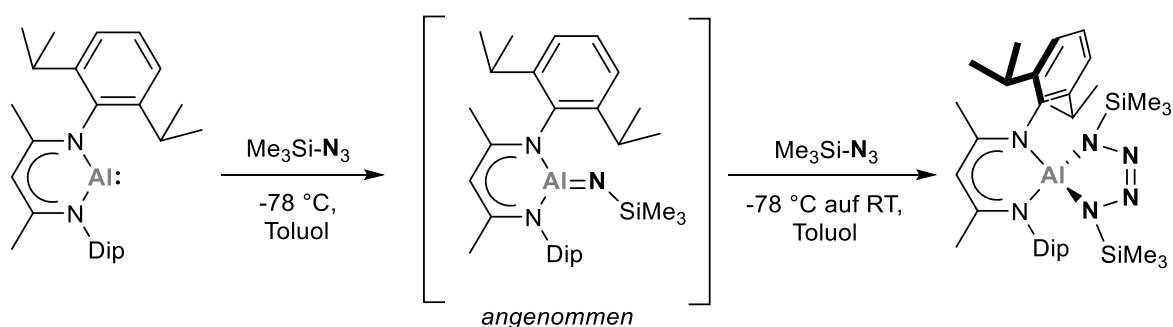


Schema 53. Die Reaktivität des transienten Boraphosphens **21**, gegenüber Alkinen (links), Phosphor-Chalkogen-Bindungen (rechts) sowie Carbonylverbindungen (unten).

Die Forschung zu Systemen mit einer B–P-Doppelbindung hat sich seit den ersten Studien von Alan Cowley *et al.* zu einem wichtigen Bereich moderner anorganischer Chemie entwickelt. Neben acyclischen Systemen wurden B–P-Doppelbindungen auch in cyclische Systeme eingebunden, wie es im vorherigen Kapitel zu Cyclooligophosphanen bereits beschrieben wurde. So wurden bisher vier-,^[185] fünf-^[186] und sechsgliedrige^[146, 187] Ringe charakterisiert, die mindestens eine B–P-Doppelbindung enthalten.

2.4.2 Mehrfachbindungen zwischen Al und N.

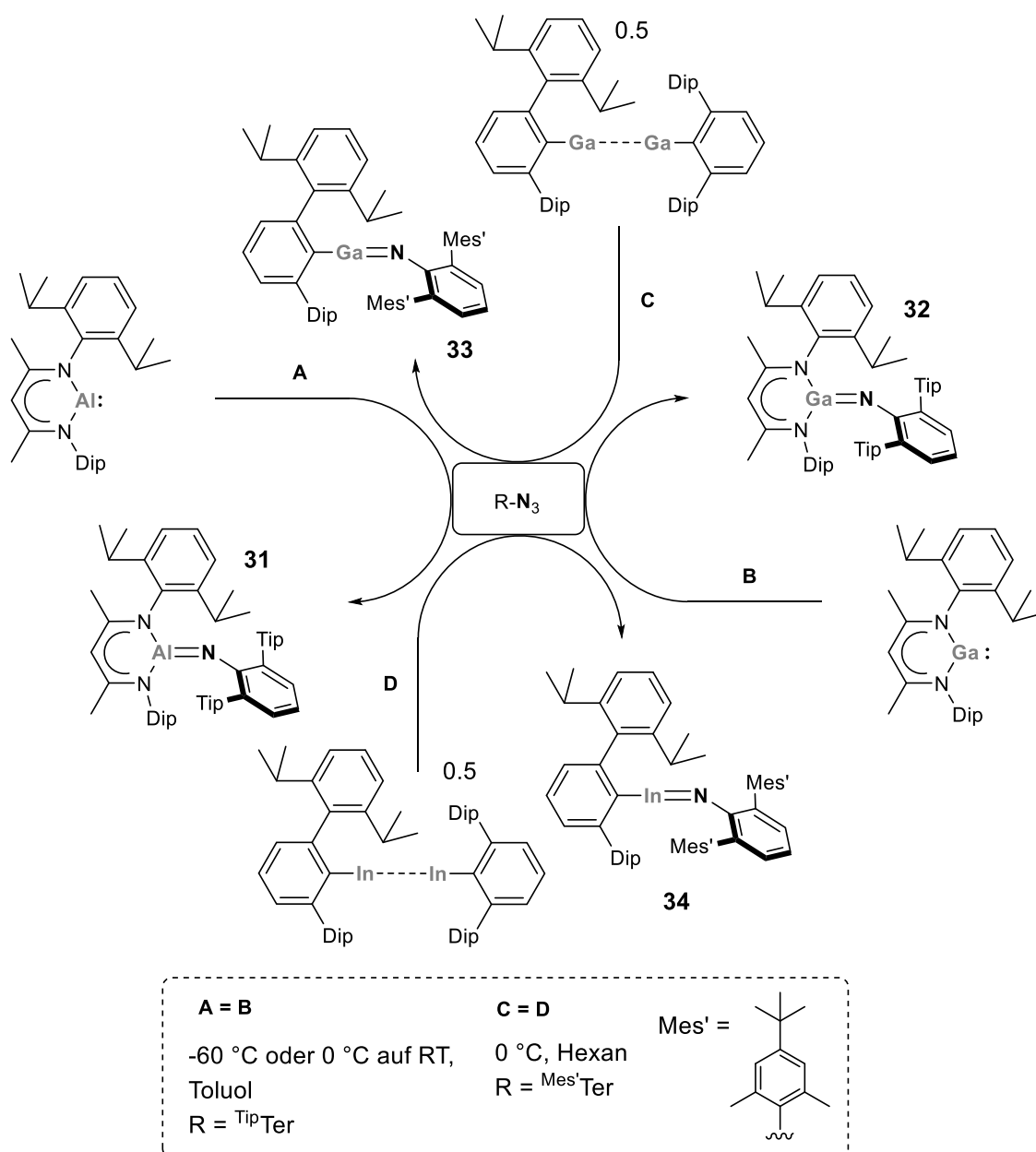
Die Chemie der Metallimide der Gruppe 13 ist etabliert,^[188] daher findet hier eine Einschränkung auf Derivate mit einer möglichen Mehrfachbindung statt. Ein Aluminium-Stickstoff-Analogon des Borazins wurde beschrieben,^[189] weist aber entgegen der Erwartung keinen Mehrfachbindungscharakter auf. Somit sind die ersten Schritte zu Al–N-Mehrfachbindungen mit der erfolgreichen Isolierung der monomeren Al(I)-Verbindung $[\text{DipNacnac}]Al$ ($\text{DipNacnac} = \text{HC}\{(\text{CMe})(\text{NDip})\}_2$) verbunden.^[190] Dieses wurde mit zwei Äquivalenten Me_3SiN_3 umgesetzt, wobei $[\text{DipNacnac}]Al[(\text{N-SiMe}_3)_2\text{N}_2]$,^[191] ein Tetrazol-Derivat, bei dem das Ringkohlenstoffatom durch ein Al-Atom ersetzt ist, erhalten wurde (Schema 54). Die Autoren stellten fest, dass Tetrazole grundsätzlich über eine [3+2]-Cycloaddition synthetisiert werden und vermuteten, dass das Iminoalan $[(\text{DipNacnac})Al=N-\text{SiMe}_3]$ an der Reaktion beteiligt gewesen sein könnte.



Schema 54. Synthese eines Aluminiumtetrazols mit einem potentiellen Iminoalan-Intermediat.

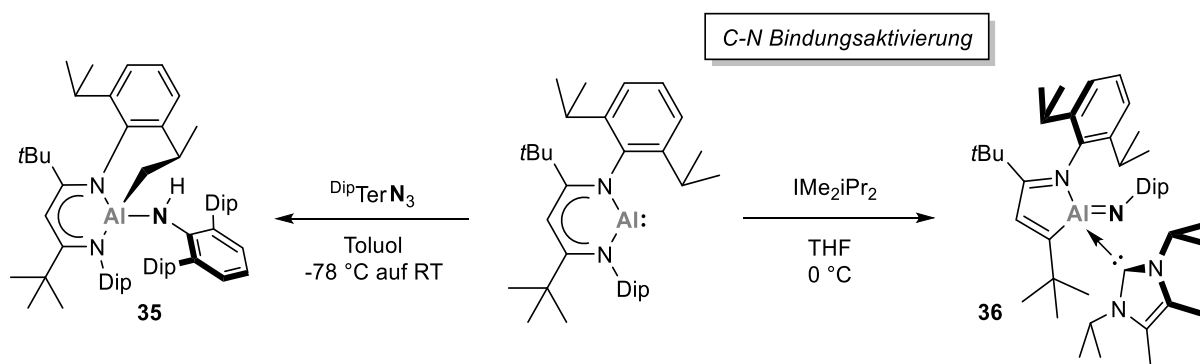
Diese Vermutung wurde nur ein Jahr später indirekt bestätigt, als Power, Roesky und Mitarbeiter Verbindungen mit Al–N- sowie Ga–N-Doppelbindungen isolierten.^[192] Es wurde gezeigt, dass die Reaktion von $[\text{DipNacnac}]Al$ sowie $[\text{DipNacnac}]Ga$ mit dem sterisch anspruchsvollen Azid TipTerN_3 die Iminotriole $[(\text{DipNacnac})M=N-\text{TipTer}]$ ($M = Al$ (**31**), Ga (**32**)) ergab, die umfassend charakterisiert wurden (Schema 55, A und B). Die NMR-Daten von $[(\text{DipNacnac})Al=N-\text{TipTer}]$ bestätigten die Charakterisierung als Aluminiumimid und die Molekülstruktur von $[(\text{DipNacnac})Ga=N-\text{TipTer}]$ zeigt ein dreifach koordiniertes Ga-Zentrum und einen Ga–N-Atomabstand von 1.742(3) Å, der im Bereich einer Doppelbindung liegt (vgl. $\Sigma r_{\text{cov}}(\text{Ga}=\text{N}) = 1.77 \text{ \AA}$).^[78] Für die Dip- und Me-Substituenten des Nacnac-Liganden werden im ^1H - und ^{13}C -NMR-Spektrum zwei Gruppen von Signalen beobachtet. Dies steht im Einklang mit einer eingeschränkten Rotation um die jeweiligen Al–N- und Ga–N- π -Bindungen. Ditrielen können als Dimere der korrespondierenden $E^{13}(\text{I})$ -Verbindungen aufgefasst werden

und daher wurde die Reaktivität von Diträlen des Typs $(\text{Dip}^i\text{TerM})_2$ ($M = \text{Ga}, \text{In}$) gegenüber $\text{Mes}'\text{TerN}_3$ ($\text{Mes}'\text{Ter} = \text{C}_6\text{H}_3\text{-2,6(Xyl-4-}t\text{Bu)}_2$) näher untersucht. In ähnlicher Weise erhält man die Iminotrielen $[(\text{Dip}^i\text{Ter})\text{M}=\text{N}-\text{Mes}'\text{Ter}]$ ($M = \text{Ga}$ (**33**), In (**34**), Schema 55, C und D), wenn beide Komponenten in einer 2:1-Stöchiometrie bei niedrigen Temperaturen miteinander umgesetzt werden (Schema 55, C und D).^[193] Bemerkenswert ist die Reaktion des Digallens $(\text{Dip}^i\text{TerGa})_2$ mit 1,2-*p*-Tolyldiazen, die zur Bildung des viergliedrigen 1,2-Diaza-3,4-digallacyclobutans $[\text{Dip}^i\text{TerGaNTol}]_2$ führte, dem formalen Dimer des korrespondierenden Iminogallans.^[194]



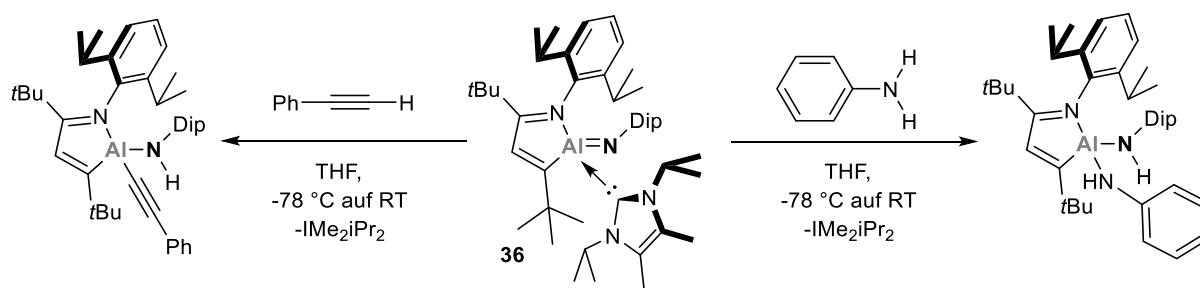
Schema 55. Synthesewege für die Herstellung von E^{13} -Imiden aus Aziden und niedervalenten E^{13} -Vorstufenmolekülen.

Cui und Mitarbeiter untersuchten die Reaktion von $[\text{DipNacnac}^*]\text{Al}$ ($\text{DipNacnac}^* = \text{HC}\{(\text{CtBu})(\text{NDip})\}_2$) mit DipTerN_3 , wobei eine der $i\text{Pr}$ -Gruppen der DipTer -Einheit CH-aktiviert wird und es zu einer CH-Addition entlang der intermediären Al–N-Mehrfachbindung kommt (Verbindung **35**; Schema 56, links).^[195] Wenig später untersuchte dieselbe Gruppe die Reaktivität von $[\text{DipNacnac}^*]\text{Al}$ gegenüber dem NHC IME_2iPr_2 ($\text{IME}_2\text{iPr}_2 = (\text{MeCNiPr})_2\text{C}:$). Das Al(I)-Zentrum insertierte hierbei nach einer C–N-Aktivierung und anschließender Umlagerung einer NDip-Gruppe in das Liganden-Gerüst des DipNacnac^* -Substituenten und das NHC-stabilisierte Aluminiumimid **36** wurde gebildet (Schema 56, rechts).



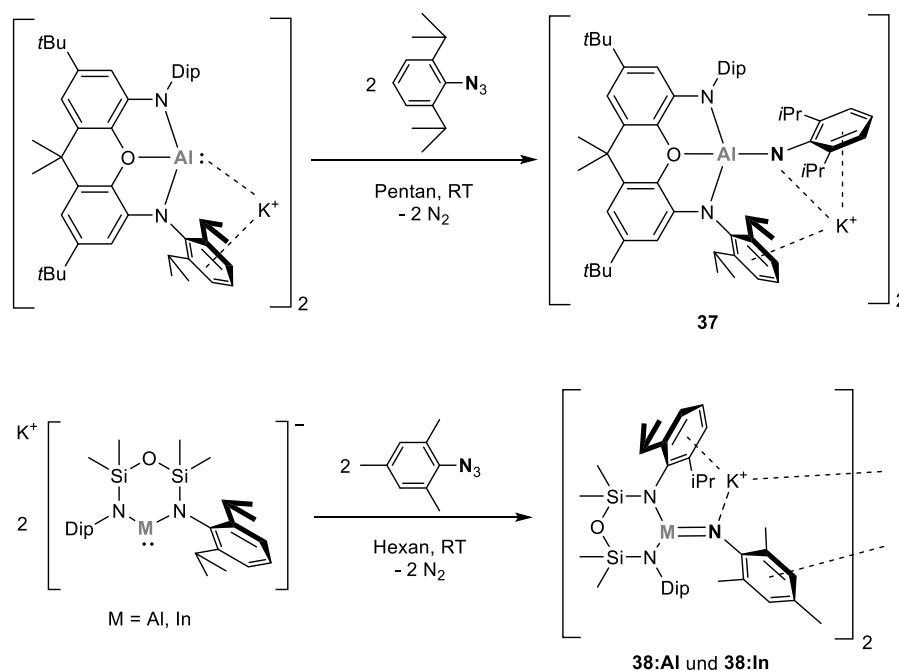
Schema 56. CH-Aktivierung entlang einer intermediären Al=N-Bindung (links) und NHC-induzierte Umlagerungsreaktion von $[\text{DipNacnac}^*]\text{Al}$ hin zum NHC-stabilisierten Iminoalan **36**.

SC-XRD-Experimente ergaben einen kurzen Al–N-Atomabstand von 1.705(2) Å ($\Sigma r_{\text{cov}}(\text{Al}=\text{N}) = 1.73$ Å),^[78] der mit dem Ga–N-Atomabstand (1.742(3) Å) in **32** vergleichbar ist. Quantenchemische Berechnungen zeigen, dass die Al–N-Bindung einen stark ionischen Charakter aufweist, obwohl die Autoren eine Formulierung als Al=N-Doppelbindung nicht ausschließen. Erste Anwendungen in der Aktivierung kleiner Moleküle wurden anschließend beschrieben. Die Reaktion von **36** mit $\text{PhC}\equiv\text{CH}$, sowie mit PhNH_2 ergaben deren oxidative Additionsprodukte entlang der Al–N-Bindung wobei das Proton unter gleichzeitiger Freisetzung von IME_2iPr_2 an das N-Atom addiert wird (Schema 57).



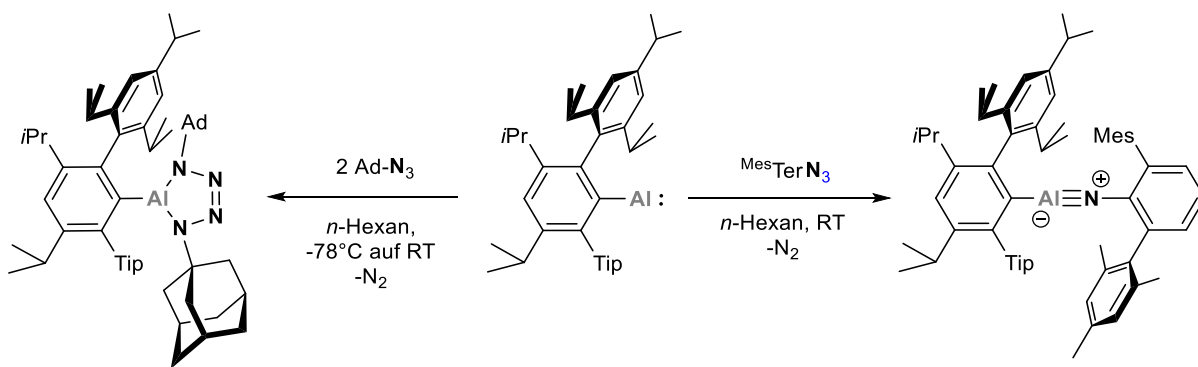
Schema 57. CH- und NH-Bindungsaktivierungen mit Hilfe des NHC-stabilisierten Iminoalans **36**.

Im Zusammenhang mit diesen Studien stehen die Arbeiten der Gruppen Goicoechea und Aldridge, die als erste über Aluminylanionen berichteten.^[196] Die Behandlung des mit Dimethylxanthin stabilisierten Kaliumaluminyls $[K\{Al(NON)\}]_2$ (NON = 4,5-Bis(2,6-diisopropylanilido)-2,7-di-tert-butyl-9,9-dimethylxanthen) mit $DipN_3$ ergab das dimere Aluminiumimid $[K\{DipNAl(NON)\}]_2$ (**37**, Schema 58). DFT-Rechnungen zeigten, dass die erhaltene Al–N-Spezies zwar formal eine Mehrfachbindung darstellt, jedoch eher als stark polarisierte Einfachbindung aufzufassen ist (WBI(Al–N) = 0.71).^[197] Anker und Coles leisteten ebenso wichtige Beiträge zur Reaktivität von Aluminyl-Anionen gegenüber Aziden. So verlaufen die Reaktionen der Trielylanionen $K[M(SiNONDip)]$ (M = Al, In; $SiNONDip = [O(SiMe_2NDip)_2]_2^-$) mit $MesN_3$ unter N_2 -Eliminierung und der Bildung der dimeren Spezies $\{K[SiNONDipM=N-Mes]\}_2$ (M = Al (**38:Al**), In (**38:In**)) (Schema 58).^[198] Für M = In konnte auch die monomere Verbindung $[K([222]crypt)][SiNONDipIn=N-Mes]$ charakterisiert werden, die nach Sequestrierung des Kations erhalten wurde. Die Festkörperstrukturen dieser Verbindungen zeigen M–N-Atomabstände von 1.7251(11) (M = Al) und 1.986(2) Å, 1.9907(18) Å (M = In). Alle diese Werte liegen im Bereich der neutralen Iminotrielen. Die Reaktivität dieser Systeme wurde untersucht, und es konnte zum einen gezeigt werden, dass das Aluminiumderivat in einer [2+2]-Cycloaddition mit CO_2 ein dimeres Carbamatdianion bildet.^[199] Andererseits führt die Reaktion des Indiumderivats mit einem zweiten Äquivalent RN_3 (R = Mes, $SiMe_3$) zu einem Indium-Tetrazol,^[198] wie es bereits für die Reaktion von $[DipNacnac]Al$ mit Me_3SiN_3 gezeigt wurde (Schema 54).



Schema 58. Reaktivität von Aluminyl- und Indenylanionen gegenüber organischen Aziden.

Power und Mitarbeiter präsentierten vor Kurzem das thermisch stabile Alandiyl [$iPr_2^{Tip}Ter-Al$] ($iPr_2^{Tip}Ter = C_6H_2-2,6-(C_6H_2-2,4,6-iPr_3)_2-3,5-iPr_2$).^[200] Mit diesem Vorläufer wurde durch die anschließende Reaktion mit $MesTerN_3$ die erste Verbindung mit einer formalen Al–N-Dreifachbindung erhalten (**39**, Schema 59).^[201] Der kristallographisch ermittelte, außerordentlich kurze Al–N-Atomabstand von 1.625(4) Å (vgl. $\Sigma r_{cov}(Al\equiv N) = 1.65$ Å)^[78] und quantenchemische Berechnungen deuten auf einen signifikanten Dreifachbindungscharakter hin. Die Kohn-Sham-Orbitale zeigen ein σ - und zwei nicht entartete π -Orbitale. Die Energiebeiträge zur Gesamtbindungsenergie wurden für jede spezifische Orbitalwechselwirkung berechnet und zeigen, dass eine Hauptkomponente (-1120 kJ·mol⁻¹, ca. 83% der gesamten Orbitalwechselwirkung von -1350 kJ·mol⁻¹) auf den Ladungsfluss von Al zu N zurückzuführen ist. Zwei kleinere Komponenten (-100 bzw. -102 kJ·mol⁻¹) beschreiben die Rückbindung von N zu Al. Obwohl der Beitrag der Rückbindung von N zu Al minimal ist, weist die Bindung die formalen Merkmale einer Al–N-Dreifachbindung auf. Die monomere Alandiyl-Vorstufe wurde mit weiteren Aziden umgesetzt, um die Reaktivität von transientem [$iPr_2^{Tip}TerAl\equiv NR$] (R = Ad, SiMe₃) zu untersuchen. Im Falle von AdN₃ (Ad = 1-Adamantyl) wurde ein Tetrazol-Derivat erhalten (Schema 59, links). Im Falle von Me₃Si–N₃ führte die Reaktion zur Bildung eines Amido-Azido-Alans.



Schema 59. Reaktivität des Alandiyls $iPr_2^{Tip}Ter-Al$ gegenüber unterschiedlichen Aziden.

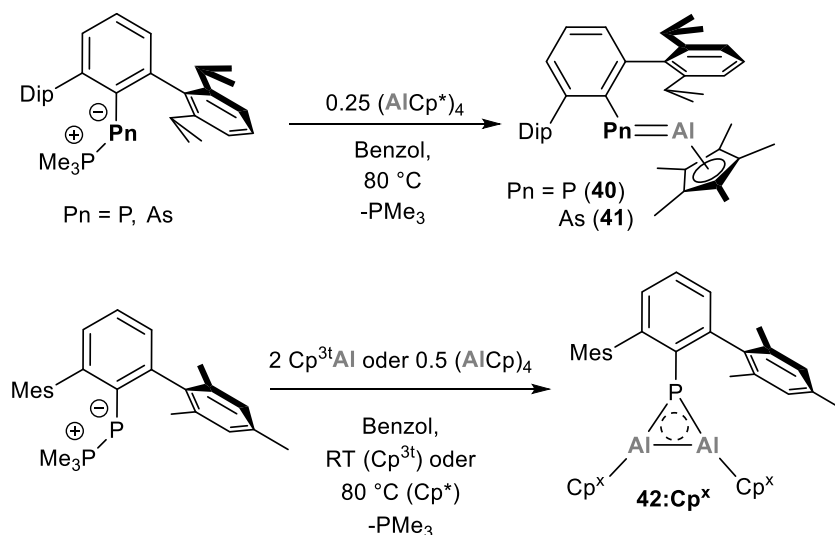
Es ist damit zu rechnen, dass die Synthese von schwereren $E^{13}-N$ -Dreifachbindungen nur eine Frage der Zeit ist. Theoretische Studien haben gezeigt, dass solche Systeme unter Verwendung von sterisch anspruchsvollen Ligandensystemen stabil sind. Es wird interessant sein, neuartige Al(I)-Vorstufen zu verwenden, um mehr monomere Aluminiumimide herzustellen und ihr Potenzial bei der Aktivierung kleiner Moleküle systematisch zu untersuchen.

2.4.3 Mehrfachbindungen zwischen Al und P, As

Bei den Mehrfachbindungen von Al–P und Al–As ist die Zahl der Verbindungen noch geringer. Es wurde über verschiedene Ansätze Al–P-Doppelbindungen zu erhalten berichtet, jedoch verhinderte die Bildung oligomerer Spezies deren Realisierung.^[175, 202] Darüber hinaus haben verschiedene Festkörperreaktionen zwar Verbindungen hervorgebracht, die der allgemeinen Formel $A_3[MPn_2]$ ($A = Na, K; M = Al, Ga, In; Pn = P, As$) genügen, aber die Struktur des Anions in diesen Salzen entspricht nicht der Propadienstruktur von $[BPn_2]^{3-}$ ($Pn = P, As$), in welchen B–Pn-Mehrfachbindungen denkbar sind. Die Substitution von B durch Al, Ga oder In ergibt vielmehr polymere Strukturen, die nach einer reduzierten Niggli-Darstellung als $\frac{1}{\infty}[(E^{13}Pn_{4/2})^{3-}]$ ($E^{13} = Al, Ga, In; Pn = Al, Ga \text{ oder } In$) beschrieben werden können.^[203] Die Stabilisierung von Al–P- oder Al–As-Mehrfachbindungen erfordert daher eine gezielte Wahl der Al- und Pn-Vorstufenmoleküle.

Im Rahmen dieser Arbeit konnte ein Syntheseprotokoll für den Zugang zu Phospha- und Arsaalumenen erarbeitet werden. Dieses Protokoll basiert auf einem Al(I)- in Kombination mit einem Pnictiniden-Vorstufenmolekül. Dies ist in Analogie zur Bildung von Al–N-Mehrfachbindungen ausgehend von Al(I)-Vorstufen in Gegenwart von Aziden, welche als maskierte Nitrene aufgefasst werden können (siehe vorheriges Kapitel). Wie bereits erwähnt, sind Pnictinidene meist kurzlebig und schwer zu handhaben. Daher erwiesen sich die zuvor diskutierten Phospha- und Arsa-Wittig-Reagenzien vom Typ $Ar-Pn(PMe_3)$ ($Pn = P$ (**9:Ar**), As (**10:Ar**)) als wertvolle synthetische Bausteine für das $Ar-Pn$ -Fragment unter der Freisetzung von PMe_3 (Schema 60). Die in Kapitel 2.2.4 beschriebenen Beispiele für eine effektive PMe_3 -Substitution veranlassten uns, die Reaktivität von $^{Dip}Ter-P(PMe_3)$ und $^{Dip}Ter-As(PMe_3)$ gegenüber geeigneten Al(I)-Vorstufen zu untersuchen. Als Al(I)-Quellen wurden $(AlCp^*)_4$, von dem bekannt ist, dass es in Lösung bei erhöhten Temperaturen in sein Monomer dissoziiert,^[204] oder das monomere $Cp^{3t}Al$ ^[205] ($Cp^{3t} = [1,2,4-tBu_3C_5H_2]^-$) verwendet. Bei 80 °C in Benzol reagierten sowohl $^{Dip}Ter-P(PMe_3)$ als auch $^{Dip}Ter-As(PMe_3)$ mit $(Cp^*Al)_4$ in einem Verhältnis von 4:1 zu den Phospha- (**40**) und Arsalumenen (**41**) $^{Dip}TerPn=AlCp^*$ ($Pn = P, As$) als bemerkenswert stabile violette bzw. blaue kristalline Verbindungen (Schema 60, oben).^[67] Dabei verdrängte das Cp^*Al -Fragment PMe_3 in einer insgesamt exergonischen Reaktion ($\Delta_R G^\circ_{298K} = -51.2$ (**40**); $-60.9 \text{ kJ}\cdot\text{mol}^{-1}$ (**41**)), wie es mit Hilfe von DFT-Rechnungen ermittelt wurde. Das ^{31}P -NMR-Signal für **40** bei -203.9 ppm lässt sich gut mit der ^{31}P -NMR-Resonanz des Phosphagallens [$(^{Dip}Nacnac)Ga=P-Ga(Cl)(^{Dip}Nacnac)$] vergleichen,^[206] die bei -245.8 ppm gefunden wurde (siehe nächstes Kapitel) und auf ein elektronenreiches Phosphoratom und eine

polarisierte P–Al-Doppelbindung hinweist. Die Atomabstände zwischen Al und P bzw. As haben Werte von 2.2113(6) Å (P) und 2.3084(4) Å (As) und stehen damit im Einklang mit einem gewissen Mehrfachbindungscharakter (Σr_{cov} (Al=P) = 2.15 Å, (Al=As) 2.27 Å) (Abbildung 8).^[78] Auf der Basis von DFT-Rechnungen konnte gezeigt werden, dass die HOMOs wesentliche Beiträge für polarisierte Pn–Al π -Bindungen zeigen, während das HOMO-1 die Pn–Al σ -Bindungen repräsentiert und das LUMO Pn–Al σ^* -Charakter hat.



Schema 60. Synthese von Phospha- (**40**) und Arsaaluminen (**41**) ausgehend von $\text{Dip}^{\text{T}}\text{Ter-Pn}(\text{PMe}_3)$ (oben), wohingegen mit $\text{Mes}^{\text{T}}\text{Ter-P}(\text{PMe}_3)$ 2π -aromatische PA_2 -Ringsysteme erhalten wurden.

Die WBOs von 1.47 (P) und 1.46 (As) zusammen mit natürlichen Ladungen von -0.37 bzw. -0.36 an den P- bzw. As-Atomen sowie positiven Partialladungen am Al-Atom (ca. $+1.3$) unterstützen das Bild von stark polarisierten (in Richtung von Pn) Pn–Al-Bindungen. Erstaunlicherweise ist keine elektronische Stabilisierung mit einer Lewis-Base notwendig, wie zuvor bei den Phosphaborenen beobachtet, jedoch ist die Rolle des η^5 -koordinierten Cp^* -Liganden entscheidend für die Stabilisierung. Dies beweist eindeutig, dass Pnicta-Wittig-Reagenzien in Kombination mit einer niedervalenten Gruppe-13-Verbindung eine ideale Kombination zur Erzeugung von Pnictatrielen darstellen. Der Wechsel von einem $\text{Dip}^{\text{T}}\text{Ter}$ - zu einem $\text{Mes}^{\text{T}}\text{Ter}$ -Substituenten ermöglichte den Zugang zu einer anderen, jedoch verwandten Klasse von Verbindungen. Die Reaktion von $\text{Mes}^{\text{T}}\text{Ter-P}(\text{PMe}_3)$ mit $(\text{Cp}^*\text{Al})_4$ sowie mit $\text{Cp}^{3\text{t}}\text{Al}$ ergab $[\text{Mes}^{\text{T}}\text{TerP}(\text{AlR})_2]$ ($\text{R} = \text{Cp}^*, \text{Cp}^{3\text{t}}$) (**42:Cp^x**; $x = 3\text{t}, *$), die als 2π -aromatische Verbindungen identifiziert wurden (Schema 60, unten) und als schwere Homologe des Cyclopropenyl-Kations aufzufassen sind.^[207]

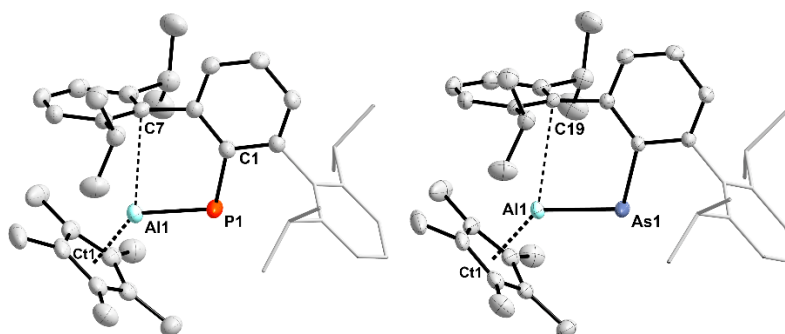
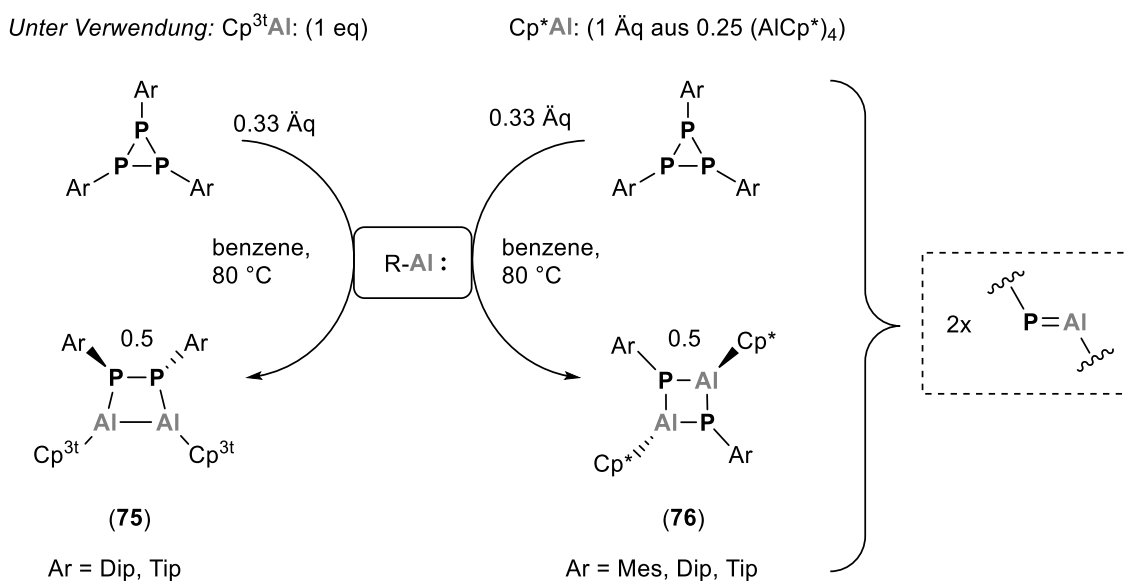


Abbildung 8. Molekülstrukturen der Pnictaalumene **40** (links) und **41** (rechts).

Zusätzlich haben wir untersucht inwieweit Cyclooligophosphane des Typs P_3Ar_3 (**18:Ar**; Ar = Mes, Dip, Tip) oder P_5Ph_5 (**16**) als Phosphiniden-Reservoir in der Reaktion mit $(Cp^*Al)_4$ und $Cp^{3t}Al$ eingesetzt werden können. Die Reaktion von **18:Ar** (Ar = Dip, Tip) mit 3 Äquivalenten $Cp^{3t}Al$ ergab die Kopf-Kopf-verbrückten 1,2-Diphospha-3,4-dialuminacyclobutane $[Cp^{3t}AlPAR]_2$ (**43**) (Schema 61, links), die formalen Dimere der gewünschten Phosphaalumene.^[170] Wenn entweder **18:Mes** oder **16** in der Reaktion mit $Cp^{3t}Al$ verwendet werden, wurden die alternierenden Dimere $[Cp^{3t}Al(\mu-PAr)]_2$ (Ar = Ph, Mes) erhalten. Ähnliche Basen-freie 1,3-Diphospha-2,4-dialane $[Cp^*Al(\mu-PAr)]_2$ (**44**, Ar = Mes, Dip, Tip) wurden unter Verwendung von $(Cp^*Al)_4$ als Aluminiumquelle erhalten (Schema 61, rechts), was auch auf die entsprechenden 1,3-Diarsa-2,4-Dialane erweitert werden konnte (siehe Kapitel 2.3.5). Versuche, das 1,3-Diphospha-2,4-dialan $[Cp^{3t}Al(\mu-PPh)]_2$ durch Zugabe des NHCs $LiPr_2$ ($LiPr_2 = (HCNiPr)_2C:$) in die NHC-stabilisierten Monomer-Einheiten zu spalten, ergaben nur das entsprechende Bis-NHC-Addukt $[Cp^{3t}(LiPr_2)Al(\mu-PPh)]_2$. In Zukunft werden wir versuchen diese Basen-freien Dimere von Phospha- und Arsaalumenen durch die Zugabe geeigneter Lewis-Säuren und -Basen oder durch Thermolyse als Vorstufen für die entsprechenden Monomere zu verwenden. Die Reaktivität der isolierbaren Phospha- und Arsaalumenen wird derzeit untersucht und sollte neue Arten der Bindungsaktivierung ermöglichen. Da immer mehr Al(I)-Spezies synthetisch hergestellt werden können, wird erwartet, dass die Zahl der isolierbaren Phosphaalumene in den kommenden Jahren erheblich steigen wird.



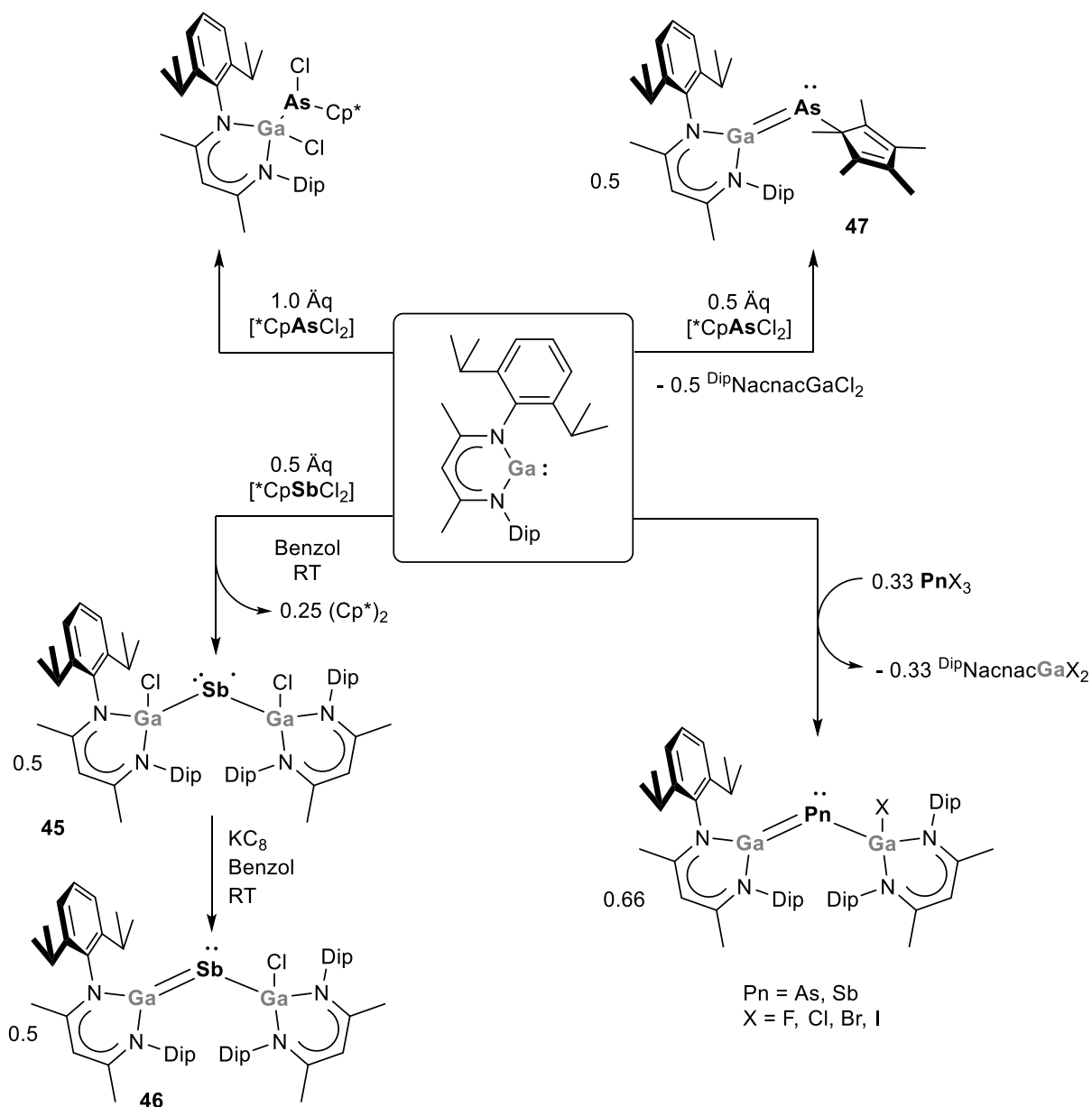
Schema 61. Synthese Basen-freier Kopf-Kopf verknüpfter 1,2-Diphospha-3,4-dialane (links) und von alternierenden 1,3-Diphospha-2,4-dialanen (rechts).

2.4.4 Mehrfachbindungen zwischen Ga und P, As, Sb

Von Hänisch und Mitarbeiter berichteten über ein Silyl-substituiertes Derivat des $[\text{Ga}_2\text{As}_4]^{6-}$ Anions, welches erstmals durch von Schnering beschrieben worden war.^[208] $[\{\text{Li}(\text{THF})_3\}_2\text{Ga}_2\{\text{As}(\text{SiiPr}_3)\}_4]$ wurde durch eine 1:2-Umsetzung von GaCl_3 mit $[\text{Li}_2\text{AsSiiPr}_3]$ in einer THF/Heptan-Lösung synthetisiert.^[209] Die Kristallstrukturbestimmung zeigte, dass die Anionen-Struktur einen Ga_2As_2 -Vierring mit zwei zusätzlichen, an Ga gebundenen exocyclischen As-Atomen aufweist. Der Abstand zwischen dem Ring-Ga- und dem exocyclischen As-Atom beträgt 2.318(2) Å (vgl. $\Sigma r_{\text{kov}}(\text{Ga}=\text{As}) = 2.31 \text{ Å}$),^[78] was auf eine Ga–As-Mehrfachbindung hinweist. Dies stellte den ersten direkten Nachweis für eine stabile Ga–Pn-Doppelbindung dar, jedoch ist die Verbindung in Lösung instabil und eine Untersuchung der Reaktivität war nicht möglich.

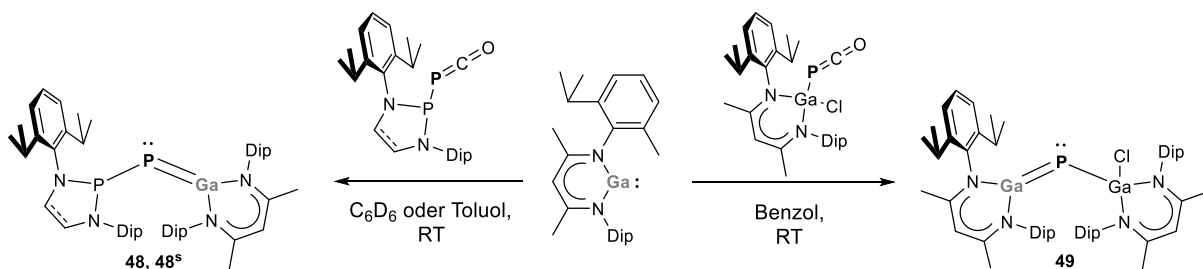
Es dauerte weitere 15 Jahre, bis Schulz und Mitarbeiter 2018 über weitere Ga–Pn-Doppelbindungen berichteten. Die Synthese des ersten Stibagallens basierte auf der Umsetzung von $[\text{DipNacnac}]\text{Ga}$ mit einem halben Äquivalent von $[\text{Cp}^*\text{SbCl}_2]$.^[210] Dabei entstand zunächst das Stibanylradikal $[\text{DipNacnac}(\text{Cl})\text{Ga}]_2\text{Sb}$ (**45**) unter gleichzeitiger Bildung eines halben Äquivalents $(\text{Cp}^*)_2$. Die chemische Reduktion von **45** mit KC_8 ergab dann $[(\text{DipNacnac})\text{Ga}=\text{Sb}-\text{Ga}(\text{Cl})(\text{DipNacnac})]$ (**46**) (Schema 16). **46** ist sowohl in Lösung als auch im festen Zustand stabil. Die Bestimmung der Molekülstruktur ergab zwei unterschiedliche Ga–Sb-Atomabstände von 2.5528(2) und 2.4629(2) Å (vgl. $\Sigma r_{\text{kov}}(\text{Ga}=\text{Sb}) = 2.50 \text{ Å}$).^[78] In ähnlicher

Weise erhielt die gleiche Gruppe in der Reaktion von $[\text{Cp}^*\text{AsCl}_2]$ mit zwei Äquivalenten $[\text{DipNacnac}]\text{Ga}$ das Arsagallen $[(\text{DipNacnac})\text{Ga}=\text{AsCp}^*]$ (**47**), eine stabile und lösliche Verbindung mit einer Ga–As-Doppelbindung (Schema 62, oben rechts).^[211] Der röntgenographisch bestimmte Ga–As-Atomabstand beträgt 2.2671(2) Å. Es ist bemerkenswert, dass die erfolgreiche Synthese von Ga–Pn-Doppelbindungen ausschließlich auf $[\text{DipNacnac}]\text{Ga}$ basiert. Durch geschickte Variationen der Stöchiometrie von $[\text{DipNacnac}]\text{Ga}$ in Kombination mit Halogen-substituierten Gruppe 15 Verbindungen wie $^{\text{Mes}}\text{TerSbCl}_2$ sowie AsX_3 (X = Cl, Br) oder SbX_3 (X = F, Cl, Br, I) konnten weitere Ga–As oder Ga–Sb-Mehrfachbindungssysteme hergestellt werden.^[212] In den letztgenannten Protokollen werden $[\text{DipNacnac}]\text{Ga}$ und PnX_3 in einem Verhältnis von 3:1 kombiniert, was $[(\text{DipNacnac})\text{Ga}=\text{Pn}-\text{Ga}(\text{X})(\text{DipNacnac})]$ (X = F, Cl, Br, I) bei gleichzeitiger Eliminierung von $[\text{DipNacnac}]\text{GaX}_2$ ergibt und einen schnellen und einfachen Zugang zu einer Reihe neuer Verbindungen ermöglicht (Schema 62, unten rechts). Diese Erfolge in der Realisierung von Ga–Pn-Mehrfachbindungen, ebneten den Weg für die Synthese von bis dahin unbekanntem Phosphagallen.



Schema 62. Synthese von Arsa- und Stibagallanen ausgehend von der Ga(I)-Verbindung $[\text{DipNacnac}]Ga$.

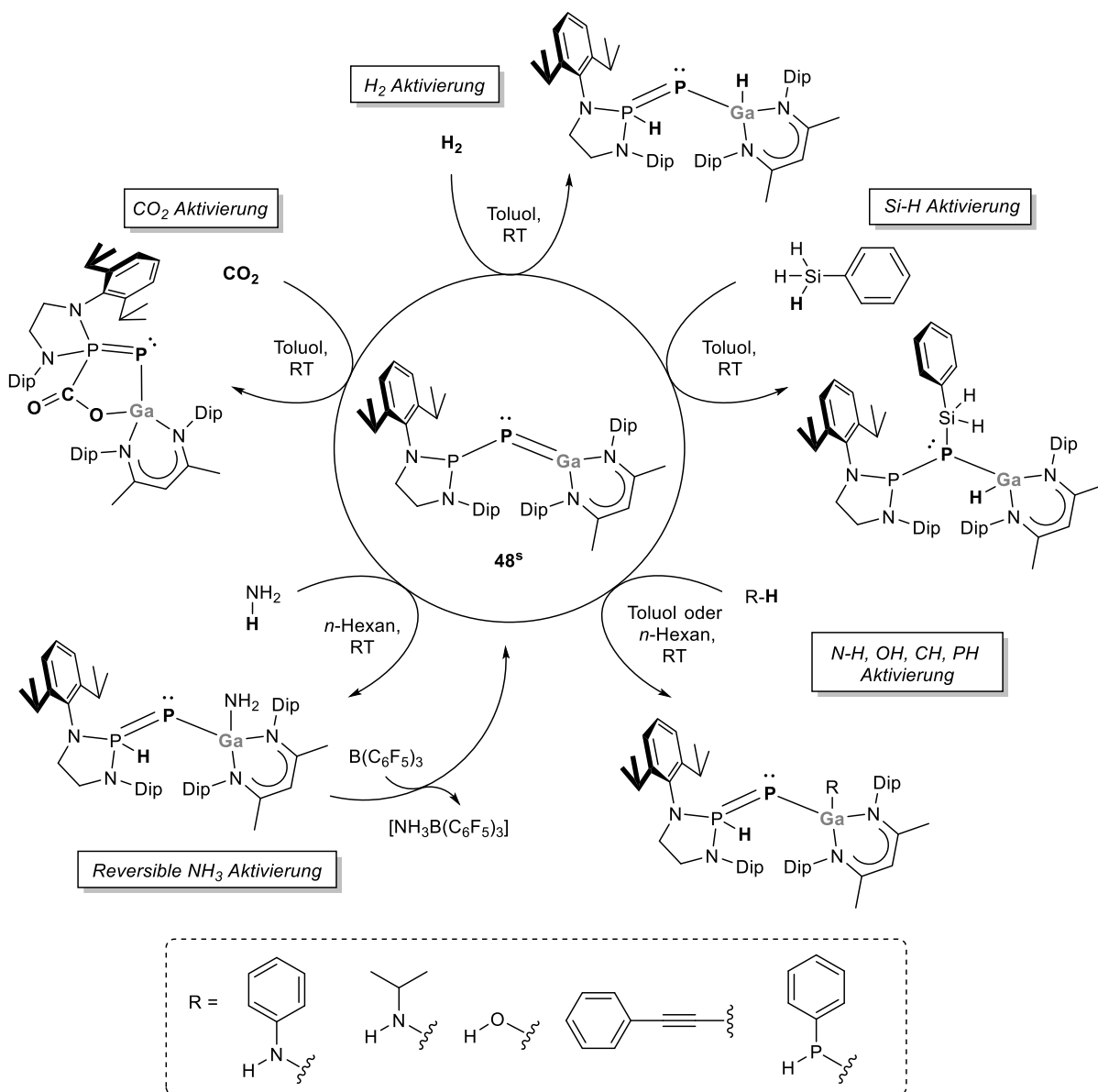
Die Gruppe um Goicoechea berichtete über die Reaktion verschiedener Phosphanylphosphaketene mit $[\text{DipNacnac}]Ga$. Die Reaktion von $[\text{P}^{\text{Dip}}]\text{PCO}$ oder $[\text{sP}^{\text{Dip}}]\text{PCO}$ ($[\text{P}^{\text{Dip}}] = [(\text{HCNDip})_2\text{P}]$) mit $[\text{DipNacnac}]Ga$ ergab unter CO-Abspaltung die Phosphagallene $[(\text{DipNacnac})Ga=\text{P}(\text{P}^{\text{Dip}})/(\text{sP}^{\text{Dip}})]$ (P^{Dip} : **48**; sP^{Dip} : **48^s**) (Schema 63, links).^[213] Anhand von SC-XRD-Experimenten wurden Ga–P-Atomabstände von 2.1650(7) bzw. 2.1766(3) Å gefunden (vgl. $\Sigma r_{\text{cov}}(\text{Ga}=\text{P}) = 2.19 \text{ \AA}$).^[78] Quantenchemische Berechnungen des gesättigten Derivats **48^s** bestätigen die kurzen Ga–P-Atomabstände, wobei das HOMO freie Elektronenpaare an beiden P-Atomen darstellt und das HOMO -1 die π -Bindungswechselwirkung widerspiegelt.



Schema 63. Phosphagallene können ausgehend von Phosphanyl- (links) und Galliumphosphaketenen (rechts) in einer Decarbonylierungsreaktion dargestellt werden.

Schulz *et al.* berichteten über einen weiteren Syntheseweg zu Phosphagallenen. In scheinbar ähnlicher Weise führte die Decarbonylierung von $[(^{\text{Dip}}\text{Nacnac})\text{Ga}(\text{Cl})\text{PCO}]$ in Gegenwart von $[(^{\text{Dip}}\text{Nacnac})\text{Ga}]$ zu $[(^{\text{Dip}}\text{Nacnac})\text{Ga}(\text{Cl})\text{-P}=\text{Ga}(^{\text{Dip}}\text{Nacnac})]$ (**49**; Schema 63, rechts).^[206] Die Molekülstruktur veranschaulicht sehr schön die Ähnlichkeiten zu den in Schema 62 dargestellten Verbindungen, und der kurze Ga=P-Atomabstand von 2.1613(6) Å weist ebenso wie die berechnete Mayer-Bindungsordnungen von 1.077 und 1.709 auf benachbarte Ga–P- und Ga=P-Bindungen hin. Die ^{31}P -NMR-Verschiebung von **49** bei –245.8 ppm zeigt eine signifikante Entschirmung im Vergleich zum Vorstufenmolekül $[(^{\text{Dip}}\text{Nacnac})\text{Ga}(\text{Cl})\text{PCO}]$ (–371,4 ppm) an.

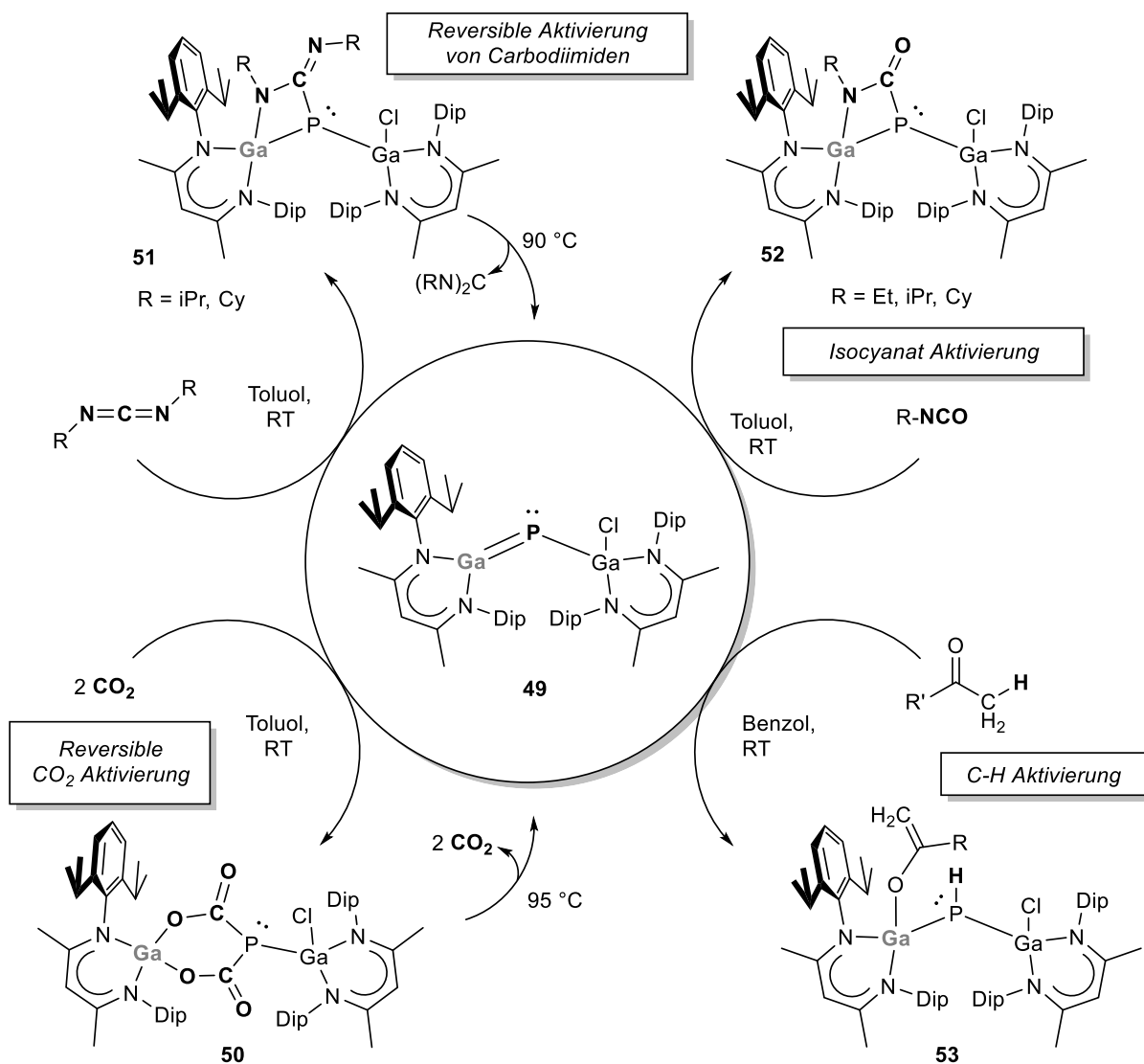
Im Folgenden soll die Reaktivität der Phosphagallene noch näher diskutiert werden. Bemerkenswert ist in diesem Zusammenhang, dass **48** mit einem ungesättigten Rückgrat in der Phosphanylgruppe empfindlich gegenüber einer Liganden-Umlagerung reagiert, ähnlich den Beobachtungen, die Cui zuvor für Al–N-Mehrfachbindungssysteme gemacht hat. Das Ga(I)-Zentrum schiebt sich in das Liganden-Rückgrat ein und bildet einen fünfgliedrigen C–N–P=P–Ga-Ring. Darüber hinaus wurde gezeigt, dass sowohl CO_2 als auch H_2 unter Verwendung des stabilen Phosphagallens **48**^s in einer FLP-artigen Reaktion aktiviert werden können.^[213] Für CO_2 wird eine Verbindung mit einem P=P–C–O–Ga-Fünfring erhalten, während H_2 in einer 1,3-Addition an die P=P=Ga-Einheit addiert wird (Schema 64). In einer Folgestudie zeigte dieselbe Gruppe, dass Ammoniak, eine Reihe primärer Amine, Wasser, Phenylacetylen und Phenylphosphin ebenfalls in einem ähnlichen 1,3-Additionsmuster E–H-aktiviert werden können (E = N, O, C, P) (Schema 64).^[214] Eine Ausnahme bildet die Si–H-Bindungsaktivierung von H_3SiPh . Hier folgt die Reaktion einer 1,2-Addition allein über die Ga–P-Doppelbindung, die nach DFT-Rechnungen als σ -Bindungsmetathese abläuft. Erstaunlich ist, dass die Addition von Ammoniak an **48**^s reversibel ist. Durch Zugabe einer Lewis-Säure wie $\text{B}(\text{C}_6\text{F}_5)_3$ wird NH_3 abstrahiert, und das Gallaphosphen wird zurückgebildet.



Schema 64. Vielseitige Reaktivität des Phosphagallens **48^s**.

Während in Phosphanylphosphagallenen zumeist 1,3-Additionen beobachtet werden, wurde festgestellt, dass **49** direkt an der Ga–P-Doppelbindung und damit immer unter 1,2-Addition reagiert. Schulz und Mitarbeiter zeigten, dass dieses System für die Aktivierung von Kohlendioxid, Carbodiimiden, Isocyanaten, Aminen, Thiolen, Selenolen und Ketonen eingesetzt werden kann (Schema 65).^[206, 215] Zum Beispiel ergab die Aktivierung von zwei Molekülen CO₂ sechsgliedrige PC₂O₂Ga-Heterocyclen (**50**) mit einer Boot-Konformation wobei die P–Ga-Bindung gespalten wurde. Die Aktivierung von Carbodiimiden (**51**) und Isocyanaten (**52**) ergab viergliedrige Metallheterozyklen nach einer [2+2]-Cycloaddition. Die Reaktionen mit CO₂ und Carbodiimiden sind vollständig reversibel und das Gallaphosphen konnte bei erhöhten Temperaturen quantitativ regeneriert werden. Ketone folgten jedoch keiner

[2+2]-Cycloaddition, stattdessen erfolgte eine chemoselektive intermolekulare C(sp³)-H-Aktivierung mit Bildung einer P-H- und einer Ga-O-Bindung (siehe 53, Schema 65). Im Gegensatz zur CO₂- und Carbodiimid-Aktivierung sind die Reaktionen mit Isocyanaten und Ketonen irreversibel.^[215a] Erst kürzlich wurde gezeigt, dass auch Amine (NH₃, NH₂R), Alkohole, Thiole und Selenole quantitativ und chemoselektiv in einer 1,2-Addition an der Ga-P-Einheit aktiviert werden, wobei das Proton jeweils am P-Atom und der Lewis-basische Rest am Ga-Atom sitzt.^[215b] Insgesamt konnte gezeigt werden, dass sowohl die P=Ga-Systeme von Goicoechea als auch die von Schulz eine Vielzahl verschiedener chemischer Bindungen aktivieren und dass die Umwandlungen in einigen Fällen reversibel sind, was eindeutig einen Durchbruch in Bezug auf mögliche katalytische Anwendungen von Pn=Ga-Mehrfachbindungen darstellt.



Schema 65. Vielseitige Reaktivitäten des Gallium-substituierten Phosphagallens **49**.

3 Zusammenfassung

Auch ca. 250 Jahre nach ersten Untersuchungen zur Synthese des Phosphobenzols (Ph-P)₂ durch Michaelis und Köhler steht die Chemie niedervalenter Phosphorverbindungen im Fokus aktueller Forschung. Insbesondere Phosphinidene und Verbindungen, die eine Phosphiniden-Einheit übertragen können, Cyclooligophosphane und Verbindungen mit Mehrfachbindungen zwischen Elementen der Gruppe 13 und 15 sind von großem wissenschaftlichem Interesse.

Wir haben verschiedene Punkte dieser Fragestellungen bearbeitet und konnten überzeugend darlegen, dass Phosphanlyliden-σ⁴-phosphorane ideale Phosphiniden-Transferreagenzien in Analogie zu organischen Aziden darstellen. So haben wir gezeigt, dass Phospha- und Arsa-Wittig-Reagenzien in großem Maßstab dargestellt und isoliert werden können, wohingegen bekannte Syntheseprotokolle zumeist die Isolierung dieser Spezies umgehen und diese *in situ* einsetzen. Darüber hinaus ist es gelungen die Phosphiniden-Einheit zu übertragen und es können auf diesem Wege NHC-Phosphiniden-Addukte, P-substituierte NHOs, Phosphaazaallene und terminale Titanocen-Phosphiniden-Komplexe dargestellt werden.

Versuche Phosphanlyliden-σ⁴-phosphorane mit kleineren Gruppen am P-Atom darzustellen waren nicht erfolgreich, jedoch wurde ein selektiver Syntheseweg zu Aryl-substituierten Cyclotriphosphanen gefunden. Diese Phosphordreiringssysteme konnten mit einem Titanocen-Vorstufen-Komplex in Titanocen-Diphosphen-Komplexe umgewandelt werden. Ebenso wurde das Syntheseprotokoll genutzt, um die ersten Beispiele von Aryl-substituierten Cyclotriarsanen zu erhalten. In diesem Zusammenhang konnte auch ein katalytischer reduktiver Pfad zu Diphosphanen und Diphosphenen etabliert werden

Auf dem Gebiet der heteroatomaren Mehrfachbindungen zwischen Aluminium und Phosphor (und Arsen) berichteten wir über die ersten Beispiele für Phospha- und Arsaalumene, sowie 2π-aromatische PA₁₂-Ringe durch die Umsetzung von Phospha- bzw. Arsa-Wittig Reagenzien mit Al(I)-Vorstufen. Die Kombination von Al(I)-Verbindungen mit Cyclotriphosphanen oder -arsanen resultierte in der Bildung von Basen-freien Dipnictadialanen, den formalen Dimeren der korrespondierenden Phospha- und Arsaalumene.

4 Referenzen

- [1] G. Ogilvy, *The Alchemist's Kitchen: Extraordinary Potions & Curious Notions*, Bloomsbury USA, **2006**.
- [2] J. Emsley, *The 13th Element: The Sordid Tale of Murder, Fire, and Phosphorus*, Wiley, **2002**.
- [3] J. P. W. Hughes, R. Baron, D. H. Buckland, M. A. Cooke, J. D. Craig, D. P. Duffield, A. W. Grosart, P. W. J. Parkes, A. Porter, *Br. J. Ind. Med.* **1962**, *19*, 83.
- [4] R. Redaktion, H. Martens, Thieme Gruppe, **2017**.
- [5] N. N. Greenwood, A. Earnshaw, *Chemistry of the Elements*, Elsevier, **2012**.
- [6] P. W. Bridgman, *J. Am. Chem. Soc.* **1914**, *36*, 1344-1363.
- [7] M. E. Schlesinger, *Chem. Rev.* **2002**, *102*, 4267-4302.
- [8] D. Warschauer, **1963**, *34*, 1853-1860.
- [9] a) R. Wild, R. Gerasimaite, J.-Y. Jung, V. Truffault, I. Pavlovic, A. Schmidt, A. Saiardi, J. Jessen Henning, Y. Poirier, M. Hothorn, A. Mayer, *Science* **2016**, *352*, 986-990; b) C. Azevedo, A. Saiardi, *Trends Biochem. Sci.* **2017**, *42*, 219-231.
- [10] F. H. Westheimer, *Science* **1987**, *235*, 1173-1178.
- [11] W. Schipper, *Eur. J. Inorg. Chem.* **2014**, *2014*, 1567-1571.
- [12] R. Scholz, in *Phosphorus recovery and recycling* (Eds.: H. Ohtake, S. Tsuneda), Springer, **2019**.
- [13] C. C. Cummins, *Daedalus* **2014**, *143*, 9-20.
- [14] H. Müller, H. Müller, *DOI* **2000**, *10*, a25_635.
- [15] M. B. Geeson, C. C. Cummins, *ACS Central Science* **2020**, *6*, 848-860.
- [16] H. Diskowski, T. Hofmann, Wiley, **2000**.
- [17] P. T. Anastas, J. C. Warner, *Frontiers* **1998**, *640*, 1998.
- [18] a) G. Wittig, G. Geissler, *Justus Liebigs Ann. Chem.* **1953**, *580*, 44-57; b) G. Wittig, U. Schöllkopf, *Chem. Ber.* **1954**, *87*, 1318-1330.
- [19] M. Oyo, Y. Masaaki, *Bull. Chem. Soc. Jpn.* **1967**, *40*, 2380-2382.
- [20] L. Schreyer, R. Properzi, B. List, *Angew. Chem. Int. Ed.* **2019**, *58*, 12761-12777.
- [21] C. D. Díaz-Oviedo, R. Maji, B. List, *J. Am. Chem. Soc.* **2021**, *143*, 20598-20604.
- [22] J. A. Gillespie, E. Zuidema, P. W. N. M. van Leeuwen, P. C. J. Kamer, in *Phosphorus(III) Ligands in Homogeneous Catalysis: Design and Synthesis*, pp. 1-26.
- [23] E. Yamasue, K. Matsubae, in *Phosphorus Recovery and Recycling* (Eds.: H. Ohtake, S. Tsuneda), Springer, Singapore, **2019**.
- [24] H. Liu, A. T. Neal, Z. Zhu, Z. Luo, X. Xu, D. Tománek, P. D. Ye, *ACS Nano* **2014**, *8*, 4033-4041.
- [25] D. Bourissou, O. Guerret, F. P. Gabbaï, G. Bertrand, *Chem. Rev.* **2000**, *100*, 39-92.
- [26] A. Igau, H. Grutzmacher, A. Baceiredo, G. Bertrand, *J. Am. Chem. Soc.* **1988**, *110*, 6463-6466.
- [27] A. J. Arduengo, R. L. Harlow, M. Kline, *J. Am. Chem. Soc.* **1991**, *113*, 361-363.
- [28] a) F. E. Hahn, M. C. Jahnke, *Angew. Chem. Int. Ed.* **2008**, *47*, 3122-3172; b) T. Dröge, F. Glorius, *Angew. Chem. Int. Ed.* **2010**, *49*, 6940-6952; c) D. Munz, *Organometallics* **2018**, *37*, 275-289.
- [29] W. A. Herrmann, *Angew. Chem. Int. Ed.* **2002**, *41*, 1290-1309.

- [30] C. A. Smith, M. R. Narouz, P. A. Lummis, I. Singh, A. Nazemi, C.-H. Li, C. M. Crudden, *Chem. Rev.* **2019**, *119*, 4986-5056.
- [31] a) L. Oehninger, R. Rubbiani, I. Ott, *Dalton Trans.* **2013**, *42*, 3269-3284; b) R. M. Mayall, C. A. Smith, A. S. Hyla, D. S. Lee, C. M. Crudden, V. I. Birss, *ACS Sensors* **2020**, *5*, 2747-2752.
- [32] R. Hoffmann, *Angew. Chem. Int. Ed. Engl.* **1982**, *21*, 711-724.
- [33] L. Dostál, *Coord. Chem. Rev.* **2017**, *353*, 142-158.
- [34] a) J. Glatthaar, G. Maier, *Angew. Chem. Int. Ed.* **2004**, *43*, 1294-1296; b) G. Bucher, M. L. G. Borst, A. W. Ehlers, K. Lammertsma, S. Ceola, M. Huber, D. Grote, W. Sander, *Angew. Chem. Int. Ed.* **2005**, *44*, 3289-3293; c) J. J. Harrison, B. E. Williamson, *J. Phys. Chem. A* **2005**, *109*, 1343-1347.
- [35] A. Mardiyukov, D. Niedek, P. R. Schreiner, *J. Am. Chem. Soc.* **2017**, *139*, 5019-5022.
- [36] X. Li, D. Lei, M. Y. Chiang, P. P. Gaspar, *J. Am. Chem. Soc.* **1992**, *114*, 8526-8531.
- [37] A. H. Cowley, F. Gabbai, R. Schluter, D. Atwood, *J. Am. Chem. Soc.* **1992**, *114*, 3142-3144.
- [38] F. Dielmann, O. Back, M. Henry-Ellinger, P. Jerabek, G. Frenking, G. Bertrand, *Science* **2012**, *337*, 1526-1528.
- [39] Z. Benkő, R. Streubel, L. Nyulászi, *Dalton Trans.* **2006**, 4321-4327.
- [40] M. T. Nguyen, A. Van Keer, L. G. Vanquickenborne, *J. Org. Chem.* **1996**, *61*, 7077-7084.
- [41] L. Liu, David A. Ruiz, D. Munz, G. Bertrand, *Chem* **2016**, *1*, 147-153.
- [42] D. Martin, A. Baceiredo, H. Gornitzka, W. W. Schoeller, G. Bertrand, *Angew. Chem. Int. Ed.* **2005**, *44*, 1700-1703.
- [43] a) N. B. Feilchenfeld, W. H. Waddell, *Chem. Phys. Lett.* **1983**, *98*, 190-194; b) N. P. Gritsan, T. Yuzawa, M. S. Platz, *J. Am. Chem. Soc.* **1997**, *119*, 5059-5060.
- [44] R. Appel, W. Paulen, *Angew. Chem. Int. Ed. Engl.* **1983**, *22*, 785-786.
- [45] J. M. Goicoechea, H. Grützmacher, *Angew. Chem. Int. Ed.* **2018**, *57*, 16968-16994.
- [46] L. Weber, *Chem. Rev.* **1992**, *92*, 1839-1906.
- [47] W. H. Powell, *Pure Appl. Chem.* **1982**, *54*, 217-228.
- [48] W. Mahler, A. B. Burg, *J. Am. Chem. Soc.* **1958**, *80*, 6161-6167.
- [49] A. B. Burg, W. Mahler, *J. Am. Chem. Soc.* **1961**, *83*, 2388-2389.
- [50] A. H. Cowley, M. C. Cushner, *Inorg. Chem.* **1980**, *19*, 515-518.
- [51] D. Weber, E. Fluck, *Z. anorg. allg. Chem.* **1976**, *424*, 103-107.
- [52] F. Zurmühlen, M. Regitz, *Angew. Chem. Int. Ed. Engl.* **1987**, *26*, 83-84.
- [53] F. Zurmühlen, M. Regitz, *New J. Chem.* **1989**, *13*, 335-340.
- [54] D. Bevern, H. Görls, S. Krieck, M. Westerhausen, *Z. anorg. allg. Chem.* **2020**, *646*, 948-958.
- [55] D. Bevern, F. E. Pröhl, H. Görls, S. Krieck, M. Westerhausen, *Organometallics* **2021**, *40*, 1744-1750.
- [56] G. Fritz, T. Vaahs, H. Fleischer, E. Matern, *Angew. Chem. Int. Ed. Engl.* **1989**, *28*, 315-316.
- [57] G. Fritz, P. Scheer, *Chem. Rev.* **2000**, *100*, 3341-3402.
- [58] E. Matern, C. E. Anson, E. Baum, E. Sattler, I. Kovács, *Eur. J. Inorg. Chem.* **2020**, *2020*, 1311-1318.
- [59] T. L. Breen, D. W. Stephan, *J. Am. Chem. Soc.* **1995**, *117*, 11914-11921.
- [60] E. Urnėžius, S. Shah, J. D. Protasiewicz, *Phosphorus Sulfur Silicon Relat. Elem.* **1999**, *144*, 137-139.
- [61] S. Shah, J. D. Protasiewicz, *Chem. Commun.* **1998**, 1585-1586.
- [62] R. C. Smith, T. Ren, John D. Protasiewicz, *Eur. J. Inorg. Chem.* **2002**, *2002*, 2779-2783.
- [63] S. Shah, G. P. A. Yap, J. D. Protasiewicz, *J. Organomet. Chem.* **2000**, *608*, 12-20.

- [64] P. Gupta, J.-E. Siewert, T. Wellnitz, M. Fischer, W. Baumann, T. Beweries, C. Hering-Junghans, *Dalton Trans.* **2021**, *50*, 1838-1844.
- [65] S. Shah, M. C. Simpson, R. C. Smith, J. D. Protasiewicz, *J. Am. Chem. Soc.* **2001**, *123*, 6925-6926.
- [66] R. C. Smith, P. Gantzel, A. L. Rheingold, J. D. Protasiewicz, *Organometallics* **2004**, *23*, 5124-5126.
- [67] M. Fischer, S. Nees, T. Kupfer, J. T. Goettel, H. Braunschweig, C. Hering-Junghans, *J. Am. Chem. Soc.* **2021**, *143*, 4106-4111.
- [68] M. Fischer, F. Reiß, C. Hering-Junghans, *Chem. Commun.* **2021**, *57*, 5626-5629.
- [69] J.-E. Siewert, A. Schumann, M. Fischer, C. Schmidt, T. Taeufer, C. Hering-Junghans, *Dalton Trans.* **2020**, *49*, 12354-12364.
- [70] P. Wawrzyniak, A. L. Fuller, A. M. Z. Slawin, P. Kilian, *Inorg. Chem.* **2009**, *48*, 2500-2506.
- [71] B. A. Surgenor, M. Bühl, A. M. Z. Slawin, J. D. Woollins, P. Kilian, *Angew. Chem. Int. Ed.* **2012**, *51*, 10150-10153.
- [72] B. A. Chalmers, M. Bühl, K. S. Athukorala Arachchige, A. M. Z. Slawin, P. Kilian, *J. Am. Chem. Soc.* **2014**, *136*, 6247-6250.
- [73] L. J. Taylor, M. Bühl, P. Wawrzyniak, B. A. Chalmers, J. D. Woollins, A. M. Z. Slawin, A. L. Fuller, P. Kilian, *Eur. J. Inorg. Chem.* **2016**, *2016*, 659-666.
- [74] D. W. N. Wilson, W. K. Myers, J. M. Goicoechea, *Dalton Trans.* **2020**, *49*, 15249-15255.
- [75] S. Bestgen, M. Mehta, T. C. Johnstone, P. W. Roesky, J. M. Goicoechea, *Chem. Eur. J.* **2020**, *26*, 9024-9031.
- [76] D. Raiser, K. Eichele, H. Schubert, L. Wesemann, *Chem. Eur. J.* **2021**, *27*, 14073-14080.
- [77] C. N. Smit, T. A. van der Knaap, F. Bickelhaupt, *Tetrahedron Lett.* **1983**, *24*, 2031-2034.
- [78] P. Pyykkö, M. Atsumi, *Chem. Eur. J.* **2009**, *15*, 12770-12779.
- [79] M. M. Hansmann, R. Jazzar, G. Bertrand, *J. Am. Chem. Soc.* **2016**, *138*, 8356-8359.
- [80] M. M. Hansmann, G. Bertrand, *J. Am. Chem. Soc.* **2016**, *138*, 15885-15888.
- [81] I. Kovacs, V. Balema, A. Bassowa, E. Matern, E. Sattler, G. Fritz, H. Borrmann, R. Bauernschmitt, R. Ahlrichs, *Z. anorg. allg. Chem.* **1994**, *620*, 2033-2040.
- [82] A. B. Burg, *J. Inorg. Nucl. Chem.* **1971**, *33*, 1575-1581.
- [83] D. V. Partyka, M. P. Washington, J. B. Updegraff III, R. A. Woloszynek, J. D. Protasiewicz, *Angew. Chem. Int. Ed.* **2008**, *47*, 7489-7492.
- [84] a) A. H. Cowley, J. E. Kilduff, J. G. Lasch, N. C. Norman, M. Pakulski, F. Ando, T. C. Wright, *J. Am. Chem. Soc.* **1983**, *105*, 7751-7752; b) A. H. Cowley, A. Decken, N. C. Norman, C. Krüger, F. Lutz, H. Jacobsen, T. Ziegler, *J. Am. Chem. Soc.* **1997**, *119*, 3389-3390.
- [85] B. A. Surgenor, B. A. Chalmers, K. S. Athukorala Arachchige, A. M. Z. Slawin, J. D. Woollins, M. Bühl, P. Kilian, *Inorg. Chem.* **2014**, *53*, 6856-6866.
- [86] A. B. Burg, K. K. Joshi, J. F. Nixon, *J. Am. Chem. Soc.* **1966**, *88*, 31-37.
- [87] I. Kovacs, G. Fritz, *Z. anorg. allg. Chem.* **1994**, *620*, 4-7.
- [88] E. Matern, G. Fritz, J. Pikies, *Z. anorg. allg. Chem.* **1997**, *623*, 1769-1773.
- [89] H. Krautscheid, E. Matern, I. Kovacs, G. Fritz, J. Pikies, *Z. anorg. allg. Chem.* **1997**, *623*, 1917-1924.
- [90] E. Matern, J. Olkowska-Oetzel, J. Pikies, G. Fritz, *Z. anorg. allg. Chem.* **2001**, *627*, 1767-1770.
- [91] Y. Masaaki, S. Takahiro, I. Naoki, *Chem. Lett.* **1988**, *17*, 1735-1738.
- [92] B. Twamley, C. D. Sofield, M. M. Olmstead, P. P. Power, *J. Am. Chem. Soc.* **1999**, *121*, 3357-3367.

- [93] R. C. Smith, S. Shah, E. Urnezius, J. D. Protasiewicz, *J. Am. Chem. Soc.* **2003**, *125*, 40-41.
- [94] X. Chen, R. C. Smith, J. D. Protasiewicz, *Chem. Commun.* **2004**, 146-147.
- [95] U. J. Kilgore, H. Fan, M. Pink, E. Urnezius, J. D. Protasiewicz, D. J. Mindiola, *Chem. Commun.* **2009**, 4521-4523.
- [96] T. Krachko, J. C. Sloopweg, *Eur. J. Inorg. Chem.* **2018**, *2018*, 2734-2754.
- [97] A. Doddi, M. Peters, M. Tamm, *Chem. Rev.* **2019**, *119*, 6994-7112.
- [98] a) K. Powers, C. Hering-Junghans, R. McDonald, M. J. Ferguson, E. Rivard, *Polyhedron* **2016**, *108*, 8-14; b) M. M. D. Roy, E. Rivard, *Acc. Chem. Res.* **2017**, *50*, 2017-2025; c) S. Naumann, *Chem. Commun.* **2019**, *55*, 11658-11670.
- [99] C. E. I. Knappke, J. M. Neudörfl, A. J. von Wangelin, *Org. Biomol. Chem.* **2010**, *8*, 1695-1705.
- [100] M. Fischer, C. Hering-Junghans, *Chem. Sci.* **2021**, *12*, 10279-10289.
- [101] A. Marinetti, F. Mathey, *Angew. Chem. Int. Ed. Engl.* **1988**, *27*, 1382-1384.
- [102] M. Yoshifuji, K. Toyota, N. Inamoto, *Tetrahedron Lett.* **1985**, *26*, 1727-1730.
- [103] a) K. W. Magnuson, S. M. Oshiro, J. R. Gurr, W. Y. Yoshida, M. Gembicky, A. L. Rheingold, R. P. Hughes, M. F. Cain, *Organometallics* **2016**, *35*, 855-859; b) P. M. Miura-Akagi, M. L. Nakashige, C. K. Maile, S. M. Oshiro, J. R. Gurr, W. Y. Yoshida, A. T. Royappa, C. E. Krause, A. L. Rheingold, R. P. Hughes, M. F. Cain, *Organometallics* **2016**, *35*, 2224-2231; c) K. Takeuchi, H.-o. Taguchi, I. Tanigawa, S. Tsujimoto, T. Matsuo, H. Tanaka, K. Yoshizawa, F. Ozawa, *Angew. Chem. Int. Ed.* **2016**, *55*, 15347-15350; d) M. L. Nakashige, J. I. P. Loristo, L. S. Wong, J. R. Gurr, T. J. O'Donnell, W. Y. Yoshida, A. L. Rheingold, R. P. Hughes, M. F. Cain, *Organometallics* **2019**, *38*, 3338-3348.
- [104] a) R. C. Smith, J. D. Protasiewicz, *J. Am. Chem. Soc.* **2004**, *126*, 2268-2269; b) R. C. Smith, J. D. Protasiewicz, *Eur. J. Inorg. Chem.* **2004**, *2004*, 998-1006.
- [105] H. Köhler, A. Michaelis, *Ber. Dtsch. Chem. Ges.* **1877**, *10*, 807-814.
- [106] a) J. J. Daly, *J. Chem. Soc.* **1964**, 6147-6166; b) J. J. Daly, L. Maier, *Nature* **1964**, *203*, 1167-1168.
- [107] M. Yoshifuji, I. Shima, N. Inamoto, K. Hirotsu, T. Higuchi, *J. Am. Chem. Soc.* **1981**, *103*, 4587-4589.
- [108] a) I. Haiduc, *The Chemistry of Inorganic Ring Systems*; Wiley-Interscience: London, **1970**, Part 1, 93; b) M. Baudler, *Angew. Chem. Int. Ed. Engl.* **1982**, *21*, 492-512; c) M. Baudler, K. Glinka, *Chem. Rev.* **1993**, *93*, 1623-1667.
- [109] K. B. Dillon, F. Mathey, J. F. Nixon, *Wiley, New York* **1998**.
- [110] J. J. Daly, *J. Chem. Soc.* **1965**, 4789-4799.
- [111] H. Schneider, D. Schmidt, U. Radius, *Chem. Commun.* **2015**, *51*, 10138-10141.
- [112] W. A. Henderson, M. Epstein, F. S. Seichter, *J. Am. Chem. Soc.* **1963**, *85*, 2462-2466.
- [113] M. Fild, I. Hollenberg, O. Glemser, *Sci. Nat.* **1967**, *54*, 89-90.
- [114] R. Wolf, A. Schisler, P. Lönnecke, C. Jones, E. Hey-Hawkins, *Eur. J. Inorg. Chem.* **2004**, *2004*, 3277-3286.
- [115] T. Grell, D. M. Yufanyi, A. K. Adhikari, M.-B. Sárosi, P. Lönnecke, E. Hey-Hawkins, *Pure Appl. Chem.* **2019**, *91*, 103.
- [116] A. K. Adhikari, M. B. Sárosi, T. Grell, P. Lönnecke, E. Hey-Hawkins, *Chem. Eur. J.* **2016**, *22*, 15664-15668.
- [117] R. Wolf, E. Hey-Hawkins, *Angew. Chem. Int. Ed.* **2005**, *44*, 6241-6244.
- [118] M. Baudler, K. Glinka, A. H. Cowley, M. Pakulski, *Inorg. Synth.: Organocyclophosphanes*, **2007**, H. R. Allcock (Ed.).
- [119] J. R. Goerlich, R. Schmutzler, *Z. anorg. allg. Chem.* **1994**, *620*, 173-176.
- [120] B. M. Cossairt, C. C. Cummins, *New J. Chem.* **2010**, *34*, 1533-1536.
- [121] A. Velian, C. C. Cummins, *J. Am. Chem. Soc.* **2012**, *134*, 13978-13981.

- [122] A. Orthaber, F. Belaj, R. Pietschnig, *J. Organomet. Chem.* **2010**, *695*, 974-980.
- [123] K. Issleib, M. Hoffmann, *Chem. Ber.* **1966**, *99*, 1320-1324.
- [124] M. Baudler, K. Hammerström, *Z. Naturforsch. B* **1965**, *20*, 810-811.
- [125] M. Scherer, D. Stein, F. Breher, J. Geier, H. Schönberg, H. Grützmacher, *Z. anorg. allg. Chem.* **2005**, *631*, 2770-2774.
- [126] J. C. Peters, A. R. Johnson, A. L. Odom, P. W. Wanandi, W. M. Davis, C. C. Cummins, *J. Am. Chem. Soc.* **1996**, *118*, 10175-10188.
- [127] M. Baudler, C. Pinner, C. Gruner, J. Hellmann, M. Schwamborn, B. Kloth, *Z. Naturforsch. B* **1977**, *32b*, 1244-1251.
- [128] C. A. Dyker, N. Burford, G. Menard, M. D. Lumsden, A. Decken, *Inorg. Chem.* **2007**, *46*, 4277-4285.
- [129] A. Schumann, F. Reiß, H. Jiao, J. Rabeah, J.-E. Siewert, I. Krummenacher, H. Braunschweig, C. Hering-Junghans, *Chem. Sci.* **2019**, *10*, 7859-7867.
- [130] R. Appel, H. Schöler, *Chem. Ber.* **1977**, *110*, 2382-2384.
- [131] J.-E. Siewert, A. Schumann, C. Hering-Junghans, *Dalton Trans.* **2021**, *50*, 15111-15117.
- [132] K. Schwedtmann, J. Haberstroh, S. Roediger, A. Bauzá, A. Frontera, F. Hennersdorf, J. J. Weigand, *Chem. Sci.* **2019**, *10*, 6868-6875.
- [133] M. C. Fermin, D. W. Stephan, *J. Am. Chem. Soc.* **1995**, *117*, 12645-12646.
- [134] J. D. Masuda, A. J. Hoskin, T. W. Graham, C. Beddie, M. C. Fermin, N. Etkin, D. W. Stephan, *Chem. Eur. J.* **2006**, *12*, 8696-8707.
- [135] a) R. Dobrovetsky, K. Takeuchi, D. W. Stephan, *Chem. Commun.* **2015**, *51*, 2396-2398; b) L. Wu, S. S. Chitnis, H. Jiao, V. T. Annibale, I. Manners, *J. Am. Chem. Soc.* **2017**, *139*, 16780-16790.
- [136] L. Wu, V. T. Annibale, H. Jiao, A. Brookfield, D. Collison, I. Manners, *Nature Comm.* **2019**, *10*, 2786.
- [137] M. R. Anneser, G. R. Elpitiya, X. B. Powers, D. M. Jenkins, *Organometallics* **2019**, *38*, 981-987.
- [138] B. Riegel, A. Pfitzner, G. Heckmann, H. Binder, E. Fluck, *Z. anorg. allg. Chem.* **1995**, *621*, 1365-1372.
- [139] C. Üffing, C. v. Hänisch, H. Schnöckel, *Z. anorg. allg. Chem.* **2000**, *626*, 1557-1560.
- [140] W. Uhl, M. Benter, *J. Chem. Soc., Dalton Trans.* **2000**, 3133-3135.
- [141] M. H. Holthausen, D. Knackstedt, N. Burford, J. J. Weigand, *Aust. J. Chem.* **2013**, *66*, 1155-1162.
- [142] S. S. Chitnis, R. A. Musgrave, H. A. Sparkes, N. E. Pridmore, V. T. Annibale, I. Manners, *Inorg. Chem.* **2017**, *56*, 4521-4537.
- [143] S. S. Chitnis, H. A. Sparkes, V. T. Annibale, N. E. Pridmore, A. M. Oliver, I. Manners, *Angew. Chem. Int. Ed.* **2017**, *56*, 9536-9540.
- [144] K. Naka, T. Umeyama, A. Nakahashi, Y. Chujo, *Macromolecules* **2007**, *40*, 4854-4858.
- [145] M. Arisawa, K. Sawahata, T. Yamada, D. Sarkar, M. Yamaguchi, *Org. Lett.* **2018**, *20*, 938-941.
- [146] J. H. Barnard, P. A. Brown, K. L. Shuford, C. D. Martin, *Angew. Chem. Int. Ed.* **2015**, *54*, 12083-12086.
- [147] R. J. Baker, C. Jones, D. P. Mills, D. M. Murphy, E. Hey-Hawkins, R. Wolf, *Dalton Trans.* **2006**, 64-72.
- [148] G. Bai, P. Wei, A. K. Das, D. W. Stephan, *Dalton Trans.* **2006**, 1141-1146.
- [149] E. A. Doud, C. J. Butler, D. W. Paley, X. Roy, *Chem. Eur. J.* **2019**, *25*, 10840-10844.
- [150] a) E. J. Popczun, J. R. McKone, C. G. Read, A. J. Biacchi, A. M. Wiltrout, N. S. Lewis, R. E. Schaak, *J. Am. Chem. Soc.* **2013**, *135*, 9267-9270; b) S. Anantharaj, S. R. Ede, K. Sakthikumar, K. Karthick, S. Mishra, S. Kundu, *ACS Catalysis* **2016**, *6*, 8069-8097.

- [151] A. Schmidpeter, W. Gebler, F. Zwaschka, W. S. Sheldrick, *Angew. Chem. Int. Ed. Engl.* **1980**, *19*, 722-723.
- [152] A. J. Arduengo, J. C. Calabrese, A. H. Cowley, H. V. R. Dias, J. R. Goerlich, W. J. Marshall, B. Riegel, *Inorg. Chem.* **1997**, *36*, 2151-2158.
- [153] I. A. J. Arduengo, D. H. V. Rasika, C. J. C., *Org. Chem. Let.* **1997**, *26*, 143-144.
- [154] O. Back, M. Henry-Ellinger, C. D. Martin, D. Martin, G. Bertrand, *Angew. Chem. Int. Ed.* **2013**, *52*, 2939-2943.
- [155] E. Tomás-Mendivil, M. M. Hansmann, C. M. Weinstein, R. Jazzar, M. Melaimi, G. Bertrand, *J. Am. Chem. Soc.* **2017**, *139*, 7753-7756.
- [156] C. M. Weinstein, G. P. Junor, D. R. Tolentino, R. Jazzar, M. Melaimi, G. Bertrand, *J. Am. Chem. Soc.* **2018**, *140*, 9255-9260.
- [157] T. Krachko, M. Bispinghoff, A. M. Tondreau, D. Stein, M. Baker, A. W. Ehlers, J. C. Slootweg, H. Grützmacher, *Angew. Chem. Int. Ed.* **2017**, *56*, 7948-7951.
- [158] A. Michaelis, C. Schulte, *Ber. Dtsch. Chem. Ges.* **1881**, *14*, 912-914.
- [159] a) P. Ehrlich, A. Bertheim, *Ber. Dtsch. Chem. Ges.* **1912**, *45*, 756-766; b) S. Riethmiller, *Bull. Hist. Chem.* **1999**.
- [160] N. C. Lloyd, H. W. Morgan, B. K. Nicholson, R. S. Ronimus, *Angew. Chem. Int. Ed.* **2005**, *44*, 941-944.
- [161] G. Thiele, G. Zoubek, H. A. Lindner, J. Ellermann, *Angew. Chem. Int. Ed. Engl.* **1978**, *17*, 135-136.
- [162] M. Baudler, P. Bachmann, *Angew. Chem. Int. Ed. Engl.* **1981**, *20*, 123-124.
- [163] C. Spang, F. T. Edelman, M. Noltemeyer, H. W. Roesky, *Chem. Ber.* **1989**, *122*, 1247-1254.
- [164] R. P. Tan, N. M. Comerlato, D. R. Powell, R. West, *Angew. Chem. Int. Ed. Engl.* **1992**, *31*, 1217-1218.
- [165] L. Weber, G. Dembeck, P. Lönneke, H.-G. Stammler, B. Neumann, *Organometallics* **2001**, *20*, 2288-2293.
- [166] C. Clobes, P. Jerabek, I. Nußbruch, G. Frenking, C. von Hänisch, *Eur. J. Inorg. Chem.* **2015**, *2015*, 3264-3273.
- [167] H. Imoto, A. Urushizaki, I. Kawashima, K. Naka, *Chem. Eur. J.* **2018**, *24*, 8797-8803.
- [168] C. K. F. von Hänisch, C. Üffing, M. A. Junker, A. Ecker, B. O. Kneisel, H. Schnöckel, *Angew. Chem. Int. Ed. Engl.* **1996**, *35*, 2875-2877.
- [169] A. Schumann, J. Bresien, M. Fischer, C. Hering-Junghans, *Chem. Commun.* **2021**, *57*, 1014-1017.
- [170] S. Nees, F. Fantuzzi, T. Wellnitz, M. Fischer, J.-E. Siewert, J. T. Goettel, A. Hofmann, M. Härterich, H. Braunschweig, C. Hering-Junghans, *Angew. Chem. Int. Ed.* **2021**, *60*, 24318-24325.
- [171] L. Pauling, *J. Am. Chem. Soc.* **1931**, *53*, 1367-1400.
- [172] a) K. S. Pitzer, *J. Am. Chem. Soc.* **1948**, *70*, 2140-2145; b) R. S. Mulliken, *J. Am. Chem. Soc.* **1950**, *72*, 4493-4503.
- [173] a) Y. Wang, G. H. Robinson, *Chem. Commun.* **2009**, 5201-5213; b) R. C. Fischer, P. P. Power, *Chem. Rev.* **2010**, *110*, 3877-3923; c) P. P. Power, *Acc. Chem. Res.* **2011**, *44*, 627-637; d) P. Bag, C. Weetman, S. Inoue, *Angew. Chem. Int. Ed.* **2018**, *57*, 14394-14413; e) T. Chu, G. I. Nikonov, *Chem. Rev.* **2018**, *118*, 3608-3680; f) J.-D. Guo, T. Sasamori, *Chem. Asian J.* **2018**, *13*, 3800-3817; g) V. A. Starodub, T. N. Starodub, *Russ. Chem. Rev.* **2019**, *88*, 717-748.
- [174] a) R. L. Wells, W. L. Gladfelter, *J. Clust. Sci.* **1997**, *8*, 217-238; b) S. Schulz, in *Advances in Organometallic Chemistry, Vol. 49*, Academic Press, **2003**, pp. 225-317; c) M. A. Malik, M. Afzaal, P. O'Brien, *Chem. Rev.* **2010**, *110*, 4417-4446.
- [175] M. Kapitein, C. von Hänisch, *Eur. J. Inorg. Chem.* **2015**, *2015*, 837-844.

- [176] a) J.-S. Lu, M.-C. Yang, M.-D. Su, *Chem. Phys. Lett.* **2017**, *686*, 60-67; b) J.-S. Lu, M.-C. Yang, M.-D. Su, *J. Phys. Chem. A* **2017**, *121*, 6630-6637; c) J.-S. Lu, M.-C. Yang, M.-D. Su, *Phys. Chem. Chem. Phys.* **2017**, *19*, 8026-8033; d) J.-S. Lu, M.-C. Yang, M.-D. Su, *ACS Omega* **2018**, *3*, 10163-10171.
- [177] A. M. Arif, J. E. Boggs, A. H. Cowley, J. G. Lee, M. Pakulski, J. M. Power, *J. Am. Chem. Soc.* **1986**, *108*, 6083-6084.
- [178] D. Geiß, M. I. Arz, M. Straßmann, G. Schnakenburg, A. C. Filippou, *Angew. Chem. Int. Ed.* **2015**, *54*, 2739-2744.
- [179] G. Linti, H. Nöth, K. Polborn, R. T. Paine, *Angew. Chem. Int. Ed. Engl.* **1990**, *29*, 682-684.
- [180] K. Knabel, T. M. Klapötke, H. Nöth, R. T. Paine, I. Schwab, *Eur. J. Inorg. Chem.* **2005**, *2005*, 1099-1108.
- [181] E. Rivard, W. A. Merrill, J. C. Fettinger, P. P. Power, *Chem. Commun.* **2006**, 3800-3802.
- [182] A. N. Price, M. J. Cowley, *Chem. Eur. J.* **2016**, *22*, 6248-6252.
- [183] A. N. Price, G. S. Nichol, M. J. Cowley, *Angew. Chem. Int. Ed.* **2017**, *56*, 9953-9957.
- [184] C. M. E. Graham, C. R. P. Millet, A. N. Price, J. Valjus, M. J. Cowley, H. M. Tuononen, P. J. Ragogna, *Chem. Eur. J.* **2018**, *24*, 672-680.
- [185] J.-B. Bourg, A. Rodriguez, D. Scheschkewitz, H. Gornitzka, D. Bourissou, G. Bertrand, *Angew. Chem. Int. Ed.* **2007**, *46*, 5741-5745.
- [186] K. G. Pearce, E. P. F. Canham, J. F. Nixon, I. R. Crossley, *Chem. Eur. J.* **2021**, *27*, 16342-16346.
- [187] a) W. Yang, K. E. Krantz, D. A. Dickie, A. Molino, D. J. D. Wilson, R. J. Gilliard Jr., *Angew. Chem. Int. Ed.* **2020**, *59*, 3971-3975; b) S. Hagspiel, F. Fantuzzi, R. D. Dewhurst, A. Gärtner, F. Lindl, A. Lamprecht, H. Braunschweig, *Angew. Chem. Int. Ed.* **2021**, *60*, 13666-13670.
- [188] M. F. Lappert, A. Protchenko, P. P. Power, A. Seeber, *Metal Amide Chemistry*, John Wiley & Sons, Ltd, Chichester, UK, **2008**.
- [189] K. M. Waggoner, H. Hope, P. P. Power, *Angew. Chem. Int. Ed. Engl.* **1988**, *27*, 1699-1700.
- [190] C. Cui, H. W. Roesky, H.-G. Schmidt, M. Noltemeyer, H. Hao, F. Cimpoesu, *Angew. Chem. Int. Ed.* **2000**, *39*, 4274-4276.
- [191] C. Cui, H. W. Roesky, H.-G. Schmidt, M. Noltemeyer, *Angew. Chem. Int. Ed.* **2000**, *39*, 4531-4533.
- [192] N. J. Hardman, C. Cui, H. W. Roesky, W. H. Fink, P. P. Power, *Angew. Chem. Int. Ed.* **2001**, *40*, 2172-2174.
- [193] R. J. Wright, A. D. Phillips, T. L. Allen, W. H. Fink, P. P. Power, *J. Am. Chem. Soc.* **2003**, *125*, 1694-1695.
- [194] R. J. Wright, M. Brynda, J. C. Fettinger, A. R. Betzer, P. P. Power, *J. Am. Chem. Soc.* **2006**, *128*, 12498-12509.
- [195] X. Li, X. Cheng, H. Song, C. Cui, *Organometallics* **2007**, *26*, 1039-1043.
- [196] J. Hicks, P. Vasko, J. M. Goicoechea, S. Aldridge, *Nature* **2018**, *557*, 92-95.
- [197] A. Heilmann, J. Hicks, P. Vasko, J. M. Goicoechea, S. Aldridge, *Angew. Chem. Int. Ed.* **2020**, *59*, 4897-4901.
- [198] M. D. Anker, M. Lein, M. P. Coles, *Chem. Sci.* **2019**, *10*, 1212-1218.
- [199] M. D. Anker, R. J. Schwamm, M. P. Coles, *Chem. Commun.* **2020**, *56*, 2288-2291.
- [200] J. D. Queen, A. Lehmann, J. C. Fettinger, H. M. Tuononen, P. P. Power, *J. Am. Chem. Soc.* **2020**, *142*, 20554-20559.
- [201] J. D. Queen, S. Irvankoski, J. C. Fettinger, H. M. Tuononen, P. P. Power, *J. Am. Chem. Soc.* **2021**, *143*, 6351-6356.

- [202] a) T. Agou, S. Ikeda, T. Sasamori, N. Tokitoh, *Eur. J. Inorg. Chem.* **2016**, 2016, 623-627; b) M. Kapitein, M. Balmer, L. Niemeier, C. von Hänisch, *Dalton Trans.* **2016**, 45, 6275-6281; c) N. A. Phan, T. J. Sherbow, J. C. Fettinger, L. A. Berben, *Z. anorg. allg. Chem.* **2021**, 647, 1824-1829.
- [203] a) M. Somer, K. Peters, H. G. von Schnering, *Z. anorg. allg. Chem.* **1992**, 613, 19-25; b) M. Somer, W. Carrillo-Cabrera, E.-M. Peters, K. Peters, H. G. von Schnering, *Z. Kristallogr. – Cryst. Mater.* **1995**, 210, 779-780.
- [204] H. Sitzmann, M. F. Lappert, C. Dohmeier, C. Üffing, H. Schnöckel, *J. Organomet. Chem.* **1998**, 561, 203-208.
- [205] A. Hofmann, T. Tröster, T. Kupfer, H. Braunschweig, *Chem. Sci.* **2019**, 10, 3421-3428.
- [206] M. K. Sharma, C. Wölper, G. Haberhauer, S. Schulz, *Angew. Chem. Int. Ed.* **2021**, 60, 6784-6790.
- [207] K. Ota, R. Kinjo, *Chem. Soc. Rev.* **2021**, 50, 10594-10673.
- [208] M. Somer, D. Thiery, K. Peters, L. Walz, M. Hartweg, T. Popp, H. G. v. Schnering, *Z. Naturforsch. B* **1991**, 46, 789-794.
- [209] C. von Hänisch, O. Hampe, *Angew. Chem. Int. Ed.* **2002**, 41, 2095-2097.
- [210] C. Ganesamoorthy, C. Helling, C. Wölper, W. Frank, E. Bill, G. E. Cutsail, S. Schulz, *Nature Comm.* **2018**, 9, 87.
- [211] C. Helling, C. Wölper, S. Schulz, *J. Am. Chem. Soc.* **2018**, 140, 5053-5056.
- [212] a) J. Krüger, C. Ganesamoorthy, L. John, C. Wölper, S. Schulz, *Chem. Eur. J.* **2018**, 24, 9157-9164; b) C. Helling, C. Wölper, Y. Schulte, G. E. Cutsail, S. Schulz, *Inorg. Chem.* **2019**, 58, 10323-10332; c) J. Schoening, L. John, C. Wölper, S. Schulz, *Dalton Trans.* **2019**, 48, 17729-17734.
- [213] D. W. N. Wilson, J. Feld, J. M. Goicoechea, *Angew. Chem. Int. Ed.* **2020**, 59, 20914-20918.
- [214] J. Feld, D. W. N. Wilson, J. M. Goicoechea, *Angew. Chem. Int. Ed.* **2021**, 60, 22057-22061.
- [215] a) M. K. Sharma, C. Wölper, G. Haberhauer, S. Schulz, *Angew. Chem. Int. Ed.* **2021**, 60, 21784-21788; b) M. K. Sharma, C. Wölper, S. Schulz, *Dalton Trans.* **2022**, 51, 1612-1616.

5 Originalpublikationen

Diese kumulative Habilitationsschrift enthält die folgenden Originalpublikationen in der entsprechenden Original-Verlagsversion. Die entsprechenden Urheberrechts-Hinweise finden sich am Anfang der jeweiligen Publikation.

In allen Fällen ist Herr Dr. Christian Hering-Junghans der Korrespondenzautor und hat die Studien entworfen, die wissenschaftliche Arbeit beaufsichtigt oder teilweise eigenständig durchgeführt, die Analyse der Daten angeleitet und alle Manuskripte in Zusammenarbeit mit den Co-Autoren verfasst. Listung der Publikationen in der Reihenfolge wie sie in Kapitel 2 diskutiert werden.

- 1) „Terphenyl(bisamino)phosphines: electron-rich ligands for gold-catalysis”
J.-E. Siewert, A. Schumann, M. Fischer, C. Schmidt, T. Taeufer, C. Hering-Junghans,*
Dalton Trans. **2020**, *49*, 12354–12364.
- 2) „Reactivity of phospho–Wittig reagents towards NHCs and NHOs”
P. Gupta, J.-E. Siewert, T. Wellnitz, M. Fischer, W. Baumann, T. Beweries,* C. Hering-Junghans,* *Dalton Trans.* **2021**, *50*, 1838–1844.
- 3) „On 1,3-phosphaazaallenes and their diverse reactivity”
M. Fischer, C. Hering-Junghans,* *Chem. Sci.* **2021**, *12*, 10279–10289.
- 4) „Titanocene pnictinidene complexes”
M. Fischer, F. Reiß,* C. Hering-Junghans,* *Chem. Commun.* **2021**, *57*, 5626–5629.
- 5) „A selective route to aryl-triphosphiranes and their titanocene-induced fragmentation”
A. Schumann, F. Reiß, H. Jiao, J. Rabeah, J.-E. Siewert, I. Krummenacher, H. Braunschweig, C. Hering-Junghans,* *Chem. Sci.* **2019**, *10*, 7859–7867.
- 6) „Phosphine-catalysed reductive coupling of dihalophosphanes”
J.-E. Siewert, A. Schumann, C. Hering-Junghans,* *Dalton Trans.* **2021**, *50*, 15111–15117.
- 7) „Aryl-substituted triarsiranes: synthesis and reactivity”
A. Schumann, M. Fischer, J. Bresien, C. Hering-Junghans,* *Chem. Commun.* **2021**, *57*, 1014–1017.

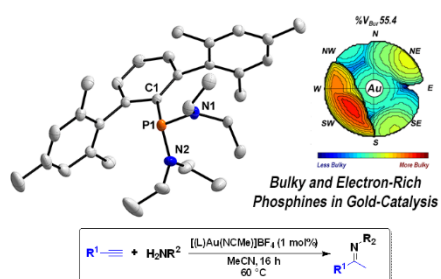
- 8) „Isolable Phospha- and Arsaalumenes”
M. Fischer, S. Nees, T. Kupfer, J. T. Goettel, H. Braunschweig,* C. Hering-Junghans*,
J. Am. Chem. Soc. **2021**, *143*, 11, 4106–4111.
- 9) „Cyclo-Dipnictadialanes”
S. Nees, F. Fantuzzi, T. Wellnitz, M. Fischer, J.-E. Siewert, J. T. Goettel, A. Hofmann,
M. Härterich, H. Braunschweig,* C. Hering-Junghans,* *Angew. Chem. Int. Ed.* **2021**, *60*,
24318–24325.

5.1 Terphenyl(bisamino)phosphines: electron-rich ligands for gold-catalysis

J.-E. Siewert, A. Schumann, M. Fischer, C. Schmidt, T. Taeufer, C. Hering-Junghans

Dalton Trans. **2020**, *49*, 12354–12364.

DOI: 10.1039/D0DT02435J



Reprinted (adapted) with permission from *Dalton Trans.*

Copyright 2020 Royal Society of Chemistry

Cite this: *Dalton Trans.*, 2020, **49**, 12354Received 9th July 2020,
Accepted 17th August 2020
DOI: 10.1039/d0dt02435j

rsc.li/dalton

Terphenyl(bisamino)phosphines: electron-rich ligands for gold-catalysis†

Jan-Erik Siewert, André Schumann, Malte Fischer, Christoph Schmidt, Tobias Taeufer and Christian Hering-Junghans*

Terphenyl(bisamino)phosphines have been identified as effective ligands in cationic gold(I) complexes for the hydroamination of acetylenes. These systems are related to Buchwald phosphines and their steric properties have been evaluated. Effective hydroamination was noted even at low catalyst loadings and a series of cationic gold(I) complexes has been structurally characterized clearly indicating stabilizing effects through gold-arene interactions.

Transition metal catalysis is governed by the influence of multiple factors; however, most crucial are the following three: metals, substrates and ligands.¹ Among the plethora of ligands used in transition metal catalysis phosphines have been demonstrated to be an invaluable ligand class in a variety of transformations. Buchwald and co-workers have developed the so-called Buchwald-type phosphines, which have been shown to occupy two coordination sites in low-valent Pd-complexes (Fig. 1A).^{2–4} In addition to the P–Pd interaction an η¹-Pd–C_{ipso} bonding interaction was found in the complex LPd(dba) (L = 2-(2',6'-dimethoxybiphenyl)dicyclohexylphosphine; dba = dibenzylidene-acetone).⁵ The 2-biphenyl moiety in this ligand class has allowed to achieve the challenging coupling of aryl chlorides and extremely hindered aryl boronic acids in Suzuki–Miyaura cross-coupling reactions. Since their initial synthesis various Buchwald-type phosphines have been presented and are now commercially available (e.g. JohnPhos).⁶

In order to access the electronic properties of phosphines usually Tolman's cone angle and/or electronic parameter (TPE) are utilized, allowing to measure direct ligand metal interactions.^{7,8} In contrast to Pd-catalysis (with mostly square planar complexes), in gold(I)-catalysis the linear coordination mode at gold is operational. This forces substrates into transposition of the ligand, which enhances its electronic effects. Cationic gold complexes are well suited for the electrophilic activation of alkynes and their subsequent functionalization with a variety of nucleophiles.^{9–11} This preference for alkyne activation has been attributed to the low LUMO energies of Au-

alkyne complexes, rendering them more electrophilic.^{12,13} In Au(I) catalysis a major drawback is the decay of the gold catalyst, which results from reduction of the cationic gold center to Au(0).¹⁴ It has been shown that in many of these transformations electron-rich phosphine ligands outperform their electron-deficient counterparts. For the intermolecular amination of alkynes electron-rich phosphines with a 2-biphenyl moiety are considered superior.¹⁵ Comparing the TEP-values of common Buchwald-type phosphines show that they do not exceed the donor strength of simple t-Bu₃P,⁸ and the prominent class of N-heterocyclic carbenes (NHCs) are stronger σ-donor ligands (Fig. 1).¹⁶ Dielmann and co-workers, as well as Sundermeyer *et al.* have recently pushed the electron-donating ability of phosphines beyond their classical endpoint through P-substitution with N-heterocyclic imines (NHIs)¹⁷ or phosphazenes,¹⁸ respectively. In addition, the NHI-functionalization allows the metal center to engage in additional interaction with the aryl-substituents in the N_{NHC}-position of the carbene (Fig. 1C).

Terphenyl-groups, of the general formula 2,6-Ar₂-C₆H₃, have played a leading role in advancing the chemistry of low-valent main group and transition metal species.^{19–23} A reagent commonly used to introduce the terphenyl moiety is Ter-Li (Ter =

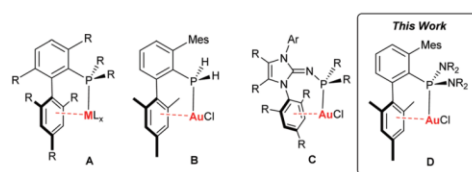


Fig. 1 General metal complexes with Buchwald-type ligands (A), related gold complexes from the literature (B and C), and synthetic targets of this study (D).

Leibniz-Institut für Katalyse e.V. Rostock Albert-Einstein-Str. 29a, 18059 Rostock, Germany. E-mail: christian.hering.junghans@catalysis.de

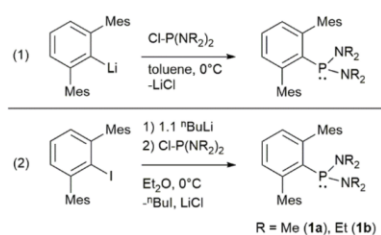
† Electronic supplementary information (ESI) available: Synthesis and characterization of compounds, NMR spectra, crystallographic, and computational details. CCDC 2014543–2014551. For ESI and crystallographic data in CIF or other electronic format see DOI: 10.1039/d0dt02435j

2,6-Mes₂-C₆H₃),²⁴ which can be treated with element halides to access Ter-EX_n species.^{17,25,26} In our hands treatment of Ter-Li with PCl₃ often resulted in trace amounts of Ter-H contaminating the desired Ter-PCl₂ product.²⁷ Thus, we were interested in a way to circumvent the formation of Ter-H. Ragnogna *et al.* have recently described the successful preparation of [TerPS]₂, a source of monomeric phosphinidene sulfides.²⁸ [TerPS]₂ is synthesized by treating Ter-PCl₂ with S(SiMe₃)₂. In their study the authors outlined an alternative route towards Ter-PCl₂. Additionally, TerPH₂ was shown to form AuCl complexes in which stabilizing arene-interactions with one of the flanking mesityl group are detected (Fig. 1B).²⁹

In this contribution we describe the application of the TerPCl₂ precursors TerP(NR₂)₂ [R = Me (**1Me**), Et (**1Et**)] as Buchwald-type phosphine ligands in gold(I)-catalyzed hydroamination reactions of terminal alkynes (Fig. 1D). The effect of the amino groups was investigated on a theoretical basis and an efficient tool for the estimation of the TEP_{Ni}-value is presented.

Results and discussion

Ragnogna and co-workers have recently described a route towards Ter-PCl₂ through aminolysis of Ter-P(NEt₂)₂ with dry HCl.^{28,30} Consequently, we prepared Ter-P(NR₂)₂ [R = Me (**1a**), Et (**1b**)] by treatment of isolated Ter-Li with ClP(NR₂)₂ (R = Me, Et; an HCl-free P-source) in toluene at ambient temperature (Scheme 1, reaction (1)). In case of **1a**, filtration over a Celite-padded frit and removal of the solvent resulted in the isolation of an analytically pure colourless solid in 67% yield. For **1b**, after stirring for 1.5 h, the solvent was removed and the residue was extracted with *n*-hexane, concentrated to incipient crystallization and standing at 5 °C overnight afforded **1b** as an analytically pure colourless crystalline solid, in a moderate yield of 40%. We found that consistently higher yields are obtained by starting from Ter-I. Lithiation of Ter-I with 2.5 M ⁿBuLi (in *n*-hexane) in Et₂O at 0 °C and subsequent treatment with ClP(NR₂)₂ afforded **1a** (79%) and **1b** (89%) in good isolated yields (Scheme 1, reaction (2)). In addition, this synthetic approach can be easily scaled and **1b** was prepared on a multi-gram scale. Ligands **1a** and **1b** are characterized by ³¹P NMR



Scheme 1 Two synthetic routes towards terphenyl-substituted bisaminophosphines **1a** (R = Me) and **1b** (R = Et).

signals at 102.5 and 100.2 ppm, respectively, upfield-shifted compared to their respective ClP(NR₂)₂ precursors. In the ¹H NMR spectrum of **1a** and **1b** two signals for the *ortho* and *para* CH₃-groups of the mesityl groups in a 2 : 1 ratio are observed. In **1a** a doublet corresponding to the two NMe₂ groups is detected, indicating C₂ symmetry in solution. In **1b** a complex multiplet is observed for the methylene protons in the Et-groups of the NEt₂-moiety, and a triplet for the Me-groups. X-ray quality crystals of **1a** and **1b** were grown from saturated *n*-hexane solutions at 5 °C over a period of 24 h. The phosphorus atoms show a coordination environment deviating significantly from an ideal trigonal pyramid [∑(<P) (**1a**) 314.03°, (**1b**) 317.26°, *cf.* TerPMe₂³¹ 309.0°, TerPCl₂³² 305.58°], which is further supported by NBO analysis [wB97XD/6-31g(d,p) level of theory] showing a 50/50 contribution of 3s and 3p orbitals for the lone pair (LP) on phosphorus.³³ The P-C_{Ter} bond lengths are [(**1a**) 1.8591(14), (**1b**) 1.813(11) Å] indicative of P-C single bonds [∑r_{cov}(P-C) = 1.85 Å].³⁴ The P-N distances [(**1a**) P1-N1 1.6981(11), P1-N2 1.6942(12) Å; (**1b**) P1-N1 1.6981(11), P1-N2 1.6942(12); *cf.* (Me₃Si)₂NPCL, P-N 1.6468(8) Å]³⁵ are contracted [∑r_{cov}(P-N) = 1.82 Å],³⁴ hinting at partial double bond character through interaction of the N-LPs with the other σ* (P-N) orbitals as shown through 2nd order perturbation analysis using NBO with stabilization energies for **1a** of 14.5 and 10.2 and for **1b** of 18.1 and 9.5 kcal mol⁻¹, respectively. The sum of angles at the N in **1b** deviate from the expected trigonal planar coordination environment, and minimal pyramidalization is observed [∑(<N1) = 352.78°] (Fig. 2).

With the structural analysis of **1a** and **1b** in hand, the structural resemblance with Buchwald's dialkylbiarylphosphines became evident. These are regarded as privileged ligands in various Pd- and Au-catalyzed reactions. In analogy to the

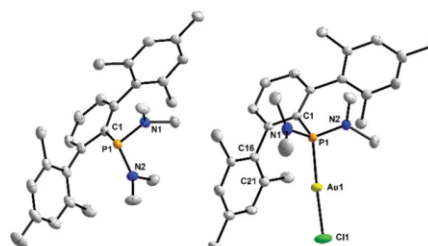
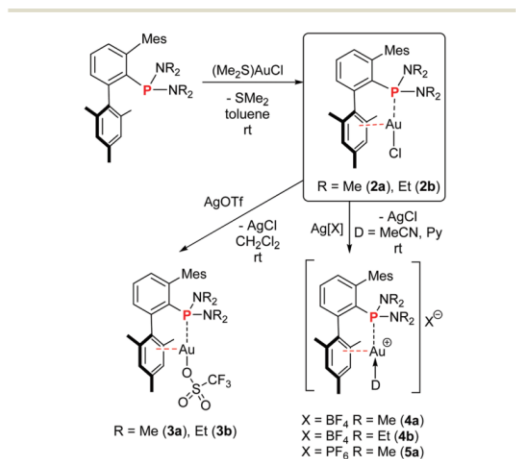


Fig. 2 POV-Ray depiction of the molecular structure of **1a** (left) and **2a** (right). Ellipsoids are drawn at 50% probability, 150(2) K. All hydrogen atoms have been omitted for clarity. Selected bond lengths (Å) and angles (°) of **1a** (left): C1-P1 1.8591(14), P1-N1 1.6827(12), P1-N2 1.6850(13), P1-C1 1.8591(14); N2-P1-N1 107.79(6), N1-P1-C1 108.37(6), N2-P1-C1 97.87(6), C25-N1-C26 112.90(13), C25-N1-P1 126.32(11), C26-N1-P1 118.37(11), C27-N2-C28 112.66(13), C27-N2-P1 117.47(10), C28-N2-P1 126.48(10). **2a** (right): P1-N2 1.657(4), P1-N1 1.659(4), P1-C1 1.846(4), P1-Au1 2.2366(11), Cl1-Au1 2.3017(14), C16-Au1 3.2839(33), C21-Au1 3.1008(43); N2-P1-N1 108.5(2), N2-P1-C1 113.3(2), N1-P1-C1 99.33(19); C25-N1-C26 112.1(4), C25-N1-P1 118.2(3), C26-N1-P1 124.0(3), C27-N2-C28 112.5(4), C27-N2-P1 123.4(3), C28-N2-P1 123.5(3); Au1-P1-C1-C2 -128.2(3).

Buchwald systems the 2,6-substitution pattern on the central aryl moiety of the terphenyl-framework, affords a binding pocket about the phosphorus that would allow for arene interactions of a coordinated metal with one of the flanking mesityl groups. Similar systems based on redox-responsive terphenyl-substituted phosphonites have been recently described by Breher and co-workers.³⁶ Jones *et al.* pushed this concept further by introducing bisbiphenyl phosphines providing enhanced stability for cationic gold centers.³⁷ In addition, the steric and electronic properties of related $\text{Ar}_2\text{C}_6\text{H}_3\text{-PR}_2$ systems have been studied in detail.^{38,39} Combination of **1a** or **1b** with one equivalent of $\text{AuCl}(\text{SMe}_2)$ in CH_2Cl_2 under the exclusion of light at room temperature for 1 h, subsequent concentration and layering with *n*-hexane afforded **2a** (67%) and **2b** (91%) in good to excellent isolated yields as colorless X-ray quality crystals (Scheme 2). Upon coordination the P atom is minimally shielded as shown by a ^{31}P NMR shift of 96.7 ppm (**2a**) and 93.3 ppm (**2b**), respectively. This trend is also reflected in the theoretic NMR shifts obtained from GIAO calculations on the wB97XD/6-31g(d,p)/ECP60MWD level of theory.³³ In the ^1H NMR spectrum both complexes show only two signals for the Me-groups of the terphenyl-moiety, indicating free rotation about the P-C_{Ter} axis on the NMR timescale at room temperature. SXRD experiments revealed the expected arene-interactions between the Au(I)-center and one of the *ortho*-mesityl groups of the terphenyl moiety. Upon coordination to AuCl the sum of angles at phosphorus increases [$\sum(\angle\text{P})$ (**2a**) 321.13°, (**2b**) 323.55°, cf. $(\text{TerPMe}_2)\text{AuCl}$ 318.33°]²⁹ and the P-N bonds are contracted by ca. 2% [(**2a**) P1-N1 1.659(4) Å, P1-N2 1.657(4) Å; (**2b**) P1-N1 1.6665(17) Å, P1-N2 1.6604(17) Å] when compared with the free ligands **1a** and **1b**. The complexes show a nearly linear P-Au-Cl arrangement with P-Au distances [(**2a**) P1-Au1 2.2366(11); (**2b**) 2.2445(5) Å; cf. $(\text{TerPMe}_2)\text{AuCl}$ 2.2964(10) Å]²⁹ in the expected range for phosphine gold complexes.



Scheme 2 Synthesis of gold complexes **2** and transformation into **3** and donor-stabilized complexes **4** and **5a**.

In **2a** and **2b** there are close contacts between Au1 and one of the flanking terphenyl groups [(**2a**) C21-Au1 3.1008(43); (**2b**) C17-Au1 2.9707(20) Å], which is in contrast to the known complex $(\text{TerPMe}_2)\text{AuCl}$.²⁹ This stabilizing arene-interaction was further authenticated through an analysis of the electron density of an optimized structure at the wB97XD/6-31g(d,p) level of theory, using the AIM (Atoms in Molecules) approach.⁴⁰ This showed a line critical point between Au and C21 (**2a**) and C17 (**2b**), respectively (see ESI† for details),⁴¹ and supports the notion that the mesityl groups provide meaningful stabilization.

Using the SambVca 2.1 online application the steric properties of ligands **1a** and **1b** were analysed (based on the molecular structures of complexes **2**).⁴² This showed percent buried volumes (% V_{bur}) of 48.8% (**1Me**) and 55.4% (**1Et**), respectively. The % V_{bur} describes how much volume of a sphere centered on the metal ($r_{\text{sphere}} = 3.5$ Å; $d_{\text{M-L}} = \mathbf{2a}$ 2.2366(11); **2b** 2.2445(5) Å) is occupied by the ligand. From the steric maps it is evident that the flanking mesityl group takes up major space in the SW-quadrant of the *xy*-plane perpendicular to the P-Au-axis (Fig. 3), while the NMe₂ groups occupy less space than the NEt₂-groups, which is clearly reflected in the NE, E and SE quadrants of the steric maps. This is in the range of JohnPhos (50.9%), however, exceeds the value of simple phosphines (PPh₃ 34.5%, P^tBu₃ 42.4%).⁴³

In a next series of experiments, we investigated the formation of cationic gold complexes. As an entry **2a** and **2b** were treated with AgOTf in benzene and ^{31}P NMR spectroscopy of the reaction mixtures showed the formation of new species with singlet resonance at 86.5 ppm and 78.9 ppm, respectively. Interestingly, the ^{19}F NMR spectrum showed a singlet at -76.6 ppm, which is in agreement with a covalently bound triflate group (cf. $\text{Ter}[\text{Me}_2(\text{OTf})\text{Si}]\text{N-Sb}(\text{Cl})\text{Me}$ $\delta(^{19}\text{F}) = -76.95$ ppm).³⁵ After removal of AgCl by filtration, concentration to incipient crystallization, and layering with *n*-hexane $[\text{TerP}(\text{NMe}_2)_2]\text{AuOTf}$ (**3a**) and $[\text{TerP}(\text{NEt}_2)_2]\text{AuOTf}$ (**3b**) were afforded as colourless solids in 64% and 49% isolated yield, respectively. X-Ray quality crystals of **3b** were obtained from a saturated CH_2Cl_2 solution layered with *n*-hexane after standing at 5 °C for 24 h (Fig. 4, left). The Au-P distance is shorter than in **2a** and **2b** [(**3b**) P1-Au1 2.2187(4) Å], hinting at a more positive Au-center. This increase is further supported by two close contacts between gold and one of the flanking mesityl groups

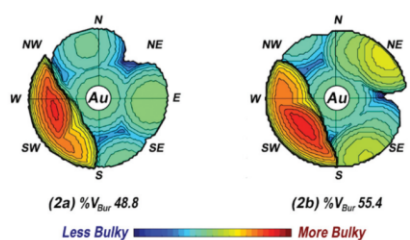


Fig. 3 Steric maps of gold complexes **2a** (left) and **2b** (right).

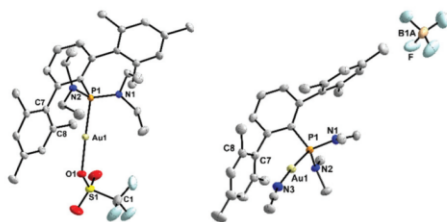
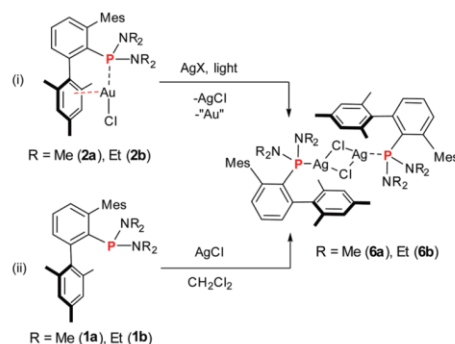


Fig. 4 POV-Ray depiction of the molecular structure of **3b** (left) and **4a** (right). Ellipsoids are drawn at 50% probability, 150(2) K. All hydrogen atoms in **4a** have been omitted for clarity. Selected bond lengths (Å) and angles (°) of **3b** (left): C1–P1 1.8632(14), P1–N1 1.6528(13), P1–N2 1.6580(13), P1–Au1 2.2187(4), P1–O1 2.0948(11), C7–Au1 3.0506(14), C8–Au1 2.9955(13); N2–P1–N1 109.44(7), N1–P1–C1 115.66(6), N2–P1–C1 100.83(6), C25–N1–C26 115.42(13), C27–N1–P1 123.76(11), C25–N1–P1 120.55(11), C29–N2–C31 115.62(12), C29–N2–P1 124.48(10), C31–N2–P1 119.79(10), O1–Au1–P1 174.42(4). **4a** (right): P1–N2 1.6559(18), P1–N1 1.6588(19), P1–C1 1.837(2), P1–Au1 2.2376(5), Au1–N3 2.0431(18), C7–Au1 3.1364(23), C8–Au1 3.0504(24); N2–P1–N1 108.69(10), N2–P1–C1 101.34(9), N1–P1–C1 113.57(10); C25–N1–C26 112.75(18), C25–N1–P1 122.20(15), C26–N1–P1 123.72(15), C27–N2–C28 112.48(18), C27–N2–P1 117.44(15), C28–N2–P1 125.49(15), N3–Au1P1 174.33(6), C29–N3–Au1 169.5(2); Au1–P1–C1–C2 47.17(16).

[C7–Au1 3.0506(14), C8–Au1 2.9955(13) Å]. Overall, the metrical parameters are close to complexes **2a** and **2b**.

To obtain an active catalyst for the hydroamination of alkynes with anilines, **2a** and **2b** were treated with AgBF_4 in CH_3CN and after filtration, an aliquot was taken for NMR analysis. In the ^{31}P NMR spectrum new signals highfield-shifted at 89.7 (**4a**) and 84.4 ppm (**4b**), respectively, compared to the starting material were detected. Broad resonances in the ^1H NMR spectrum at 0.98 and 1.46 ppm, respectively, indicate a coordinated CH_3CN molecule, which is further supported by a ^{19}F NMR shift for both complexes of -150.2 ppm, showing a non-interacting $[\text{BF}_4]^-$ anion. Colourless X-ray quality crystals of **4a** were obtained from a saturated C_6D_6 solution and revealed the expected ion-separated structure with a threefold disordered $[\text{BF}_4]^-$ anion (Fig. 4, right). Additionally, we treated **2a** with AgPF_6 in CH_2Cl_2 , added an excess of pyridine and the mixture was stirred overnight. Upon removal of the solvent and excess pyridine, X-Ray quality crystals were obtained from a saturated CH_2Cl_2 solution layered with *n*-hexane. In analogy to complex **4a** the base adduct, pyridine in this case, of the cationic gold complex was obtained with a non-coordinating $[\text{PF}_6]^-$ anion in $[\text{TerP}(\text{NMe}_2)_2\text{Au}(\text{py})][\text{PF}_6]$ (**5a**). In **4a** and **5a** the Au–P distances are similar to complexes **2** [P1–Au1 (**4a**) 2.2376 (5); (**5a**) 2.247(3) Å; cf. $(\text{TerPMe}_2)_2\text{AuCl}$ 2.2964(10) Å] and two contacts with the flanking mesityl group below 3.1 Å are detected in the base-stabilized cations. Overall, the structural parameters clearly show that the terphenyl structural motif gives rise to stabilizing Au–arene interactions, which should prove beneficial in catalytic trials, as was shown by Xu and co-workers in terms of complex stability in intermolecular hydroamination reactions.¹⁵



Scheme 3 Serendipitous decomposition of cationic gold complexes into $([\text{1aAgCl}]_2)$ dimeric complexes **6** (i) and their rational synthesis from **1** and AgCl (ii).

Preparing complexes **3–5**, sometimes the formation of a new species characterized by a doublet of doublets in the ^{31}P NMR spectrum was noted. This species was only observed if AgCl was not completely removed during filtration and when the solution was kept in daylight. In one instance we obtained X-ray quality crystals that were identified as the neutral silver chloride complex $([\text{1aAgCl}]_2)$ (**6a**). We therefore conclude that it is of the utmost importance to carefully remove any traces of silver chloride and work in the dark, when preparing cationic gold complexes, as the formation of the respective ligand silver chloride complexes might proceed unnoticed and influence catalytic tests.⁴⁴ **6a** and the related complex $([\text{1bAgCl}]_2)$ (**6b**) were independently synthesized by combining **1** with AgCl in a 1:1 stoichiometry in CH_2Cl_2 and continued stirring for 16 h under the exclusion of light afforded **6a** and **6b** as colourless air and moisture stable crystalline solids (Scheme 3). In the ^{31}P NMR spectra **6a** and **6b** show two doublets due to coupling with the two spin $\frac{1}{2}$ silver isotopes (^{107}Ag and ^{109}Ag) at 99.3 ($^1J_{^{109}\text{Ag},\text{P}} = 862.3$ Hz, $^1J_{^{107}\text{Ag},\text{P}} = 746.4$ Hz) and 94.3 ppm ($^1J_{^{109}\text{Ag},\text{P}} = 864.0$ Hz, $^1J_{^{107}\text{Ag},\text{P}} = 748.9$ Hz), respectively. X-ray quality crystals were grown from saturated acetone solutions in air and **6a** and **6b** (Fig. 5) crystallize as centrosymmetric dimers.³³

The molecular structures show a $\mu\text{-Cl}$ bridged dimer with a deltoid Ag_2Cl_2 core coordinated by two ligands **1a** or **1b**, respectively. The solid structures of **6a** and **6b** are closely related to that of $[\text{XPhosAg}(\mu\text{-Cl})_2]$.⁴⁵ Complexes with a $(\text{Ag}-\mu\text{-Cl})_2$ core comprising a single phosphine ligand on Ag are rare and restricted to bulky monodentate phosphine ligands, such as $\text{P}(\text{NC}_4\text{H}_8\text{NMe})_3$,⁴⁶ $\text{Ph}_2\text{P}(\text{CH}_2)\text{PPh}_2\text{C}(\text{H})\text{C}(\text{O})\text{C}_6\text{H}_4\text{Cl}$,⁴⁷ and the simple $\text{P}(\text{Cy})_3$.⁴⁸

To further characterize the electronic character of terphenyl (bisamino)phosphine ligands DFT calculations were carried out to determine the theoretical TEP-value ($\text{TEP}_{\text{Ni,theo}}$) of terphenyl(bisamino)phosphines **1**. Therefore, the complexes $([\text{1a}]\text{Ni}(\text{CO})_3)$ and $([\text{1b}]\text{Ni}(\text{CO})_3)$ were constructed *in silico* and their gas-phase structures were optimized at the BP86/def2SVP

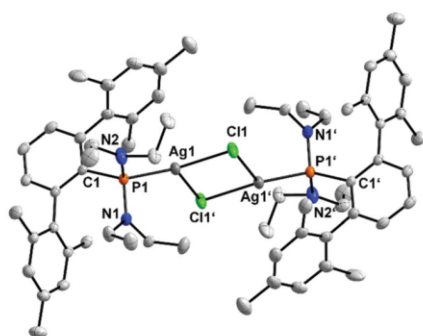


Fig. 5 POV-Ray depiction of the molecular structure of **6b**. Ellipsoids are drawn at 30% probability, 150(2) K. All hydrogen atoms have been omitted for clarity. Selected bond lengths (Å) and angles (°): C1–P1 1.8652(18), P1–N1 1.6701(17), P1–N2 1.6700(17), P1–Ag1 2.4038(6), Ag1–Cl1 2.5060(6), Ag1–Cl1' 2.6120(6), Ag1–Ag1' 3.6518(7) Å; P1–Ag1–Cl1 135.850(19), Ag1–Cl1–Ag1' 91.017(18).

level of theory and confirmed as minima by frequency analyses.³³

Of the resulting unscaled frequencies, the A_1 symmetrical CO stretching mode was chosen for the evaluation of the donor parameters. To fit the theoretical frequencies to experimental values the $\nu_{\text{theor}}(\text{CO})$ for eleven different complexes $[\text{LNi}(\text{CO})_3]$ were calculated and a linear dependency with respect to their experimental TEP values was noted (Fig. 6).³³ Complexes were chosen to span from extremely electron-rich phosphazenyphosphines to electron-poor phosphines such as PCl_3 and PF_3 giving a range of experimental TEPs from 2017.3 to 2110.8 cm^{-1} .^{7,8,17,18,32,49,50} A linear regression allowed to derive the TEP_{Ni} values for ligands **1a** and **1b** of 2059.6 cm^{-1} and 2053.0 cm^{-1} , respectively. This is more electron rich than classical PPh_3 and approaches the donor strength of IMes, while the more electron rich IAPs and phosphazenyphosphines are not surpassed. Especially **1b** is a stronger donor (based on TEP_{Ni}) than P^tBu_3 and falls in the range of newly developed YPhos ligands.⁵¹ 2019 Carmona, Nicasio and co-workers described a series of nickel carbonyl complexes of dialkylterphenyl phosphines, and the A_1 mode for $[(\text{TerPMe}_2)\text{Ni}(\text{CO})_3]$ was detected at 2063 cm^{-1} .³⁹ This illustrates the influence of the amino groups on phosphorus to render ligands **1a** and **1b** more electron rich and thus as a class with superior donor properties for the gold-catalyzed hydroamination of alkynes.

In order to evaluate the catalytic activity of complexes **4a** and **4b** in the hydroamination of aryl alkynes with anilines we first did a screening of the general reaction conditions, such as catalyst loading, solvent, temperature and reaction time using the phenylacetylene, *p*-toluidine pairing. Monitoring of the hydroamination between phenylacetylene and *p*-toluidine with 2 mol% of **4a** or **4b** in MeCN at 60 °C *via* NMR spectroscopy (1,3,5-(OMe)₃-C₆H₃ as internal standard) showed that

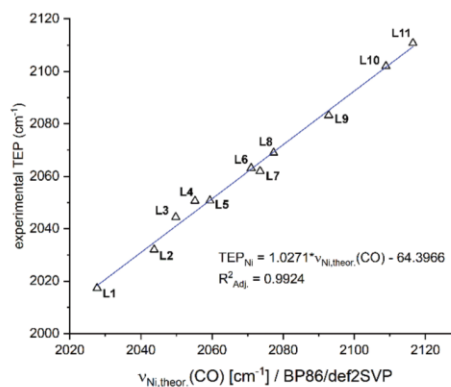
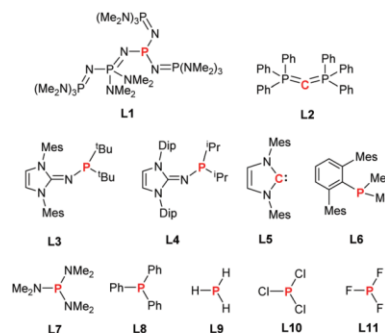


Fig. 6 Diagram showing the correlation between experimental TEP_{Ni} -values of selected complexes $[\text{LNi}(\text{CO})_3]$ and their corresponding theoretical $A_1(\text{CO})$ values obtained at the BP86/def2SVP level of theory.

conversion plateaued after *ca.* 6 h, we therefore decided to run catalytic reactions overnight (*ca.* 16 h) to take into account different sterics of the substrates to be used. Variation of the catalyst loading revealed that no significant drop of conversion occurs going from 2 mol% to 1 mol% and minimally worse results were obtained with 0.5 mol%. Catalytic activity ceases when only 0.1 mol% of **4a** or **4b** were used as catalyst. Considering that in many gold-catalyzed transformations catalyst loadings in excess of 5 mol% are present,^{9–11} this catalyst system is competitive with known systems. To further underline this, complex **4b** was compared with $[(\text{JohnPhos})\text{Au}(\text{CNMe})\text{BF}_4]$ using the *p*-toluidine phenylacetylene pairing in MeCN at 80 °C and after 2 h GC yields (*vs.* biphenyl as internal standard) in excess of 89% and 84%, respectively, were recorded. In contrast, $[(\text{Ph}_3\text{P})\text{Au}(\text{NCMe})\text{BF}_4]$ only gave 12% of the respective imine after 5 h under the same conditions.³³ In a next series of experiments, we changed the solvent from MeCN to benzene and a minimal drop in conversion was noted. We therefore chose MeCN for our substrate scope. Lowering the temperature at optimized conditions from 60 °C to 40 °C resulted in a consistent drop of the isolated yield from

78% to 65%. We thus chose 60 °C to evaluate the substrate scope.

With the optimized parameters in hand we tested both, different anilines and acetylenes (Scheme 4). To investigate the influence of the steric bulk of the aniline, *p*-toluidine, Mes-NH₂ (Mes = 2,4,6-Me₃-C₆H₃) and Dip-NH₂ (Dip = 2,6-diisopropylphenyl) were tested. Overall, 12 different derivatives could be synthesized using different aryl-substituted alkynes. It should be noted that the electron-rich alkynes 4-MeO- and 4-^tBu-phenylacetylene could be converted into the respective imines quantitatively as determined by ¹H NMR spectroscopy, using 1,3,5-(OMe)₃-C₆H₃ as an internal standard. However, attempts to isolate these electron-rich imines after column chromatography on silica with *n*-Hex/EtOAc (4:1) as the eluent, resulted in the isolation of the corresponding benzophenone derivatives in good isolated yields (Scheme 4, bottom). The isolated yields for the hydroamination of phenylacetylene are generally good, with up to 97% yield for the reaction with Mes-NH₂. Interestingly, for F₃C-C₆H₄-CCH the yield increases with the steric demand of the respective aniline and up to 92% of the respective Dip-substituted imine were isolated. In general, we observed that the isolated yields are usually over 70% and nearly independent of whether **1a** or **1b** were used as a ligand. In summary, ligands of the type **1** rep-

resent a potent class of electron-rich Buchwald-type phosphines, which have proven to be efficient in stabilizing gold(I) complexes for the intermolecular hydroamination of alkynes. It is known that in the presence of amines the corresponding amine complexes [LAu(H₂N-R)]X form and inhibit coordination of the alkyne to the metal. In the presence of a strongly donating ligand, amine dissociation should be more favourable.⁵² We therefore independently synthesized [(**1a**)Au(NH₂-*p*-Tol)]BF₄ (**7a**) by addition of *p*-toluidine to **4a**. **7a** was characterized by multinuclear NMR spectroscopy, showing a ³¹P NMR signal at 93.8 ppm and a broad signal for the *p*-toluidine-NH₂ at 4.5 ppm in the ¹H NMR spectrum. Using 1 mol% of **7a** as a catalyst for the hydroamination of *p*-toluidine with phenylacetylene at 80 °C, showed a yield of the desired imine of 72% (GC). This clearly shows that electron rich ligands favour amine dissociation and therefore enhance turnover even at low catalyst loadings.

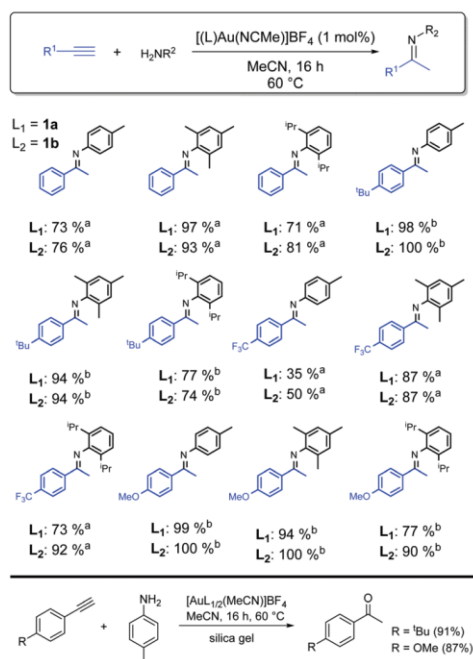
Conclusions

Overall, we report the isolation, spectroscopic and structural characterization of bulky terphenyl(bisamino)phosphines **1**. These Buchwald-type ligands with flanking mesityl groups have been shown to possess attractive interactions between the gold center and one of the flanking mesityl groups, as was ascertained by determination of the molecular structures of a series of gold complexes **2**, **3**, **4** and **5**. The percent buried volume of **1b** amounts to ca. 55% and a linear fit of known TEP-values with their respective gas phase structures (obtained by DFT studies) revealed that particularly **1b** can be classified as an electron-rich phosphine and their application in the intermolecular hydroamination of alkynes was tested. Preparing catalyst solutions by chloride ion abstraction from **2** with AgX salts, sometimes the formation of the respective dimeric Ag-complexes [(L)Ag-μ-Cl]₂ **6a** and **6b** was noted, which were independently synthesized. This is another example that AgCl contamination can result in erroneous catalyst screening results. Screening of the catalytic reaction conditions showed efficient hydroamination to take place at 60 °C in MeCN with a catalyst loading of **4** of 1 mol% and moderate to excellent yields were achieved for bulky anilines such as Dip-NH₂ and different phenyl acetylene derivatives. No obvious difference in performance between ligands **1a** and **1b** was noted. In summary, terphenylbisaminophosphines meet the criteria of efficient ligands for intermolecular gold-catalyzed hydroamination reactions, as they combine strong donor properties with the 2-biphenyl structural motif, which is needed to enhance complex stability and dissociation of additives during catalysis.

Experimental

General methods

All reactions were performed under oxygen- and moisture-free conditions under an inert atmosphere of argon using standard



Scheme 4 Substrate scope of the gold-catalyzed hydroamination of various aryl alkynes with anilines of varying bulk. ^a Isolated yields; ^b NMR yields, (MeO)₃C₆H₃ as internal standard.

Schlenk techniques or an inert atmosphere glovebox (MBraun LABstar ECO). Acetonitrile, diethylether, toluene, *n*-hexane and dichloromethane were purified with the Grubbs-type column system "Pure Solve MD-5" and dispensed into thick-walled Schlenk bombs equipped with Young-type Teflon valve stopcocks and stored under an atmosphere of argon prior to use. Benzene was refluxed over Na/benzophenone and freshly distilled prior to use. Dichloromethane was additionally refluxed over CaH₂ and freshly distilled prior to use. Acetonitrile was additionally stored over molecular sieves (4 Å, 4–8 mesh) prior to use. C₆D₆ was refluxed over Na and freshly distilled prior to use. CDCl₃ was refluxed over P₄O₁₀ and distilled prior to use. CD₂Cl₂ was refluxed over P₄O₁₀ and distilled onto CaH₂ and was refluxed again and then distilled prior to use.

2,6-Mes₂-C₆H₃-I (Ter-I),⁵³ 2,6-Mes₂-C₆H₃-Li (Ter-Li),²⁴ and ClP(NEt₂)₂⁵⁴ have been reported previously and were prepared according to modified literature procedures. *n*-BuLi (2.5 M in *n*-hexane, ACROS), ClP(NMe₂)₂ (99%, Alfa Aesar), AuCl(SMe₂) (>97%, TCI), AgPF₆ (98%, TCI), AgSO₃CF₃ (≥99%, Sigma Aldrich), AgCl (99%, Sigma Aldrich), JohnPhos (97%, Sigma Aldrich), PPh₃ (95%, Sigma Aldrich) and AgBF₄ (98%, Sigma Aldrich) were stored under an argon atmosphere and used as received. DippNH₂ (ABCR, 90%) and MesNH₂ (98% Alfa Aesar) were distilled prior to use. Acetylenes PhCCH (98%, Sigma Aldrich), 4-OMe-C₆H₄-CCH (97%, Sigma Aldrich), 4-CF₃-C₆H₄-CCH (97% Sigma Aldrich) and 4-*t*-Bu-C₆H₄-CCH (96%, Acros Organics) were recondensed, degassed three times and stored over sieves (4 Å) prior to use. Pyridine (99.8%, Sigma Aldrich) was refluxed over KOH, distilled and stored over molecular sieves (3 Å) prior to use.

¹H, ¹³C{¹H} of, ¹¹B, ¹⁹F{¹H} and ³¹P{¹H} NMR spectra were recorded on BRUKER AV300, AV400 or Fourier 300 spectrometers. All ¹H NMR and ¹³C NMR spectra are referenced using the chemical shifts of residual proton solvent resonances (benzene-d₆: δ_H 7.16, δ_C 128.06; chloroform-d: δ_H 7.26, δ_C 77.16; dichloromethane-d₂: δ_H 5.32, δ_C 53.84). Chemical shifts are reported in ppm (δ) relative to tetramethylsilane. The ³¹P{¹H} NMR spectra were referenced to external 85% H₃PO₄ and the ¹⁹F NMR spectra to CFCl₃ as external standard. IR spectra were recorded in ATR mode on a Bruker Alpha II IR spectrometer under an atmosphere of argon. Elemental analysis was done using a Leco Tru Spec elemental analyzer. Melting points were determined on a Mettler-Toledo MP 70 apparatus. Melting points are uncorrected and were measured in sealed capillaries under an Ar atmosphere. Mass spectra were recorded on a MAT 95XP Thermo Fisher mass spectrometer in electrospray ionization mode.

Synthesis of TerP(NMe₂)₂ (1a)

From Ter-Li: Terphenyllithium (0.994 g, 3.106 mmol) was suspended in toluene (80 mL) and the yellowish suspension was cooled to –78 °C. ClP(NMe₂)₂ (0.479 g, 3.106 mmol) in toluene (5 mL) was added dropwise over a period of 5 min. The cooling bath was removed, and the mixture was allowed to warm to ambient temperature over a period of 1 h. The resulting white suspension was filtered using a Celite-padded frit. The filtrate

was then concentrated to incipient crystallization (*ca.* 5 mL) and placed in the fridge (*ca.* 5 °C) for 72 h. This resulted in clear colorless blocks of TerP(NMe₂)₂ (1a, 0.898 g, 2.078 mmol, 67%). X-Ray quality crystals were obtained from a saturated *n*-hexane solution at 5 °C after 24 h.

From Ter-I: Ter-I (2.500 g, 5.677 mmol) was suspended in Et₂O and cooled to –78 °C and *n*-BuLi (2.49 mL, 2.5 M, 1.1 eq.) was added dropwise over a period of 5 min. The yellowish solution was allowed to warm to ambient temperatures over a period of 1 h and was then stirred for an additional 30 min. Subsequently, ClP(NMe₂)₂ (0.930 g, 6.016 mmol, 1.05 eq.) in Et₂O (10 mL) was added dropwise at –78 °C. The reaction mixture was slowly warmed to ambient temperature and stirred overnight. Afterwards, the solvent was removed under reduced pressure and the remaining white powder was extracted with toluene (65 mL) and filtered using a G4 frit, packed with Celite. The volume of the clear filtrate was reduced to *ca.* 4 mL and the flask was placed in the freezer (–30 °C) for 48 h. This resulted in clear colorless blocks of TerP(NMe₂)₂ (1a, 1.940 g, 4.485 mmol, 79%).

¹H NMR (300 MHz, C₆D₆): δ = 7.12 (td, ³J_{HH} = 7.2 Hz, ⁵J_{HH} = 0.7 Hz, 1H, *p*-C₆H₃), 6.90 (dd, ³J_{HH} = 7.2 Hz, ⁴J_{PH} = 2.7 Hz, 2H, *m*-C₆H₃), 6.89 (s (br), 4H, *m*-CH-Mes), 2.24 (s, 6H, Ar-CH₃), 2.22 (s, 12H, Ar-CH₃), 2.21 (d, ³J_{PH} = 8.6 Hz, 12H, NCH₃). ¹³C {¹H} NMR (75 MHz, CDCl₃): δ = 144.1, 140.5, 140.4, 135.6 (d, *J*_{CP} = 27.7 Hz), 130.5, 127.8, 127.7, 42.4 (d, *J*_{CP} = 19.5 Hz), 21.4 (d, ⁵J_{PC} = 5.0 Hz), 21.2. ³¹P{¹H} NMR (122 MHz, C₆D₆): δ = 103.42. IR (ATR, 32 scans, cm⁻¹): ν = 2967 (w), 2915 (w), 2855 (m), 2827 (m), 2785 (m), 1608 (w), 1558 (w), 1478 (w), 1443 (m), 1375 (w), 1267 (m), 1197(m), 1059 (w), 979 (m), 964 (s), 848 (s), 809 (m), 773 (m), 755(m), 719 (w), 672 (s), 646 (m), 576 (m), 561 (m), 550 (m), 534 (w), 452 (m), 409 (m). MS (ESI-TOF): expected *m/z* = 433.2773, found: *m/z* = 433.2767. EA: calc.: C 77.74, H 8.62, N 6.48, found: C 77.39, H 8.54, N 6.08%.

Synthesis of TerP(NEt₂)₂ (1b)

From Ter-Li: Terphenyllithium (0.465 g, 1.428 mmol) was suspended in toluene (15 mL) and the yellowish suspension was cooled to –78 °C. To this suspension ClP(NEt₂)₂ (0.360 g, 1.571 mmol) in toluene (5 mL) was added dropwise over a period of 5 min. The cooling bath was removed, and the mixture was allowed to warm to ambient temperature over a period of 1 h. Subsequently, toluene was removed using an external solvent trap, resulting in a yellowish pasty material, which was then extracted with *n*-hexane (20 mL) and filtered using a Celite-padded frit (G4). The filtrate was then concentrated to incipient crystallization (*ca.* 2 mL) and placed in the fridge (*ca.* 5 °C) for 72 h. This resulted in colorless, X-ray quality blocks of TerP(NEt₂)₂ (1b, 0.273 g, 0.568 mmol, 40%).

From Ter-I: Ter-I (2.500 g, 5.677 mmol) was suspended in Et₂O and cooled to –78 °C and *n*-BuLi (2.49 mL, 2.5 M, 1.1 eq.) was added dropwise. The yellowish solution was allowed to warm to ambient temperatures over a period of 1 h and stirred for an additional 30 minutes. Then ClP(NEt₂)₂ (1.311 g, 6.245 mmol, 1.1 eq.) in Et₂O (10 mL) was added dropwise at –78 °C. The reaction mixture was slowly warmed to ambient

temperature and was further stirred overnight. Afterwards the volatiles were evaporated, *n*-hexane (70 mL) was added to the solid yellow residue and the mixture was then filtered using a G4 frit packed with Celite. The volume of the clear filtrate was reduced to ca. 4 mL and the flask was placed in the freezer (−30 °C) for 48 h. This resulted in the deposition of colorless, crystalline blocks, which were washed with 5 mL of cold *n*-hexane (−30 °C). **TerP(NEt₂)₂ (1b)**, 2.472 g, 5.150 mmol, 89%.

¹H NMR (300 MHz, C₆D₆): δ = 7.10 (td, ³J_{HH} = 7.1 Hz, ⁵J_{HP} = 0.6 Hz, 1H, *p*-C₆H₃), 6.89 (d, ⁴J_{HH} = 0.7 Hz, 4H, *m*-Mes), 6.84 (dd, ³J_{HH} = 7.1 Hz, ⁴J_{PH} = 2.6 Hz, 2H, *m*-C₆H₃), 2.83–2.46 (m, 8H, NCH₂), 2.26 (s, 12H, Ar-CH₃), 2.24 (s, 6H, Ar-CH₃), 0.84 (t, ³J_{HH} = 7.1 Hz, 12H, NCH₂CH₃). **¹³C{¹H} NMR** (75 MHz, C₆D₆): δ = 144.7 (d, *J*_{CP} = 18.38 Hz), 142.1 (d, *J*_{CP} = 34.7 Hz), 141.2 (d, *J*_{CP} = 3.41 Hz), 136.2 (d, *J*_{CP} = 1.33 Hz), 135.7, 130.9, 128.6, 132.7 (w), 129.3 (w), 127.7 (w), 118.9 (m), 118.0 (s), 111.7 (w), 107.4 (w), 102.6 (m), 101.4 (s), 90.7 (m), 85.0 (s), 80.4 (m), 78.7 (m), 75.0 (m), 71.8 (w), 66.4 (m), 63.6 (m), 57.7 (w), 55.9 (w), 55.1 (w), 53.5 (w), 49.1 (w), 47.3 (m), 43.7 (m). **MS** (ESI-TOF): expected *m/z* = 489.3398, found: *m/z* = 489.3394, **EA**: calc.: C 78.65, H 9.28, N 5.73, found: C 78.49, H 9.10, N 5.51%.

Synthesis of TerP(NMe₂)₂AuCl (2a)

TerP(NMe₂)₂ (0.130 g, 0.30 mmol) and ClAu(SMe₂) (0.110 g, 0.30 mmol) were dissolved in dichloromethane (5 mL) under the exclusion of light (wrap flask with tin foil) and stirred at ambient temperature for 1 h. Subsequently, the volume of the reaction mixture was reduced to ca. 1 mL, layered with *n*-hexane (3–5 mL) and placed in the fridge (ca. 5 °C) for 72 h. This resulted in the deposition of colorless, X-ray quality crystals of [(TerP(NMe₂)₂)₂AuCl] (**2a**, 0.130 g, 0.20 mmol, 66%).

¹H NMR (300 MHz, CDCl₃): δ = 7.51 (td, ³J_{HH} = 7.1 Hz, ⁵J_{HP} = 1.6 Hz, 1H, *p*-C₆H₃), 7.04 (dd, ³J_{HH} = 7.6 Hz, ⁴J_{PH} = 4.0 Hz, 2H, *m*-C₆H₃), 6.89 (d, ⁶J_{PH} = 0.7 Hz, 4H, *m*-Mes), 2.34 (s, 12H, Ar-CH₃), 2.31 (s, 6H, Ar-CH₃), 2.06 (s, 12H, NCH₃). **¹³C NMR** (75 MHz, CDCl₃): δ = 145.8 (d, *J*_{CP} = 12.1 Hz), 138.5 (d, *J*_{CP} = 5.3 Hz), 137.2, 135.6, 132.0 (d, ³J_{CP} = 8.4 Hz), 131.4 (d, ⁴J_{CP} = 2.0 Hz), 129.0, 41.2 (d, ²J_{CP} = 9.1 Hz), 21.9, 21.2. **³¹P{¹H} NMR** (122 MHz, CDCl₃): δ = 96.94. **MS** (ESI-TOF): expected *m/z* = 629.2360, found: *m/z* = 629.2368. **EA**: calc.: C 50.57, H 5.61, N 4.21, found: C 50.67, H 5.61, N 4.24%.

Synthesis of TerP(NEt₂)₂AuCl (2b)

TerP(NEt₂)₂ (0.960 g, 2.000 mmol) and ClAu(SMe₂) (0.600 g, 2.000 mmol) were dissolved in dichloromethane (20 mL) under the exclusion of light (wrap flask with tin foil) and stirred at ambient temperature for 1 h. The solvent was removed *in vacuo*, resulting in an off-white solid of [(TerP(NEt₂)₂)₂AuCl] (**2b**, 1.313 g, 1.821 mmol, 91%). X-ray quality crystals were obtained from layering a saturated CH₂Cl₂ solution with *n*-hexane (5 °C for 72 h).

¹H NMR (300 MHz, C₆D₆): δ = 6.99 (t (br), ³J_{HH} = 7.5, 1H, *p*-C₆H₃), 6.95 (m, 4H, *m*-Mes), 6.66 (dd, ³J_{HH} = 7.5, ⁴J_{PH} = 3.9 Hz, 2H, *m*-C₆H₃), 2.59 (q, ³J_{HH} = 7.1 Hz, 4H, NCH₂), 2.56 (q, ³J_{HH} = 7.1 Hz, 4H, NCH₂), 2.30 (s, 6H, Ar-CH₃), 2.09 (s, 12H, Ar-CH₃), 0.77 (t, ³J_{HH} = 7.1 Hz, 12H, NCH₂CH₃). **¹³C{¹H} NMR** (101 MHz, C₆D₆): δ = 146.1 (d, *J*_{CP} = 12.1 Hz), 139.6 (d, *J*_{CP} = 5.2 Hz), 137.4, 135.7, 134.3, 132.4 (d, *J*_{CP} = 8.0 Hz), 130.9 (d, *J*_{CP} = 2.1 Hz), 129.7, 44.7 (d, ³J_{CP} = 10.0 Hz), 22.4, 21.3, 15.3 (d, ⁴J_{CP} = 1.9 Hz). **³¹P{¹H} NMR** (122 MHz, C₆D₆): δ = 93.26. **MS** (ESI-TOF): expected *m/z* = 743.2571, found: *m/z* = 743.2574. **EA**: calc.: C 53.30, H 6.29, N 3.88, found: C 53.26, H 6.25, N 3.64. **MP** (°C): dec. >160 °C.

Synthesis of TerP(NMe₂)₂AuOTf (3a)

In a round-bottomed flask TerP(NMe₂)₂AuCl (66.5 mg, 0.100 mmol) and AgOTf (25.7 mg, 0.100 mmol) are suspended in 5 mL benzene under the exclusion of light. The solution was stirred at room temperature for 2 h and subsequently filtered using a filter canula. The volume of the filtrate was reduced to ca. 1 mL, layered with *n*-hexane (4 mL) and placed in the fridge (5 °C, 72 h). This resulted in the deposition of [(TerP(NMe₂)₂)₂AuOTf] (50.1 mg, 0.064 mmol, 64%) as an amorphous powder.

¹H NMR (300 MHz, C₆D₆): δ = 6.95 (td, ³J_{HH} = 7.6 Hz, ⁵J_{PH} = 1.7 Hz, 1H, *p*-C₆H₃), 6.91–6.82 (m, 4H, *m*-Mes), 6.62 (dd, ³J_{HH} = 7.6 Hz, ⁴J_{PH} = 4.3 Hz, 2H, *m*-C₆H₃), 2.28 (s, 6H, Ar-CH₃), 1.89 (s, 12H, Ar-CH₃), 1.84 (d, ³J_{PH} = 11.3 Hz, 12H, NCH₃). **¹⁹F{¹H} NMR** (282 MHz, C₆D₆): −76.8. **³¹P{¹H} NMR** (122 MHz, C₆D₆): δ = 86.5.

X-Ray quality crystals of this compound could not be grown. CHN and MS were not obtained for this compound.

Synthesis of TerP(NEt₂)₂AuOTf (3b)

In a round-bottomed flask TerP(NEt₂)₂AuCl (0.100 g, 0.140 mmol) and AgOTf (0.036 mg, 0.140 mmol) are suspended in CH₂Cl₂ (5 mL) and the mixture stirred under the exclusion of light at room temperature for 1 h. Afterwards the mixture is filtered using a filter canula. The volume of the filtrate is reduced to ca. 1 mL, layered with *n*-hexane (4 mL) and placed in the fridge (5 °C, 72 h). This resulted in the deposition of colorless, X-ray quality crystals of [(TerP(NEt₂)₂)₂AuOTf] (0.054 g, 0.069 mmol, 49%).

¹H NMR (300 MHz, C₆D₆): δ = 7.02–6.94 (m, 1H, *p*-C₆H₃), 6.92 (s, 4H, *m*-Mes), 6.62 (dd, 2H, *m*-C₆H₃), 2.63–2.44 (m, 8H, NCH₂), 2.31 (s, 6H, Ar-CH₃), 2.02 (s, 12H, Ar-CH₃), 0.76 (t, ³J_{PH} = 7.1 Hz, 12H, NCH₂CH₃) ppm. **¹³C{¹H} NMR** (75 MHz, CD₂Cl₂): δ = 146.28 (d, *J*_{CP} = 12.4 Hz), 139.18 (d, *J*_{CP} = 5.8 Hz), 138.13, 136.23, 133.12 (d, *J*_{CP} = 8.6 Hz), 132.25 (d, *J*_{CP} = 2.4 Hz), 129.5, 128.7, 44.5 (d, *J* = 9.6 Hz), 22.3, 21.3, 15.1. **¹⁹F{¹H} NMR** (376 MHz, CD₂Cl₂): δ = −76.62 ppm. **³¹P{¹H} NMR** (162 MHz, CD₂Cl₂): δ = 78.89 ppm. **MS** (ESI-TOF): expected *m/z* = 834.2506, found: *m/z* = TerP(NEt₂)₂Au 685.2980, AuOTf 345.1763. **EA**: calc.: C 47.48, H 5.43, N 3.36, S 3.84, found: C 47.02, H 5.69, N 3.38, S 3.89%.

Synthesis of [TerP(NMe₂)₂Au-MeCN]BF₄ (4a)

Complex **2a** (0.030 g, 0.045 mmol) and AgBF₄ (0.009 g, 0.045 mmol) were combined in a round-bottomed flask, dis-

solved in acetonitrile (2.5 mL) and stirred under the exclusion of light for 30 min at room temperature. The solution was then filtered using a canula fitted with a glass microfiber filter. This mixture was then dried and extracted with benzene-*d*⁶ and filtered into an NMR-tube equipped with a *J*-young-type screw cap. X-ray quality crystals of [(TerP(NMe₂)₂)Au(MeCN)]BF₄ (4a) were obtained upon standing at room temperature for 48 h.

¹H NMR (300 MHz, C₆D₆) δ = 6.97 (td, ³J_{HH} = 7.6 Hz, ⁵J_{PH} = 1.7 Hz, 1H, *p*-C₆H₃), 6.88 (s, 4H, *m*-Mes), 6.62 (dd, ³J_{HH} = 7.6 Hz, ⁴J_{PH} = 4.2 Hz, 2H, *m*-C₆H₃), 2.27 (s, 6H, Ar-CH₃), 2.12 (d, ³J_{PH} = 11.3 Hz, 12H, NMe₂), 1.93 (s, 12H, Ar-CH₃), 0.98 (s, 3H, CH₃CN). ¹⁹F{¹H} NMR (282 MHz, C₆D₆): -150.24 ppm. ³¹P{¹H} NMR (122 MHz, C₆D₆): δ = 89.7 ppm.

¹³C NMR, CHN and MS were not obtained for this compound.

Synthesis of [TerP(NEt₂)₂Au-MeCN]BF₄ (4b)

Complex **2b** (0.032 g, 0.045 mmol) and AgBF₄ (0.009 g, 0.045 mmol) combined in a round-bottomed flask, dissolved in acetonitrile (2.5 mL) and stirred under exclusion of light for 30 min at room temperature. The solution was then filtered using a canula fitted with a glass microfiber filter. This mixture was then dried and extracted with benzene-*d*⁶ and filtered into an NMR-tube equipped with a *J*-young-type screw cap.

¹H NMR (300 MHz, C₆D₆) δ = 6.99 (td, ³J_{HH} = 7.6 Hz, ⁵J_{PH} = 1.7 Hz, 1H, *p*-C₆H₃), 6.94 (s, 4H, *m*-Mes), 6.60 (dd, ³J_{HH} = 7.6 Hz, ⁴J_{PH} = 4.0 Hz, 2H, *m*-C₆H₃), 2.67–2.52 (m, 8H, NCH₂CH₃), 2.41 (s, 6H, Ar-CH₃), 2.01 (s, 12H, Ar-CH₃), 1.46 (s, 3H, CH₃CN), 0.80 (t, ³J_{HH} = 7.1 Hz, 12H, NCH₂CH₃). ¹⁹F{¹H} NMR (282 MHz, C₆D₆): -150.22 ppm. ³¹P{¹H} NMR (122 MHz, C₆D₆): δ = 84.4 ppm.

Single crystal X-ray analysis, ¹³C NMR, CHN and MS were not obtained for this compound.

Synthesis of [TerP(NMe₂)₂Au-py]PF₆ (5a)

TerP(NMe₂)₂AuCl (0.066 g, 0.1 mmol) and AgPF₆ (0.025 g, 0.1 mmol) were dissolved in 5 mL dichloromethane. 10 μL pyridine was added to the solution and stirred overnight. After canula filtration the clear solution is reduced to 1 mL, layered with 5 mL *n*-hexane and placed in the freezer (-70 °C) for 4 h. The solvent was removed and the resulting colorless crystals of [(TerP(NMe₂)₂)Au(py)]PF₆ (0.062 g, 0.088 mmol, 88%) were dried *in vacuo*.

¹H NMR (300 MHz, CD₂Cl₂) δ = 8.15–8.10 (m, 3H, *p,m*-CH-py), 7.73–7.68 (m, 2H, *o*-CH-py), 7.67–7.58 (m, 1H, *p*-CH-Ph), 7.09 (dd, ¹J_{HH} = 7.6 Hz, ¹J_{HP} = 4.2 Hz, 2H, *m*-CH-Ph), 6.88 (s, 4H, *m*-CH-Ph), 2.40 (s, 6H, NCH₃), 2.36 (s, 6H, NCH₃), 2.14 (s, 6H, Ar-CH₃), 2.07 (s, 6H, Ar-CH₃). ¹³C NMR (75 MHz, CD₂Cl₂): δ = 150.95, 146.30, 146.13, 142.04, 138.97 (d, ²J_{CP} = 5.8 Hz), 137.78, 136.82, 132.76 (d, ¹J_{CP} = 8.8 Hz), 129.26, 127.10, 40.81 (d, ¹J_{CP} = 8.7 Hz), 22.00, 21.15. ¹⁹F NMR (282 MHz, CD₂Cl₂): δ = -73.38 (d, *J* = 707.6 Hz). ³¹P NMR (122 MHz, CD₂Cl₂): δ = 91.49, -144.45 (septet, ¹J_{P-F} = 707.6 Hz).

Sufficient CHN analyses for this compound were not obtained, despite crystals showing no impurities on the basis of ¹H NMR spectroscopy.³³

Synthesis of [TerP(NMe₂)₂AgCl]₂ (6a)

AgCl (0.019 g, 0.129 mmol) and TerP(NMe₂)₂ (0.056 g, 0.129 mmol) were dissolved in 5 mL of dichloromethane under the exclusion of light (wrap flask with tin foil) and the reaction mixture was stirred for 16 h at room temperature, which was accompanied by precipitation of slight amounts of solid material. After canula filtration all volatile components were removed under vacuum, the residue was washed with small amounts of *n*-hexane (2 × 2 mL) and dried under vacuum to yield **6a** 0.046 g (0.040 mmol; 62%) as a colorless solid.

Crystals suitable for single-crystal X-ray diffraction were obtained by slow evaporation of a solution of **6a** in acetone.

¹H NMR (300 MHz, CDCl₃, 298 K): *d* = 2.04 (s, 24H, *o*-CH₃C₆H₃), 2.25 (s, 12H, N(CH₃)₂), 2.28 (s, 12H, N(CH₃)₂), 2.34 (s, 12H, *p*-CH₃C₆H₃), 6.99–7.00 (m, 8H, CH_{Mes}), 7.00–7.03 (m, 4H, *m*-CH_{Ar}IP), 7.47–7.51 (m, 2H, *p*-CH_{Ar}IP) ppm. ¹³C{¹H} NMR (75 MHz, CDCl₃, 298 K): *d* = 21.2 (*p*-CH₃C₆H₃), 21.55 (*o*-CH₃C₆H₃), 21.57 (*o*-CH₃C₆H₃), 41.78 (d, ²J_{P,C} = 13.5 Hz, N(CH₃)₂), 41.80 (d, ²J_{P,C} = 13.7 Hz, N(CH₃)₂), 129.2 (CH_{Mes}), 130.9 (*p*-CH_{Ar}IP), 131.4 (d, ³J_{P,C} = 5.8 Hz, *m*-CH_{Ar}IP), 133.7 (m, C_{q,Ar}IP), 135.2 (*o*-C_{q,Mes}C₆H₃), 137.4 (*p*-C_{q,Mes}C₆H₃), 138.0 (d, ³J_{P,C} = 6.1 Hz, C_{q,Mes}), 144.5 (d, ²J_{C,P} = 15.3 Hz, *o*-C_{q,Ar}IP) ppm. ³¹P{¹H} NMR (122 MHz, CDCl₃, 298 K): *d* = 99.3 (dd, ¹J_{Ag,P} = 862.3 Hz, ¹J_{Ag,P} = 746.4 Hz) ppm. MS (ESI-TOF): expected: *m/z* = 1113.3184 [M - Cl]⁺; found: *m/z* = 1113.3202. EA: calculated: C 58.40, H 6.48, N 4.86; found: C 58.56, H 6.96, N 4.34%.

Synthesis of [TerP(NEt₂)₂AgCl]₂ (6b)

AgCl (0.147 g, 1.023 mmol) and TerP(NEt₂)₂ (0.500 g, 1.023 mmol) were dissolved in 15 mL of dichloromethane under the exclusion of light (wrap flask with tin foil) and the reaction mixture was stirred for 16 h at room temperature which was accompanied by precipitation of slight amounts of solid material. After canula filtration all volatile components were removed under vacuum, the residue was washed with *n*-hexane (2 × 5 mL) and dried under vacuum to yield **6b** 0.546 g (0.422 mmol; 83%) as a colorless solid. Crystals suitable for single-crystal X-ray diffraction were obtained by slow evaporation of a solution of **6b** in acetone.

¹H NMR (300 MHz, CDCl₃, 298 K): *d* = 0.91 (t, ³J_{H,H} = 7.1 Hz, 24H, NCH₂CH₃), 2.10 (s, 24H, *o*-CH₃C₆H₃), 2.36 (s, 12H, *p*-CH₃C₆H₃), 2.54–2.79 (m, 16H, NCH₂CH₃), 6.94–6.97 (m, 4H, *m*-CH_{Ar}IP), 7.00–7.01 (m, 8H, CH_{Mes}), 7.44–7.48 (m, 2H, *p*-CH_{Ar}IP) ppm. ¹³C{¹H} NMR (75 MHz, CDCl₃, 298 K): *d* = 15.1 (d, ³J_{P,C} = 2.7 Hz, NCH₂CH₃), 21.3 (*p*-CH₃C₆H₃), 21.83 (*o*-CH₃C₆H₃), 21.84 (*o*-CH₃C₆H₃), 45.0 (d, ²J_{P,C} = 17.0 Hz, NCH₂CH₃), 129.6 (CH_{Mes}), 130.6 (*p*-CH_{Ar}IP), 131.8 (d, ³J_{P,C} = 5.5 Hz, *m*-CH_{Ar}IP), 133.9 (m, C_{q,Ar}IP), 135.2 (*o*-C_{q,Mes}C₆H₃), 137.7 (*p*-C_{q,Mes}C₆H₃), 138.8 (d, ³J_{P,C} = 6.3 Hz, C_{q,Mes}), 144.5 (m, *o*-C_{q,Ar}IP) ppm. ³¹P{¹H} NMR (122 MHz, CDCl₃, 298 K): *d* = 94.3 (dd, ¹J_{Ag,P} = 864.0 Hz, ¹J_{Ag,P} = 748.9 Hz) ppm. MS (ESI-TOF): expected: *m/z* = 1227.4428 [M - Cl]⁺; found: *m/z* = 1227.4449. EA: calculated: C 60.81, H 7.18, N 4.43; found: C 60.83, H 7.74, N 4.28%.

Synthesis of [TerP(NMe₂)₂Au(H₂N-*p*-Me-C₆H₄)₂] (7a)

Complex **2a** (0.100 g, 0.150 mmol) and AgBF₄ (0.031 g, 0.159 mmol) were combined in a round-bottomed flask, dissolved in acetonitrile (5 mL) and stirred under exclusion of light for 30 min at room temperature. The solution was then filtered using a canula fitted with a glass microfiber filter. To the filtrate *p*-toluidine (0.020 g, 0.186 mmol) was added, resulting in the formation of a white precipitate. The supernatant solution was removed by canula filtration and the residual off-white solid triturated with *n*-pentane and dried *in vacuo*. This afforded [(TerP(NMe₂)₂)Au(H₂N-*p*-Me-C₆H₄)] (**7a**, 0.095 g, 0.113 mmol, 75%) as a greyish powder.

¹H NMR (300 MHz, CDCl₃) δ = 7.55 (td, ³J_{HH} = 7.6 Hz, ⁵J_{PH} = 1.7 Hz, 1H, *p*-C₆H₃), 7.09–7.00 (m, 4H, *m*-C₆H₃, *p*-Tol), 6.88 (d, br ²J_{HH} = 8.4 Hz, 2H, *p*-Tol), 4.50 (br, 2H, *p*-Tol-NH₂), 2.32 (s, 6H, Ar-CH₃), 2.28 (s, 3H, *p*-Tol *p*-CH₃), 2.27 (d, ³J_{PH} = 11.2 Hz, 12H, NCH₃), 2.02 (s, 12H, Ar-CH₃). ¹⁹F{¹H} NMR (282 MHz, CDCl₃): -151.15 ppm. ³¹P{¹H} NMR (122 MHz, CDCl₃): δ = 93.77 ppm.

Catalytic hydroamination of acetylenes

The complexes [Au(L)Cl] (0.045 mmol, 1 equiv.; L = **1a**, **1b**) and AgBF₄ (0.045 mmol, 1 equiv.) were dissolved in MeCN (2.5 mL) and stirred under exclusion of light for 30 min at room temperature and the solution was then filtered using a filter canula fitted with a glass microfiber filter. This 0.018 M solution was used as a stock solution. Acetylenes (0.455 mmol) and aryl amines (0.503 mmol) were weighed in a glovebox and were dissolved in 1.75 mL MeCN in a vial fitted with a septum screw cap. Afterwards 0.25 mL of the respective catalyst standard solutions were added and stirred for 16 h at 60 °C. The NMR yields were determined by ¹H NMR spectroscopy as an average of two runs using 1,3,5-MeO-C₆H₃ as an internal standard. The characteristic singlet of the CH₃ group of the imines that appears around 2.3 ppm was used for the integration. For the isolated yields, the products were purified by column chromatography on silica gel. Spectroscopic data is provided in the ESI.[†]³³

Conflicts of interest

There are no conflicts to declare.

Acknowledgements

C. H.-J. thanks Prof. M. Beller for his support, the European Union for funding (H2020-MSCA-IF-2017 792177), the Max Buchner-Foundation for a Scientific Fellowship and support by an Exploration Grant of the Boehringer Ingelheim Foundation (BIS) is acknowledged. We thank our technical and analytical staff for assistance, especially Dr Anke Spannenberg for her support regarding X-ray analysis. Dr Alexander Villinger is acknowledged for assistance with the X-ray analysis of **4a**. Dr Jonas Bresien is kindly acknowledged for help with

vibrational spectroscopy and fruitful discussions on DFT calculations.

Notes and references

- 1 B. F. Straub, *Angew. Chem., Int. Ed.*, 2010, **49**, 7622–7622.
- 2 D. W. Old, J. P. Wolfe and S. L. Buchwald, *J. Am. Chem. Soc.*, 1998, **120**, 9722–9723.
- 3 B. P. Fors, D. A. Watson, M. R. Biscoe and S. L. Buchwald, *J. Am. Chem. Soc.*, 2008, **130**, 13552–13554.
- 4 T. Ikawa, T. E. Barder, M. R. Biscoe and S. L. Buchwald, *J. Am. Chem. Soc.*, 2007, **129**, 13001–13007.
- 5 T. E. Barder, S. D. Walker, J. R. Martinelli and S. L. Buchwald, *J. Am. Chem. Soc.*, 2005, **127**, 4685–4696.
- 6 D. S. Surry and S. L. Buchwald, *Angew. Chem., Int. Ed.*, 2008, **47**, 6338–6361.
- 7 C. A. Tolman, *J. Am. Chem. Soc.*, 1970, **92**, 2956–2965.
- 8 C. A. Tolman, *Chem. Rev.*, 1977, **77**, 313–348.
- 9 A. S. K. Hashmi, *Chem. Rev.*, 2007, **107**, 3180–3211.
- 10 A. Arcadi, *Chem. Rev.*, 2008, **108**, 3266–3325.
- 11 Z. Li, C. Brouwer and C. He, *Chem. Rev.*, 2008, **108**, 3239–3265.
- 12 R. H. Hertwig, W. Koch, D. Schröder, H. Schwarz, J. Hrušák and P. Schwerdtfeger, *J. Phys. Chem.*, 1996, **100**, 12253–12260.
- 13 D. J. Gorin and F. D. Toste, *Nature*, 2007, **446**, 395–403.
- 14 A. S. K. Hashmi, *Angew. Chem., Int. Ed.*, 2010, **49**, 5232–5241.
- 15 W. Wang, G. B. Hammond and B. Xu, *J. Am. Chem. Soc.*, 2012, **134**, 5697–5705.
- 16 D. G. Gusev, *Organometallics*, 2009, **28**, 6458–6461.
- 17 T. Wittler, H. Darmandeh, P. Mehlmann and F. Dielmann, *Organometallics*, 2018, **37**, 3064–3072.
- 18 S. Ullrich, B. Kovačević, X. Xie and J. Sundermeyer, *Angew. Chem., Int. Ed.*, 2019, **58**, 10335–10339.
- 19 J. A. C. Clyburne and N. McMullen, *Coord. Chem. Rev.*, 2000, **210**, 73–99.
- 20 T. Nguyen, A. D. Sutton, M. Brynda, J. C. Fettinger, G. J. Long and P. P. Power, *Science*, 2005, **310**, 844.
- 21 E. Rivard and P. P. Power, *Inorg. Chem.*, 2007, **46**, 10047–10064.
- 22 R. C. Fischer and P. P. Power, *Chem. Rev.*, 2010, **110**, 3877–3923.
- 23 D. L. Kays, *Chem. Soc. Rev.*, 2016, **45**, 1004–1018.
- 24 K. Ruhlandt-Senge, J. Ellison, R. Wehmschulte, F. Pauer and P. Power, *J. Am. Chem. Soc.*, 1993, **115**, 11353–11357.
- 25 C. Gerdes, W. Saak, D. Haase and T. Müller, *J. Am. Chem. Soc.*, 2013, **135**, 10353–10361.
- 26 A. J. Veinot, A. D. K. Todd and J. D. Masuda, *Angew. Chem., Int. Ed.*, 2017, **56**, 11615–11619.
- 27 E. Urnéžius and J. D. Protasiewicz, *Main Group Chem.*, 1996, **1**, 369–372.
- 28 C. M. E. Graham, T. E. Pritchard, P. D. Boyle, J. Valjus, H. M. Tuononen and P. J. Ragogna, *Angew. Chem., Int. Ed.*, 2017, **56**, 6236–6240.

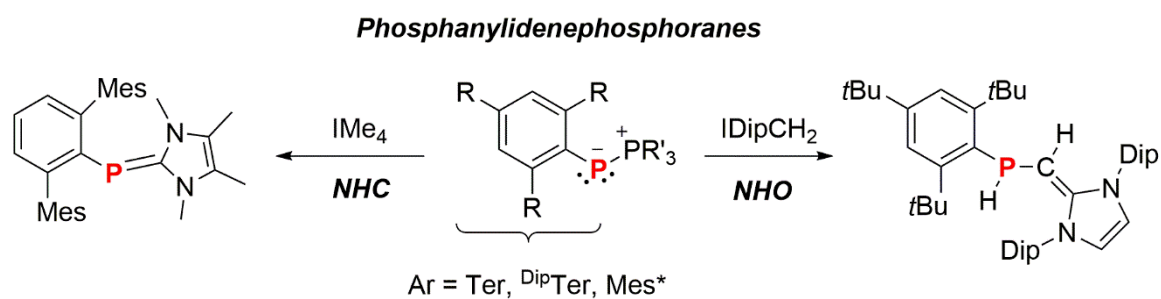
- 29 D. V. Partyka, M. P. Washington, J. B. Updegraff, X. Chen, C. D. Incarvito, A. L. Rheingold and J. D. Protasiewicz, *J. Organomet. Chem.*, 2009, **694**, 1441–1446.
- 30 A. Orthaber, F. Belaj, J. H. Albering and R. Pietschnig, *Eur. J. Inorg. Chem.*, 2010, **2010**, 34–37.
- 31 R. C. Smith, R. A. Woloszynek, W. Chen, T. Ren and J. D. Protasiewicz, *Tetrahedron Lett.*, 2004, **45**, 8327–8330.
- 32 B. Buster, A. A. Diaz, T. Graham, R. Khan, M. A. Khan, D. R. Powell and R. J. Wehmschulte, *Inorg. Chim. Acta*, 2009, **362**, 3465–3474.
- 33 Experimental, computational, and details on the X-ray diffraction studies are included in the ESI.†
- 34 P. Pyykkö and M. Atsumi, *Chem. – Eur. J.*, 2009, **15**, 12770–12779.
- 35 C. Hering, M. Lehmann, A. Schulz and A. Villinger, *Inorg. Chem.*, 2012, **51**, 8212–8224.
- 36 E. Deck, H. E. Wagner, J. Paradies and F. Breher, *Chem. Commun.*, 2019, **55**, 5323–5326.
- 37 C. Griebel, D. D. Hodges, B. R. Yager, F. L. Liu, W. Zhou, K. J. Makaravage, Y. Zhu, S. G. Norman, R. Lan, C. S. Day and A. C. Jones, *Organometallics*, 2020, **39**, 2665–2671.
- 38 M. Marín, J. J. Moreno, M. M. Alcaide, E. Álvarez, J. López-Serrano, J. Campos, M. C. Nicasio and E. Carmona, *J. Organomet. Chem.*, 2019, **896**, 120–128.
- 39 M. Marín, J. J. Moreno, C. Navarro-Gilabert, E. Álvarez, C. Maya, R. Peloso, M. C. Nicasio and E. Carmona, *Chem. – Eur. J.*, 2019, **25**, 260–272.
- 40 R. F. W. Bader, *Acc. Chem. Res.*, 1985, **18**, 9–15.
- 41 S. Shahbazian, *Chem. – Eur. J.*, 2018, **24**, 5401–5405.
- 42 L. Falivene, R. Credendino, A. Poater, A. Petta, L. Serra, R. Oliva, V. Scarano and L. Cavallo, *Organometallics*, 2016, **35**, 2286–2293.
- 43 H. Clavier and S. P. Nolan, *Chem. Commun.*, 2010, **46**, 841–861.
- 44 A. Homs, I. Escofet and A. M. Echavarren, *Org. Lett.*, 2013, **15**, 5782–5785.
- 45 A. Gorrane, E. Álvarez, H. García and A. Corma, *Chem. – Eur. J.*, 2016, **22**, 340–354.
- 46 C. Ganesamoorthy, J. T. Mague and M. S. Balakrishna, *Eur. J. Inorg. Chem.*, 2008, **2008**, 596–604.
- 47 S. J. Sabounchei, M. Pourshahbaz, S. Salehzadeh, M. Bayat, R. Karamian, M. Asadbegyan and H. R. Khavasi, *Polyhedron*, 2015, **85**, 652–664.
- 48 G. A. Bowmaker, Effendy, P. J. Harvey, P. C. Healy, B. W. Skelton and A. H. White, *J. Chem. Soc., Dalton Trans.*, 1996, 2459–2465.
- 49 W. Petz, F. Weller, J. Uddin and G. Frenking, *Organometallics*, 1999, **18**, 619–626.
- 50 R. Dorta, E. D. Stevens, N. M. Scott, C. Costabile, L. Cavallo, C. D. Hoff and S. P. Nolan, *J. Am. Chem. Soc.*, 2005, **127**, 2485–2495.
- 51 T. Scherpf, C. Schwarz, L. T. Scharf, J.-A. Zur, A. Helbig and V. H. Gessner, *Angew. Chem., Int. Ed.*, 2018, **57**, 12859–12864.
- 52 K. D. Hesp and M. Stradiotto, *J. Am. Chem. Soc.*, 2010, **132**, 18026–18029.
- 53 F. Reiß, A. Schulz, A. Villinger and N. Weding, *Dalton Trans.*, 2010, **39**, 9962–9972.
- 54 P. Wucher, J. B. Schwaderer and S. Mecking, *ACS Catal.*, 2014, **4**, 2672–2679.

5.2 Reactivity of phospho–Wittig reagents towards NHCs and NHOs

P. Gupta, J.-E. Siewert, T. Wellnitz, M. Fischer, W. Baumann, T. Beweries, C. Hering-Junghans

Dalton Trans. **2021**, *50*, 1838–1844.

DOI: 10.1039/D1DT00071C



Reprinted (adapted) with permission from *Dalton Trans.*.

Copyright 2021 Royal Society of Chemistry

Cite this: *Dalton Trans.*, 2021, **50**, 1838

Received 8th January 2021.

Accepted 12th January 2021

DOI: 10.1039/d1dt00071c

rsc.li/dalton

Reactivity of phospho–Wittig reagents towards
NHCs and NHOs†‡Priyanka Gupta, Jan-Erik Siewert, Tim Wellnitz, Malte Fischer, Wolfgang Baumann,
Torsten Beveries* and Christian Hering-Junghans*

Phospho–Wittig reagents, RPPMe₃ (R = Mes* 2,4,6-*t*Bu₃-C₆H₂; ^{Me}Ter 2,6-(2,4,6-Me₃C₆H₂)-C₆H₃; ^{DIP}Ter 2,6-(2,6-*i*Pr₂C₆H₃)-C₆H₃), can be considered as phosphine-stabilized phosphinidenes. In this study we show that PMe₃ can be displaced by NHCs or NHOs. Interestingly, phosphinidene-like reactivity results in a subsequent C(sp²)-H activation of the exocyclic CH₂ group in NHOs. This concept was further extended to allyl-apeded NHOs, which resulted in phosphine-substituted allyl species.

In 1953 Wittig and Geisler reported the olefination of carbonyl groups with the aid of phosphorus ylides, the so-called Wittig reaction.^{1,2} This protocol allows the chemo- and regioselective conversion of carbonyl functionalities into olefins and has been widely utilized, even on large industrial scale.^{3–5} Phosphorus ylides of the type R₃P⁽⁺⁾-C⁽⁻⁾R₂ are generated by the alkylation of phosphines and subsequent treatment with stoichiometric amounts of base. The reaction with a carbonyl compound then furnishes the desired alkene and phosphine oxides, which are the driving force of this transformation.

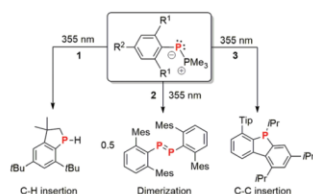
Burg and Mahler investigated the action of an excess of PMe₃ on the cyclophosphanes (PCF₃)₄ and (PCF₃)₅, noting the reversible formation of F₃CP=PMe₃, a phosphanylidene phosphorane,⁶ and the concentration-dependent exchange of PMe₃ was later detected, indicating exchange of coordinated PMe₃.⁷ Investigating the reactivity of [Cp₂Zr(PR₃)P^{Me}Ter] (R = Me, *n*Bu; ^{Me}Ter = 2,6-(2,4,6-Me₃C₆H₂)₂-C₆H₃) Protasiewicz and co-workers noted the formation of ^{Me}TerP=PR₃.⁸ In general compounds of the type RP=PR₃ are referred to as phospho–Wittig reagents by isolobal replacement of the CR₂ in R₂C=PR₃ with a phosphinidene fragment PR.⁹ The term “phospho–Wittig” reaction was originally introduced by Mathey for the reaction of (RO)₂P(O)-P⁽⁻⁾[W(CO)₅]R' with ketones to give (CO)₅W-coordinated phosphoalkenes.¹⁰ The Protasiewicz group then showed that unsupported phospho–

Wittig reagents can be isolated when the group R on phosphorus is kinetically stabilizing and to date four examples of ArP=PMe₃ (Ar = 2,4,6-*t*Bu₃-C₆H₂, Mes* (1); ^{Me}Ter (2);¹¹ 2,6-(2,4,6-*i*Pr₃C₆H₂)-C₆H₃, ^{TIP}Ter (3);¹² 1,1,3,3,5,5,7,7-octaethyl-1,2,3,5,6,7-hexahydro-*s*-indacen-4-yl, EIND¹³) have been described in the literature. In addition, the difunctional phospho–Wittig material (*E*),(*E*)-1,4-bis-(Me₃P=P)-(3,5-dimethylstyryl)-2,5-di-*n*-hexyloxybenzene was shown to afford diphosphene containing polymers upon photolysis or thermolysis.¹⁴ Phospho–Wittig reagents are generally obtained by the combination of the respective dichlorophosphine Ar-PCl₂ with zinc powder and an excess of PMe₃, whereby PMe₃ acts as the active reductant (with concomitant formation of Cl₂PMe₃),^{15,16} and stabilizing base. Zinc dust seems to be redundant here, however, high yields are not obtained when only using PMe₃, *vide infra*. The role of PR₃ and PR₃Cl₂ was studied in detail and it was shown that PMe₃ can catalyse the chlorine atom transfer between ArPPMe₃ and Ar'PCl₂.¹⁵ Using ArP=PMe₃ in the reaction with aldehydes (note ketones cannot be converted using this methodology) phosphoalkenes, RP=CR'H, are obtained, with the concomitant formation of Me₃P=O. Thus, this reactivity can be classified as Wittig-type, as the driving force in the classical Wittig reaction is the formation of R₃P=O as well. Furthermore, phosphanylidene phosphoranes have been shown to display phosphinidenoid reactivity. For example, laser irradiation of 1–3 at 355 nm facilitates PMe₃ cleavage,¹² and in case of 1 a C–H activation of one *o*-*t*Bu-group of Mes* results in the formation of a phosphindane (Scheme 1).^{17–19} For 2 phosphinidene recombination and formation of (PTer)₂ prevails, whereas C–C bond activation and phosphoalkene formation is the major pathway for 3 (Scheme 1, middle and right).²⁰ Moreover, the cyclo-addition of 1 and 2 with quinones affords 1,3,2-dioxophospholanes rather than producing the expected 1,2-diphosphoalkenes.²¹ Phosphinidene transfer was shown for 2 when combined with Cp₂Zr(PMe₃)₂ yielding

Leibniz-Institut für Katalyse e.V. (LIKAT Rostock), Albert-Einstein-Str. 29a, 18059 Rostock, Germany. E-mail: torsten.beweries@catalysis.de, christian.hering-junghans@catalysis.de

†Dedicated to Prof. Dr Paul Kamer for his achievements in Phosphorus Chemistry.

‡Electronic supplementary information (ESI) available: Synthesis and characterization of compounds, NMR spectra, crystallographic, and computational details. CCDC 2046859–2046869. For ESI and crystallographic data in CIF or other electronic format see DOI: 10.1039/d1dt00071c



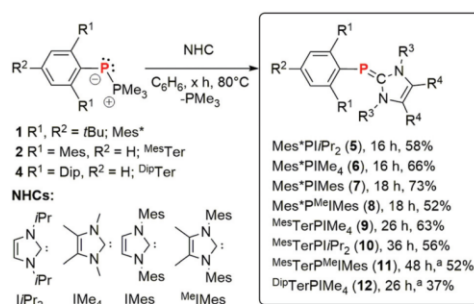
Scheme 1 Photolytic cleavage of **1** (R^1 , R^2 = *t*Bu), **2** (R^1 = Mes, R^2 = H) and **3** (R^1 = Tip, R^2 = H) and the products of phosphinidene quenching.

$\text{Cp}_2\text{Zr}(\text{P}^{\text{Mes}}\text{Ter})(\text{PMe}_3)$, while combination of **1** with (PNP)V(CH_2tBu)₂ (PNP = $\text{N}[\text{C}_2\text{-P}(\text{CHMe}_2)_2\text{-4-methylphenyl}]_2$) furnished the first V(v) terminal phosphinidene complex.²²

Recently, phosphanylphosphaketenes $\text{R}_2\text{P-PCO}$ have emerged as a synthetic surrogate for phosphinidenes, which unlocked a pathway towards an isolable room-temperature stable singlet phosphinidene [P]P ([P] = $(\text{H}_2\text{CNAr}^{**})_2\text{P}$, Ar^{**} = 2,6-bis[(4-*tert*-butylphenyl)methyl]-4-methylphenyl).²³ In addition, Bertrand and co-workers showed facile ligand exchange of CO in $[\text{P}]\text{PCO}$ ($[\text{P}]$ = $(\text{H}_2\text{CNDip})_2\text{P}$) for PR_3 , CNAd, IiPr_2 and EtCAAC , with calculations supporting an associative mechanism with a T-shaped transition state.²⁴ Just recently, the decarbonylation of $[\text{P}]\text{PCO}$ in the presence of $(\text{Dip})\text{NacnacGa}$ afforded a phosphagallene with a $\text{P}=\text{Ga}$ double bond.²⁵ Gallium phosphaketenes also show CO for PMe_3 exchange, affording gallium-substituted phospho-Wittig reagents.²⁶

Phospha-Wittig reagents are moreover isovalence-electronic to carbene phosphinidene adducts,²⁷ an emerging compound class in main group and transition metal chemistry²⁸ and thus, phosphanylidenephosphoranes should be easily converted into such by replacement of the phosphine with a carbene. In addition, the NHC phosphinidene adduct $\text{PhP}=\text{IME}_2$ has been shown to be transferred onto organic substrates in the presence of ZnCl_2 ,²⁹ furthermore underlining the potential of this compound class. We now report on the facile synthesis of a variety of NHC phosphinidene adducts derived from ArPPR_3 and show that in case of N-heterocyclic olefins (NHOs) PMe_3 release is followed by an intramolecular $\text{C}(\text{sp}^2)\text{-H}$ activation to afford phosphine-substituted NHOs.

Phospha-Wittig reagents are usually synthesized *in situ* and directly used in subsequent reactions, mostly with aldehydes in the synthesis of phosphalkenes. Herein, modified literature procedures were used to allow for the isolation of the phospho-Wittig reagents **1** and **2** in up to a multigram scale (Scheme 2, for detailed synthetic procedures please refer to the ESI p.S4ff†).³⁰ DipTerPPMe_3 (**4**), has not been reported previously and was synthesized by reduction of DipTerPCL_2 with Zn/PMe_3 in a 1:2:10 ratio in THF. Full conversion was achieved after stirring the mixture for 24 h and after filtration and removal of the solvent **4** was afforded as a yellow, thermally stable solid in 50% yield. In the ^{31}P NMR spectrum **4** is characterized by two doublet signals at -116.5 ppm (P^{DipTer})



Scheme 2 Synthesis of NHC phosphinidene adducts **5–12** in the reaction of various NHCs with **1**, **2** or **4**, respectively. (†Mixture was heated to 115 °C in toluene-*d*₈).

and -3.1 (PMe_3) ppm, respectively and a $^1J_{\text{PP}}$ coupling constants of 560 Hz. X-ray quality crystals of **4** were grown from a saturated *n*-hexane solution at -30 °C (Fig. S13†). The P1-P2 distance [2.0955(7) Å] is significantly shorter than typical P-P single bonds ($\sum r_{\text{cov}}(\text{P-P}) = 2.22$ Å)³¹ and slightly elongated compared to typical $\text{P}=\text{P}$ double bonds ($\sum r_{\text{cov}}(\text{P}=\text{P}) = 2.04$ Å),³¹ thus being, as expected, in good accordance to the other structurally characterized phospho-Wittig reagent **2** (2.084(2) Å).³² With **1**, **2** and **4** available on a gram-scale we systematically studied their reactivity.

In a first sequence $\text{Mes}^*\text{PPMe}_3$ (**1**) was combined with IiPr_2 in C_6D_6 at room temperature, resulting in a color change from yellow to orange and the appearance of a signal at -62.6 ppm for free PMe_3 in the ^{31}P NMR spectrum and at -50.7 ppm suggested formation of the corresponding NHC phosphinidene adduct $\text{Mes}^*\text{P}=\text{IiPr}_2$ (**5**) (Scheme 2).^{27,33} Clean conversion to **5** is achieved upon heating to 80 °C over a period of 16 h. To gauge the scope of the substitution reaction, carbenes with different steric profiles were tested. Complete PMe_3 for NHC exchange in **1** at 80 °C was achieved for IME_4 , IMes and MeIMes , while no conversion was achieved with IiPr_2Me_2 , which is most likely due to steric reasons. $\text{Mes}^*\text{P}=\text{IME}_4$ (**6**), $\text{Mes}^*\text{P}=\text{IMes}$ (**7**) and $\text{Mes}^*\text{P}=\text{MeIMes}$ (**8**) are deep yellow thermally stable (melting points >138 °C) solids and X-Ray quality crystals of **5**, **6** and **8** were grown from saturated *n*-hexane solutions at -30 °C. **6** shows a ^{31}P NMR signal at -47.5 ppm, while **7** and **8** appear less shielded at -29.8 and -33.2 ppm, respectively. In the ^1H NMR spectrum three signals are detected for the Mes* group and two sets of signals for the *N*-substituents of the NHCs as well as for the backbone protons (**5**, **7**) or methyl groups (**6**, **8**), respectively, indicating C_2 symmetry on the NMR time-scale. The molecular structures of **6** and **8** display P-C_{NHC} distances [**6** 1.7709(12), **8** 1.7630(19) Å] (Fig. 1) similar to that reported in $(\text{EIND})\text{P}=\text{IME}_4$ [$d(\text{P-C}_{\text{NHC}})$ 1.767(3) Å],³⁴ and $\text{Mes}^*\text{P}=\text{IMes}$ [$d(\text{P-C}_{\text{NHC}})$ 1.769(3) Å].³⁵ The CPC_{NHC} angles [**6** 102.58(5), **8** 106.38(8) °] are in the expected range for NHC phosphinidene adducts and the planes of the central phenyl group in Mes^* and the imidazolidine unit are offset from a

perpendicular arrangement by 10–15°. One of the *N*-mesityl substituents in **8** is parallel to the Mes* group indicating arene–arene interactions. The concept of NHC for PMe₃ exchange could be extended to **2** and Mes*TerP=IMe₄ (**9**),³⁶ and Mes*TerP=IPr₂ (**10**) were afforded as yellow crystalline solids in moderate isolated yields solids after heating **2** and the respective NHC at 80 °C overnight (Scheme 2). The combination of **2** and Me*IMes gave only minimal conversion at 80 °C, however, heating the mixture to 115 °C in toluene-*d*₈ for 48 h facilitated full conversion to Mes*TerP=Me*IMes (**11**). Again, no conversion was observed with IPr₂Me₂, even though Mes*TerP=IPr₂Me₂ has been previously reported by Ragona *et al.* through the desulfurization of [SP^{Mes*Ter}]₂ with 2 equivalents of IPr₂Me₂. With **4** only the reaction with IMe₄ yielded the corresponding^{Dip}TerP=IMe₄ (**12**) in low isolated yields of 37% (Scheme 2). The P–C_{NHC} distances in **10** [1.786(2) Å] and **12** [1.8074(11) Å] are minimally longer compared to **6** and **8**, the CPC_{NHC} angles are similar [**10** 104.21(5), **12** 102.90°] and the imidazolidine and central phenyl plane deviate from a perpendicular arrangement by *ca.* 35° (Fig. 1). This indicates a more electron-rich phosphorus center compared to the Mes* substituted derivatives **5–8** as further evidenced by the ³¹P NMR shift of **9** [–76.9 ppm], **10** [–79.8 ppm], **11** [–45.1 ppm] and **12** [–63.2 ppm]. In addition, the ¹³C NMR signal of the C_{NHC} atom is detected at *ca.* 170 ppm with a ¹J_{PC} coupling constant that directly corresponds to the P–C bond lengths,³³ with J_{PC} values being smaller when the P–C bond is longer.

To elucidate the reaction mechanism we conducted DFT calculations at the B3LYP/6-311G(d,p) gd3 smd(C₆H₆) level of theory, which reproduced the metrical parameters of **1**, **2**, **4** and **5–12** well with respect to their molecular structures.³⁰ In addition, the calculated ³¹P NMR shifts are in good agreement with experimental values and reflect the trends observed for **5–12**.³⁰ Starting from **1** a T-shaped transition state in the reaction with IPr₂ was found, in line with the observed exchange of PMe₃ for a NHC in **1** to afford **5–8**.²⁴ The activation barrier was determined to be Δ_RG[‡] = 23.8 kcal mol^{–1} for IPr₂ and overall the formation of **5** and release of PMe₃ is exergonic by Δ_RG⁰ = –17.9 kcal mol^{–1}. A lower barrier was found for the reaction with IMe₄ [Δ_RG[‡] = 20.4 kcal mol^{–1}], whereas for IMes and Me*IMes the barriers are the highest. Furthermore, the

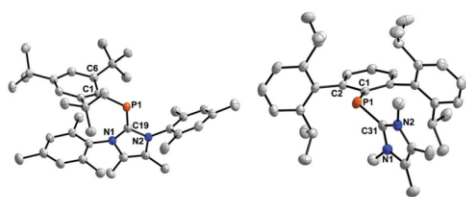
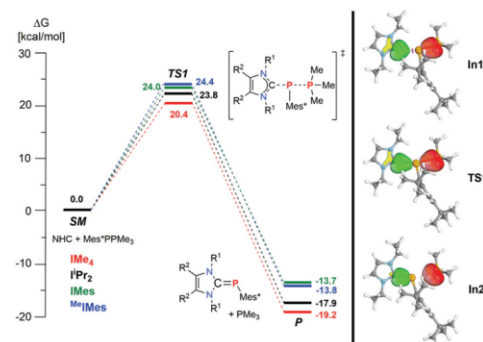


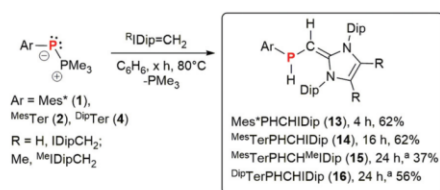
Fig. 1 POV-ray depiction of the molecular structure of **8** and **12**. ORTEPs drawn at 50% probability, all H-atoms are omitted for clarity. Selected bond lengths (Å) and angles (°) of **8** (values from 2nd molecule in the asymmetric unit): P1–C19 1.7630(19) (1.7594(19)), P1–C1 1.8683(18) (1.8639(18)), C19–P1–C1 106.38(8) (105.22(8)); **12**: P1–C19 1.8074(11), P1–C1 1.8280(10), C31–P1–C1 104.21(5).

associative transition state explains that the formation of the C–H-activated phosphaindane is not detected.³⁰ In accordance with experimental findings, the exchange in **2** was shown to possess higher Δ_RG[‡] energy barriers, with a similar exergonic overall reaction. The reaction of **2** with Me*IMes only proceeded at 115 °C, which is clearly reflected by a high activation barrier of 35.9 kcal mol^{–1} for this reaction, while the overall reaction is exergonic by –5.0 kcal mol^{–1}. To achieve a better understanding of this substitution reaction, IBO analyses of stationary points of selected species along the intrinsic reaction coordinate (IRC) from **1** with IPr₂ leading to **5** were performed (Scheme 3, right). IBOs have been shown to illustrate electronic structure changes in intuitive terms.^{37,38} In the case of **5**, the IBO associated with the IPr₂ lone pair (LP; Scheme 3, **IN1**, green/yellow) is transformed into a newly formed C–P σ-bond (Scheme 3, **IN2**, green/yellow), and the IBO for the P–P bonds converts into the PMe₃ lone pair of electrons (Scheme 3, **IN2**, red). The transformation clearly involves initial nucleophilic attack by the NHC LP onto the σ*-antibonding orbital of the P–P bond in **1**, **2** and **4** (Scheme 3, **TS1**), concurrent with the proposed S_N2-type substitution.

Having shown the facile PMe₃ for NHC exchange in **1**, **2** and **4** we wanted to investigate whether strongly σ-donating NHOs could also facilitate PMe₃ exchange to give more labile phosphinidene NHO adducts. NHOs are characterized by a highly polarized exocyclic double bond,^{39,40} placing considerable electron density on the terminal =CH₂ group, and determinations of their TEP values have shown that they are strong donors.^{33,41,42} In contrast to NHCs however, they are not π-accepting, facilitating the formation of Pd nanoparticles when using [(Me^cIdipCH₂)PdCl(Cin)] as a precatalyst in Buchwald–Hartwig aminations.⁴³ Beller and coworkers introduced 2-phosphanylmethyl-*N,N'*-biarylimidazolium salts as ligand precursors in palladium-catalysed C–O and C–N coupling reactions, which under the respective reaction conditions (*e.g.* CsOH as a base) should be deprotonated to give P-substituted NHOs.^{44,45} Moreover, isolable P-substituted



Scheme 3 DFT predicted free energy profile for the reaction of Mes*PPMe₃ with NHCs (left). Selected IBOs along the reaction coordinate (right).



Scheme 4 Synthesis of P-substituted NHOs (**13–16**) starting from **1**, **2** or **4** in the reaction with IDipCH₂ or MeIDipCH₂, respectively. (Sample was heated to 105 °C).

NHOs have been reported and Ghadwal *et al.* showed facile access to ^RIDip=C(Ph)PCl₂,⁴⁶ whereas IDipCH(PR₂) (R = *i*Pr, Ph) was reported by Rivard *et al.*⁴⁷ Using a bis(NHO)-ligand Kinjo and co-workers reported on aromatic isophosphindolium derivatives.⁴⁸ Combining **1** with IDipCH₂ in C₆D₆ and heating the 1:1 mixture to 80 °C overnight resulted in consumption of **1** and formation of a new species with a doublet of doublets in the ¹H NMR spectrum centred at 5.20 ppm (¹J_{PH} = 216.2 Hz, ³J_{HH} = 1.0 Hz) indicating the formation of Mes*PHCHIDip (**13**) (Scheme 4). This assignment was confirmed by SC-XRD experiments on crystals grown from saturated *n*-hexane solutions at –30 °C (Fig. 2, left). The P–H protons in **13** could be located on the Fourier map and a 1:1 ratio between *R* and *S* configurations was identified.

13 can be considered as a P-substituted NHO with a C=C_{NHC} [1.360(2), *cf.* Σ*r*_{cov}(C=C) = 1.34 Å]³¹ double bond and a P–C_{NHO} [1.8013(18), *cf.* Σ*r*_{cov}(P–C) = 1.86 Å]³¹ single bond in accord with the related IDipCH(P*i*Pr₂) [*cf.* *d*(C=C_{NHC}) 1.364(4), *d*(P–C_{NHO}) 1.780(3) Å].⁴⁷ To show that this reactivity is not only restricted to Mes*PPMe₃, **2** was treated with one equivalent

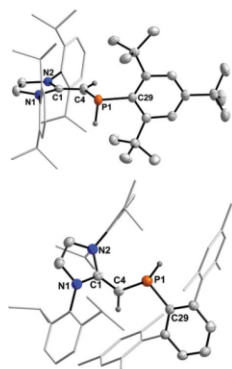
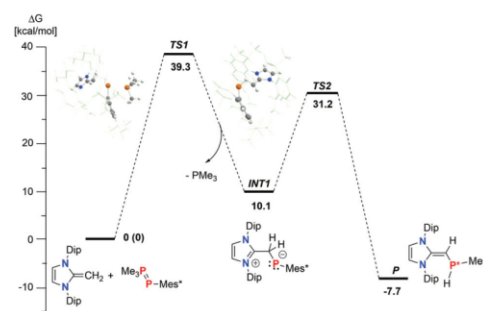


Fig. 2 POV-ray depiction of the molecular structure of **13** and **14**. ORTEPs drawn at 50% probability, all H atoms are omitted for clarity. Selected bond lengths (Å) and angles (°) of **13**: P1–C4 1.8013(18), P1–C29 1.8679(17), C1–C4 1.360(2); C1–C4–P1 126.51(14), C4–P1–C29 105.12(8); **14**: P1–C4 1.8540(13), P1–C29 1.8540(13), C1–C4 1.3580(18); C1–C4–P1 126.93(10), C4–P1–C29 100.59(6).

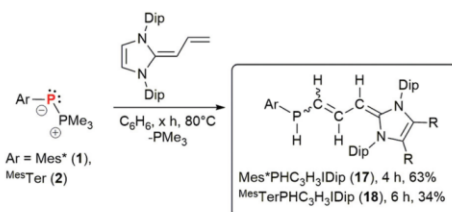
IDipCH₂ or MeIDipCH₂, and after heating to 80 °C or 105 °C the corresponding P-substituted NHOs Mes*TerPHCHIDip (**14**) and Mes*TerPHCHMeIDip (**15**) were afforded in 62 and 37% yield, respectively (Scheme 4). In addition, DipTerPHCHIDip (**16**) was afforded when utilizing **4** as a starting material. As mentioned above, the formation of **13–16** can be clearly identified by the appearance of a doublet of doublets between 4.11–5.29 ppm with a characteristic ¹J_{PH} and ³J_{HH} coupling constant of *ca.* 210 Hz and *ca.* 2 Hz, respectively. Additionally, the ¹³C NMR signal of the vinyl C-atom appears as a characteristic doublet (¹J_{PC} = 7–15 Hz) at *ca.* 42 ppm (**14–16**) and 52.5 ppm (**13**) [*cf.* IDipCH(P*i*Pr₂) δ(¹³C) = 51.4 ppm].⁴⁷ Moreover, IR spectroscopy revealed characteristic P–H stretching modes at *ca.* 2300 cm^{–1}.³⁰ A similar C–H activation process was discussed by Ghadwal *et al.* for IDipCH(SiCl₂H), readily accessible from the combination of two equivalents IDipCH₂ with HSiCl₃, with concomitant formation of [IDipCH₃]Cl. Interestingly, IDipCH(SiCl₂H) is also formed when IDipSiCl₂ is reacted with IDipCH₂, with a formal insertion of the silylene SiCl₂ into the exocyclic CH₂ group of IDipCH₂.⁴⁹

This C(sp²)-H bond activation in NHOs with the aid of the phosphinidenoid species **1**, **2** and **4** was theoretically investigated by DFT studies. A potential energy surface scan was carried out for the reaction of **1** with IDipCH₂ and a first T-shaped transition state was located with a high barrier of Δ_RG[‡] = 39.3 kcal mol^{–1} (Scheme 5), in line with these reactions going to completion only after prolonged heating at 80 °C. The intermediate INT1, an NHO-phosphinidene adduct through release of PMe₃ is endergonic and in a second reaction step an H-Shift from IDipCH₂ to PMe₃ occurs with a barrier (TS2, Δ_RG[‡] = 21.1 kcal mol^{–1}) that is lower than TS1. Therefore, the NHO for PMe₃ substitution is the rate-determining step, in line with INT1 not being observed in this transformation. It needs to be pointed out that the energy barrier TS1 is rather high, however, the full model was used for these calculations and the trends observed experimentally are clearly supported.

Having observed this C(sp²)-H activation we turned to the allyl-appended NHO IDipC₃H₄, to elucidate whether the C–H activation pathway is more general. Enediamine IDipC₃H₄ was



Scheme 5 DFT predicted free energy profile for the reaction of Mes*PPMe₃ with IDipCH₂. The free enthalpies are given in kcal mol^{–1}.



Scheme 6 Synthesis of P-substituted enediamines **17** and **18** starting from **1** or **2** in the reaction with IDipC₃H₄.

first reported by Jacobi von Wangelin *et al.* and has two potential nucleophilic sites in α and γ position.^{50,51} Rivard and coworkers have shown coordination to Pd(II),⁴³ and AlMe₃,⁵² through the γ -position. Heating a mixture of **1** or **2** with IDipC₃H₄ in C₆H₆ to 80 °C, conversion into the new species Mes*PHC₃H₃IDip (**17**) and TerPHC₃H₃IDip (**18**) and release of PMe₃ were noted by ³¹P{¹H} NMR spectroscopy (Scheme 6). Pale yellow X-ray quality crystals of **17** and **18** could be grown from saturated *n*-hexane solutions at –30 °C and revealed in case of **17** a *Z*-configuration of the C5–C6 double bond, so that the vinylic proton on C4 and the PH point into one direction, even though they are not in one plane (Fig. 3, note that in solution *E*-**17** is the major component, but *Z*-**17** is detected as well). In solution a spatial correlation *via* dipolar couplings, in particular homonuclear NOE, between C(4)–H and P(1)–H in *Z*-**17** is detected.

For **18** a *E*-configuration is observed for the C5–C6 bond, which in solution was corroborated by dipolar coupling of C(4)–H and C(6)–H.³⁰ The bonding parameters of **17** and **18** correspond with P-substituted enediamines [C1–C4 1.376(2) (**17**), 1.3734(16) (**18**); C4–C5 1.422(2) (**17**), 1.4309(15) (**18**); C5–C6 1.355(2) (**17**), 1.3483(16) (**18**) Å] with trigonal pyramidal P atoms. The C₄P unit minimally deviates from a planar arrange-

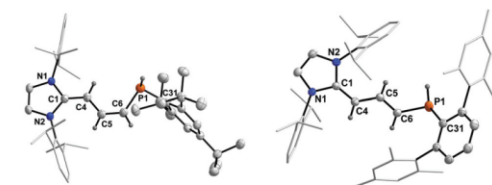
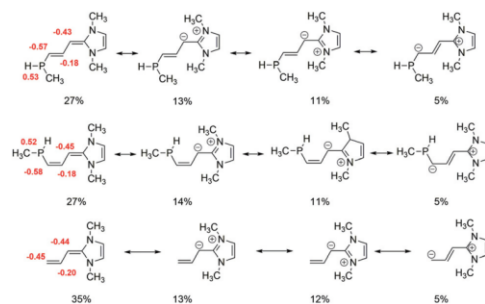


Fig. 3 POV-ray depiction of the molecular structure of **17** and **18**. ORTEPs drawn at 50% probability, all H-atoms are omitted for clarity. Selected bond lengths (Å) and angles (°) of **17**: C1–C4 1.376(2), C4–C5 1.422(2), C5–C6 1.355(2), P1–C31 1.8623(16), P1–C6 1.8157(18); C31–P1–C6 97.74(8), P1–C6–C5 125.03(13), C6–C5–C4 127.50(16), C5–C4–C1 127.72(16); C1–C4–C5–C6 –178.81(17), C4–C5–C6–P1 –1.7(3); **18**: C1–C4 1.3734(16), C4–C5 1.4309(15), C5–C6 1.3483(16), P1–C31 1.8523(12), P1–C6 1.7876(12); C31–P1–C6 108.27(5), P1–C6–C5 123.74(9), C6–C5–C4 123.78(11), C5–C4–C1 128.19(10); C1–C4–C5–C6 –170.82(11), C4–C5–C6–P1 –175.64(9).



Scheme 7 Natural resonance theory (NRT) performed on model compounds to investigate the allyl character in corresponding phosphines **17** and **18** in their *E*- (top) and *Z*-configuration (middle) compared to unsubstituted enediamines (bottom). Formula weights below 5% are not depicted and NPA-charges are given in red.

ment in **17** and **18** as judged by the dihedral angles (Fig. 3). In solution both **17** and **18** mainly exist as *E*-configured 1,3-dienes, with **17** showing the *Z*-configured diene as a minor isomer. An NRT analysis using the truncated model H₃CP(H)C₃H₃Ime₂ revealed four major resonance structures, clearly showing effective π -delocalization into the imidazole ring system and the NPA charges suggest charge accumulation on the γ -C atom (Scheme 7). This delocalization is also evident from inspection of the Kohn–Sham orbitals of **17** and **18**, which show delocalization in the HOMO–1 and HOMO, the LUMO and LUMO+1, however, are localized on the flanking aryl groups (Fig. S78 and 79†).³⁰

Conclusions

In summary we have shown facile substitution of the phosphine in phospho–Wittig reagents for NHCs, affording a variety of novel NHC–phosphinidene adducts. When using NHOs a substitution of PMe₃ was observed in all cases, however, in a second reaction step a C(sp²)–H activation of the =CH₂ moiety in the NHO occurs to give P-substituted NHOs in a facile manner. This C–H activation was shown to be more general and P-substituted dienes were obtained when **1** or **2** were treated with the enediamine IDipC₃H₄. These reactions clearly show the potential of phospho–Wittig reagents beyond the formation of phosphoalkenes and offer access to bulky phosphines. Of particular interest will be the potential of **17** to act as a dianionic ligand scaffold through twofold deprotonation in the vinylic position and the P–H group. Studies utilizing P-substituted NHOs **13–16** as ligands are currently ongoing in this laboratory.

Conflicts of interest

There are no conflicts to declare.

Acknowledgements

C. H.-J. thanks Prof. M. Beller for his support, the Max Buchner-Foundation for a Scientific Fellowship and support by an Exploration Grant of the Boehringer Ingelheim Foundation (BIS) is acknowledged. We thank our technical and analytical staff for assistance, especially Dr Anke Spannenberg for her support regarding X-ray analysis. We thank Dr Alexander Villinger for his help with obtaining the molecular structure of **5** by SC-XRD. J.-E. S. wishes to thank Dr Jonas Bresien for helpful discussions and the ITMZ at the University of Rostock for access to the Cluster Computer and especially Malte Willert for technical support.

Notes and references

- G. Wittig and G. Geissler, *Justus Liebigs Ann. Chem.*, 1953, **580**, 44–57.
- G. Wittig and U. Schöllkopf, *Chem. Ber.*, 1954, **87**, 1318–1330.
- H. Ernst, *Pure Appl. Chem.*, 2002, **74**, 2213.
- C. Mercier and P. Chabardes, *Pure Appl. Chem.*, 1994, **66**, 1509.
- K. C. Nicolaou, M. W. Härter, J. L. Gunzner and A. Nadin, *Liebigs Ann.*, 1997, **1997**, 1283–1301.
- A. B. Burg and W. Mahler, *J. Am. Chem. Soc.*, 1961, **83**, 2388–2389.
- A. H. Cowley and M. C. Cushner, *Inorg. Chem.*, 1980, **19**, 515–518.
- E. Urnezius, S. Shah and J. D. Protasiewicz, *Phosphorus, Su für Silicon Relat. Elem.*, 1999, **144**, 137–139.
- J. D. Protasiewicz, *Eur. J. Inorg. Chem.*, 2012, **2012**, 4539–4549.
- A. Marinetti and F. Mathey, *Angew. Chem., Int. Ed. Engl.*, 1988, **27**, 1382–1384.
- S. Shah and J. D. Protasiewicz, *Chem. Commun.*, 1998, 1585–1586.
- S. Shah, M. C. Simpson, R. C. Smith and J. D. Protasiewicz, *J. Am. Chem. Soc.*, 2001, **123**, 6925–6926.
- K. Takeuchi, H.-o. Taguchi, I. Tanigawa, S. Tsujimoto, T. Matsuo, H. Tanaka, K. Yoshizawa and F. Ozawa, *Angew. Chem., Int. Ed.*, 2016, **55**, 15347–15350.
- R. C. Smith and J. D. Protasiewicz, *J. Am. Chem. Soc.*, 2004, **126**, 2268–2269.
- R. C. Smith, S. Shah, E. Urnezius and J. D. Protasiewicz, *J. Am. Chem. Soc.*, 2003, **125**, 40–41.
- A. Schumann, F. Reiß, H. Jiao, J. Rabeah, J.-E. Siewert, I. Krummenacher, H. Braunschweig and C. Hering-Junghans, *Chem. Sci.*, 2019, **10**, 7859–7867.
- Y. Masaaki, S. Takahiro and I. Naoki, *Chem. Lett.*, 1988, **17**, 1735–1738.
- A. H. Cowley, F. Gabbai, R. Schluter and D. Atwood, *J. Am. Chem. Soc.*, 1992, **114**, 3142–3144.
- X. Li, D. Lei, M. Y. Chiang and P. P. Gaspar, *J. Am. Chem. Soc.*, 1992, **114**, 8526–8531.
- B. Twamley, C. D. Sofield, M. M. Olmstead and P. P. Power, *J. Am. Chem. Soc.*, 1999, **121**, 3357–3367.
- X. Chen, R. C. Smith and J. D. Protasiewicz, *Chem. Commun.*, 2004, 146–147.
- U. J. Kilgore, H. Fan, M. Pink, E. Urnezius, J. D. Protasiewicz and D. J. Mindiola, *Chem. Commun.*, 2009, 4521–4523.
- L. Liu, D. A. Ruiz, D. Munz and G. Bertrand, *Chem*, 2016, **1**, 147–153.
- M. M. Hansmann and G. Bertrand, *J. Am. Chem. Soc.*, 2016, **138**, 15885–15888.
- D. W. N. Wilson, J. Feld and J. M. Goicoechea, *Angew. Chem.*, 2020, **59**, 20914.
- D. W. N. Wilson, W. K. Myers and J. M. Goicoechea, *Dalton Trans.*, 2020, **49**, 15249.
- T. Krachko and J. C. Slootweg, *Eur. J. Inorg. Chem.*, 2018, **2018**, 2734–2754.
- A. Doddi, M. Peters and M. Tamm, *Chem. Rev.*, 2019, **119**, 6994–7112.
- T. Krachko, M. Bispinghoff, A. M. Tondreau, D. Stein, M. Baker, A. W. Ehlers, J. C. Slootweg and H. Grützmacher, *Angew. Chem., Int. Ed.*, 2017, **56**, 7948–7951.
- Experimental and computational details, and details on the X-ray diffraction studies are included in the ESI. CCDC 2046859–2046869† contain the supplementary crystallographic data for this paper.
- P. Pyykkö and M. Atsumi, *Chem. – Eur. J.*, 2009, **15**, 12770–12779.
- S. Shah, G. P. A. Yap and J. D. Protasiewicz, *J. Organomet. Chem.*, 2000, **608**, 12–20.
- O. Back, M. Henry-Ellinger, C. D. Martin, D. Martin and G. Bertrand, *Angew. Chem., Int. Ed.*, 2013, **52**, 2939–2943.
- N. Hayakawa, K. Sadamori, S. Tsujimoto, M. Hatanaka, T. Wakabayashi and T. Matsuo, *Angew. Chem., Int. Ed.*, 2017, **56**, 5765–5769.
- K. Pal, O. B. Hemming, B. M. Day, T. Pugh, D. J. Evans and R. A. Layfield, *Angew. Chem., Int. Ed.*, 2016, **55**, 1690–1693.
- C. M. E. Graham, C. R. P. Millet, A. N. Price, J. Valjus, M. J. Cowley, H. M. Tuononen and P. J. Ragogna, *Chem. – Eur. J.*, 2018, **24**, 672–680.
- J. E. M. N. Klein and G. Knizia, *Angew. Chem., Int. Ed.*, 2018, **57**, 11913–11917.
- G. Knizia, *J. Chem. Theory Comput.*, 2013, **9**, 4834–4843.
- M. M. D. Roy and E. Rivard, *Acc. Chem. Res.*, 2017, **50**, 2017–2025.
- S. Naumann, *Chem. Commun.*, 2019, **55**, 11658–11670.
- K. Powers, C. Hering-Junghans, R. McDonald, M. J. Ferguson and E. Rivard, *Polyhedron*, 2016, **108**, 8–14.
- M. M. Hansmann, P. W. Antoni and H. Pesch, *Angew. Chem.*, 2020, **59**, 5782–5787.
- I. C. Watson, A. Schumann, H. Yu, E. C. Davy, R. McDonald, M. J. Ferguson, C. Hering-Junghans and E. Rivard, *Chem. – Eur. J.*, 2019, **25**, 9678–9690.
- A. Dumrath, X.-F. Wu, H. Neumann, A. Spannenberg, R. Jackstell and M. Beller, *Angew. Chem., Int. Ed.*, 2010, **49**, 8988–8992.

Paper

Dalton Transactions

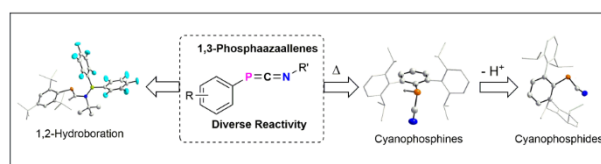
- 45 A. Dumrath, C. Lübbe, H. Neumann, R. Jackstell and M. Beller, *Chem. – Eur. J.*, 2011, **17**, 9599–9604.
- 46 D. Rottschäfer, M. K. Sharma, B. Neumann, H.-G. Stämmler, D. M. Andrada and R. S. Ghadwal, *Chem. – Eur. J.*, 2019, **25**, 8127–8134.
- 47 N. R. Paisley, M. W. Lui, R. McDonald, M. J. Ferguson and E. Rivard, *Dalton Trans.*, 2016, **45**, 9860–9870.
- 48 C. C. Chong, B. Rao, R. Ganguly, Y. Li and R. Kinjo, *Inorg. Chem.*, 2017, **56**, 8608–8614.
- 49 R. S. Ghadwal, S. O. Reichmann, F. Engelhardt, D. M. Andrada and G. Frenking, *Chem. Commun.*, 2013, **49**, 9440–9442.
- 50 C. E. I. Knappke, A. J. Arduengo III, H. Jiao, J.-M. Neudörfl and A. Jacobi von Wangelin, *Synthesis*, 2011, 3784–3795.
- 51 C. E. I. Knappke, J. M. Neudörfl and A. Jacobi von Wangelin, *Org. Biomol. Chem.*, 2010, **8**, 1695–1705.
- 52 I. C. Watson, Y. Zhou, M. J. Ferguson, M. Kränzlein, B. Rieger and E. Rivard, *Z. Anorg. Allg. Chem.*, 2020, **646**, 547–551.

5.3 On 1,3-phosphaazaallenes and their diverse reactivity

M. Fischer, C. Hering-Junghans

Chem. Sci. **2021**, *12*, 10279–10289.

DOI: 10.1039/D1SC02947A



Reprinted (adapted) with permission from *Chem. Sci.*.

Copyright 2021 Royal Society of Chemistry

Cite this: *Chem. Sci.*, 2021, 12, 10279

All publication charges for this article have been paid for by the Royal Society of Chemistry

Received 31st May 2021
Accepted 30th June 2021DOI: 10.1039/d1sc02947a
rsc.li/chemical-science

On 1,3-phosphaazaallenes and their diverse reactivity†

Malte Fischer^{1b} and Christian Hering-Junghans^{1b*}

1,3-Phosphaazaallenes are heteroallenes of the type $RP=C=NR'$ and little is known about their reactivity. In here we describe the straightforward synthesis of $ArPCNR$ ($Ar = Mes^*$, 2,4,6-*t*-Bu-C₆H₂; ^{Mes}Ter, 2,6-(2,4,6-Me₃C₆H₂)-C₆H₃; ^{Dip}Ter, 2,6-(2,6-*i*-Pr₂C₆H₂)-C₆H₃; R = *t*Bu; Xyl, 2,6-Me₂C₆H₃) starting from phospho-Wittig reagents $ArPPMe_3$ and isonitriles CNR . It is further shown that $ArPCNtBu$ are thermally labile with respect to the loss of iso-butene and it is shown that the cyanophosphines $ArP(H)CN$ are synthetically feasible and form the corresponding phosphanitilium borates with $B(C_6F_5)_3$, whereas deprotonation of ^{Dip}TerP(H)CN was shown to give an isolable cyanidophosphide. Lastly, the reactivity of $ArPCNR$ towards Pier's borane was investigated, showing hydroboration of the C=N bond in $Mes^*PCNtBu$ to give a hetero-butadiene, while with ^{Dip}TerPCNXyl the formation of the Lewis acid–base adduct with a B–P linkage was observed.

Introduction

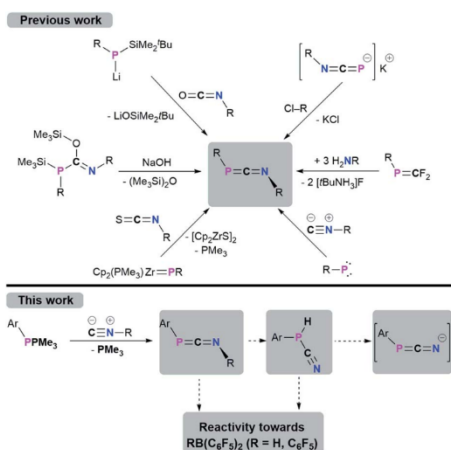
1,3-Phosphaazaallenes ($RP=C=NR$) are a heteroallene subclass. The first derivative $tBuPCNtBu$ was obtained by combining $tBuP(SiMe_3)C(OSiMe_3)=NtBu$ with NaOH under the release of hexamethyldisiloxane.^{1,2} Although known for almost 40 years, 1,3-phosphaazaallenes have been scarcely investigated, especially when compared to the “lighter” carbodiimides and other heteroallene analogues. Another synthetic route was disclosed by Yoshifuji,^{3,4} and Appel,⁵ who reacted $Mes^*P(Li)SiMe_3tBu$ ($Mes^* = 2,4,6-tBu_3C_6H_3$) with isocyanates in a Peterson-type reaction to give Mes^*PCNR (R = Ph, *n*Pr, *t*Bu). In 2000, Zhou and co-workers expanded this series to include $Mes^*PCN(4-ClC_6H_4)$,⁶ $Mes^*PCN(4-ClC_6H_4)$ and Mes^*PCNPh ⁴ are the only structurally characterized 1,3-phosphaazaallenes bearing classic organic substituents. Sterically demanding groups on the P atom suppress dimerization to the corresponding 1,3-diphosphetanes, which can only be reconverted to the 1,3-phosphaazaallenes by flash vacuum pyrolysis.^{2,7} Even Mes^*PCNPh slowly dimerizes in solution, whereas in the presence of catalytic amounts of $Pd(PPh_3)_4$ the unsymmetric four-membered heterocycle is obtained.⁸ Derivatives with a bulky cyclopropen-1-yl substituent at the phosphorus were synthesized by Regitz *et al.*⁹

In 1991 Grobe and co-workers demonstrated that the metastable $(F_3C)PCNtBu$ (can be handled at -40 °C) is feasible by reacting the phosphoalkene precursor $(F_3C)P=CF_2$ with three equivalents of H_2NtBu .¹⁰ Instead of dimerizing at higher temperatures, $(F_3C)PCNtBu$ decomposes to give fluorinated cyclophosphanes $(PCF_3)_n$ and the isocyanide $CNtBu$. Stephan *et al.* showed that the zirconocene phosphinidene $Cp_2(PMe_3)Zr=PMe^*$ reacts with an isothiocyanate in a [2 + 2] cycloaddition/cycloreversion sequence to yield Mes^*PCNPh and $[Cp_2ZrS]_2$.¹¹ That 1,3-phosphaazaallenes can function as ligands for transition metals was established by Streubel and Jones.¹² Photochemical ring opening in the presence of an isocyanide of a $W(CO)_5$ -stabilized 2*H*-azaphosphirene resulted in the formation of an 1,3-phosphaazaallene with the P atom remaining coordinated to $W(CO)_5$. A transient terminal phosphinidene complex is assumed to react in a 1,1-addition with the respective isocyanide. The motif to generate 1,3-phosphaazaallenes directly in the coordination sphere of a transition metal by reactions of metal-bound phosphinidenes with isocyanides is more common in the literature.¹³ A trimethylstannyl substitution at the phosphorus centre in 1,3-phosphaazaallenes was achieved by reacting the potassium 1,3-azaphosphaallene $K[PrNCP]$ with $ClSnMe_3$ in a salt metathesis reaction, thus revealing another access to this substance class.¹⁴ The most recent examples of 1,3-phosphaazaallenes were synthesized by Bertrand *et al.* in coupling reactions of (phosphino)phosphinidenes with isocyanides.¹⁵ Moreover, Scheschkewitz *et al.* showed that a phosphasilene with a mobile NMe_2 -functionality on the phosphorus atom undergoes an NMe_2 -shift in the reaction with $CNtBu$ to give a P-silyl-substituted 1,3-phosphaazaallene.¹⁶ The synthetic protocols towards 1,3-phosphaazaallenes are summarized in Scheme 1. Even though

Leibniz Institut für Katalyse e.V. (LIKAT), A.-Einstein-Str. 3a, 18059 Rostock, Germany. E-mail: christian.hering.junghans@catalysis.de; Web: [https://www.catalysis.de/forschung/aktivierung-kleiner-molekuele.]

† Electronic supplementary information (ESI) available: Synthesis and characterization of compounds, NMR spectra, crystallographic, and computational details. CCDC 2086496–2086506. For ESI and crystallographic data in CIF or other electronic format see DOI: 10.1039/d1sc02947a





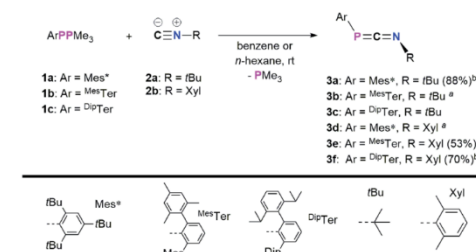
Scheme 1 Syntheses of 1,3-phosphaazaallenes and scope of this work.

1,3-phosphaazaallenes are without a doubt an interesting class of compounds, it is surprising that their general reactivity has not been studied in detail.

Recently, we have revisited the chemistry of phosphanylidene phosphoranes, so-called phospho-Wittig reagents, ArPPMe_3 (**1a-c**) (**1a**: Ar = Mes^{*}; **1b**: Ar = 2,6-(2,4,6-Me₃C₆H₂)-C₆H₃, ^{Mes}Ter; **1c**: Ar = 2,6-(2,6-*i*Pr₂C₆H₃)-C₆H₃, ^{Dip}Ter).¹⁷ We successfully used them as phosphinidene transfer reagents in reactions with N-heterocyclic carbenes (NHCs) or N-heterocyclic olefins (NHOs),¹⁷ towards Al(i) species to give phosphaalumenes,¹⁸ and with $\text{Cp}_2\text{Ti}(\text{C}_2(\text{SiMe}_3)_2)$ to afford terminal titanium phosphinidene complexes, respectively.¹⁹ In this contribution, the reactivity of the phospho-Wittig reagents **1a-c** towards isocyanides is presented (Scheme 1, bottom), giving a series of 1,3-phosphaazaallenes. The *t*Bu-substituted 1,3-phosphaazaallenes can be converted into primary cyanophosphines, which in one case can be transformed to the corresponding cyanophosphides. Finally, the reactivity of 1,3-phosphaazaallenes and primary cyanophosphines towards the perfluorinated arylboranes $\text{RB}(\text{C}_6\text{F}_5)_2$ (R = H, C₆F₅) is illustrated.

Results and discussion

In a first series of experiments Mes^{*}PPMe₃ (**1a**)¹⁴ was dissolved in C₆D₆, and an excess of CN*t*Bu (**2a**) was added (Scheme 2).²⁰ Within 16 h at room temperature, two new signals were observed in the ³¹P{¹H} NMR spectrum at -62.6 and -103.8 ppm, respectively, along with mostly unreacted starting materials. Heating to 60 °C for 24 h resulted in the consumption of **1a** and one equivalent of CN*t*Bu to give the targeted 1,3-phosphaazaallene Mes^{*}PCN*t*Bu (**3a**, $\delta^{31}\text{P}\{^1\text{H}\} = -103.8$ ppm) upon PMe_3 release. This is in contrast to the reaction of the phosphaketene [sP]PCO ([sP] = (H₂CNDip)₂P) with CN-Ad (Ad = adamantyl), which did not result in a CO for isonitrile



Scheme 2 Reactions of **1a-c** with isocyanides to give 1,3-phosphaazaallenes **3a-f**,^a obtained as a mixture with the diphosphenes Mes^{*}PPMes^{*} and ^{Mes}TerPP^{Mes}Ter, respectively; heated to 60 °C (**3a**) or 80 °C (**3f**).

substitution, but in the formation of a P₂C₂ heterocycle through attack of CN-Ad on the PCO carbon atom.²¹ However, sequential treatment of [sP]PCO with PPh₃ and CNAd was shown to afford the corresponding heteroallenes [sP]PCNAd.²² Phosphaketenes are related to the 1,3-phosphaazaallenes through isolobal CO for CNR replacement.²³ To further investigate the scope of this reaction, **1a-c** were each reacted with both **2a** and CNXyl (Xyl = 2,6-Me₂C₆H₃, **2b**) (Scheme 2). It was found that the desired 1,3-phosphaazaallene formation is generally faster at higher temperatures but accompanied by diphosphene ArP=PAR formation unless ^{Dip}TerPPMe₃ (**1c**) is used. It is worthy to note that **3b** and **3d** could only be obtained as mixtures with the corresponding diphosphenes ^{Mes}TerP=P^{Mes}Ter,²⁴ and Mes^{*}P=P^{Mes}*,²⁵ respectively, even if an excess of isocyanide was employed (Fig. S8 and S18†). Theoretical investigations at the PBE0-D3/def2SVP//DNLPO-CCSD(T)/def2TZVP level of theory revealed that the formation of **3a-f** are exergonic (Fig. S86†).^{26,27} However, diphosphene formation from ArPPMe₃ through recombination of ArP upon PMe_3 release, has been calculated to be even more exergonic at the same level of theory, therefore explaining that formation of diphosphenes cannot be completely suppressed (Fig. S18†). Using a thermal approach, a diphosphene-poly(phenylenevinylene) has been prepared from the corresponding phospho-Wittig monomers upon PMe_3 release. The monomer showed the same 2,6-Mes₂Ar structural motif as in phospho-Wittig reagent **1b**.²⁸ In case of 1a free phosphinidenes are unlikely, as cyclometalated species are not

Table 1 Characteristic ³¹P{¹H} and ¹³C{¹H} NMR data of **3a-f**. Calculated ³¹P NMR shifts (PBE0-D3/def2SVP) are given in parentheses

Compound	$\delta^{31}\text{P}\{^1\text{H}\}^a$ ($\delta_{\text{calc}}^{31\text{P}}\}^a$	$\delta^{13}\text{C}\{^1\text{H}\}(\text{PCN})^a$	$^1J_{\text{P,C}}(\text{PCN})^a$
3a	-103.9 (-124.4)	192.2	76.8
3b	-125.4 (-161.1)	186.6	73.0
3c	-134.8 (-164.8)	177.9	77.9
3d	-120.6 (-157.9)	191.5	78.8
3e	-145.4 (-179.4)	183.7	78.1
3f	-144.8 (-164.1)	179.6	77.2

^a In C₆D₆ at room temperature; values given in ppm (δ) or Hz (*f*).



observed.²⁹ The NMR data of **3a–f** are in accordance to the previously reported data of **3a** in CDCl₃ (Table 1).⁴ The ³¹P{¹H} NMR signals of **3a–3f** range from –103.9 to –145.4 ppm and are generally shifted to higher field when the N-substituent is aromatic with the P-substituent being the same. This was corroborated by DFT calculations at the PBE0-D3/def2SVP level of theory, which gave $\delta_{\text{calc}}(^{31}\text{P})$ values that are systematically at lower ppm values, though the experimentally observed trends are followed (Table 1).

Highly characteristic for **3a–f** are the ¹³C{¹H}NMR signals of the two-coordinate carbon atoms of the PCN moieties, being significantly deshielded ($\delta(^{13}\text{C}\{^1\text{H}\}) = 177.9$ to 192.2 ppm) and showing ¹J_{P,C} coupling constants of 73.0 to 78.1 Hz (Table 1). Additionally, the molecular structures of **3a**, **3e**, and **3f** could be determined by single crystal X-ray diffraction (SC-XRD, Fig. 1, Table 2). The P–C bond lengths of **3a**, **3e**, and **3f** of 1.6658(15) Å (**3a**) to 1.6785(12) Å (**3f**) are slightly elongated compared to **I** (1.651 Å) and **II** (1.642(5) Å), respectively, but are shorter than the sum of the covalent double bond radii ($\Sigma r_{\text{cov}}(\text{P}=\text{C}) = 1.69$ Å).³⁰ The N–C bond lengths of **3a**, **3e**, and **3f** (1.2009(15) Å to 1.2037(19) Å) are in the expected range for heteroallenes (cf. XylN=C=NXYl d(C–N) 1.197(2), 1.206(3) Å).^{31,32} Noteworthy, the P–C–N angles deviate from linearity (as expected for sp-hybridized carbon atoms) but are in good agreement to previously structurally characterized 1,3-phosphaazaallenes (Table 2).

The bonding in **3a–f** was studied using the truncated model compound MesPCNMe on the PBE0-D3/def2SVP level of theory. Inspection of the Kohn–Sham orbitals revealed a HOMO best described as a polarized P–C π-bond, while the LUMO shows major contribution from the C–N π* orbital interacting with a s-type lone pair on phosphorus (Fig. 2, top). With an energetically high lying HOMO the 1,3-phosphaazaallenes might be potentially oxidized to give the corresponding radical cation, as was recently shown for vinyl-substituted diphosphenes.³³ CV studies on **3a** show an irreversible oxidation event at $E_{1/2} = 0.38$ V vs. Fc/Fc⁺ (Fig. S82–S84[†]), and the corresponding radical cation might be synthetically feasible. We next evaluated the NPA (Natural Population Analysis) charges indicating a minimal charge transfer from the MesP-fragment to the CNMe moiety by –0.196e, with a positive partial charge on P of 0.37e and 0.07e

on the two-coordinate C atom. Natural Bond Orbital (NBO) analysis supports the description as an heteroallene, with a LP of electrons on P and polarized σ- and π-P=CNMe (WBI 1.64) and PC=NMe (WBI 2.05) double bonds, respectively. In agreement with the KS-orbitals the π-component is polarized towards the P atom (58.3% P, 41.7% C), whereas the σ-component is inversely polarized (34.5% P, 65.5% C). Analysis of the second order perturbation of the Fock matrix revealed delocalization of the lone pair of electrons (LP) on P into the CN π*-orbital resulting in a stabilization energy of 12.7 kcal mol^{–1}. Natural resonance theory analysis (NRT) revealed two leading resonance structures, with the 1,3-phosphaazaallene being the dominant form (31.7%) and an ylidic formulation with a C≡N triple bond and thus two LPs on P (14.8%) (Fig. 2, bottom).

Formation of cyanophosphines starting from **3a–c**

When a solution of **3a** was heated to 105 °C in toluene-*d*₈ a new species with a ³¹P{¹H} NMR chemical shift of –105.6 ppm (cf. **3a** $\delta(^{31}\text{P}\{^1\text{H}\}) = -103.9$ ppm) was observed along with minimal amounts of the diphosphene Mes*P=PMe* ($\delta(^{31}\text{P}\{^1\text{H}\}) = 493.2$ ppm). This transformation is accompanied by the formation of iso-butene, as evident from two signals in the ¹H NMR spectrum in a 3 : 1 ratio at 1.60 (triplet) and 4.75 (heptet) ppm, respectively. Finally, the multinuclear and multidimensional NMR data clearly showed that the new compound is the cyanophosphine Mes*P(H)CN (**4a**) (Scheme 3). Isobutene elimination and formal HCN transfer has been previously observed with disilynes,³⁴ whereas with boracumulenes and transient borylenes CN[–] transfer was observed, with formation of a mixture of isobutane and -butene.^{35,36} Streubel and co-workers showed that the η¹-1,3-phosphaazaallene complex (Me₃Si)₂HC–P(W(CO)₅)CNtBu undergoes thermal loss of iso-butene to give the corresponding cyanophosphine tungsten complex.¹² The thermodynamic feasibility of this transformation was elucidated at the PBE0-D3/def2SVP//DNLPO-CCSD(T)/def2TZVP level of theory, showing that the formation of **4a** is exergonic by –36.93 kJ mol^{–1}, whereas the dimerization of **3a** to give Mes*P=PMe* and CNtBu is less favored ($\Delta_{\text{R}}G = -5.68$ kJ mol^{–1}). A scan of the potential energy surface revealed that the H-shift from the *t*Bu-group to P occurs intramolecularly



Fig. 1 Molecular structures of **3a** (left), **3e** (middle), and **3f** (right). Hydrogen omitted and parts of the molecule rendered as wireframe for clarity. Thermal ellipsoids are drawn at the 50% probability level. Structural parameters are summarized in Table 2.



Table 2 Selected bond lengths [Å] and angles [°] of **3a**, **3e** and **3f** (literature known species I and II for comparison)

Compound	P–C	N–C	P–C–N	C–P–C	C–N–C
3a	1.6690(15)	1.2034(18)	170.38(12)	97.92(6)	130.02(13)
3e	1.6658(15)	1.2037(19)	167.14(13)	103.06(7)	139.44(15)
3f	1.6785(12)	1.2009(15)	160.00(10)	107.53(5)	143.24(12)
Mes*PCNPh (I) ^d	1.651	1.209	171.1	99.2	130.5
Mes*PCN(<i>p</i> -ClC ₆ H ₄) (II) ^e	1.642(5)	1.214(6)	170.8(4)	99.8(2)	128.3(4)

via a six-membered transition state ($\Delta_r G = 156.1 \text{ kJ mol}^{-1}$), resulting in P–H bond formation as the C(sp³)–H and N–C_{tBu} bonds are cleaved (Fig. S87†). This rather high energy barrier is in line with prolonged heating of the reaction mixture at 105 °C. An alternative radical pathway through N–C_{tBu} bond homolysis and formation of a *t*Bu• radical was excluded as this would result in disproportionation and a mixture of iso-butene and iso-butane. The intermediate formation of free phosphinidenes is also unlikely, as this would give rise to cyclo-metalated species in case of Mes* and ^{DIP}Ter, which were not observed by NMR spectroscopy. Alternatively, **4a** can be prepared directly in one pot starting from **1a** and **2a** (Scheme 3, bottom).¹⁶ Following this route **4a** was isolated as a colourless solid in good yields of 75%. Given the PH functionality, the ¹H NMR spectrum shows a characteristic doublet at 5.57 ppm with a ¹J_{P,H} coupling constant of 252.3 Hz, which is corroborated by the ³¹P NMR spectrum. To further elaborate the scope of this reaction, the

analogous ^{Mes*}TerP(H)CN (**4b**) and ^{DIP}TerP(H)CN (**4c**) derivatives were synthesized, and their characteristic NMR data is shown in Table 3. Surprisingly, in the IR spectrum of **4a** and **4c** no characteristic CN band is detected, in agreement with frequency analyses at the PBE0-D3/def2SVP level of theory. The presence of a P–H moiety was corroborated by a band at 2411 and 2310 cm⁻¹ for **4a** and **4c**, respectively. Cyanophosphines of the general type RP(H)CN (R = alkyl, aryl) have long remained elusive and were either found to be unstable,³⁷ or to be stabilized by coordination to a transition metal.³⁸

In 2001 the reaction of dicyanophosphines (RP(CN)₂) with equimolar amounts of Schwartz's reagent ([Cp₂Zr(H)Cl]_n) was shown to afford the methyl, *tert*-butyl, and Mes* derivatives, respectively.³⁹ However, structural data of this compound class is missing in the literature and the molecular structures of **4a–c** could be determined by SC-XRD (Fig. 3, Table 4). The C–N bond lengths in **4a–c** average 1.146 Å and indicate triple bonds ($\Sigma r_{\text{cov}}(\text{C}\equiv\text{N}) = 1.14 \text{ \AA}$),³⁰ in agreement with the formulation as cyanophosphines. The average P–C bond length of 1.791 Å is shorter than the respective single bond covalent radii ($\Sigma r_{\text{cov}}(\text{P–C}) = 1.86 \text{ \AA}$),³⁰ with a nearly linear arrangement of the P–C–N unit (>176°). Similar bond lengths were reported for Mes*P(CN)₂ (P–C_{avg} 1.80 Å, N–C_{avg} 1.14 Å).³⁹ NBO analyses of **4a–c** at the PBE0-D3/def2SVP//PBE0/def2SVP level of theory support the notation as cyanophosphines with CN triple bonds (WBI C≡N **4a** 2.88, **4b** 2.87, **4c** 2.87), a polar $\delta^{\oplus}\text{C}^{\ominus}\text{CN}$ single bond and a LP on P, which is minimally delocalized into two π^* orbitals of the CN group with a stabilization energy of ca. 12 kcal mol⁻¹.¹⁷

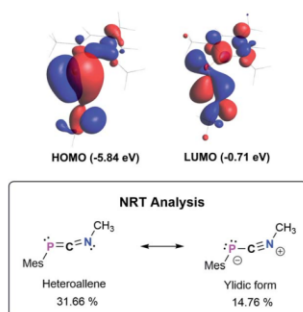
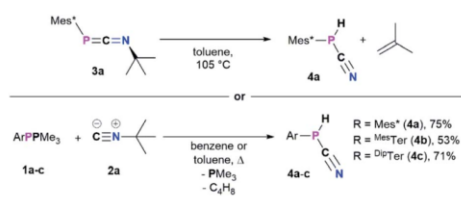


Fig. 2 Selected Kohn–Sham orbitals of the truncated model compound MesPCNMe (PBE0-D3/def2SVP) and leading resonance structures according to NRT analysis.



Scheme 3 Formation of the cyanophosphines **4a–c** from **3a–c** (top) or directly from **1a–c** and *t*BuNC (**2a**).

Reactivity of cyanophosphines towards B(C₆F₅)₃

4a–c possess two potential binding sites for Lewis acids, the LPs on P and N, even though steric congestion should render the phosphorus rather inaccessible. By reacting **4a–c** with B(C₆F₅)₃, the first examples of the corresponding phosphanitrilium borates RP(H)CNB(C₆F₅)₃ (R = Mes* (**5a**), R = ^{Mes*}Ter (**5b**), R = ^{DIP}Ter (**5c**)) were prepared (Scheme 4). The reactions were performed on NMR scale and **5a** was exemplarily isolated as a colourless solid in a moderate yield of 55%. The coordination to the borane moiety results in a minimal deshielding of the PH unit accompanied by a slight increase of the ¹J_{P,H} coupling constant in both the ¹H and ³¹P NMR spectra ($\delta(^1\text{H}) = 5.61 \text{ ppm}$, $\delta(^{31}\text{P}) = -99.2 \text{ ppm}$, ¹J_{P,H} = 260.0 Hz; $\delta_{\text{calc}}(^{31}\text{P}) = -140.9 \text{ ppm}$), respectively, when compared to the starting material **4a** ($\delta(^1\text{H}) = 5.57 \text{ ppm}$, $\delta(^{31}\text{P}) = -105.4 \text{ ppm}$, ¹J_{P,H} = 252.3 Hz). The signals of the C≡N group are unaltered (**5a**: $\delta(^{13}\text{C}\{^1\text{H}\}) = 121.0 \text{ ppm}$, *c.f.* **4a**: $\delta(^{13}\text{C}\{^1\text{H}\}) = 120.8 \text{ Hz}$), while the ¹J_{P,C} coupling constant



Table 3 Characteristic $^{31}\text{P}\{^1\text{H}\}$ and $^{13}\text{C}\{^1\text{H}\}$ NMR data of **4a–c**. Calculated ^{31}P NMR shifts (PBE0-D3/def2TZVP) are given in parentheses

Compound ^a	$\delta^1\text{H}$ (PH)	$\delta^{31}\text{P}$ ($\delta_{\text{calc}}^{31}\text{P}$)	$^1J_{\text{P,H}}$ (PH)	$\delta^{13}\text{C}$ (C≡N)	$^1J_{\text{P,C}}$ (C≡N)
4a	5.57 [5.95] ^b	−105.4 [−101.6] ^b (−139.1)	252.3 [249.7] ^b	120.8 [121.2] ^b	76.3 [74.4] ^b
4b	4.38	−120.6 (−154.9)	244.8	116.7	76.7
4c	4.35	−120.4 (−154.6)	247.2	116.6	75.3
5a	5.61	−99.2 ()	260.0	121.0	106.8
5b	4.61	−115.1	250.9	—	—
5c	5.03	−108.3	256.1	—	—
MeP(H)CN ³⁹	4.15	−119.9	227.5	119.6	70.9

^a In C_6D_6 at room temperature; values in ppm (δ) or Hz (J). ^b previously reported NMR data for **4a** was collected in CD_2Cl_2 [values given in brackets].³⁹

increases significantly to $^1J_{\text{P,C}} = 106.8$ Hz (cf. **4a** $^1J_{\text{P,C}} = 76.3$ Hz). Interestingly, in the IR spectrum the CN stretch is now visible as a weak band at 2265 cm^{-1} . The $^{11}\text{B}\{^1\text{H}\}$ NMR resonance at -10.3 ppm is consistent with tetra-substituted boron atoms bearing perfluorinated aryl groups (cf. [K(18-crown-6)] [SCNB(C₆F₅)₃]: $\delta(^{11}\text{B}\{^1\text{H}\}) = -12.4$ ppm).⁴⁰ The three C₆F₅ groups are equivalent as verified by the respective ^{19}F NMR spectrum ($\delta(^{19}\text{F}\{^1\text{H}\}) = -133.9$ (*meta*), -155.8 (*para*), and -163.4 (*ortho*) ppm; $\Delta(\delta)^{19}\text{F}_{m,p} = 7.6$ Hz), which is in agreement with other nitrilium borates with a heteroatom at the carbon atom of the C≡N triple bond (cf. PhSCNB(C₆F₅)₃; $\delta(^{19}\text{F}\{^1\text{H}\}) = -134.0$ (*meta*), -155.7 (*para*), and -163.3 (*ortho*) ppm; $\Delta(\delta)^{19}\text{F}_{m,p} = 7.6$ Hz).⁴¹ The molecular structure of **5a** (Fig. 4) confirms the four-coordinate boron atom and the BNCP axis is in a nearly linear arrangement (P1–C19–N1 $175.7(2)^\circ$, C19–N1–B1 $178.3(2)^\circ$). The N1–C19 bond length of $1.136(3)$ Å is still diagnostic of a triple bond (cf. **4a** $1.143(4)$ Å; $\Sigma r_{\text{cov}}(\text{C}\equiv\text{N}) = 1.14$ Å).³⁰ The newly formed N1–B1 bond ($1.584(3)$ Å) is in the same range as reported for PhSCNB(C₆F₅)₃ ($1.5829(10)$ Å)⁴¹ and slightly shorter when compared to classic nitrile–B(C₆F₅)₃ adducts (cf. MeCNB(C₆F₅)₃ $1.616(3)$ Å).⁴²

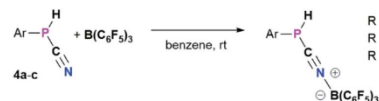
Attempted syntheses of cyanophosphides

With **4a–c** in hand, we envisioned to synthesize the corresponding cyanophosphides [RPCN][−] through simple deprotonation of **4a–c**. The first dicyanophosphides [P(CN)₂]M were isolated by Schmidpeter *et al.* through reductive decyanation of P(CN)₃,⁴³ and alternative synthetic strategies have surfaced since this initial report.^{44–46} Schmidpeter and co-workers then

Table 4 Selected bond lengths (Å) and angles [°] of **4a–c** and **5a**

Compound	P–C	N–C	P–C–N	C–P–C
4a	1.796(3)	1.143(4)	176.4(3)	97.49(11)
4b	1.7853(18)	1.148(2)	177.41(16)	100.31(6)
4c	1.793(2)	1.146(3)	177.5(2)	99.32(9)
5a	1.799(3)	1.136(3)	175.7(2)	97.71(11)

synthesized [PhPCN]M (M⁺ = Na, K, [(Ph₃P)₂N]) by reacting Ph₅P₅ with the corresponding cyanides as equilibrium mixtures, which is shifted to [PhPCN]M when using weakly-coordinating cations.^{47–49} Recently, Grützmacher *et al.* introduced alkali phosphanyl cyanophosphides [[NHP]PCN]M (NHP = N-heterocyclic phosphonium, M = Na, K) as versatile PCN building blocks, by an oxygen for nitrogen exchange from phosphanyl phosphaketenes of the general type (NHP)PCO with (M(NSiMe₃)₂) (M = alkali metal) and concomitant formation of O(SiMe₃)₂.⁵⁰ Wolf, Weigand and co-workers observed the formation of the phosphanyl-substituted cyanophosphides



Scheme 4 Synthesis of phosphanitriumborates ArP(H)CNB(C₆F₅)₃ **5a–c**. ^a NMR reactions, products were not isolated.

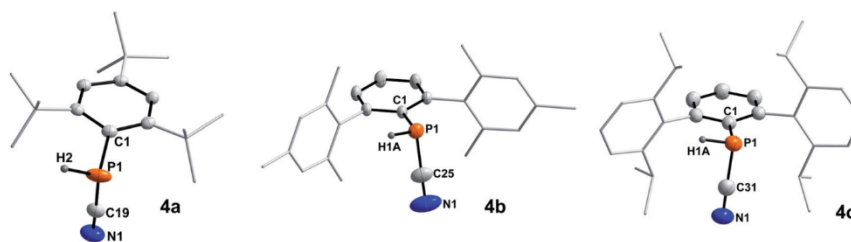


Fig. 3 Molecular structures of **4a** (left), **4b** (middle), and **4c** (right). Hydrogen atoms (except on P1) omitted and parts of the molecules rendered as wireframe for clarity. Thermal ellipsoids are drawn at the 50% probability level. Structural parameters are summarized in Table 4.



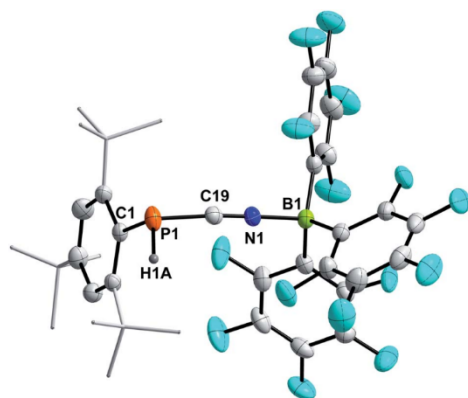


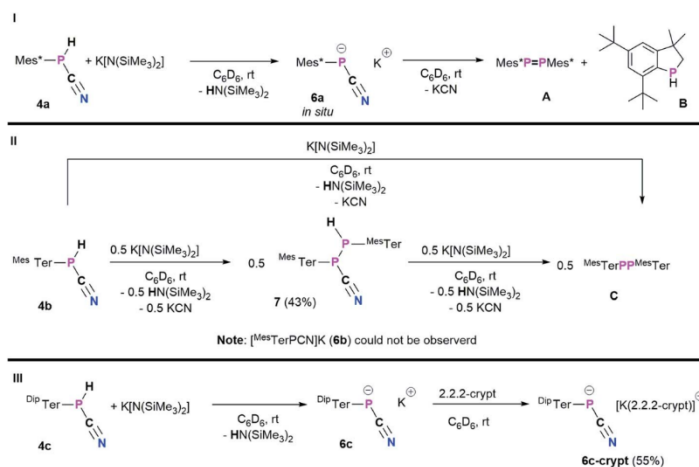
Fig. 4 Molecular structure of **5a**. Hydrogen atoms (except H1) omitted and *t*Bu-groups on Mes* rendered as wireframe for clarity. Thermal ellipsoids are drawn at the 50% probability level. Selected bond lengths (Å) and angles (°): P1–C19 1.799(3), N1–C19 1.136(3), N1–B1 1.584(3), P1–C19–N1 175.7(2), C19–N1–B1 178.3(2), C19–P1–C1 97.71(11).

$[(R_3PPCN)]^-$; R = Ph, Cy, *t*Bu, $N(iPr)_2$) as counter-anions for anionic *cyclo*-triphosphido cobalt complexes.³¹ Inspired by these results, the potential of **4a–c** being deprotonated by $K[N(SiMe_3)_2]$ (KHMDS) was investigated (Scheme 5).

As a starting point, the cyanophosphine Mes*P(H)CN (**4a**) and KHMDS were combined on an NMR scale, accompanied by a color change from colorless to yellow and formation of a colorless precipitate. 1H and $^{31}P\{^1H\}$ NMR spectra were immediately recorded and show that the main species at this

point showed a $^{31}P\{^1H\}$ NMR signal at -146.2 ppm, which according to 1H NMR spectroscopy does not bear a P–H function and $HN(SiMe_3)_2$ (HMDS, $\delta(^1H) = 0.10$ ppm) was observed as well.²⁰ This indicated successful deprotonation to give $[Mes^*PCN]K$ (**6a**).

Nevertheless, **6a** is unstable at room temperature and after 16 h at room temperature, the $^{31}P\{^1H\}$ NMR data revealed three signals at 493.2 (Mes^*PPMes^* , **A**),²⁵ -79.7 , and -146.2 ppm, respectively.²⁰ The signal at -79.7 ppm is now the main species and was assigned to the known 3,3-dimethyl-5,7-di-*tert*-butylphosphindane (**B**).⁵² Unfortunately, up to now all attempts to isolate, crystallize or trap **6a** have not been successful and only crystals of **A** and **B** could be obtained. From a mechanistic point of view, we assume that deprotonation of **4a** by KHMDS leads to the formation of HMDS and **6a**, the latter then eliminates KCN to give a reactive phosphinidene intermediate capable of both dimerization to give **A** and capable of insertion of the phosphinidene fragment into one methyl group of one *tert*-butyl group of the Mes* substituent to yield **B**.⁵² Burg and Slota noted that the stability of species of the type RPHX is greatly enhanced by the steric profile of the substituent R.⁵³ Therefore, the terphenyl-based cyanophosphines **4b** and **4c** were expected to make the anions isolable. The reaction of $Mes^*TerP(H)CN$ (**4b**) and KHMDS resulted in an immediate color change of the reaction mixture from colorless to yellow and precipitation of a colorless solid. Interestingly, the clean formation of $Mes^*TerPPMes^*Ter$ (**C**) ($\delta(^{31}P\{^1H\}) = 492.5$ ppm) and HMDS were observed even when the reaction mixture is directly analyzed by NMR spectroscopy after reacting both substrates.²⁰ To get information whether any other phosphorus containing species can be observed (*e.g.* intermediate formation of a phosphinidene which dimerizes to **C**), **4b** and 0.5 eq. of KHMDS were



Scheme 5 Reactivity of **4a–c** towards KHMDS: (I) *in situ* synthesis of $[Mes^*PCN]K$ (**6a**) and decomposition towards phosphindane **A**, diphosphene **B** and KCN; (II) synthesis of $Mes^*TerP(H)P(CN)Mes^*Ter$ (**7**) or diphosphene **C** dependent on the used stoichiometry; (III) synthesis of $[DipTerPCN]K$ (**6c**) and $[DipTerPCN]K(2.2.2-crypt)$ (**6c-crypt**).





combined and the solution was directly analyzed by NMR spectroscopy. Intriguingly, two doublet signals were observed in the $^{31}\text{P}\{^1\text{H}\}$ NMR spectrum at -78.2 and -82.6 ppm with a coupling constant of $^1J_{\text{P,P}} = 326.6$ Hz. The corresponding ^{31}P NMR spectrum revealed the existence of two doublets of doublets with additional coupling constants of 38.3 Hz and 216.3 Hz, respectively. In addition, a highly diagnostic doublet of doublet signal in the ^1H NMR spectrum at 3.97 ppm confirms that the above mentioned coupling constants correspond to $^1J_{\text{P,H}}$ and $^2J_{\text{P,H}}$ coupling, thus the obtained molecule bears a unique P(H)–P moiety.²⁰ In accordance with the NMR data and high-resolution mass spectrometry, SC-XRD verified the formation of the diphosphane $^{\text{Mes}}\text{TerP}(\text{H})\text{P}(\text{CN})^{\text{Mes}}\text{Ter}$ (**7**, Fig. S1†). Treatment of **7** with additional amounts of KHMDS then resulted in the clean conversion to give diphosphane **6** as shown by $^{31}\text{P}\{^1\text{H}\}$ NMR spectroscopy. It is worth mentioning, that the reaction of **4a** with half an equivalent of KHMDS only leads to the described concomitant formation of **6a**, **A**, **B**, **KCN**, and HMDS with parts of **4a** remaining unreacted. Finally, the even bulkier cyanophosphine $^{\text{Dip}}\text{TerP}(\text{H})\text{CN}$ (**4c**) was reacted with equimolar amounts of KHMDS, giving an immediate color change to yellow. A significantly shielded signal in the $^{31}\text{P}\{^1\text{H}\}$ NMR spectrum at -142.0 ppm (*c.f.* *in situ* prepared **6a**: $\delta(^{31}\text{P}\{^1\text{H}\}) = -146.2$ ppm; $[(\text{NHP})\text{PCN}]\text{M}$: $\delta(^{31}\text{P}\{^1\text{H}\}) = -124$ to -84 ppm⁵⁰) indicated the formation of the corresponding cyanophosphide $[\text{Dip}^{\text{Ter}}\text{PCN}]^{\text{K}}$ (**6c**). **6c** proved to be stable in C_6D_6 solution for at least one week at room temperature. Subsequently, the potassium cation could be sequestered by adding 2.2.2-cryptand to quantitatively give the ion separated salt $[\text{Dip}^{\text{Ter}}\text{PCN}][\text{K}(2.2.2\text{-crypt})]$ (**6c-crypt**). The ion separation leads to the expected low-field shift in the $^{31}\text{P}\{^1\text{H}\}$ NMR of approximately 20 ppm so that a signal at -120.7 ppm is detected. In addition, the molecular structure of **6c-crypt** was determined by SC-XRD (Fig. 5).

The structural parameters of the $\text{P}^{\ominus}\text{CN}$ unit indicate that the negative charge is mainly located at the phosphorus, with a N1–C31 bond length of $1.1585(19)$ Å ($\Sigma r_{\text{cov}}(\text{C}\equiv\text{N}) = 1.14$ Å,³⁰ *c.f.* $\text{Ph}_3\text{PC}(\text{H})\text{CN}$ $1.158(3)$ Å).⁵⁴ This is minimally longer than in

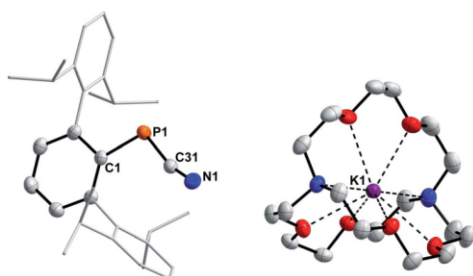


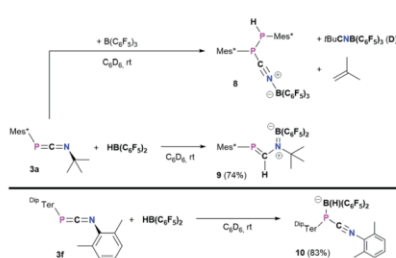
Fig. 5 Molecular structure of **6c-crypt**. Hydrogen atoms omitted and Dip-groups rendered as wireframe for clarity. Thermal ellipsoids are drawn at the 50% probability level. Selected bond lengths (Å) and angles (°): P1–C31 $1.7680(14)$, N1–C31 $1.1585(19)$, P1–C31–N1 $165.45(12)$, C1–P1–C31 $106.73(6)$.

starting material **4a** ($1.146(3)$ Å), whereas the P1–C31 bond length is slightly shortened ($1.7680(14)$ Å; *c.f.* **4a**: $1.793(2)$ Å). Therefore a major contribution from the resonance structure $\text{R}^{\ominus}\text{P}^{\ominus}\text{C}\equiv\text{N}$ and a minor contribution from the resonance structure $\text{R}-\text{P}=\text{C}=\text{N}^{\ominus}$ is reasonable, and is further supported by the C–N stretching frequency of 2053 cm^{-1} . The only other structurally characterized cyanophosphides bear phosphorus based substituents at the phosphorus atom of the PCN moiety but show nearly identical bond lengths across the PCN axis (*c.f.* $[\text{iPr}_2\text{PPCN}]^-$: P–C $1.763(1)$ Å, N–C $1.160(2)$ Å;⁵¹ $[(\text{NHP})\text{PCN}]^-$: P–C_{avg.} 1.75 Å, N–C_{avg.} 1.16 Å).⁵⁰ Whereas for the previously described cyanophosphides nearly linear arrangements of the PCN moieties are observed (N–C–P $> 177^\circ$),^{50,51} the P1–C31–N1 bond angle of $165.45(12)^\circ$ deviates significantly from linearity which might be caused by steric repulsion of the sterically demanding $^{\text{Dip}}\text{Ter}$ group.

Reactivity of selected 1,3-phosphaazaallenes towards $\text{B}(\text{C}_6\text{F}_5)_3$ and Pier's borane $\text{HB}(\text{C}_6\text{F}_5)_2$

Heteroallenes like carbodiimides, isocyanates, and isothiocyanates have shown a diverse reactivity towards the perfluorinated boranes $\text{B}(\text{C}_6\text{F}_5)_3$ and $\text{HB}(\text{C}_6\text{F}_5)_2$ (Pier's borane), ranging from the development of new heterocycles to the formation of classic and frustrated Lewis pairs (FLPs) and 1,2-hydroboration reactions.^{41,55–58}

Treatment of **3a** with $\text{B}(\text{C}_6\text{F}_5)_3$ in toluene afforded a colorless suspension (Scheme 6, top). After stirring for 16 h and subsequent workup,²⁰ the isolated colorless solid was hardly soluble in aromatic hydrocarbons and started to polymerize tetrahydrofuran within minutes. From a saturated C_6D_6 solution sufficient ^1H , $^{11}\text{B}\{^1\text{H}\}$, $^{19}\text{F}\{^1\text{H}\}$, and $^{31}\text{P}\{^1\text{H}\}$ data was obtained and the $^{31}\text{P}\{^1\text{H}\}$ NMR spectrum showed two characteristic signals at -46.8 and -53.3 ppm, respectively with a characteristic $^1J_{\text{P,P}} = 247.5$ Hz coupling constant, reminiscent of $^{\text{Mes}}\text{TerP}(\text{H})\text{P}(\text{CN})^{\text{Mes}}\text{Ter}$ (**7**) (*c.f.* $\delta(^{31}\text{P}\{^1\text{H}\}) = -78.2$ and -82.6 ppm, $^1J_{\text{P,P}} = 326.6$ Hz). The existence of a P(H)–P moiety was supported by the ^1H and ^{31}P NMR data, which show that the signal at -53.3 ppm is a doublet of doublets with $^1J_{\text{P,H}} = 224.0$ Hz, which is further corroborated by a doublet signal with the same $^1J_{\text{P,H}}$ coupling constant in the ^1H NMR spectrum at 5.44 ppm. The reaction is accompanied by significant amounts of



Scheme 6 Reactivity of **3a** towards $\text{B}(\text{C}_6\text{F}_5)_3$ and $\text{HB}(\text{C}_6\text{F}_5)_2$, and reactivity of **3f** towards $\text{HB}(\text{C}_6\text{F}_5)_2$ to give **10**.

byproducts as evident from two signals in the $^{11}\text{B}\{^1\text{H}\}$ NMR spectrum at -7.9 (significantly broadened) and -20.7 ppm, respectively. Similarly, the $^{19}\text{F}\{^1\text{H}\}$ NMR spectrum shows a total of nine signals. Moreover, iso-butene was identified as byproduct ($\delta(^1\text{H}) = 1.60$ and 4.74 ppm, Fig. S67[†]), similarly to the synthesis of the cyanophosphines **4a-c**.

Crystallization attempts gave two types of colorless crystals, and SC-XRD confirmed that indeed the diphosphane $\text{Mes}^*\text{P}(\text{H})\text{P}(\text{CNB}(\text{C}_6\text{F}_5)_3)\text{Mes}^*$ (**8**, Fig. 6) was formed alongside the literature known nitrile-borane adduct $t\text{BuCNB}(\text{C}_6\text{F}_5)_3$ (**D**) (Scheme 6, top).⁴² It is worth mentioning, that all attempts to isolate **8** in pure fashion failed up to now, which is attributed to quite similar solubilities of **8** and **D**. In **8** the newly formed P1-P2 and N1-B1 bond lengths of $2.2464(8)$ Å and $1.572(3)$ Å are in good accordance with the formulation as single bonds ($\Sigma r_{\text{cov}}(\text{P-P}) = 2.22$ Å; $\Sigma r_{\text{cov}}(\text{N-B}) = 1.56$ Å).³⁹ The N1-C37 bond length of $1.140(3)$ Å is a typical carbon nitrogen triple bond ($\Sigma r_{\text{cov}}(\text{C}\equiv\text{N}) = 1.14$ Å),³⁹ and the P1,C37,N1,B1 axis is minimally bent (*e.g.* C37-N1-B1 $174.9(2)^\circ$).

All these metrics agree with phosphanitrilium borate **5a** (Fig. 4). It is noteworthy that the phosphaketene $[\text{SP}]\text{PCO}$ reacted with $\text{B}(\text{C}_6\text{F}_5)_3$ to give a zwitterionic diphosphirenium with a P_2C three-membered ring with an exocyclic C-O-B(C_6F_5)₃ moiety.²¹ We continued to investigate the reactivity of **3a** towards Pier's borane ($\text{HB}(\text{C}_6\text{F}_5)_2$) to check its potential for hydroboration chemistry.³⁹

The reaction of **3a** and $\text{HB}(\text{C}_6\text{F}_5)_2$ yielded a yellow solid after workup (isolated yield 74%, Scheme 6, middle). Single crystals grown from layering a saturated C_6D_6 solution with *n*-hexane revealed the product to be $\text{Mes}^*\text{PC}(\text{H})\text{N}(t\text{Bu})\text{B}(\text{C}_6\text{F}_5)_3$ (**9**, Fig. 7), showing that 1,2-hydroboration across the C=N bond of **3a** had occurred (Scheme 6, middle). Remarkably, the molecular structure of **9** reveals a novel heterodiene ($\text{P}=\text{C}-\text{N}^{(+)}=\text{B}^{(-)}$) structural motif. Both, the P1-C19 and N1-B1 bond lengths of

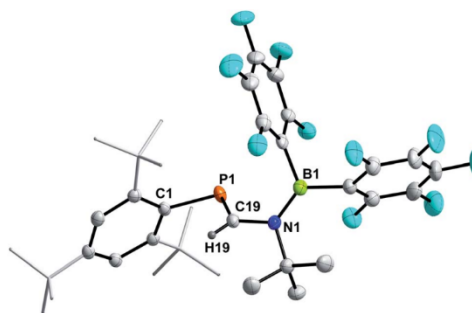


Fig. 7 Molecular structure of **9**. Hydrogen (except H19) omitted and *t*Bu-groups on Mes^* rendered as wireframe for clarity. Thermal ellipsoids are drawn at the 50% probability level. Selected bond lengths (Å) and angles ($^\circ$): P1-C19 $1.6751(13)$, N1-C19 $1.4278(15)$, N1-B1 $1.3995(18)$; C1-P1-C19 $98.93(6)$, P1-C19-N1 $123.69(9)$, C19-N1-B1 $120.15(10)$.

$1.6751(13)$ Å and $1.3995(18)$ Å are best described as double bonds, respectively, which is also illustrated in the KS orbitals (PBE0-D3/def2-SVP, Fig. S91[†]). The HOMO is best described as the P-C and B-N π -bonds, respectively, with one node. The LUMO has π^* character for P-C and B-N bonds resulting in two nodes and with π -character between C and N, as expected for a heterodiene.⁶⁰ The nature of BN multiple bonds has been in the focus of recent computational studies,^{61,62} and NBO results for **9** show a σ (N 79.5, B 20.5%) and π (N 86.1, B13.9%) NBO, which are mainly formed by the natural atomic hybrid orbitals located on N. This agrees well with the values obtained for 9,10-diimino-9,10-dihydro-9,10-diboraanthracene.^{62,63} Topological analysis of the electron density using the QT-AIM approach revealed an electron density ($\rho_{(3,-1)}$ [e bohr^{-3}]) of 0.198 at the BN bond critical point (BCP), as well as an electron density Laplacian (∇^2 [e bohr^{-5}]) of 0.651, which corresponds nicely with the aforementioned diminodiboraanthracene.^{30,62} In addition, the sum of angles around C19, N1, and B1 all add up to over 359.8° , in line with sp^2 -hybridization. The solution NMR spectra of **9** are indicative that this diene structure sustains in solution, with one resonance in the ^{11}B NMR spectrum at 36.4 ppm, indicating a tri-coordinated boron atom (*cf.* $(\text{C}_6\text{F}_5)_2\text{BNMe}_2$ 33.7 ppm).⁶⁴ Given the double bond character of the B=N bond, two distinct C_6F_5 groups are detected giving two sets of signals in the ^{19}F NMR spectrum. Highly diagnostic is the ^1H NMR chemical shift of the P=C(H) proton at 7.80 ppm as a doublet with a $^2J_{\text{P,H}}$ coupling constant of 18.5 Hz (*cf.* $\text{Mes}^*\text{P}=\text{C}(\text{H})\text{N}(\text{SiMe}_3)_2$ (ref. 65) $\delta(^1\text{H}) = 8.24$ (d, $^2J_{\text{P,H}} = 16.8$ Hz)). The aforementioned ^1H NMR signal, the deshielded $^{31}\text{P}\{^1\text{H}\}$ NMR signal at 228.5 ppm and the $^{13}\text{C}\{^1\text{H}\}$ NMR signal of the P=C(H) functionality ($\delta(^{13}\text{C}\{^1\text{H}\}) = 177.5$ ppm, $^1J_{\text{P,C}} = 37.3$ Hz) clearly indicate a phosphalkene (*cf.* $2,6\text{-}(\text{Mes}^*\text{P}=\text{C}(\text{H}))_2(\text{NC}_5\text{H}_5)$ $\delta(^{31}\text{P}) = 249.1$ ppm).⁶⁶ Interestingly, carbodiimides react with Pier's Borane to the corresponding four-membered boron amidinates.⁵⁵ Similar four-membered heterocycles are formed when isothiocyanates are treated with $\text{HB}(\text{C}_6\text{F}_5)_2$.⁴¹

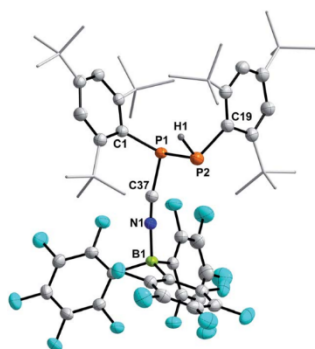


Fig. 6 Molecular structure of **8**. Hydrogen atoms (except H1) omitted and *t*Bu-groups on Mes^* rendered as wireframe for clarity. Thermal ellipsoids are drawn at the 50% probability level. Selected bond lengths (Å) and angles ($^\circ$): P1-P2 $2.2464(8)$, N1-B1 $1.572(3)$, P1-C37 $1.784(2)$, P1-C1 $1.844(2)$, P2-C19 $1.852(2)$, N1-C37 $1.140(3)$; P1-C37-N1 $165.4(2)$, C37-N1-B1 $174.9(2)$.



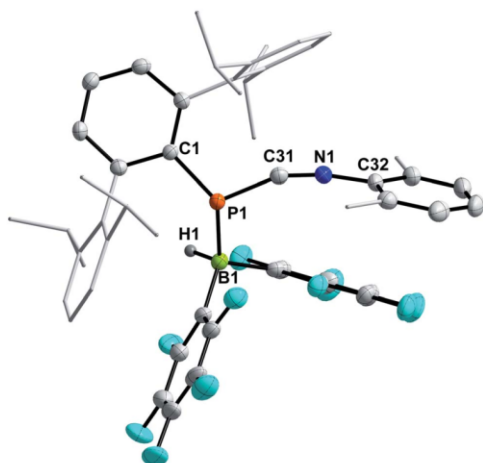


Fig. 8 Molecular structure of **10**. Hydrogen (except H1) omitted and Dip and Xyl groups rendered as wireframe for clarity. Thermal ellipsoids are drawn at the 50% probability level. Selected bond lengths (Å) and angles (°): P1–C31 1.754(3), N1–C31 1.161(3), P1–B1 2.060(3), P1–C31–N1 157.7(2).

Finally, the influence of the substitution pattern at both the phosphorus and nitrogen atoms was investigated exemplarily by reacting the 1,3-phosphaazaallene **3f** (bearing ^{Dip}Ter and Xyl substituents) with HB(C₆F₅)₂ (Scheme 6, bottom). One singlet signal in the ¹¹B{¹H} NMR spectrum at –19.3 ppm, indicated a four-coordinate boron atom. In contrast to **9**, only three signals are observed in the ¹⁹F{¹H} NMR spectrum and the ³¹P{¹H} signal is observed at –83.1 ppm, over 300 ppm shifted towards higher field when compared to **9**. These data together with the data obtained by SC-XRD showed that instead of 1,2-hydroboration, the Lewis acid base adduct ^{Dip}TerP(HB(C₆F₅)₂)CNXyl (**10**) with a newly formed P–B bond was obtained (Fig. 8). The C1–N1 bond length of 1.161(3) Å is shortened by approximately 0.04 Å when compared to the starting material **3f** (*c.f.* 1.2009(15) Å) and is now close to a carbon nitrogen triple bond ($\Sigma r_{\text{cov}}(\text{C}\equiv\text{N}) = 1.14$ Å).²⁵ Accordingly, the C31–N1–C32 bond angle increases to 165.1(3)° (*c.f.* 143.24(12)° (**3f**)). The P1–C31 bond length of 1.754(3) Å also increases compared to **3f** (1.6785(12) Å) indicative of a single bond (*c.f.* ^{Dip}TerP(H)CN **4c** 1.793(2) Å). The P1–B1 bond length of 2.060(3) Å is 0.1 Å longer than the respective sum of the covalent radii ($\Sigma r_{\text{cov}}(\text{P–B}) = 1.96$ Å)²⁵ and corresponds with dative bonding as further ascertained by a low WBI for the P–B bond of 0.85.

Conclusions

Phospha-Wittig reagents have been shown to react with isocyanides to give 1,3-phosphaazaallenes **3a–f**. In case of the CN^tBu-derivatives these were further transformed in the corresponding cyanophosphines **4a–c**. CN^tBu acts in this case as a disguised HCN transfer reagent. This allowed the structural

characterization of this underrepresented class of phosphines and deprotonation yielded in one case a rare example of an aryl-substituted cyanophosphide anion. Moreover, **3a** was shown to be 1,2-hydroborylated along the C=N bond to give the unique heterodiene **9** with alternating PC and BN double bonds. Studies using cyanophosphide **6c** as a ligand and exploiting heterodiene **9** in FLP-type chemistry are currently underway.

Data availability

All experimental, crystallographic and computational data are provided in the ESI.

Author contributions

M. F. discovered and optimized the formation of 1,3-phosphaazaallenes, studied the scope and studied the reactivity of compounds **3a–f**. M. F. prepared the experimental part and the first draft of the manuscript. C. H.-J. designed the overall research, supervised the work, carried out the computational work, contributed to IR analysis, finalized the manuscript, proofread the experimental part and coordinated the overall project.

Conflicts of interest

There are no conflicts to declare.

Acknowledgements

C. H.-J. thanks Prof. M. Beller for his continuous support and the Boehringer Ingelheim Stiftung (BIS) is acknowledged for an Exploration Grant. We thank our technical and analytical staff for assistance, especially Dr Anke Spannenberg for her support regarding X-ray analysis. J.-E. Siewert is gratefully acknowledged for assisting with CV measurements. We wish to thank the ITMZ at the University of Rostock for access to the Cluster Computer and especially Malte Willert for technical support and Dr Jonas Bresien for helpful discussions.

Notes and references

- O. I. Kolodiazny, *Tetrahedron Lett.*, 1982, **23**, 4933–4936.
- O. I. Kolodiazny, *Phosphorus Sulphur Relat. Elem.*, 1983, **18**, 39–42.
- M. Yoshifuji, K. Toyota, K. Shibayama and N. Inamoto, *Tetrahedron Lett.*, 1984, **25**, 1809–1812.
- M. Yoshifuji, T. Niitsu, K. Toyota, N. Inamoto, K. Hirotsu, Y. Odagaki, T. Higuchi and S. Nagase, *Polyhedron*, 1988, **7**, 2213–2216.
- R. Appel and C. Behnke, *Z. Anorg. Allg. Chem.*, 1987, **555**, 23–35.
- X.-G. Zhou, L.-B. Zhang, R.-F. Cai, Q.-J. Wu, L.-H. Weng and Z.-E. Huang, *J. Organomet. Chem.*, 2000, **604**, 260–266.
- C. Wentrup, H. Briehl, G. Becker, G. Uhl, H. J. Wessely, A. Maquestiau and R. Flammang, *J. Am. Chem. Soc.*, 1983, **105**, 7194–7195.



- 8 M.-A. David, J. B. Alexander, D. S. Glueck, G. P. A. Yap, L. M. Liabre-Sands and A. L. Rheingold, *Organometallics*, 1997, **16**, 378–383.
- 9 T. Wegmann, M. Hafner and M. Regitz, *Chem. Ber.*, 1993, **126**, 2525–2530.
- 10 J. Grobe, D. Le Van and T. Großpietsch, *Z. Naturforsch. B*, 1991, **46**, 978–984.
- 11 T. L. Breen and D. W. Stephan, *J. Am. Chem. Soc.*, 1995, **117**, 11914–11921.
- 12 E. Ionescu, G. von Frantzius, P. G. Jones and R. Streubel, *Organometallics*, 2005, **24**, 2237–2240.
- 13 F. Basuli, L. A. Watson, J. C. Huffman and D. J. Mindiola, *Dalton Trans.*, 2003, 4228–4229.
- 14 G. Becker, H. Brombach, S. T. Horner, E. Niecke, W. Schwarz, R. Streubel and E.-U. Würthwein, *Inorg. Chem.*, 2005, **44**, 3080–3086.
- 15 L. Liu, D. A. Ruiz, D. Munz and G. Bertrand, *Chem*, 2016, **1**, 147–153.
- 16 P. Willmes, M. J. Cowley, M. Hartmann, M. Zimmer, V. Huch and D. Scheschke, *Angew. Chem., Int. Ed.*, 2014, **53**, 2216–2220.
- 17 P. Gupta, J.-E. Siewert, T. Wellnitz, M. Fischer, W. Baumann, T. Beverley and C. Hering-Junghans, *Dalton Trans.*, 2021, **50**, 1838–1844.
- 18 M. Fischer, S. Nees, T. Kupfer, J. T. Goettel, H. Braunschweig and C. Hering-Junghans, *J. Am. Chem. Soc.*, 2021, **143**, 4106–4111.
- 19 M. Fischer, F. Reiß and C. Hering-Junghans, *Chem. Commun.*, 2021, **57**, 5626–5629.
- 20 Experimental and computational details, and details on the X-ray diffraction studies are included in the ESI.† CCDC 2086496–2086506 contain the X-Ray data.
- 21 M. M. Hansmann, D. A. Ruiz, L. L. Liu, R. Jazzar and G. Bertrand, *Chem. Sci.*, 2017, **8**, 3720–3725.
- 22 M. M. Hansmann and G. Bertrand, *J. Am. Chem. Soc.*, 2016, **138**(49), 15885–15888.
- 23 J. Escudié, H. Ranaivonjatovo and L. Rigon, *Chem. Rev.*, 2000, **100**, 3639–3696.
- 24 E. Urnéžius and J. D. Protasiewicz, *Main Group Chem.*, 1996, **1**, 369–372.
- 25 M. Yoshifuji, I. Shima, N. Inamoto, K. Hirotsu and T. Higuchi, *J. Am. Chem. Soc.*, 1981, **103**, 4587–4589.
- 26 C. Riplinger and F. Neese, *J. Chem. Phys.*, 2013, **138**, 034106.
- 27 C. Riplinger, B. Sandhoefer, A. Hansen and F. Neese, *J. Chem. Phys.*, 2013, **139**, 134101.
- 28 R. C. Smith and J. D. Protasiewicz, *J. Am. Chem. Soc.*, 2004, **126**, 2268–2269.
- 29 S. Shah, M. C. Simpson, R. C. Smith and J. D. Protasiewicz, *J. Am. Chem. Soc.*, 2001, **123**, 6925–6926.
- 30 P. Pykkö and M. Atsumi, *Chem.–Eur. J.*, 2009, **15**, 12770–12779.
- 31 M. B. Smith and J. March, Localized Chemical Bonding, In *March's Advanced Organic Chemistry*, ed. M. B. Smith and J. March, 2006, pp. 3–31.
- 32 T. Peddarao, A. Baishya, M. K. Barman, A. Kumar and S. Nembenna, *New J. Chem.*, 2016, **40**, 7627–7636.
- 33 M. K. Sharma, D. Rottschäfer, S. Blomeyer, B. Neumann, H.-G. Stammer, M. van Gastel, A. Hinz and R. S. Ghadwal, *Chem. Commun.*, 2019, **55**, 10408–10411.
- 34 K. Takeuchi, M. Ichinohe and A. Sekiguchi, *J. Am. Chem. Soc.*, 2012, **134**, 2954–2957.
- 35 J. Böhnke, H. Braunschweig, T. Dellermann, W. C. Ewing, T. Kramer, I. Kruppenacher and A. Vargas, *Angew. Chem., Int. Ed.*, 2015, **54**, 4469–4473.
- 36 H. Braunschweig, I. Kruppenacher, M.-A. Légaré, A. Matler, K. Radacki and Q. Ye, *J. Am. Chem. Soc.*, 2017, **139**, 1802–1805.
- 37 R. C. Dobbie, P. D. Gosling and B. P. Straughan, *J. Chem. Soc., Dalton Trans.*, 1975, 2368–2373.
- 38 C. Schulten, G. von Frantzius, G. Schnakenburg and R. Streubel, *Heteroat. Chem.*, 2011, **22**, 275–286.
- 39 A. Maraval, A. Igau, C. Lepetit, A. Chrostowska, J.-M. Sotiropoulos, G. Pfister-Guillouzo, B. Donnadiu and J. P. Majoral, *Organometallics*, 2001, **20**, 25–34.
- 40 I. C. Vei, S. I. Pascu, M. L. H. Green, J. C. Green, R. E. Schilling, G. D. W. Anderson and L. H. Rees, *Dalton Trans.*, 2003, 2550–2557.
- 41 M. Fischer and M. Schmidtman, *Chem. Commun.*, 2020, **56**, 6205–6208.
- 42 H. Jacobsen, H. Berke, S. Döring, G. Kehr, G. Erker, R. Fröhlich and O. Meyer, *Organometallics*, 1999, **18**, 1724–1735.
- 43 A. Schmidpeter and F. Zwaschka, *Angew. Chem., Int. Ed. Engl.*, 1977, **16**, 704–705.
- 44 A. Schmidpeter, G. Burget, F. Zwaschka and W. S. Sheldrick, *Z. Anorg. Allg. Chem.*, 1985, **527**, 17–32.
- 45 A. Schmidpeter, F. Zwaschka and W. S. Sheldrick, *Chem. Ber.*, 1985, **118**, 1078–1085.
- 46 J. F. Binder, S. C. Kosnik, P. B. J. St Onge and C. L. B. Macdonald, *Chem.–Eur. J.*, 2018, **24**, 14644–14648.
- 47 A. Schmidpeter, K.-H. Zirzow, G. Burget, G. Huttner and I. Jibril, *Chem. Ber.*, 1984, **117**, 1695–1706.
- 48 A. Schmidpeter and G. Burget, *Z. Naturforsch. B*, 1985, **40**, 1306–1313.
- 49 R. M. K. Deng and K. B. Dillon, *J. Chem. Soc., Chem. Commun.*, 1981, 1170–1171.
- 50 Z. Li, J. E. Borger, F. Müller, J. R. Harmer, C.-Y. Su and H. Grützmacher, *Angew. Chem., Int. Ed.*, 2019, **58**, 11429–11433.
- 51 C. M. Hoidn, T. M. Maier, K. Trabitsch, J. J. Weigand and R. Wolf, *Angew. Chem., Int. Ed.*, 2019, **58**, 18931–18936.
- 52 A. H. Cowley, F. Gabbai, R. Schluter and D. Atwood, *J. Am. Chem. Soc.*, 1992, **114**, 3142–3144.
- 53 A. B. Burg and P. J. Slota, *J. Am. Chem. Soc.*, 1958, **80**, 1107–1109.
- 54 C. Schwarz, L. T. Scharf, T. Scherpf, J. Weismann and V. H. Gessner, *Chem.–Eur. J.*, 2019, **25**, 2793–2802.
- 55 M. A. Dureen and D. W. Stephan, *J. Am. Chem. Soc.*, 2010, **132**, 13559–13568.
- 56 M. H. Holthausen, M. Colussi and D. W. Stephan, *Chem.–Eur. J.*, 2015, **21**, 2193–2199.



Edge Article

- 57 A. C. McQuilken, Q. M. Dao, A. J. P. Cardenas, J. A. Bertke, S. Grimme and T. H. Warren, *Angew. Chem., Int. Ed.*, 2016, **55**, 14335–14339.
- 58 M. Mehta and J. M. Goicoechea, *Chem. Commun.*, 2019, **55**, 6918–6921.
- 59 E. A. Patrick and W. E. Piers, *Chem. Commun.*, 2020, **56**, 841–853.
- 60 G. Desimoni and G. Tacconi, *Chem. Rev.*, 1975, **75**, 651–692.
- 61 S. Berski, Z. Latajka and A. J. Gordon, *New J. Chem.*, 2011, **35**, 89–96.
- 62 G. Mierzwa, A. J. Gordon and S. Berski, *J. Mol. Model.*, 2020, **26**, 136.
- 63 P. Müller, S. Huck, H. Köppel, H. Pritzkow and W. Siebert, *Z. Naturforsch., B: Chem. Sci.*, 1995, **50**, 1476–1484.
- 64 D. Winkelhaus, Y. V. Vishnevskiy, R. J. F. Berger, H.-G. Stammer, B. Neumann and N. W. Mitzel, *Z. Anorg. Allg. Chem.*, 2013, **639**, 2086–2095.
- 65 M. Song, B. Donnadiou, M. Soleilhavoup and G. Bertrand, *Chem.–Asian J.*, 2007, **2**, 904–908.
- 66 Y.-H. Chang, Y. Nakajima and F. Ozawa, *Organometallics*, 2013, **32**, 2210–2215.

Open Access Article. Published on 30 June 2021. Downloaded on 2/14/2022 4:03:10 PM.
This article is licensed under a Creative Commons Attribution-NonCommercial 3.0 Unported Licence.



5.4 Titanocene pnictinidene complexes

M. Fischer, F. Reiß, C. Hering-Junghans

Chem. Commun. **2021**, 57, 5626–5629.

DOI: 10.1039/D1CC01305J



Reprinted (adapted) with permission from *Chemical Communications*.

Copyright 2021 Royal Society of Chemistry






Titanocene pnictinidene complexes†

Cite this: *Chem. Commun.*, 2021, 57, 5626Received 10th March 2021
Accepted 10th May 2021

DOI: 10.1039/d1cc01305j

rsc.li/chemcomm

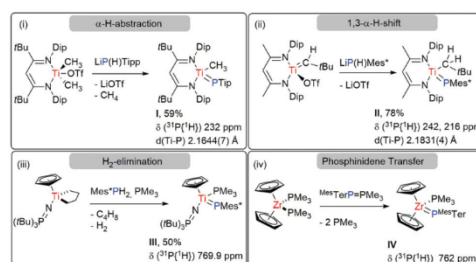
Malte Fischer,  Fabian Reiß * and Christian Hering-Junghans *

The phospho–Wittig reagent ^{Mes}TerPPMe₃ (^{Mes}Ter = 2,6-(2,4,6-Me₃-C₆H₂)-C₆H₃) and arsa–Wittig reagent ^{Dip}TerAsPMe₃ (^{Dip}Ter = 2,6-(2,6-iPr₂-C₆H₃)-C₆H₃) have been employed to synthesize the titanocene complexes Cp₂Ti(PMe₃)PnAr (Pn = P, As) with terminal phosphinidene or arsinidene ligands, respectively. *Ab initio* studies show that the description as singlet biradicaloids in their ground state is warranted.

Phosphinidenes, the isovalent analogues of carbenes, are in most cases transient species that stand in stark contrast to the widely applied, bottleable N-heterocyclic carbenes (NHCs),^{1–3} and cyclic alkyl amino carbenes (cAACs).^{4,5} Just recently, the first example of a free kinetically stabilized phosphino-phosphinidene has been reported by Bertrand *et al.*⁶ Nevertheless, most phosphinidenes are stabilized by coordination to a transition metal fragment,⁷ or by cycloaddition reactions to (conjugated) multiple bond systems as was recently shown for RP(anthracene) systems.⁸ Together with free phosphinidenes, terminal phosphinidene complexes of the type [L_nM=PR] are highly desirable compounds to access a carbene-like chemistry for phosphorus-element bond formation and phosphinidene-transfer reactions.^{9–12} Nucleophilic phosphinidene complexes are preferred when the spectator ligands L are strong σ-donors, while strong π-accepting ligands render the phosphinidene unit more electrophilic.¹³ In contrast to the rich chemistry of phosphinidene-bridged dinuclear complexes,¹⁴ terminal phosphinidene complexes are rare. To access the first terminal titanium phosphinidenes Mindiola *et al.* used sterically demanding β-diketiminato supporting ligands on Ti (Scheme 1, i and ii). Oxidation of a dimethyl complex with AgOTf and subsequent addition of LiP(H)Tip (Tip = 2,4,

6-iPr₃C₆H₂) furnished [(^tBuNacnac)(Me)Ti=PTip] (**I**, ^tBuNacnac = CH(C(^tBu)NDip)₂; Dip = 2,6-iPr₂C₆H₃) with concomitant release of methane and LiOTf.¹⁵ [(^{Mes}Nacnac)(CH₂^tBu)Ti=PMe^{*}] (**II**, ^{Mes}Nacnac = CH(C(CH₃)NDip)₂; Me^{*} = 2,4,6-^tBu₃C₆H₂) was prepared from a putative neopentylidene phosphide *via* a 1,3-*H*-shift of the α-hydrogen (Scheme 1, ii).¹⁶ The same synthetic strategy was utilized to synthesize a Ti(IV) phosphinidene complex bearing a mono-anionic PNP-pincer ligand.¹⁷ Reaction of the Ti(II) synthon [CpTi(NP(^tBu)₃)(CH₂)₄] with Me^{*}PH₂ in the presence of PMe₃ afforded the corresponding base-stabilized complex [(Cp)NP(^tBu)₃](PMe₃)Ti=PMe^{*}] (**III**), which shows three characteristic resonances in the ³¹P NMR spectrum at 769.9, 35.3, and –10.3 ppm for the phosphinidene, phosphinimide, and PMe₃ phosphorus atoms, respectively (Scheme 1, iii).¹⁸ Efficient transfer of a PAr unit can also be achieved by so-called phospho-Wittig reagents of the general type ArPPMe₃.¹⁹ The combination of the Zr(II) synthon [Cp₂Zr(PMe₃)₂] and ^{Mes}TerPPMe₃ (^{Mes}Ter = 2,6-Me₂C₆H₃, Mes = 2,4,6-Me₃C₆H₃) afforded [(Cp)₂(PMe₃)Zr=P^{Mes}Ter] (**IV**) with a characteristic deshielded phosphinidene phosphorus showing a ³¹P NMR signal at 762 ppm (Scheme 1, iv).²⁰

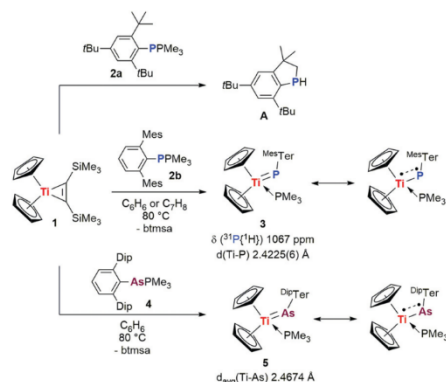
Recently, we attempted the synthesis of terminal titanocene phosphinidene complexes by treatment of the Ti(II) synthon



Scheme 1 Reported syntheses of selected group 4 phosphinidene complexes I–IV with the respective Ti–P bond lengths (I, II) and ³¹P NMR shifts of the phosphinidene units (I–IV).

Leibniz-Institut für Katalyse e.V. (LIKAT Rostock), Albert-Einstein-Str. 29a, Rostock 18059, Germany. E-mail: fabian.reiss@katalyse.de, christian.hering-junghans@katalyse.de

† Electronic supplementary information (ESI) available: Synthesis and characterization of compounds, NMR spectra, crystallographic, and computational details. CCDC 2060154–2060157. For ESI and crystallographic data in CIF or other electronic format see DOI: 10.1039/d1cc01305j



Scheme 2 Synthesis of phosphaindane **A** and the titanocene phosphinidene complexes **3** and **5** (the dotted line between the electrons on Ti and E indicates antiferromagnetic coupling).

$[\text{Cp}_2\text{Ti}(\text{btmsa})]$ ($\text{btmsa} = \text{C}_2(\text{SiMe}_3)_2$),²¹ with aryl substituted triphosphiranes P_3Ar_3 ($\text{Ar} = \text{Tip}, \text{Dip}, \text{Mes}$), which afforded the titanocene diphosphene complexes $[\text{Cp}_2\text{Ti}(\text{P}_2\text{Ar}_2)]$ instead.²²

In this contribution we present the synthesis and characterization of the first terminal titanocene phosphinidene and arsinidene complexes. The bonding has been thoroughly studied by combined DFT and *ab initio* studies.

As a synthetic entry we chose the titanocene precursor $[\text{Cp}_2\text{Ti}(\text{btmsa})]$ (**1**),^{23,24} in combination with the phospho-Wittig reagents Mes^*PMe_3 (**2a**), $\text{Mes}^*\text{TerPMe}_3$ (**2b**) and $\text{Dip}^*\text{TerPMe}_3$ (**2c**, $\text{Dip}^*\text{Ter} = 2,6\text{-Dip}_2\text{C}_6\text{H}_3$).²⁵ We first studied the formal ligand exchange reaction of btmsa for PAR between **1** and **2** to give $[\text{Cp}_2\text{Ti}(\text{PMe}_3)\text{PAR}]$ *in silico*, to evaluate its thermodynamic feasibility. For all three combinations an exergonic Gibbs Free Enthalpy change to give the complexes $[(\text{Cp}_2(\text{PMe}_3)\text{Ti}=\text{PAR})]$ according to Scheme 2 ($\Delta_{\text{R}}G^\ddagger = -5.8$ (**2a**), -11.2 (**2b**), -9.0 (**2c**) kcal mol^{-1} , Table S4, ESI†) was obtained.²⁶

Then **1** and **2a** were combined in C_6D_6 . At room temperature no reaction was observed after 16 h, but warming to 40°C resulted in the formation of the known 3,3-dimethyl-5,7-di-*tert*-butylphosphaindane (**A**) (Scheme 2, top and Fig. S5–S7, ESI†).^{18,26,27} This suggests phosphinidene release and formal insertion of the phosphinidene unit into a C–H-bond of one *tert*-butyl methyl group, which is faster than recombination with Cp_2Ti . Phosphaindane formation is reminiscent of the reaction of the stable phosphinidene complex $[\text{Cp}_2\text{U}=\text{PMe}_3^*]$ with diphenylacetylene, which results in the formation of **A** and $[\text{Cp}_2\text{U}(\text{C}_2\text{Ph}_2)]$.²⁸ In contrast, treatment of **1** with **2b** on an NMR scale in C_6D_6 at 80°C for 16 h indicated the complete consumption of both starting materials, accompanied by the release of btmsa ($\delta(^1\text{H}) = 0.15$ ppm) (Scheme 2, middle). No indications for a CH-activation of the Mes^*Ter -moiety were observed, which was corroborated by DFT studies (Table S5, ESI†). The product could be unambiguously characterized to be the PMe_3 -stabilized titanocene phosphinidene complex $[\text{Cp}_2(\text{PMe}_3)\text{Ti}=\text{P}^{\text{Mes}^*\text{Ter}}]$ (**3**) by combined spectroscopic methods.

An unsymmetrical coordination environment at titanium is indicated by two signals for the Cp_2Ti unit ($\delta(^1\text{H}) = 5.22, 5.23$ ppm) in the ^1H NMR spectrum. Broad signals for the terphenyl moiety suggest hindered rotation within the molecule. In the $^{31}\text{P}\{^1\text{H}\}$ NMR spectrum two diagnostic doublets ($^2J_{\text{P,P}} = 21.7$ Hz) at 8.0 (PMe_3) and 1067.3 (P^{Ter}) ppm ($\delta_{\text{calc}}(^{31}\text{P}\{^1\text{H}\}) = -41.3$ (PMe_3), 1162.1 (P^{Ter}) ppm) were detected, respectively.²⁶ The latter being significantly deshielded by *ca.* 300 ppm compared to the titanium phosphinidene complex $[(\text{Cp})(\text{N}^t\text{PrBu})(\text{PMe}_3)\text{Ti}=\text{PMe}_3^*]$ (**III**, Scheme 1).¹⁸ X-Ray quality intensely coloured brown crystals of **3** were obtained by slowly cooling a saturated toluene solution of **3** from 80°C to room temperature (Fig. 1, left).

The central titanium atom is in a distorted trigonal-pyramidal coordination environment according to $\tau_4 = 0.80$ (τ_4 is a simple metric for evaluating the geometry of four-coordinate compounds).²⁹ The Ti1–P1–C1 bond angle of $122.12(6)^\circ$ is significantly more bent as in structurally characterized **I** ($159.95(7)^\circ$)^[6] and **II** ($164.44(5)^\circ$),^{15,16} respectively, but agrees with the analogous zirconium complex $[\text{Cp}_2(\text{PMe}_3)\text{Zr}=\text{PMe}_3^*]$ ($116.1(4)^\circ$).³⁰ Comparable base-stabilized titanium imido complexes of the general type $[\text{Cp}_2(\text{NCMe})\text{Ti}=\text{N}^{\text{Mes}^*\text{Ter}}]$ (**V**) also show Ti–N–C_{Ter} angles of over 155° .³¹ However, it is accepted that the M–N–C angle in metal imido complexes is mostly an artefact of crystal packing and the energy penalty for changing the angle is generally low. The Ti1– PMe_3 bond length of $2.5688(6)$ Å is significantly longer than typical titanium phosphorus single bonds ($\sum r_{\text{cov}}(\text{Ti}-\text{P})$ 2.47 Å)³² and corresponds to dative bonding, whereas the Ti1–P1 bond ($2.4225(6)$ Å) does not approach a double bond ($\sum r_{\text{cov}}(\text{P}=\text{P})$ 2.19 Å).³² In the structurally characterised NaacnacTiPAR species **I** ($2.1644(7)$ Å) and **II** ($2.1831(4)$ Å) significantly shorter titanium phosphorus bond lengths were found (Scheme 1), in line with pseudo-triply bound species.^{15,16} Attempts to synthesize a base-free titanocene phosphinidene complex using phospho-Wittig reagent **2c** with a sterically more demanding Dip^*Ter group did only result in decomposition of **1** at higher

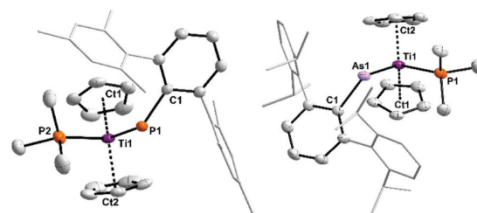


Fig. 1 ORTEP drawing of the molecular structures of **3** (left) and **5** (right, one of three independent molecules in the asymmetric unit). Hydrogen atoms omitted for clarity and thermal ellipsoids drawn at 50% (**3**) and at 30% (**5**) probability, respectively. Ct corresponds to the centroids of the respective Cp rings. Selected bond lengths (Å) and angles ($^\circ$) of **3**: Ti1–P1 $2.4225(6)$, Ti1–P2 $2.5688(6)$; C1–P1–Ti1 $122.12(6)$, P1–Ti1–P2 $86.823(19)$; **5**: Ti1–As1 $2.4726(8)$, Ti1–P1 $2.5545(11)$; C1–As1–Ti1 $121.73(10)$, P1–Ti1–As1 $88.05(3)$.

temperatures.²⁶ Interestingly, no decomposition of **2c** was noted, illustrating the stabilizing effect of the ^{Dip}Ter group.

The successful isolation of **3** prompted us to test whether a terminal arsinidene complex is feasible as well. To date there are two potential arsa-Wittig reagents described in the literature, ^{TiP}TerAsPMe₃,³³ and ^{Dip}TerAsPMe₃ (**4**).³⁴ Using an equimolar mixture of **4** and **1** in C₆D₆ at room temperature revealed a new signal in the ³¹P NMR spectrum at 16.7 ppm after 8 h at room temperature. Heating the mixture to 80 °C over a period of 16 h gave full conversion of both **1** and **4** to the titanocene arsinidene complex [Cp₂(PMe₃)Ti=As^{Dip}Ter] (**5**) was detected (Scheme 2, bottom). We note that using sub-stoichiometric amounts of **1** in the reaction with **4** reproducibly gave rise to the formation of the diarsene (^{Dip}TerAs)₂ (**6**) as a side product. We independently showed that heating **4** to 105 °C in C₆D₆ over a period of 130 h afforded **6** quantitatively based on ¹H NMR spectroscopy. Recrystallization from *n*-pentane at -30 °C allowed the isolation of **6** in 54% yield as a yellow crystalline solid and two modifications of the diarsene (**6_i** and **6_ii**) were identified by SC-XRD experiments (Fig. S3 and S4, ESI†).

X-Ray quality deep brown crystals of **5** were obtained from saturated *n*-hexane solutions at -30 °C.²⁶ **5** crystallizes in the triclinic spacegroup *P* $\bar{1}$ with three independent molecules in the asymmetric unit (Fig. S2, ESI†). As in **3**, the value of $\tau_4 = 0.80$ is diagnostic of a distorted trigonal-pyramidal coordination environment at titanium,²⁹ with a similar Ti1-As1-C1 bond angle of 121.73(10)° (*cf.* **3** 122.12(6)°) (Fig. 1, right). Transition metal complexes with an arsinidene ligand are rare and the herein reported **5** is the first arsinidene complex of a group 4 metal. Wolczanski *et al.* synthesized the first transition metal arsinidene complex (tBuSiO)₃Ta=AsPh with a Ta-As-C bond angle of 107.2(4)° and a Ta-As bond length of 2.428(2) Å ($\sum r_{\text{cov}}(\text{Ta}=\text{As})$ 2.40 Å).^{32,35} The Ti1-As1 bond length in **5** of 2.4726(8) Å (Ti-As_{avg} 2.4674 Å) ($\sum r_{\text{cov}}(\text{Ti}=\text{As})$ 2.31 Å, (Ti-As) 2.57 Å)³² indicates a weak π -component within this bond. Other structurally characterized arsinidene complexes were reported with tungsten,³⁶ iron,³⁷ and uranium metal centers.³⁸

To gain a better understanding of the bonding situation in **3** and **5** we first performed an NBO analysis of the B3LYP/GD3BJ/def2svp optimized structures to analyse the natural localized molecular orbitals (NLMO).²⁶ This revealed a double bond between P1 and Ti1, in agreement with the Lewis structure in Scheme 2, however, both the π -type NBO as well as the LP at P1 are occupied by only 1.8 electrons, indicating a potential biradical character. A similar picture is shown by the NBO analysis of **5**. When evaluating the NLMO's of **3** and **5** (Tables S11 and S12, ESI†), it is immediately apparent that they are very similar and describe the Ti=E bond as π -type. The results from NBO-analysis were corroborated by quantum theory of atoms in molecules analysis (Fig. S20 and S21, ESI†) and electron localization function (ELF) analysis (Fig. S22 and S23, ESI†), the latter also showing a dative Ti-PMe₃ bond and a lone pair of electrons at the P1 (**3**) and As1 (**5**) atom, respectively. Inspection of the Wiberg Bond Indices of the Ti-Pn linkage gave values of 1.73 (**3**) and 1.72 (**5**), respectively. However, both the NBO analyses and the ¹³C-NMR high field shift of the Cp

substituents of **3** (104 ppm; *cf.* **1** $\delta = 118$ ppm) indicate an electron rich titanium center,^{39,40} which led us to inspect the stability of the wave function with respect to RHF/UHF or RKS/UKS instabilities, in order to analyse a potential biradical character of complex **3** and **5**.

While the Kohn-Sham wave function showed no instabilities, the Hartree-Fock solution exhibited a low-lying, "broken-symmetry" open-shell singlet state. Therefore, we used the *Complete Active Space* (CAS(2,2)) method^{41,42} to obtain a multi-determinant open-shell singlet wave function, which potentially describes the bonding situation in **3** and **5** more precisely. This calculation determined the biradical character of **3** and **5** ($\beta(\mathbf{3}) = 37\%$; $\beta(\mathbf{5}) = 40\%$) to be considerable.⁴³ This is in line with the rather long Ti-P and Ti-As bonds, respectively. The contributions to the multi-determinant wave function are characterized by two determinants placing two electrons either in the formal HOMO (ϕ_1) or LUMO (ϕ_2) (Fig. 2). The singlet state is calculated to be the ground state ($\Delta E_{\text{S-T}}(\mathbf{3}) = -106.2$ KJ mol⁻¹; $\Delta E_{\text{S-T}}(\mathbf{5}) = -96.6$ KJ mol⁻¹); *i.e.*, the radical centres, Ti(III) and the pnictogen-centred radical, are strongly antiferromagnetically coupled (Fig. 2, active orbitals and bonding in **3**, for **5** see Fig. S25, ESI†). In line with this both complexes **3** and **5** show no indication for paramagnetically shifted NMR spectra. To proof the general description of group 4 pnictinidenes as biradicaloids we further performed the same calculations for the literature known complexes (**II-V**). These complexes also showed a non-neglectable biradical character, besides a small degree of formal tetradical character in species **II** and **V**, which is due to the presence of two Ti-E π -bonds in them (Table S14, ESI†). Therefore, the Lewis-representation of group 4 pnictinidenes should be best written as a resonance between a classical M=E double bond and antiferromagnetically coupled electrons on Ti and E (Scheme 2 and Fig. 2).

In summary, the syntheses of the titanocene phosphinidene and arsinidene complexes **3** and **5** are outlined, the latter being an elusive example with a titanium arsenic double bond. The bonding in titanium pnictinidene complexes was shown to be best described as singlet biradicaloids. These compounds became available by employing [Cp₂Ti(btmsa)] and phosphora- or arsa-Wittig reagents, respectively. Based on this study, we

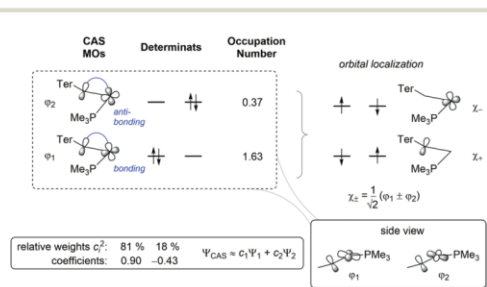


Fig. 2 Schematic depiction of the active orbitals of Cp₂Ti(PMe₃)PMe₃Ter (**3**) (CAS(2,2)/def2svp).

Communication

expect an ambivalent reactivity of complexes **3** and **5**, which is now under further examinations in our laboratory.

C. H.-J. thanks Prof. M. Beller for his support, and support by an Exploration Grant of the Boehringer Ingelheim Foundation (BIS) is acknowledged. We thank our technical and analytical staff, especially Dr A. Spannenberg for her support regarding X-ray analysis. F. R. thanks Dr Jonas Bresien for fruitful discussions about the computational results, the ITMZ at the University of Rostock for access to the Cluster Computer and especially M. Willert for technical support.

Conflicts of interest

There are no conflicts to declare.

Notes and references

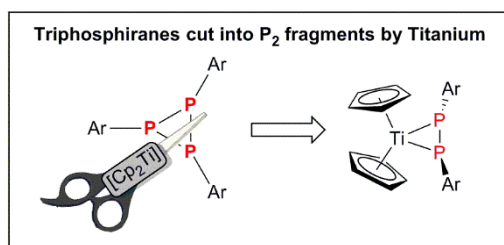
- F. E. Hahn and M. C. Jahnke, *Angew. Chem., Int. Ed.*, 2008, **47**, 3122–3172.
- M. Melaimi, M. Soleilhavoup and G. Bertrand, *Angew. Chem., Int. Ed.*, 2010, **49**, 8810–8849.
- D. Munz, *Organometallics*, 2018, **37**, 275–289.
- M. Melaimi, R. Jazzar, M. Soleilhavoup and G. Bertrand, *Angew. Chem., Int. Ed.*, 2017, **56**, 10046–10068.
- U. S. D. Paul and U. Radius, *Eur. J. Inorg. Chem.*, 2017, 3362–3375.
- L. Liu, D. A. Ruiz, D. Munz and G. Bertrand, *Chem*, 2016, **1**, 147–153.
- A. H. Cowley, *Acc. Chem. Res.*, 1997, **30**, 445–451.
- W. J. Transue, A. Velian, M. Nava, C. García-Iriepa, M. Temprado and C. C. Cummins, *J. Am. Chem. Soc.*, 2017, **139**, 10822–10831.
- R. Waterman, *Dalton Trans.*, 2009, 18–26.
- F. Mathey, *Dalton Trans.*, 2007, 1861–1868.
- K. Lammertsma and M. J. M. Vlaar, *Eur. J. Org. Chem.*, 2002, 1127–1138.
- F. Mathey, *Angew. Chem., Int. Ed. Engl.*, 1987, **26**, 275–286.
- H. Aktas, J. C. Slootweg and K. Lammertsma, *Angew. Chem., Int. Ed.*, 2010, **49**, 2102–2113.
- M. E. García, D. García-Vivó, A. Ramos and M. A. Ruiz, *Coord. Chem. Rev.*, 2017, **330**, 1–36.
- G. Zhao, F. Basuli, U. J. Kilgore, H. Fan, H. Aneetha, J. C. Huffman, G. Wu and D. J. Mindiola, *J. Am. Chem. Soc.*, 2006, **128**, 13575–13585.
- F. Basuli, J. Tomaszewski, J. C. Huffman and D. J. Mindiola, *J. Am. Chem. Soc.*, 2003, **125**, 10170–10171.
- B. C. Bailey, J. C. Huffman, D. J. Mindiola, W. Weng and O. V. Ozerov, *Organometallics*, 2005, **24**, 1390–1393.
- J. D. Masuda, A. J. Hoskin, T. W. Graham, C. Beddie, M. C. Fermin, N. Etkin and D. W. Stephan, *Chem. – Eur. J.*, 2006, **12**, 8696–8707.
- J. D. Protasiewicz, *Eur. J. Inorg. Chem.*, 2012, 4539–4549.
- U. J. Kilgore, H. Fan, M. Pink, E. Urnezus, J. D. Protasiewicz and D. J. Mindiola, *Chem. Commun.*, 2009, 4521–4523.
- U. Rosenthal, *Organometallics*, 2020, **39**, 4403–4414.
- A. Schumann, F. Reiß, H. Jiao, J. Rabeah, J.-E. Siewert, I. Kruppenacher, H. Braunschweig and C. Hering-Junghans, *Chem. Sci.*, 2019, **10**, 7859–7867.
- U. Rosenthal, V. V. Burlakov, P. Arndt, W. Baumann and A. Spannenberg, *Organometallics*, 2003, **22**, 884–900.
- M. Fischer, L. Vincent-Heldt, M. Hillje, M. Schmidtman and R. Beckhaus, *Dalton Trans.*, 2020, **49**, 2068–2072.
- P. Gupta, J.-E. Siewert, T. Wellnitz, M. Fischer, W. Baumann, T. Beveries and C. Hering-Junghans, *Dalton Trans.*, 2021, **50**, 1838–1844.
- Experimental, computational, and details on the X-ray diffraction studies are included in the ESL† CCDC 2060154–2060157 contain the supplementary crystallographic data for this paper.
- Y. Mataka, S. Takahiro and I. Naoki, *Chem. Lett.*, 1988, 1735–1738.
- D. Wang, W. Ding, G. Hou, G. Zi and M. D. Walter, *Chem. – Eur. J.*, 2020, **26**, 16888–16899.
- L. Yang, D. R. Powell and R. P. Houser, *Dalton Trans.*, 2007, 955–964.
- Z. Hou, T. L. Breen and D. W. Stephan, *Organometallics*, 1993, **12**, 3158–3167.
- M. Fischer, M. C. Wolff, E. del Horno, M. Schmidtman and R. Beckhaus, *Organometallics*, 2020, **39**, 3232–3239.
- P. Pyykkö and M. Atsumi, *Chem. – Eur. J.*, 2009, **15**, 12770–12779.
- R. C. Smith, P. Gantzel, A. L. Rheingold and J. D. Protasiewicz, *Organometallics*, 2004, **23**, 5124–5126.
- M. Fischer, S. Nees, T. Kupfer, J. T. Goettel, H. Braunschweig and C. Hering-Junghans, *J. Am. Chem. Soc.*, 2021, **143**, 4106–4111.
- J. B. Bonanno, P. T. Wolczanski and E. B. Lobkovsky, *J. Am. Chem. Soc.*, 1994, **116**, 11159–11160.
- N. C. Mösch-Zanetti, R. R. Schrock, W. M. Davis, K. Wanninger, S. W. Seidel and M. B. O'Donoghue, *J. Am. Chem. Soc.*, 1997, **119**, 11037–11048.
- M. K. Sharma, B. Neumann, H.-G. Stammer, D. M. Andrada and R. S. Ghadwal, *Chem. Commun.*, 2019, 55, 14669–14672.
- B. M. Gardner, G. Balázs, M. Scheer, F. Tuna, E. J. L. McInnes, J. McMaster, W. Lewis, A. J. Blake and S. T. Liddle, *Nat. Chem.*, 2015, **7**, 582–590.
- F. Reiss, M. Reiss, J. Bresien, A. Spannenberg, H. Jiao, W. Baumann, P. Arndt and T. Beveries, *Chem. Sci.*, 2019, **10**, 5319–5325.
- E. P. Beaumier, C. P. Gordon, R. P. Harkins, M. E. McGreal, X. Wen, C. Copéret, J. D. Goodpaster and I. A. Tonks, *J. Am. Chem. Soc.*, 2020, **142**, 8006–8018.
- M. Klene, M. A. Robb, M. J. Frisch and P. Celani, *J. Chem. Phys.*, 2000, **113**, 5653–5665.
- N. Yamamoto, T. Vreven, M. A. Robb, M. J. Frisch and H. Bernhard Schlegel, *Chem. Phys. Lett.*, 1996, **250**, 373–378.
- E. Miliordos, K. Ruedenberg and S. S. Xantheas, *Angew. Chem., Int. Ed.*, 2013, **52**, 5736–5739.

5.5 A selective route to aryl-triphosphiranes and their titanocene-induced fragmentation.

A. Schumann, F. Reiß, H. Jiao, J. Rabeah, J.-E. Siewert, I. Krummenacher, H. Braunschweig, C. Hering-Junghans

Chem. Sci. **2019**, *10*, 7859–7867.

DOI: 10.1039/C9SC02322D



Reprinted (adapted) with permission from *Chem. Sci.*.

Copyright 2019 Royal Society of Chemistry



Cite this: *Chem. Sci.*, 2019, 10, 7859

All publication charges for this article have been paid for by the Royal Society of Chemistry

Received 12th May 2019
Accepted 26th July 2019

DOI: 10.1039/c9sc02322d

rsc.li/chemical-science

A selective route to aryl-triphosphiranes and their titanocene-induced fragmentation†

André Schumann,^a Fabian Reiß,^a Haijun Jiao,^a Jabor Rabeah,^a Jan-Erik Siewert,^a Ivo Krummenacher,^{b,c} Holger Braunschweig^{b,c} and Christian Hering-Junghans^{b,*a}

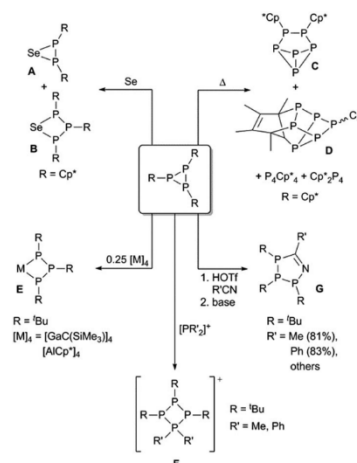
Triphosphiranes are three-membered phosphorus cycles and their fundamental reactivity has been studied in recent decades. We recently developed a high-yielding, selective synthesis for various aryl-substituted triphosphiranes. Variation of the reaction conditions in combination with theoretical studies helped to rationalize the formation of these homoleptic phosphorus ring systems and highly reactive intermediates could be isolated. In addition we showed that a titanocene synthon $[\text{Cp}_2\text{Ti}(\text{btmsa})]$ facilitates the selective conversion of these triphosphiranes into titanocene diphosphene complexes. This unexpected reactivity mode was further studied theoretically and experimental evidence is presented for the proposed reaction mechanism.

Introduction

Triphosphiranes are three-membered cyclo-phosphines, which are promising synthons in inorganic chemistry (Scheme 1). As early as 1877 the first cyclic oligophosphine was synthesized by Köhler and Michaelis in an attempt to prepare a phosphorus analogue of azobenzene with a PP double bond.¹ Almost 100 years later in 1964 the molecular structure of the product could be identified as P_3Ph_3 by X-ray crystal structure analysis.² Although, Cowley *et al.* already mentioned the synthesis of $\text{P}_3(\text{C}_2\text{F}_5)_3$ in 1970,³ it was later discussed that in fact the tetramer and pentamer were formed under the reaction conditions described.⁴ The first stable triphosphirane P_3^tBu_3 was reported by Baudler and co-workers in 1976,^{5,6} and various synthetic approaches towards triphosphiranes have since emerged.⁷ Reductive approaches starting from dihalophosphines RPX_2 ($\text{X} = \text{Cl}, \text{Br}$) result in a mixture of oligophosphines of different ring sizes of P_nR_n ($n = 3, 4, 5, 6$) and are thus regarded as unspecific.⁸ The ratio of the different oligomers heavily depends on the steric demand of the substituent R .⁹ Cyclo-condensation reactions, which also allow the preparation of unsymmetrically substituted triphosphiranes, and

cyclization by reductive dehalogenation of dihalotriphosphines have emerged as more selective synthetic pathways.¹⁰ Nevertheless, the presence of other cyclic oligophosphines as side products is often observed.

Jutzi and co-workers have shown that selenium inserts into one P–P bond of P_3Cp^*_3 ($\text{Cp}^* = \text{pentamethylcyclopentadienyl}$), affording a mixture of cyclic selenotriphosphabutanes (Scheme 1, **A**) and cyclic selenodiphosphopropanes (Scheme 1, **B**).¹¹ In contrast, thermolysis of P_3Cp^*_3 in xylene resulted in the



Scheme 1 Selected reactivity modes of differently substituted triphosphiranes.

^aLeibniz-Institut für Katalyse e.V. an der Universität Rostock, Albert-Einstein-Str. 29a, 18059 Rostock, Germany. E-mail: christian.hering-junghans@catalysis.de

^bInstitut für Anorganische Chemie, Julius-Maximilians-Universität Würzburg, Am Hubland, 97074 Würzburg, Germany

^cInstitute for Sustainable Chemistry & Catalysis with Boron, Julius-Maximilians-Universität Würzburg, Am Hubland, 97074 Würzburg, Germany

† Electronic supplementary information (ESI) available: Synthesis and characterization of compounds, NMR spectra, crystallographic, EPR and computational details. CCDC 1915056–1915060. For ESI and crystallographic data in CIF or other electronic format see DOI: 10.1039/c9sc02322d



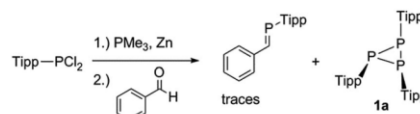
formation of different phosphorus clusters, some of which are structurally related to Hittorf's-phosphorus (Scheme 1, C and D).¹² Ring expansion reactions were reported by Uhl and Benter by the insertion of Ga(i) into a P–P bond of $P_3^tBu_3$, thus establishing a way to prepare cyclo-galliumtriphosphabutanes (Scheme 1, E, M = Ga).¹³ A similar reactivity is observed when Al(i) compound $(AlCp^*)_4$ reacts with $P_3^tBu_3$ (Scheme 1, E, M = Al).¹⁴ In addition, the reaction of $P_3^tBu_3$ with PMe_2Cl or PPh_2Cl in the presence of Me_3SiOTf or $GaCl_3$, respectively, resulted in the selective ring expansion with insertion of $[PMe_2]^+$ into the P–P bond between the two identical P atoms of $P_3^tBu_3$ to afford $[R_2P(P_3^tBu_3)]^+$ (Scheme 1, F; R = Me, Ph).^{15,16} More recently, Manners and co-workers showed the addition of $P_3^tBu_3$ to organic nitriles after activation of the three-membered ring by electrophiles to yield differently substituted 1-aza-2,3,4-triphospholenes in a click-type reaction (Scheme 1, G).^{17,18} Underlining the value of triphosphiranes as synthons in synthetic inorganic chemistry. Fragmentation of $P_3^tBu_3$ was observed by Fenske and Ahlrichs in the reaction with $Ni(CO)_4$, resulting in the formation of $[Ni_5(P^tBu)_3(P_3^tBu_3)(CO)_5]$ with μ_4 - and μ_3 -bridging P^tBu ligands as well as a $P_3^tBu_3$ chain, acting as a $\mu_4(\eta^3, \eta^1, \eta^1, \eta^3)$ ligand to three Ni atoms of the cluster.¹⁹

To the best of our knowledge, only four aryl-substituted triphosphiranes are reported in the literature. P_3Ph_3 was described as early as 1973 as a labile solid with respect to P_2Ph_5 ,²⁰ and it has been shown that this compound is part of an equilibrium mixture consisting of different oligomers with ring sizes of $n = 3, 4, 5, 6$.²¹ Tokitoh *et al.* synthesized (Anth = 9-anthryl, Bbt = 2,6-bis[bis(trimethylsilyl)methyl]-4-[tris(trimethylsilyl)phenyl]) in good yield by heating a mixture of $AnthP=PBbt$ and $^tBu_3P=Te$.²² P_3Tipp_3 (Tipp = 2,4,6- $iPr_3C_6H_2$) and P_3Mes_3 (Mes = 2,4,6-Me $_3C_6H_2$) were described as one of a mixture of products when free phosphinidenes were generated by reductive dechlorination of RP_3Cl_2 (R = Tipp, Mes).^{23–25} Moreover, Gaspar and co-workers reported on the photochemical release of the triplet phosphinidene $MesP(C_2H_4)$ in 1992.²⁶ In the absence of a trapping reagent these triplet phosphinidenes oligomerize to give a mixture containing P_3Mes_3 and P_4Mes_4 .

Using $[W(PMe_3)_6]$ as a reducing agent the quantitative coupling of RP_3Cl_2 (R = Mes* = 2,4,6- $iPr_3C_6H_2$; 2,4,6-(CF $_3$) $_3C_6H_2$) to the respective diphosphenes $RP=PR$ was detected. Starting from $TippP_3Cl_2$, the initial formation of the diphosphene is detected by ^{31}P NMR spectroscopy, however, the reaction continues to produce $Tipp_3P_3$ as the final product, clearly pointing to the intermediacy of $W=PR$ species.²⁷ Moreover, it was shown that the reductive degradation of P_4 with mesityl-radicals (generated from Mes-Br and Ti(iii)-based chlorine atom abstracting reagent $[Ti\{N(^tBu)(3,5-C_6H_3Me_2)_3\}_3]$) yields P_3Mes_3 as the main product in good isolated yields.²⁸

In 1998 Shah and Protasiewicz reported the formation of the triphosphirane P_3Tipp_3 (**1a**) by treatment of $TippP_3Cl_2$ with PMe_3 and Zn and subsequent reaction with benzaldehyde (Scheme 2).²⁹ This so-called phospho-Wittig reaction afforded a mixture of P_3Tipp_3 and traces of the desired phosphoalkene $Ph(H)C=P^tTipp$.

In this contribution, we report on the synthesis of aryl substituted triphosphiranes using a modified synthesis on the



Scheme 2 Formation of $Tipp_3P_3$ (**1a**) and trace amounts of phosphoalkene $H(Ph)C=P^tTipp$ in a so-called phospho-Wittig protocol.

basis of the studies by Protasiewicz *et al.* Furthermore, we report on the selective degradation of these P_3Ar_3 systems using $[Cp_2Ti(btmsa)]$ (Cp = cyclopentadienyl, btmsa = $C_2(SiMe_3)_2$) as a Ti(ii) synthon.

Results

In an attempt to prepare new variants of pyridinephosphoalkenes,³⁰ we utilized the phospho-Wittig protocol described by Protasiewicz *et al.* with $DippP_3Cl_2$ ($Dipp = 2,6\text{-}iPr_2C_6H_3$), PMe_3 and excess of Zn powder in a strict low-temperature regime ($-78^\circ C$); after subsequent treatment with pyridine-2-carbaldehyde at that temperature and warming to room temperature the formation of the respective phosphoalkene was not observed. The ^{31}P NMR spectrum of the reaction mixture displayed a major product with an A_2B spin system with a doublet at -99.47 ppm and a triplet at -132.90 ppm with a coupling constant of 178.5 Hz, which was identified as P_3Dipp_3 (**1b**), in line with attempted synthesis of the phospho-Wittig reagent $TippPPMe_3$ as discussed before.²⁹ X-ray quality crystals of **1b** were grown from a saturated *n*-hexane solution at $5^\circ C$ (Fig. 1). **1b** crystallises in the monoclinic space group $P2_1/c$ with four molecules in the unit cell. The molecular structure of **1b** shows the expected down-down-up orientation of the Dipp groups with respect to the central P_3 plane, with a minimally distorted central P_3 -ring [P1–P2 2.1991(4), P2–P3

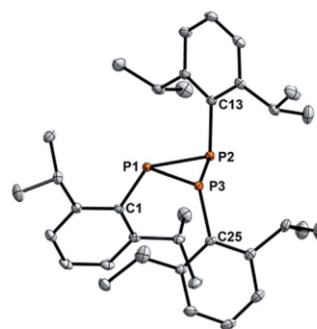


Fig. 1 POV-ray depiction of the molecular structure of **1b**. ORTEPs drawn at 30% probability, H atoms are omitted for clarity. Selected bond lengths (Å) and angles ($^\circ$): P1–P2 2.1991(4), P2–P3 2.2440(4), P1–P3 2.2124(3), P1–C1 1.8526(10), P2–C13 1.8594(10), P3–C25 1.8507(10); P1–P2–P3 59.718(11), P2–P1–P3 61.147(12), P1–P3–P2 59.135(11).



2.2440(4); P1–P3 2.2124(3) Å] (Fig. 1). These metric parameters are in line with those detected for **1a** and **1c** (Table S1†),³¹ of which the molecular structures have been reported previously.^{32,33}

We then utilized the sterically more demanding PEt₃ to better stabilize the reactive phosphanylidene phosphorane intermediate TippP=PEt₃. Phosphanylidene phosphoranes have been identified as a source of the triplet phosphenes Ar₃P.³⁴

Additionally, we switched to TippPBr₂, as its reduction should be more facile. TippPBr₂, PEt₃ (1.2 equiv.) and Zn (3 equiv.) were combined in THF at –78 °C and the formation of a deep yellow to orange suspension was observed, which again showed P₃Tipp₃ (**1a**) as the major species in the ³¹P NMR spectrum.

After removal of the solvent and extraction with *n*-hexane minimal amounts (<0.01 g) of yellow needles suitable for single crystal X-ray analysis were obtained and identified as the elusive diphosphene P₂Tipp₂ (**2**) (Fig. 2), which has only been observed in solution in the [W(PMe₃)₆] mediated coupling of ArPCl₂ (Ar = Tipp, Mes*, 2,4,6-(CF₃)₃C₆H₂) by ³¹P NMR experiments to date.³⁷ The ³¹P NMR spectrum of isolated **2** showed P₂Tipp₂ (δ(³¹P) = 517.4 ppm) to be the major species, whereas minor amounts of P₃Tipp₃ and P₄Tipp₄ were also detected. Monitoring a C₆D₆ solution of **2** over time at room temperature revealed that P₂Tipp₂ slowly converts into P₃Tipp₃ and its dimer P₄Tipp₄, *vide infra*.³¹ **2** crystallises as its *trans*-conformer in the triclinic space group *P1* with one molecule in the unit cell. The P1–P1' distance [2.0290(5) Å] (*cf.* d(P=P) P₂Mes*₂ 2.034(2);³⁵ P₂Ter₂ 2.029(1);³⁶ P₂Bbt₂ 2.043(1)³⁷) is in the expected range for a diphosphene (Σ*r*_{cov}(P=P) = 2.04 Å,³⁶ and rather acute C–P–P' [99.61(3)°] angles at the dicoordinate P center are detected.

Theoretical investigations at the M062X/TZVP level of density functional theory were carried out, assuming that transient phosphenes are formed. The gas-phase trimerization of Dipp–P with a triplet ground state (the corresponding singlet state is less stable by 26.01 kcal mol^{–1}) is exergonic (–91.39 kcal mol^{–1}). In addition, we computed the transfer reaction of a Dipp–P fragment (which may be formed intermediately at low temperatures) *via* DippPPMe₃ to P₂Dipp₂ and

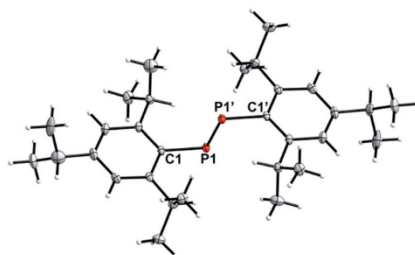


Fig. 2 POV-ray depiction of the molecular structure of **2**. ORTEPs drawn at 30% probability. Selected bond lengths (Å) and angles (°): P1–P1' 2.0290(5), P1–C1 1.8439(10); C1–P1–P1' 99.61(3); P1'–P1–C1–C6 91.34(8), C1–C2–C3–C4 1.25(16).

found this reaction to be exergonic by –15.74 kcal mol^{–1} (energy barriers were not calculated). This is in line with the isolation of **2**.

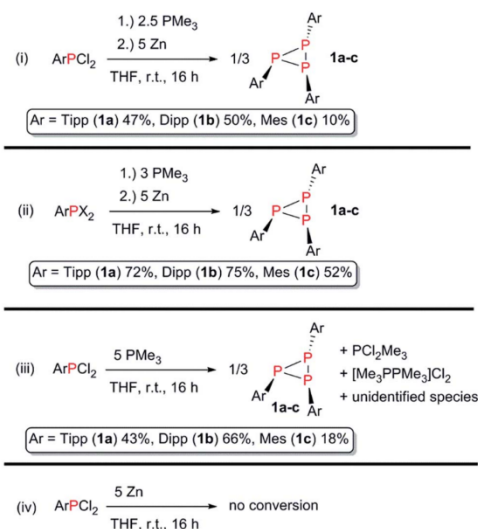
Since there are only few high-yielding, selective methods for the preparation of aryl-substituted triphosphiranes outlined in the literature, we decided to take a closer look at this synthetic approach. We therefore tested different aryl(dichloro)phosphines ArPCl₂ (Ar = Mes, Dipp, Tipp) to elucidate whether treatment with PR₃ (R = Me, Et) and Zn gives general access to aryl-substituted triphosphiranes (Scheme 3).

The reaction of ArPCl₂ with PMe₃ (2.5 equiv.) and an excess of Zn (5 equiv.) in anhydrous THF afforded P₃Ar₃ (Ar = Tipp (**1a**), Dipp (**1b**), Mes (**1c**)) as expected (Scheme 3, reaction (i)).

Purification by recrystallisation from a saturated *n*-hexane solution at 5 °C yielded **1a–c** as colourless crystalline solids in 47, 50 and 10% isolated yield, respectively.

Starting from the easily accessible mixed dihalophosphines ArPX₂ (Ar = Tipp, Dipp, Mes; X = Cl, Br; obtained through treatment of ArMgBr with PCl₃),³⁹ with PMe₃ and Zn in a 1/2/2.5 molar ratio in THF at room temperature (Scheme 3, reaction (ii)), **1a**, **1b** and **1c** could be obtained in up to 72%, 75% and 52% isolated yield, respectively, after extraction with benzene or Et₂O in case of **1c**. **1a–c** show good thermal stability with melting points of higher than 167 °C.³¹ Heating a solution of **1a** in C₆D₆ for 36 h at 80 °C showed no decomposition or rearrangement products in the ³¹P NMR spectrum.

Since either PMe₃ or Zn can act as reducing agents, we reduced TippPCl₂ with each reductant separately (Scheme 3(iii) and (iv)). While there is no reaction observed, when TippPCl₂ or TippPBr₂ are stirred with an excess of Zn in THF over a period of



Scheme 3 (i) and (ii) General procedure for the preparation of **1a–c**; (iii) identification of PMe₃ as the active reductant; (iv) Zn can be excluded as active reductant.



24 h, treatment of ArPCL_2 with a fivefold excess of PMe_3 afforded **1a-c** in 43, 66 and 18% isolated yield, respectively. The potential of PMe_3 to act as a chlorine abstracting reagent is documented in the literature and results in oxidation to the respective dichlorophosphorane,^{40,41} or the homoleptic dication salt $[\text{Me}_3\text{PPMe}_3]_2\text{Cl}_2$. This concept has been used to access *cyclo*-tetra(stibinophosphonium) triflate salts of the type $[\text{Sb}_4(\text{PR}_3)_4][\text{OTf}]_4$ ($\text{R} = \text{Me}, \text{Et}, \text{Pr}, \text{Bu}$), cationic antimony compounds related to the cyclic oligophosphines.⁴² To shed light on this proposition, we independently synthesized PMe_3Cl_2 and treated it with an excess of zinc dust in the presence of TippPCL_2 in a mixture of MeCN/THF (3 : 1) over 24 h. A ^{31}P NMR spectrum of the reaction mixture indeed showed **1a** to be the main product of this reaction.³¹ It can thus be concluded that PMe_3Cl_2 is a plausible by-product of the reduction with PMe_3 and zinc can reduce it back to PMe_3 , *vide infra*. This opens the pathway for potential catalytic reduction of ArPCL_2 with PMe_3 and Zn as a sacrificial reductant. In another experiment DippPCL_2 was reduced with an excess of PMe_3 and the white precipitate was carefully washed with benzene and *n*-hexane. Subsequently, the precipitate was treated with AgOTf in CH_2Cl_2 . After filtration a colourless solid was obtained, which was dissolved in CD_3CN , allowing to unambiguously identify $[\text{Me}_3\text{PCL}]\text{OTf}$ ($\delta^{31}\text{P}\{^1\text{H}\} = 93.6$ ppm),⁴³ and $[\text{Me}_3\text{P-PMe}_3][\text{OTf}]_2$ ($\delta^{31}\text{P}\{^1\text{H}\} = 28.4$ ppm)⁴⁴ among three unidentified PMe_3 containing species (Scheme 3(iii)).³¹

The synthetic approach using Zn/PMe_3 showed a high selectivity towards the respective triphosphiranes. In the case of **1a** and **1b** just little amounts of the corresponding cyclic tetraphosphines P_4Ar_4 were detected as side products by ^{31}P NMR spectroscopy of the reaction mixture. When MesPCL_2 is applied in our approach, the selectivity decreases and the formation of little amounts of the cyclic tetraphosphine P_4Mes_4 , and the cyclic pentaphosphine P_5Mes_5 species can be detected. We conclude that this is due to lesser steric bulk imposed by the mesityl substituent. The sterically more demanding substituents *Tipp* and *Dipp* promote the formation of the three-membered phosphorus ring more effectively.⁷

Having prepared **1a-c** we wanted to explore their reactivity with the titanocene synthon $[\text{Cp}_2\text{Ti}(\text{btmsa})]$ in order to access titanium phosphinidene complexes.

Titanocene-induced degradation of R_3P_3

Stephan and co-workers have shown the phospho-Wittig-type phosphinidene transfer for $[\text{Cp}_2\text{Zr}=\text{PMes}^*(\text{PMe}_3)]$ resulting in the formation of phosphalkenes in the reaction with aldehydes along with the formation of $[\text{Cp}_2\text{ZrO}]_n$.⁴⁵ Similar reactivity was observed by Cummins and Schrock for the terminal tantalum phosphinidene complexes, $[(\text{N}_3\text{N})\text{Ta}=\text{PR}]$ ($\text{N}_3\text{N} = (\text{Me}_3\text{Si-NCH}_2\text{CH}_2)_3\text{N}$).⁴⁶

With the series of triphosphiranes **1a-c** synthesized, we wanted to investigate the propensity to access monomeric, terminal $\text{Cp}_2\text{Ti}=\text{PR}$ complexes, by reaction of **1** with the titanocene synthon $[\text{Cp}_2\text{Ti}(\text{btmsa})]$. $\text{Cp}_2\text{Ti}=\text{PR}$ has not been described in the literature. There are reports of neutral and zwitterionic terminal titanium phosphinidene complexes of the

type $[(^{\Delta}\text{Nacnac})\text{Ti}=\text{PAr}'(\text{R})]$ ($\text{Ar}' = \text{Tipp}, \text{Mes}^*$; $\text{R} = \text{CH}_2^t\text{Bu}, \text{CH}_3, \text{CH}_3[\text{B}(\text{C}_6\text{F}_5)_3]$) by Mindiola and co-workers with a bulky β -diketiminato ligand ($^{\Delta}\text{Nacnac} = [\text{Ar}]\text{NC}(\text{Me})\text{CHC}(\text{Me})\text{N}[\text{Ar}]$, $\text{Ar} = \text{Dipp}$) on titanium.^{47,48} $[\text{Cp}_2\text{Ti}(\text{btmsa})]$ is obtained by reduction of Cp_2TiCl_2 in the presence of *btmsa*. In these complexes *btmsa* acts as a spectator ligand and its facile release under the respective reaction conditions generates the highly reactive 14-electron $[\text{Cp}_2\text{Ti}]$ fragment *in situ*.⁴⁹ Combination of three equivalents $[\text{Cp}_2\text{Ti}(\text{btmsa})]$ with **1b** in C_6D_6 at room temperature and monitoring by ^{31}P NMR spectroscopy revealed slow, but selective, conversion into a phosphorus-containing species with a singlet resonance at 283.8 ppm. Heating this reaction mixture to 80 °C over a period of 16 h in a sealed NMR tube resulted in consumption of $[\text{Cp}_2\text{Ti}(\text{btmsa})]$ according to ^1H NMR spectroscopy. However, unreacted P_3Ar_3 remained in the reaction mixture and thus, more $[\text{Cp}_2\text{Ti}(\text{btmsa})]$ was added to the reaction mixture and heating to 80 °C was continued. Fractional crystallisation from C_6D_6 and determination of the molecular structure by single crystal X-ray analysis revealed the formation of the η^2 -diphosphene complex $[\text{Cp}_2\text{Ti}(\text{P}_2\text{Dipp}_2)]$ (**3b**) (Fig. 3, right). Consequently, the reaction was repeated in the correct stoichiometry with $[\text{Cp}_2\text{Ti}(\text{btmsa})]$ and **1b** in a 3 : 2 molar ratio in benzene, which allowed for full conversion into **3b** after stirring at 80 °C over a period of 16 h. In analogy, **1a** and **1c** were converted into the respective titanocene diphosphene complexes $[\text{Cp}_2\text{Ti}(\text{P}_2\text{Tipp}_2)]$ (**3a**, Fig. 3, left) and $[\text{Cp}_2\text{Ti}(\text{P}_2\text{Mes}_2)]$ (**3c**) (Scheme 4). Filtration and subsequent concentration of the reaction mixtures and standing overnight at 5 °C resulted in the formation of deep yellow crystals of **3a** suitable for X-ray analysis, whereas formation of **3c** was authenticated by NMR spectroscopy, elemental analysis and HR-MS studies.³¹ Interestingly, in the ^1H NMR spectrum three or two independent septets are detected for **3a** and **3b**, respectively. This indicates hindered rotation about the P-C_{Ar} bond and the Me group of the isopropyl moiety in close proximity to the Cp_2Ti -fragment is significantly upfield-shifted, resonating at -0.99 ppm in **3a** and **3b**. This hindered rotation is also evident in **3c**, in which three ^1H NMR signals are detected for the Me groups of the Mes moiety.

3a crystallises in the monoclinic space group *C2/c* with four molecules in the unit cell as a benzene solvate. **3b** crystallises in

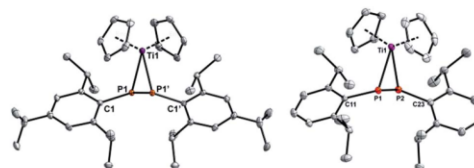
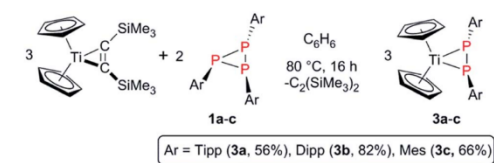


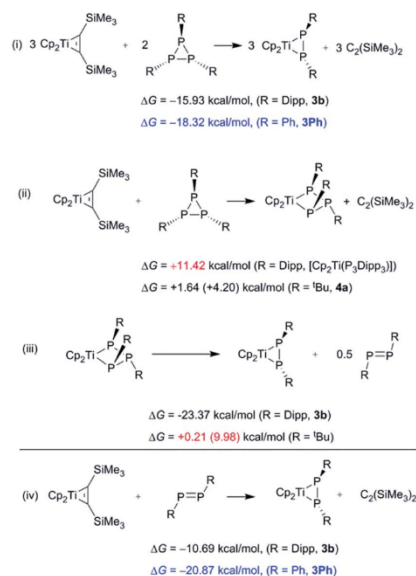
Fig. 3 POV-ray depiction of the molecular structure of **3a** and **3b**. ORTEPs drawn at 30% probability, all H-atoms are omitted for clarity. Selected bond lengths (Å) and angles (°) of **3a**: P1–P1' 2.1826(7), P1–C1 1.8548(13), P1–Ti1 2.5329(5); C1–P1–P1' 108.39(5), P1–Ti1–P1' 51.042(17). **3b**: P1–P2 2.1699(5), P1–Ti1 2.5425(5), P2–Ti1 2.5230(5), P1–C11 1.8548(13), P2–C23 1.8495(13); C11–P1–P2 108.88(4), C23–P2–P1 112.53(4), P1–Ti1–P2 50.725(12).



Scheme 4 Selective degradation of P_3Ar_3 (**1a-c**) into $[Cp_2Ti(P_2Ar_2)]$ (**3a-c**) complexes using $[Cp_2Ti(btmsa)]$ as a synthon for $[Cp_2Ti]$.

the monoclinic space group $P2_1/c$ with four molecules of **3b** and four C_6D_6 molecules in the unit cell. **3a** is located on a special position and thus shows C_2 symmetry in the solid state. The P–P distances in **3a** [2.1826(7) Å] and **3b** [2.1699(5) Å] are intermediate between a P–P single and double bond ($\sum r_{cov}(P=P) = 2.04$ Å; (P–P) 2.22 Å)³⁸ and are in line with the P–P distance [2.173(4) Å] in $[rac-(EBTHI)Ti(P_2Ph_2)]$ (ETBHI = ethylene-1,2-bis(5-4,5,6,7-tetrahydro-1-indenyl)), the only titanium diphosphene complex known to date.³⁹ It is worth noting that green $[rac-(EBTHI)Ti(P_2Ph_2)]$ is insoluble in common non-halogenated organic solvents and thus, NMR data was not obtained. It is formed through the dehydrocoupling of $PhPH_2$ in the presence of the Ti(m)-hydride dimer $[rac-(EBTHI)-TiH]_2$.²¹ η^2 -Diphosphene complexes of various transition metals have been known and were thoroughly reviewed by Weber.²² Noteworthy, is the formation of $[(Ph_3P)_2M(P_2C_6F_5)_2]$ with an *E*-configured diphosphene ligand in the presence of $M(PPh_3)_4$ ($M = Pt$,²³ Pd ²⁴). Other known diphosphene complexes of group 4 include the anionic species $[Cp_2Zr(PPh)_2Br]^-$ with a P–P distance [2.145(3) Å] shorter than in **3a** and **3b**,²⁵ and the related Mes-substituted complex $[Cp_2Zr(P_2Mes)_2]$ with a similar P–P distance [2.188(3) Å].²⁶ The Ti–P distances in **3a** [2.5425(5), 2.5230(5) Å] and **3b** [2.5329(5) Å], as well as the P–Ti–P angles (**3a** 50.725(12)°; **3b** 51.042(17)°), are similar to that in $[Cp_2Zr(PPh)_2Br]^-$ [d(Ti–P) 2.525(2) Å; <(P–Ti–P) 51.00(6)°] and point to a Ti(IV) center and an overall titana-cyclo-propane, rather than a titana-cyclo-propene type structure.

The surprising selective formation of the titanocene diphosphene species **3**, prompted us to study the reactivity by DFT calculations on the M062X/TZVP level of theory. The calculated gas phase structure of **1b** and **3b** and the metric parameters derived from X-ray crystallography are in good agreement. In a next step the reaction of $[Cp_2Ti(btmsa)]$ with **1b** in a 3 : 2 ratio was investigated. It is found that the gas phase reaction is exergonic by -15.93 kcal mol⁻¹, indicating that the reaction is accessible thermodynamically, even though energy barriers for this transformation could not be determined (Scheme 5(i)). Using the truncated model compound P_3Ph_3 (**1Ph**) the same exergonic character was calculated ($\Delta G = -18.32$ kcal mol⁻¹) for this transformation. Additionally, we were interested to determine whether the free *trans*-diphosphenes P_2Dipp_2 and P_2Ph_2 can displace the btmsa molecule in $[Cp_2Ti(btmsa)]$ to afford complexes **3b** and $[Cp_2Ti(P_2Ph_2)]$ (**3Ph**), respectively (Scheme 7, bottom). Interestingly, this reaction is



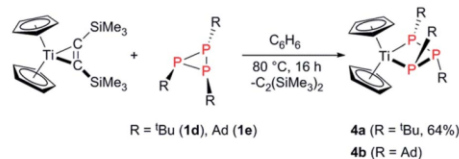
Scheme 5 M062X/TZVP (i and iv) and BP86/TZVP (ii and iii) (M062X) for $R = {}^tBu$ computed reaction free energies for possible paths of formation of $[Cp_2Ti(P_2R_2)]$ in the gas phase.

also exergonic for P_2Dipp_2 and P_2Ph_2 by -10.69 and -20.87 kcal mol⁻¹, respectively, illustrating that diphosphenes are potential intermediates along the reaction pathway (Scheme 5(iv)).

With minimal amounts of the free diphosphene $Tipp_2P_2$ (**2**) in hand, we treated **2** with $[Cp_2Ti(btmsa)]$ in a 1 : 1 ratio at room temperature in C_6D_6 . Having shown that the reaction of **1a** with $[Cp_2Ti(btmsa)]$ is slow at room temperature and full conversion is only achieved at 80 °C, we were delighted to see the disappearance of the diagnostic diphosphene signal at 517.4 ppm and formation of **3a** with a characteristic ³¹P NMR shift of 290.7 ppm. This clearly shows, that diphosphenes are potential intermediates in the reaction of **1** with $[Cp_2Ti(btmsa)]$. Furthermore, this shows the drastic influences of the sterically demanding groups attached to phosphorus, as the diphosphene $P_2Mes^*_2$ was shown to not afford the respective diphosphene complex in the reaction with $[Cp_2Ti(btmsa)]$.²⁷

To compare the reactivity of the aryl-substituted triphosphiranes with alkyl-substituted derivatives we treated $[Cp_2Ti(btmsa)]$ with the known triphosphiranes $P_3{}^tBu_3$ (**1d**) and P_3Ad_3 (Ad = adamantyl),^{28,29} in a 1 : 1 ratio in benzene at 80 °C in C_6D_6 (Scheme 6). Interestingly, in the case of **1d** full consumption of both starting materials was noted, with a new characteristic A_2B spin system in the ³¹P NMR spectrum. **1e** also cleanly reacted in similar fashion, however full consumption was not achieved due to the poor solubility of **1e**. Compared to **1d** and **1e** the A_2 -part of the ³¹P NMR signal is downfield-shifted, thus indicating selective insertion into the P–P bond with the





Scheme 6 Formation of the cyclo-titanatrichosphabutanes $[\text{Cp}_2\text{-Ti}(\text{P}_3\text{R}_3)]$ (R = ^tBu (4a), Ad (4b)) starting from $[\text{Cp}_2\text{Ti}(\text{btmsa})]$ and triphosphiranes 1d and 1e.

two identical P atoms and the formation of the triphosphanato-complexes $[\text{Cp}_2\text{Ti}(\text{P}_3^t\text{Bu}_3)]$ (4a) and $[\text{Cp}_2\text{Ti}(\text{P}_3\text{Ad}_3)]$ (4b).³¹ Complex 4a among other $[\text{Cp}_2\text{Ti}(\text{P}_3\text{R}_3)]$ species has been described before by Köpf and co-workers in the reaction of Cp_2TiCl_2 with the salt $\text{K}_2[\text{P}_3^t\text{Bu}_4]$ in a salt elimination reaction on the basis of NMR experiments.⁶⁰ Extraction of the reaction mixture with Et_2O , concentration to incipient crystallisation and standing at 5 °C overnight, afforded deeply coloured brown crystals of 4a suitable for X-ray analysis (Fig. 4) in 64% yield. To the best of our knowledge this is the first structural characterization of a cyclo-titanatrichosphine.

4a crystallises in the orthorhombic space group $P2_12_12_1$ with four molecules in the unit cell. The P–P distances [P1–P2 2.1953(8), P2–P3 2.1840(8)] are shorter than a P–P single bond ($\sum r_{\text{cov}}(\text{P–P}) = 2.22 \text{ \AA}$)³⁸ and the P–Ti–P angle [90.34(2)°] is wider than in 3a and 3b and compares nicely with the P–Zr–P angle [89.8(2)°] found in the related compound $[\text{Cp}_2\text{Zr}(\text{P}_3\text{Ph}_3)]$.⁵⁵

To rationalize the contrasting reactivity of alkyl- and aryl-substituted triphosphiranes noted in this study, we calculated the free enthalpies for the gas phase reaction of $[\text{Cp}_2\text{Ti}(\text{btmsa})]$ with Dipp_3P_3 to afford the insertion product $[\text{Cp}_2\text{Ti}(\text{P}_3\text{Dipp}_3)]$ under liberation of btmsa at the BP86//TZVP/LANL2DZ level of theory.³¹ This transformation was found to be endergonic by 11.41 kcal mol⁻¹, whereas this insertion process was computed to be almost thermo-neutral for P_3^tBu_3 (+1.64 (+4.20 M062X) kcal mol⁻¹) to give 4a (Scheme 5(ii)). The selective

degradation of $[\text{Cp}_2\text{Ti}(\text{P}_3\text{Dipp}_3)]$ to yield 3b and half an equivalent of P_2Dipp_2 was also considered and is shown to be exergonic by $-23.27 \text{ kcal mol}^{-1}$, whereas the same process is endergonic by +0.21 (+9.97 M062X) kcal mol⁻¹ for 4a (Scheme 5(iii)). These results are in line with the observed difference in reactivity of alkyl- and aryl-substituted triphosphiranes and that the reactions only take place at elevated temperatures. We then wanted to determine whether single electron transfer (SET) is preferred over reduction of the cyclo- P_3R_3 in two electron steps by comparison of the free energies of the reduction products. It is noted from successive theoretical one-electron addition to triphosphiranes P_3R_3 that the single-electron transfer step is exergonic and favoured thermodynamically, while the two-electron transfer process is endergonic and thermodynamically not favored.³¹

On the basis of these results, one can expect a stepwise reaction mechanism for the electron transfer reactions. Furthermore one of the P–P bonds in the radical anion species $[\text{P}_3\text{R}_3]^-$ is considerably elongated [2.814 (R = Dipp), 2.973 Å (R = Ph)], which would allow for the liberation of a phosphinidene fragment or the recombination of two radical anions, under formal exchange of P–R groups. If arylphosphinidenes were formed in this transformation these would be triplet species, with the triplet state being thermodynamically favored by -26.01 (R = Dipp) and $-33.71 \text{ kcal mol}^{-1}$ (R = Ph), respectively. With these insights we set out to generate experimental evidence for these assumptions.

On the basis of these results, one can expect a stepwise reaction mechanism for the electron transfer reactions and the possible intermediary formation of a titanocene phosphinidene species. Electrochemical studies revealed an electrochemically irreversible reduction of 1b in THF at a potential of -3.09 V (vs. F_c/F_c^+), which is in line with degradation of the aryl-substituted triphosphiranes into diphosphene fragments upon treatment with $[\text{Cp}_2\text{Ti}(\text{btmsa})]$. Investigation of the reaction mixture of $[\text{Cp}_2\text{Ti}(\text{btmsa})]$ and 1a (3 : 2 ratio, after heating to 80 °C for 1 h) at room temperature by electron paramagnetic resonance (EPR) spectroscopy revealed the occurrence of an EPR-active intermediate (Fig. 5) with an isotropic g -factor of 1.978. This doublet signal shows strong coupling to one ^{31}P nucleus with $a(^{31}\text{P}) = 72 \text{ MHz}$ and hyperfine coupling to titanium $a(^{49/47}\text{Ti}) = 22 \text{ MHz}$. The rather large g -value and small hyperfine coupling to Ti indicates a species with a high spin density on phosphorus, in which only one phosphorus is attached to titanium, as a more complex EPR-signal would be expected otherwise.⁶¹ In addition, there is an underlying signal stemming from $[\text{Cp}_2\text{Ti}(\text{btmsa})]$, which could be fitted to a species with $g_{\text{iso}} = 1.973$ and $a(^1\text{H}) = 32 \text{ MHz}$.⁶² This could indicate a hydridic species such as $[\text{Cp}_2\text{-Ti}(\text{III})\text{-H}]$, which has been discussed as resting state of $[\text{Cp}_2\text{Ti}]$ in solution. In this case hydrogen release would generate the free titanocene and subsequent addition of H_2 regenerates the $[\text{Cp}_2\text{TiH}]$ species.⁶³

We then wanted to generate more evidence for the end group liberation and formation of free phosphinidenes during the reaction. If this is the case, starting from a 1 : 1 mixture of differently substituted triphosphiranes P_3Ar_3 and $\text{P}_3\text{Ar}'_3$ should result in the formation of the mixed diphosphene complex

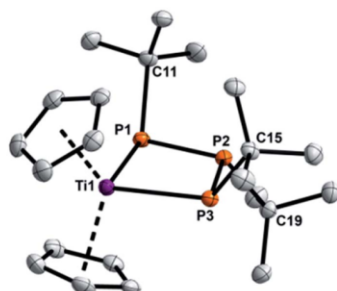


Fig. 4 POV-ray depiction of the molecular structure of 4a. ORTEPs drawn at 30% probability, H atoms are omitted for clarity. Selected bond lengths (Å) and angles (°): P1–P2 2.1953(8), P2–P3 2.1840(8), Ti1–P1 2.5354(6), Ti1–P2 3.0348(7), Ti1–P3 2.5480(7); P1–Ti1–P3 90.34(2).



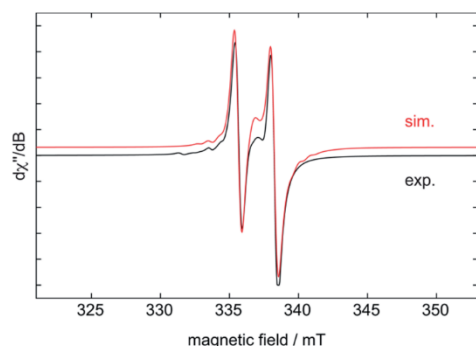


Fig. 5 Experimental (black) and simulated (red) X-band EPR spectra of the intermediate formed in the reaction of $[\text{Cp}_2\text{Ti}(\text{btmsa})]$ with Tipp_3P_3 to yield **3a** in benzene solution at room temperature. The simulation includes an impurity ($g_{\text{iso}} = 1.973$, $a(^1\text{H}) = 32$ MHz) which is present in the titanium precursor $[\text{Cp}_2\text{Ti}(\text{btmsa})]$. Simulation parameters: $g_{\text{iso}} = 1.978$, $a(^{31}\text{P}) = 72$ MHz, and $a(^{47,49}\text{Ti}) = 22$ MHz.

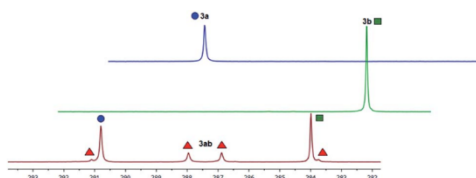
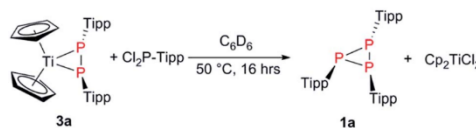


Fig. 6 Formation of the mixed diphosphene complex **3ab** in a scrambling experiment utilizing a 1 : 1 mixture of **3a** and **3b** in the presence of 1.5 equiv. $[\text{Cp}_2\text{Ti}(\text{btmsa})]$.

$[\text{Cp}_2\text{TiP}_2\text{ArAr}']$ (from recombination of differently substituted phosphinidenes) along with $[\text{Cp}_2\text{TiP}_2\text{Ar}_2]$ and $[\text{Cp}_2\text{TiP}_2\text{Ar}'_2]$. Therefore, a 1 : 1 mixture of **1a** and **1b** (1 equiv.) was mixed with 1.5 equiv. of $[\text{Cp}_2\text{Ti}(\text{btmsa})]$ in C_6D_6 in an NMR scale reaction.

The ^{31}P NMR spectrum of the resulting product solution is shown in Fig. 6. For comparison the spectra of the pure compounds **3a** and **3b** are depicted as well. In the spectrum of the product mixture the singlet signals of the symmetric compounds **3a** and **3b** can be seen clearly at 283.8 and 290.7 ppm, respectively. Additionally, there are two doublets, indicating the formation of the mixed diphosphene complex $[\text{Cp}_2\text{Ti}(\text{P}_2\text{DippTipp})]$ (**3ab**). We conclude from this experiment that an exchange of P–R end groups or the intermediacy of phosphinidenes P–R are likely in the course of the reaction.



Scheme 7 Transmetalation of **3a** with Tipp-PCl_2 , resulting in the formation of **1a**.

Moreover, titana- and zirconacycles are regularly applied in the formation of main group element substituted heterocycles.^{64,65} We wanted to probe this reactivity by treating isolated **3a** with TippPCl_2 and found **1a** as the product along with the formation of Cp_2TiCl_2 (Scheme 7),³¹ which clearly shows the potential of complexes **3** for the formation of small inorganic ring systems.

Conclusions

We have shown in here a simple and selective synthetic protocol for the formation of aryl-substituted triphosphiranes **1** of the type P_3Ar_3 and identified PMe_3 as the active reductant. These findings open the way for future studies to render these transformations catalytic with respect to PMe_3 . Moreover, we have shown that the $\text{Ti}(\text{II})$ synthon $[\text{Cp}_2\text{Ti}(\text{btmsa})]$ reacts with **1** to yield the respective titanocene diphosphene complexes **3** in straightforward fashion. Combined theoretical and experimental studies suggest the intermediate formation of a paramagnetic titanium phosphorus species, indicating single electron transfer steps. Moreover, experimental evidence is presented for the intermediacy of free diphosphenes, authenticated by reaction of the elusive diphosphene P_2Tipp_2 (**2**) with $[\text{Cp}_2\text{Ti}(\text{btmsa})]$. In first reactivity studies we have shown that **3** can be utilized as a P_2R_2 -transfer reagent in transmetalation protocols using TippPCl_2 . This opens the pathway to generate new P_2R_2 -containing heterocycles.

Studies to further elucidate the reaction mechanism of the P_3Ar_3 degradation reaction are ongoing, to further investigate the nature of the paramagnetic intermediate. Additionally, application of the P_3Ar_3 systems in phosphinidene transfer reactions will be investigated.

Conflicts of interest

There are no conflicts to declare.

Acknowledgements

C. H.-J. thanks Prof. M. Beller for his support, the European Union for funding (H2020-MSCA-IF-2017 792177) and the Max Buchner-Foundation for a Scientific Fellowship. The CV studies were co-funded through the Leibniz Science Campus Phosphorous Research Rostock and the FCI (SK 202/22). We thank our technical and analytical staff for assistance, especially Dr Anke Spannenberg for her support regarding X-ray analysis. Dr Jonas Bresien is kindly acknowledged for help with vibrational spectroscopy.

Notes and references

- H. Köhler and A. Michaelis, *Ber. Dtsch. Chem. Ges.*, 1877, **10**, 807.
- J. J. Daly and L. Maier, *Nature*, 1964, **203**, 1167.
- A. H. Cowley, T. A. Furtch and D. S. Dierdorf, *J. Chem. Soc., Chem. Commun.*, 1970, 523.



- 4 P. S. Elmes, M. E. Redwood and B. O. West, *J. Chem. Soc. D*, 1970, 1120.
- 5 M. Baudler, B. Carlsohn, W. Böhm and G. Reuschenbach, *Z. Naturforsch., B: Anorg. Chem., Org. Chem.*, 1976, **31**, 558.
- 6 M. Baudler, B. Carlsohn, B. Kloth and D. Koch, *Z. Anorg. Allg. Chem.*, 1977, **432**, 67.
- 7 M. Baudler and K. Glinka, *Chem. Rev.*, 1993, **93**, 1623.
- 8 W. Mahler and A. B. Burg, *J. Am. Chem. Soc.*, 1957, **79**, 251.
- 9 M. Baudler, J. Hahn and E. Clef, *Z. Naturforsch., B: Anorg. Chem., Org. Chem.*, 1984, **39**, 438.
- 10 M. Baudler and J. Hellmann, *Z. Naturforsch., B: Anorg. Chem., Org. Chem.*, 1981, **36**, 266.
- 11 P. Jutzi, N. Brusdeilins, H.-G. Stammer and B. Neumann, *Chem. Ber.*, 1994, **127**, 997.
- 12 P. Jutzi and N. Brusdeilins, *Z. Anorg. Allg. Chem.*, 1994, **620**, 1375.
- 13 W. Uhl and M. Benter, *J. Chem. Soc., Dalton Trans.*, 2000, 3133.
- 14 C. Üffing, C. v. Hänisch and H. Schnöckel, *Z. Anorg. Allg. Chem.*, 2000, **626**, 1557.
- 15 C. A. Dyker, N. Burford, G. Menard, M. D. Lumsden and A. Decken, *Inorg. Chem.*, 2007, **46**, 4277.
- 16 M. H. Holthausen, D. Knackstedt, N. Burford and J. J. Weigand, *Aust. J. Chem.*, 2013, **66**, 1155.
- 17 S. S. Chitnis, R. A. Musgrave, H. A. Sparkes, N. E. Pridmore, V. T. Annibale and I. Manners, *Inorg. Chem.*, 2017, **56**, 4521.
- 18 S. S. Chitnis, H. A. Sparkes, V. T. Annibale, N. E. Pridmore, A. M. Oliver and I. Manners, *Angew. Chem., Int. Ed.*, 2017, **56**, 9536.
- 19 R. Ahlrichs, D. Fenske, H. Oesen and U. Schneider, *Angew. Chem., Int. Ed. Engl.*, 1992, **31**, 323–326.
- 20 M. Baudler and M. Bock, *Z. Anorg. Allg. Chem.*, 1973, **395**, 37.
- 21 K. Schwedtmann, R. Schoemaker, F. Hennesdorf, A. Bauzá, A. Frontera, R. Weiss and J. J. Weigand, *Dalton Trans.*, 2016, 45, 11384.
- 22 N. Tokitoh, A. Tsurusaki and T. Sasamori, *Phosphorus, Su.fur Silicon Relat. Elem.*, 2009, **184**, 979.
- 23 C. N. Smit, T. A. van der Knaap and F. Bickelhaupt, *Tetrahedron Lett.*, 1983, **24**, 2031.
- 24 L. Weber, D. Bungardt, R. Boese and D. Bläser, *Chem. Ber.*, 1988, **121**, 1033.
- 25 D. G. Yakhvarov, E. Hey-Hawkins, R. M. Kagirov, Y. H. Budnikova, Y. S. Ganushevich and O. G. Sinyashin, *Russ. Chem. Bull.*, 2007, **56**, 935.
- 26 X. Li, D. Lei, M. Y. Chiang and P. P. Gaspar, *J. Am. Chem. Soc.*, 1992, **114**, 8526.
- 27 K. B. Dillon, V. C. Gibson and L. J. Sequeira, *J. Chem. Soc., Chem. Commun.*, 1995, 2429.
- 28 B. M. Cossairt and C. C. Cummins, *New J. Chem.*, 2010, **34**, 1533.
- 29 S. Shah and J. D. Protasiewicz, *Chem. Commun.*, 1998, 1585.
- 30 P. Le Floch, *Coord. Chem. Rev.*, 2006, **250**, 627.
- 31 Experimental and computational details, and details on the X-ray diffraction studies are included in the ESI.†
- 32 K. S. A. Motolko, D. J. H. Emslie, H. A. Jenkins and J. F. Britten, *Eur. J. Inorg. Chem.*, 2017, 2920.
- 33 C. Frenzel and E. Hey-Hawkins, *Phosphorus, Su.fur Silicon Relat. Elem.*, 1998, **143**, 1.
- 34 J. D. Protasiewicz, *Eur. J. Inorg. Chem.*, 2012, 4539.
- 35 M. Yoshifuji, I. Shima, N. Inamoto, K. Hirotsu and T. Higuchi, *J. Am. Chem. Soc.*, 1981, **103**, 4587.
- 36 J. D. Protasiewicz, M. P. Washington, V. B. Gudimetla, J. L. Payton and M. C. Simpson, *Inorg. Chim. Acta*, 2010, **364**, 39.
- 37 T. Sasamori, N. Takeda and N. Tokitoh, *J. Phys. Org. Chem.*, 2003, **16**, 450.
- 38 P. Pyykkö and M. Atsumi, *Chem.–Eur. J.*, 2009, **15**, 12770.
- 39 D. Dhara, D. Mandal, A. Maiti, C. B. Yildiz, P. Kalita, N. Chrysochos, C. Schulzke, V. Chandrasekhar and A. Jana, *Dalton Trans.*, 2016, **45**, 19290.
- 40 A. Aistars, R. J. Doedens and N. M. Doherty, *Inorg. Chem.*, 1994, **33**, 4360.
- 41 R. Appel and H. Schöler, *Chem. Ber.*, 1977, **110**, 2382.
- 42 S. S. Chitnis, A. P. M. Robertson, N. Burford, J. J. Weigand and R. Fischer, *Chem. Sci.*, 2015, **6**, 2559.
- 43 J. J. Weigand, N. Burford, A. Decken and A. Schulz, *Eur. J. Inorg. Chem.*, 2007, 4868.
- 44 A. P. M. Robertson, S. S. Chitnis, H. A. Jenkins, R. McDonal, M. J. Ferguson and N. Burford, *Chem.–Eur. J.*, 2015, **21**, 7902.
- 45 T. L. Breen and D. W. Stephan, *J. Am. Chem. Soc.*, 1995, **117**, 11914.
- 46 C. C. Cummins, R. R. Schrock and W. M. Davis, *Angew. Chem., Int. Ed. Engl.*, 1993, **32**, 756.
- 47 F. Basuli, J. Tomaszewski, J. C. Huffman and D. J. Mindiola, *J. Am. Chem. Soc.*, 2003, **125**, 10170.
- 48 G. Zhao, F. Basuli, U. J. Kilgore, H. Fan, H. Aneetha, J. C. Huffman, G. Wu and D. J. Mindiola, *J. Am. Chem. Soc.*, 2006, **128**, 13575.
- 49 T. Beweries, M. Haehnel and U. Rosenthal, *Catal. Sci. Technol.*, 2013, **3**, 18.
- 50 S. Xin, H. G. Woo, J. F. Harrod, E. Samuel and A.-M. Lebus, *J. Am. Chem. Soc.*, 1997, **119**, 5307.
- 51 S. Xin, J. F. Harrod and E. Samuel, *J. Am. Chem. Soc.*, 1994, **116**, 11562.
- 52 L. Weber, *Chem. Rev.*, 1992, **92**, 1839.
- 53 P. S. Elmes, M. L. Scudder and B. O. West, *J. Organomet. Chem.*, 1976, **122**, 281.
- 54 J. Chatt, P. B. Hitchcock, A. Pidcock, C. P. Warrens and K. R. Dixon, *J. Chem. Soc., Dalton Trans.*, 1984, 2237.
- 55 J. Ho, T. L. Breen, A. Ozarowski and D. W. Stephan, *Inorg. Chem.*, 1994, **33**, 865.
- 56 S. Kurz and E. Hey-Hawkins, *J. Organomet. Chem.*, 1993, **462**, 203.
- 57 M. Schaffrath, A. Villinger, D. Michalik, U. Rosenthal and A. Schulz, *Organometallics*, 2008, **27**, 1393.
- 58 M. Baudler, K. Glinka, A. H. Cowley and M. Pakulski, Organocyclophosphanes, in *Inorg. Synth.*, ed. H. R. Allcock, 2007.
- 59 J. R. Goehlich and R. Schmutzler, *Z. Anorg. Allg. Chem.*, 1994, **620**, 173.
- 60 H. Köpf and R. Voigtländer, *Chem. Ber.*, 1981, **114**, 2731.



Edge Article

- 61 A. T. Normand, Q. Bonnin, S. Brandès, P. Richard, P. Fleurat-Lessard, C. H. Devillers, C. Balan, P. Le Gendre, G. Kehr and G. Erker, *Chem.-Eur. J.*, 2019, **25**, 2803.
- 62 J. Pinkas, R. Gyepes, I. Císařová, J. Kubišta, M. Horáček, N. Žilková and K. Mach, *Dalton Trans.*, 2018, **47**, 8921.
- 63 M. Polásek and J. Kubišta, *J. Organomet. Chem.*, 2007, **692**, 4073.
- 64 X. Yan and C. Xi, *Acc. Chem. Res.*, 2015, **48**, 935.
- 65 T. Baumgartner and R. Réau, *Chem. Rev.*, 2006, **106**, 4681.

Open Access Article. Published on 30 July 2019. Downloaded on 2/14/2022 4:47:31 PM.
This article is licensed under a Creative Commons Attribution-NonCommercial 3.0 Unported Licence.

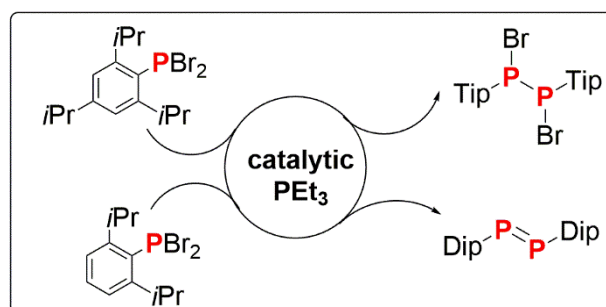


5.6 Phosphine-catalysed reductive coupling of dihalophosphanes

J.-E. Siewert, A. Schumann, C. Hering-Junghans

Dalton Trans. **2021**, *50*, 15111–15117.

DOI: 10.1039/D1DT03095G



Reprinted (adapted) with permission from *Dalton Trans.*.

Copyright 2021 Royal Society of Chemistry

Cite this: *Dalton Trans.*, 2021, **50**, 15111Received 12th September 2021.
Accepted 29th September 2021

DOI: 10.1039/d1dt03095g

rsc.li/dalton

Phosphine-catalysed reductive coupling of dihalophosphanes†

Jan-Erik Siewert, André Schumann and Christian Hering-Junghans *

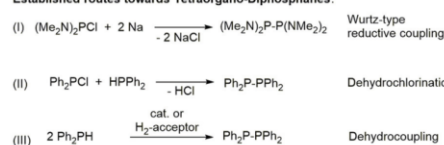
Classically tetraaryl diphosphanes have been synthesized through Wurtz-type reductive coupling of halo-phosphanes R_2PX or more recently, through the dehydrocoupling of phosphines R_2PH . Catalytic variants of the dehydrocoupling reaction have been reported, but are limited to R_2PH compounds. Using PEt_3 as a catalyst, we now show that $TipPBr_2$ ($Tip = 2,4,6\text{-}iPr_3C_6H_2$) is selectively coupled to give the dibromodiphosphane ($TipPBr_2$) (1), a compound not accessible using classic Mg reduction. Surprisingly, when using $DipPBr_2$ ($Dip = 2,6\text{-}iPr_3C_6H_3$) in the PEt_3 catalysed reductive coupling the diphosphene ($PDip_2$) (2) with a $P=P$ double was formed selectively. In benzene solutions ($PDip_2$) has a half life time of ca. 28 days and can be utilized with NHCs to access NHC-phosphinidene adducts. To show that this protocol is more widely applicable, we show that Ph_2PBr and Mes_2PX ($X = Cl, Br$) are efficiently coupled using 10 mol% of PEt_3 to give $(Ph_2P)_2$ and $(Mes_2P)_2$, respectively. Control experiments show that $[BrPEt_3]Br$ is a potential oxidation product in the catalytic cycle, which can be debrominated by Zn dust as a sacrificial reductant.

Introduction

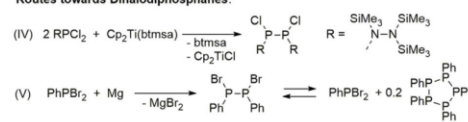
The formation of element–element bonds in main group chemistry is still dominated by classic stoichiometric salt metathesis and reductive coupling reactions. Only in recent years, catalytic protocols for the dehydrocoupling of main group (p-block) substrates to species with homonuclear (E–E) or heteronuclear (E–E') bonds have emerged.^{1–3} Catalysis with earth-abundant metals, in particular Zr, Fe and Ni,⁴ has been shown to be a viable alternative to using rather expensive systems based on Rh,^{5–7} Ir^{7–10} and Ru.¹¹ Moving to main-group species to facilitate the homo- or heterocoupling of p-block elements has also been the focus of current research. Among potential coupling products, diphosphanes have received attention as both synthetic targets as well as undesired byproducts, for example in the synthesis of tertiary phosphines.^{12–17} Diphosphanes have been shown to readily react with alkenes and alkynes to give diphos-type ligands and to be of interest for dynamic covalent chemistry.^{13,17} Classically, tetraorgano-diphosphanes have been synthesized through Wurtz-type reductive coupling of R_2PBr using various

metals (Li, Na, K, Mg and Hg) (Scheme 1, I).^{18–21} Alternatively, chlorophosphanes react with simple phosphines HPR_2 to give R_2P-PR_2 under HCl elimination (Scheme 1, II),²² which can be improved by the addition of tertiary amines.²³ Another viable pathway is the salt metathesis between R_2PBr and R_2PLi , which can be enhanced by BH_3 -stabilization of the lithium phosphide.^{13,24} The dehydrocoupling of HPR_2 (Scheme 1,

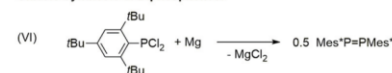
Established routes towards Tetraorgano-Diphosphanes:



Routes towards Dihalodiphosphanes:



Classic Synthesis of Diphosphenes:



Scheme 1 Synthetic pathways (I–III) towards R_2P-PR_2 , $R(x)P-P(x)R$ (IV, V) and diphosphenes (VI).

Leibniz Institut für Katalyse e.V. (LIKAT), A-Einstein-Str. 29a, 18059 Rostock, Germany. E-mail: Christian.hering.junghans@catalysis.de; <https://www.catalysis.de/forschung/aktivierung-kleiner-molekuele>

† Electronic supplementary information (ESI) available: Synthesis and characterization of compounds, NMR and IR spectra, crystallographic, and computational details. CCDC 2098825–2098829. For ESI and crystallographic data in CIF or other electronic format see DOI: 10.1039/d1dt03095g

III),^{25–28} chlorosilane elimination from R_2PSiMe_3 and R_2PCL or P–N/P–P bond metathesis reactions are other synthetic pathways described in the literature.^{29,30}

Even though still limited to select examples, Zr,³¹ Fe,³² and Rh-based³³ metal complexes have been successfully used in the catalytic dehydrocoupling of phosphines to make P–P bonds.^{1,34} Just recently, *t*BuOK was shown to efficiently catalyse the dehydrocoupling of phosphines using imines or azobenzene as a hydrogen acceptor.³⁵ In comparison to tetraorgano-diphosphanes, diorgano-dihalo-diphosphanes of the type R(X)P–P(X)R are rare (X = Cl, Br, I). The stoichiometric reduction of $((Me_3Si)_2N_2(SiMe_3))PCL_2$ with $Cp_2Ti(btmsa)$ in a 2:1 ratio, yielded the corresponding dichlorodiphosphane R(Cl)P–P(Cl)R (R = N(SiMe₃)N(SiMe₃)₂, Scheme 1, IV).³⁶ Ph(Br)P–P(Br)Ph was obtained by reduction of PhPBr₂ with Mg metal in 80% yield and was shown to reversibly disproportionate in solution giving (PPh)₃ and PhPBr₂ (Scheme 1, V).³⁷ Another class of P–P bonded species are the diphosphenes,³⁸ comprising a P=P double bond and the first variant Mes*P=PMe* (Mes* = 2,4,6-*t*Bu₃C₆H₃) was synthesized through the reductive coupling of Mes*PCL₂ with Mg metal (Scheme 1, VI).³⁹ Since its initial discovery in the early 1980s diphosphenes have emerged as a well-studied class of compounds and alternative synthetic pathways,³⁸ including the dimerization of phospho-Wittig reagents upon loss of PMe₃ has been established by Protasiewicz and co-workers.⁴⁰ Moreover, both PMe₃ and *Pn*Bu₃ have been shown to catalyse the chlorine atom transfer between ArPPMe₃ and ArPCL₂ to give ArPCL₂ and ArPPMe₃.⁴¹ This clearly shows the potential of phosphines to catalytically dehalogenate halophosphines. Even though a large variety of diphosphenes is known, sterically demanding and therefore kinetically stabilizing groups attached to phosphorus are needed to stabilize the reactive P=P double bond, as formation of larger oligomers, namely *cyclo*-oligophosphanes, is observed otherwise.^{42,43} Recent studies in the area of diphosphenes have been focused on tuning the HOMO–LUMO gap of diphosphenes,^{44,45} and to synthesize radical cations and anions derived from the diphosphenes as well as making charged variants.^{46–48} The interaction of NHCs with diphosphenes has also been investigated in terms of their coordination chemistry and the influence on their hydrolysis.^{49–52}

Our group has shown that aryldihalophosphanes of the type ArPX₂ (Ar = 2,4,6-Me₃C₆H₃, Mes; 2,6-*i*Pr₂C₆H₃, Dip; 2,4,6-*i*Pr₃C₆H₂, Tip; X = Cl, Br) are selectively coupled using a mixture of PMe₃ and Zn to give the corresponding triphosphiranes (PAr)₃. PMe₃ was identified as the active reductant.⁵³ By using PMe₃Cl₂⁵⁴ with Zn as the sacrificial reductant in the reaction with TipPCL₂ we demonstrated that (PTip)₃ is the major product formed. This is in line with the seminal work of Sisler on the reductive coupling of chlorophosphanes with trialkylphosphines.^{55–57} Moreover, we noticed the formation of the diphosphene TipP=PTip when TipPBr₂ was reacted with 1.3 equiv. of PEt₃.⁵³ This raised the question whether catalytic amounts of PR₃ (R = Me, Et) will facilitate the reductive coupling of ArPX₂.

Results and discussion

In this study we focused on two ArPBr₂ (Ar = Dip, Tip) derivatives. As a first entry we revisited the reduction of TipPBr₂ with PEt₃. PEt₃ was chosen, as we expected a higher solubility of the oxidation product [BrPEt₃]₂Br,^{58,59} compared to the insoluble by-product when TipPCL₂ was reduced with PMe₃.⁵³ At first THF was selected as solvent in conjunction with 20 mol% PEt₃ as the catalyst and 3 equiv. zinc dust and the reaction mixture was analysed by ³¹P NMR spectroscopy after stirring 1 h at –78 °C. This revealed the formation of diphosphane (TipPBr)₂ (1) in 36% as a diastereomeric mixture, namely the *meso*- and *rac*-compounds, with 64% of unconverted TipPBr₂ (Table 1, entry 1). Better conversion into (TipPBr)₂ (77%) was noted when the mixture was stirred at room temperature for 1 h under otherwise same conditions (Table 1, entry 2). However, continued stirring at ambient temperature for 16 h afforded a mixture of (PTip)₃ and (PTip)₄ and minimal amounts of the diphosphane (PTip)₂ were detected (Table 1, entry 3). Lowering the amount of PEt₃ to 10 mol% in THF after 1 h at room temperature, a conversion of TipPBr₂ (54%) into 1 of 46% was achieved. Increasing the reaction time to 3 h the conversion into 1 increased to 69%. Using these conditions 1 (Table 1, entry 5) was isolated as yellow crystalline solid after evaporation of the volatiles and extraction of the crude mixture with toluene. Concentration to incipient crystallization and storage at –78 °C for 48 h gave 1 as a yellow crystalline solid in moderate isolated, yet reproducible yields of ca. 30%. Further decreasing the catalyst loading to 5 mol%, full conversion could not be achieved even after 16 h (Table 1, entries 6 and 7). It needs to be noted that the formation of (PTip)₃ and (PTip)₄ was not detected when using 10 or 5 mol% of PEt₃, respectively. This clearly shows the potential of PEt₃ to act as a catalyst for the reductive coupling of halophosphines, giving the diphosphane (TipPBr)₂ (1) rather selectively. We note that when using *Pn*Bu₃ (10 mol%, 2 eq. Zn, 3 h) 1 is formed, albeit

Table 1 Screening different amounts of PEt₃ in the catalytic coupling of TipPBr₂ in THF after different reaction times using Zn dust as a sacrificial reductant

Entry	PEt ₃ [mol%]	T [°C]	t [h]	A ^a	B ^a	C ^a	D ^a	E ^a
1	20	–78	1	64	36	0	0	0
2	20	r.t.	1	23	77	0	0	0
3	20	r.t.	16	0	0	36	41	23
4	10	r.t.	1	54	46	0	0	0
5	10	r.t.	3	31	69	0	0	0
6	5	r.t.	1	100	0	0	0	0
7	5	r.t.	16	42	58	0	0	0

^a Conversion determined by ³¹P NMR spectroscopy, normalized to A, duplicate runs.

in significantly lower yields (21%) compared to using PET_3 (Fig. S21†).

X-ray quality crystals of **1** were grown from saturated *n*-hexane solutions at 5 °C. Testing different crystals revealed that both *R,S*-**1** (*meso*) and *S,S*-**1** (*rac*) crystallize in the form of yellow crystals, which can only be distinguished by cell determination. Dissolving the isolated crystals of **1** in C_6D_6 indicates that a 4.7 : 1 ratio between the two forms is still present in solution, as indicated by two signals at 65.4 and 64.4 ppm in the ^{31}P NMR spectrum, respectively (Fig. S34†). In the ^1H NMR spectrum the expected 2 : 1 ratio between the *o*- and *p*-*i*Pr groups was found. However, one of the two forms shows rather featureless, broad signals, thereby precluding a clean assignment in both, the ^1H and ^{13}C NMR spectrum. The purity of the bulk material was established by CHN analysis. **1** is rather stable with respect to disproportionation into TipPBr_2 and $(\text{TipP})_n$ ($n = 3, 4$) and heating a C_6D_6 solution of **1** to 80 °C over a period of 33 h gives a mixture of TipPBr_2 (16%), **1** (62%), $(\text{TipP})_4$ (11%) and $(\text{TipP})_3$ (11%) (Fig. S36†).

R,S-**1** and *S,S*-**1** crystallize in the triclinic space group $P\bar{1}$ with one inversion symmetric molecule in the case of *R,S*-**1** and two molecules in the unit cell in *S,S*-**1**, respectively (Fig. 1). In *R,S*-**1** the bromine atoms are arranged in *trans* fashion across the P–P bond [2.2402(8) Å] ($\sum_{\text{cov}}(\text{P}-\text{P}) = 2.22$ Å, *cf.* $(\text{R}(\text{Cl})\text{P})_2$ $\text{R} = \text{N}_2(\text{SiMe}_3)_3$ $d(\text{P}-\text{P})$ 2.255(1) Å),³⁶ with the phosphorus atoms being in a trigonal pyramidal coordination environment [$\sum(\angle\text{P})$ 303.4°] (Fig. 1, left). In *S,S*-**1** the bromine atoms are arranged in *cis* fashion on the same side of the P–P bond [2.2382(6) Å] with a dihedral Br–P–P–Br angle of 55.2(2)° (Fig. 1, right).

Next, DipPBr_2 was employed as a substrate and to our surprise the diphosphane (DipPBr_2) was not formed using 10 mol% of PET_3 as a catalyst at room temperature. Instead, the major species detected in the ^{31}P NMR spectrum showed a significantly deshielded signal at 513.0 ppm (Scheme 2, top). This hinted at the formation of the diphosphane (PDip_2) (*cf.* $(\text{PTip})_2$ $\delta(^{31}\text{P}\{^1\text{H}\}) = 517.4$ ppm),⁵³ which was confirmed by SC-XRD experiments on crystals grown from a saturated *n*-hexane solution at –30 °C. Using the same conditions that allowed the isolation of **1** (10 mol% PET_3 , 3 equiv. Zn dust, THF, 3 h), **2** was isolated in reproducible yields of ca. 30% in

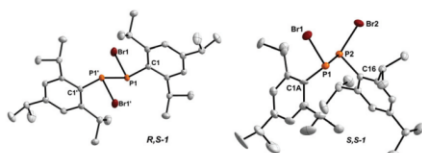
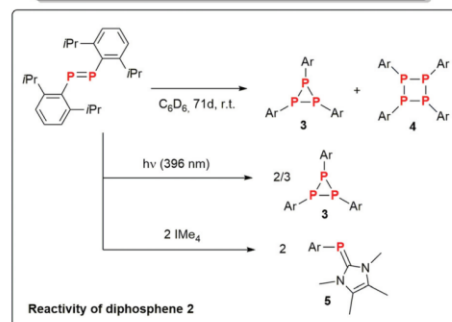
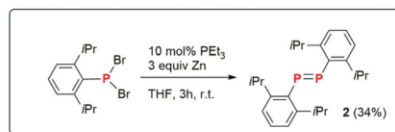


Fig. 1 Molecular structures of **1**. Hydrogen atoms have been omitted for clarity. Thermal ellipsoids are drawn at the 50% probability level. Selected bond lengths (Å) and angles (°): *R,S*-**1**: P1–P1' 2.2402(8), P1–C1 1.8337(15), P1–Br1 2.2592(4), C1–P1–Br1 105.94(5), C1–P1–P1' 102.10(5), P1'–P1–Br1 95.36(2). *S,S*-**1**: P1–P2 2.2382(6), P1–Br1 2.2512(4), P2–Br2 2.2478(5), C1A–P1–Br1 104.2(4), P2–P1–Br1 103.243(19), C1A–P1–P2 92.1(4).



Scheme 2 Synthesis of diphosphane (PDip_2) (**2**) (top) and its reactivity (bottom).

the form of yellow crystals. It needs to be noted that the direct reduction of DipPBr_2 with 1 equivalent magnesium turnings gave the triphosphirane (PDip_3) as the major product (Fig. S30†). Using half an equivalent of Mg full conversion was not achieved after 3 h with $(\text{DipPBr}_2)_2$ being formed in ca. 20% in rather unselective fashion (Fig. S31†). With PnBu_3 (10 mol%, 3 h) DipPBr_2 is converted into $(\text{DipPBr}_2)_2$ (55%, Fig. S20†). The formation of **2** is remarkable, as usually aryl groups with a greater steric profile are needed to stabilize diphosphenes, *vide infra*. Alternatively, thermodynamic stabilization of diphosphenes can be achieved by using amino functions on phosphorus, however, dimerization to the corresponding *cyclo*-tetraphosphanes has been described for $[(\text{Me}_3\text{Si})_2\text{NP}]_2$.⁶¹

2 crystallizes in the triclinic space group $P\bar{1}$ with one inversion symmetric molecule in the unit cell (Fig. 2). The Dip-substituents are arranged in *trans* fashion with the P–P bond [2.0293(7) Å] in the expected range for diphosphenes [*cf.*

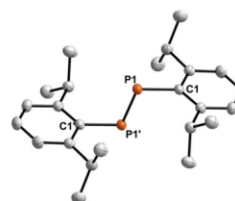


Fig. 2 Molecular structure of **2**. Hydrogen atoms have been omitted for clarity. Thermal ellipsoids are drawn at the 50% probability level. Selected bond lengths (Å) and angles (°): P1–P1' 2.0293(7), P1–C1 1.8471(10), C1–P1–P1' 99.59(4), C2–C1–P1–P1' 91.75(8).

(*i*Pr⁴CpP)₂ 2.0282(10) Å).⁶² The C–P–P angles [99.59(4)°] are narrower compared to (Mes*P)₂ [*i.e.* 102.8(1)°] in agreement with the lesser steric demand of the Dip-substituent compared to Mes*. To determine the kinetic stability of **2** a solution in C₆D₆ was kept at room temperature under the exclusion of light and was monitored over a period of 71 d (Fig. S43–44 and Table S4†). The half-life time of **2** is *ca.* 28 d, which is considerably more stable than [(Me₃Si)₂C(H)P]₂ with a half-life time of *ca.* 7 d at room temperature,⁶³ or the ruby red liquid [(Me₃Si)₂NP]₂ which in isolated form dimerizes to the corresponding tetraphosphane within hours.⁶¹ The thermal decomposition products have been shown to be the triphosphirane (PDip)₃ (**3**) and the dimerization product (PDip)₄ (**4**) in a 3 : 1 ratio. Irradiation of **2** with an LED ($\lambda = 396$ nm) resulted in the immediate and clean formation of **3**, which was corroborated by UV-Vis studies (Scheme 2 and Fig. S46–48†). The yellow colour of **2** stems from a HOMO–1 and HOMO–3 to LUMO (π – π^*) transition according to TD-DFT calculations on the PBE0-D3/def2-TZVP level of theory (Table S7, and Fig. S61†). The cyclic voltammogram of **2** in THF (0.1 M [*n*Bu₄N][PF₆]) showed a reversible reduction event at –2.10 V (*vs.* Cp₂Fe/Cp₂Fe⁺; Fig. S42†), which is higher than that of (Mes*P)₂ (–2.36 V),⁶⁴ and ([sB]P)₂ (–2.24 V) ([sB] = (H₂CNDip)₂)⁶⁵ suggesting a lower LUMO level in **2** compared to these species.

With compound **2** accessible we became interested in its reactivity towards N-heterocyclic carbenes (NHCs). Jana and co-workers have recently shown reversible NHC binding to (Mes*TerP)₂,⁴⁹ whereas Matsuo *et al.* showed cleavage of the P=P bond in (RIND-P)₂ (RIND = 1,1,3,3,5,5,7,7-octa-R-substituted s-hydrindacen-4-yl) to give NHC phosphinidene adducts.⁶⁶ Combination of **2** with two molar equiv. of IMe₄ (IMe₄ = (MeCNMe)₂C) resulted in the formation of DipP=IMe₄ (**5**), which was isolated in pure form in 50% yield after recrystallization from saturated *n*-hexane solutions at –30 °C. **5** shows a characteristic ³¹P{¹H} NMR signal at –86.3 ppm (*i.e.* EIND-PIMe₄ $\delta^{(31P)} = -63.9$ ppm) and one set of signals for the *i*Pr-groups for the Dip group in the expected 1 : 6 ratio and two signals for the Me-groups of IMe₄ in a 1 : 1 ratio, indicating C_s symmetry in solution. **5** crystallizes in the monoclinic spacegroup *P*2₁/*n* with four molecules in the unit cell. The P–C_{NHC} [1.7730(13) Å] agrees with the formulation as an inversely polarized phosphalkene (*i.e.* EIND-PIMe₄ 1.767(3) Å, Fig. 3).^{66,67}

Attempts to prepare metal complexes of **2** proved unsuccessful, however, we noted the dimerization of **2** to give *cyclo*-tetraphosphane **4** as the main product in the presence of one molar equivalent of PdCl₂. This allowed isolation of some colourless crystals of **4** and its molecular structure was determined by means of X-Ray crystallography (Fig. S57†).

To further elaborate on whether the PEt₃-catalyzed reductive coupling can be more generally applied, we tested Mes₂PX (X = Cl, Br) as a substrate. Mes₂PX was chosen, as it can be conveniently prepared by addition of PCl₃ to MesMgBr in THF, and the exact molar mass is then derived from integration of the Mes₂PCL and Mes₂PBR species in the ³¹P NMR spectrum

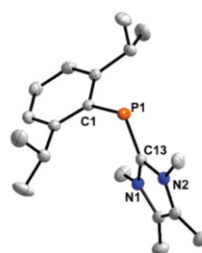
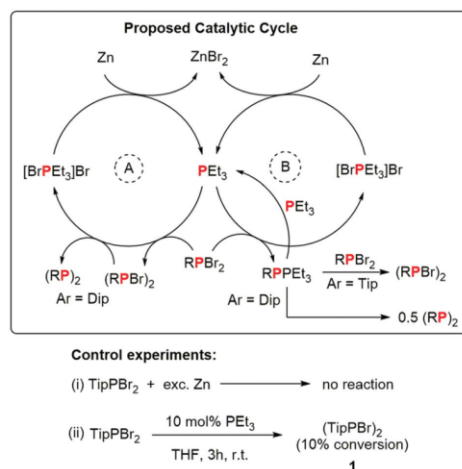


Fig. 3 Molecular structure of **5** (left). Hydrogen atoms have been omitted for clarity. Thermal ellipsoids are drawn at the 50% probability level. Selected bond lengths (Å) and angles (°): P1–C1 1.8490(12), P1–C13 1.7730(13); C1–P1–C13 103.60(5), C13–P1–C1–C6 66.95(11).

(see ESI† for details). Using the conditions established for TipPBr₂, Mes₂PX was efficiently coupled (10 mol% PEt₃, 2 eq. Zn, 6 h) to give (Mes₂P)₂ (**6**) in good isolated yield (86%) after extracting the dried reaction mixture with benzene. Compared to reported synthetic procedures for **6**, in which mainly Mes₂PH is used in dehydrocoupling reactions,^{25,35,68} the protocol applied in here eliminates the extra reduction step needed to go from Mes₂PX to Mes₂PH, *vide infra*. Moreover, we show that Ph₂PCL can be coupled to give (Ph₂P)₂ (**7**) in moderate isolated yields (58%) using the same reaction conditions that gave **6**.

Control experiments were carried out to better understand this trialkylphosphine-catalyzed coupling of dibromophosphanes. Using the corresponding dichlorophosphanes DipPCL₂ and TipPCL₂ under optimized conditions, the formation of the dichlorodiphosphanes (ArPCL)₂ was observed after 3 h in THF, however, conversions lack behind those observed for the dibromophosphanes. We then tested whether [BrPEt₃]Br can be used to generate PEt₃ in the presence of Zn in THF. When employing 10 mol% [BrPEt₃]Br with DipPBr₂ the starting material was mostly consumed after 3 h and a nearly equimolar mixture of diphosphane (DipPBr)₂ and (PDip)₃ was obtained (Fig. S9†). Similarly, half of TipPBr₂ is converted into **1** using [BrPEt₃]Br as the catalyst (Fig. S8†). This clearly underlines that [BrPEt₃]Br is a potential oxidation product, however, the formation of [Et₃PPEt₃]Br₂ cannot be excluded, as diphosphonium salts were shown to be formed upon reduction of Sb(OTf)₃ with PR₃ (R = Me, Et).⁶⁹ Using PMe₃ (10 mol%, 2 equiv. Zn) as a catalyst DipPBr₂ was coupled to give (DipPBr)₂ and (PDip)₃ in a 2 : 1 ratio and DipPBr₂ was fully consumed after 3 h, however, attempts to isolate (DipPBr)₂ have proven unsuccessful to date. In contrast, with TipPBr₂ and 10 mol% of PMe₃ a 1 : 1 mixture of TipPBr₂ and **1** was detected. To identify Zn as the sacrificial reductant both TipPBr₂ and DipPBr₂ were stirred over an excess of Zn dust in the absence of PEt₃ and no conversion was observed (Scheme 3, reaction (i)) after 3 h at room temperature. When only using 10 mol% of PEt₃ without adding Zn dust in the coupling of TipPBr₂ and DipPBr₂ only 10% of the starting



Scheme 3 Proposed catalytic cycles (A and B) and control experiments to determine the role of Zn and PEt_3 .

material was converted into **1** (Scheme 3, reaction (ii)). In light of these observations we propose a catalytic cycle (A, Scheme 3) in which in a first step ArPBr_2 is coupled to give **1** (Ar = Tip) with concomitant formation of $[\text{BrPEt}_3]\text{Br}$, which is then reduced by zinc to regenerate PEt_3 . The formation of **2** is surprising and therefore an alternative pathway (B, Scheme 3) is the intermediate formation of short-lived $\text{ArP}=\text{PEt}_3$, which can then either react with a second equivalent of TipPBr_2 to **1** and release of PEt_3 , which re-enters the cycle or through PEt_3 liberation (Ar = Dip) and recombination of the free phosphinidene to give **2**. The formation of phosphanylidene phosphoranes ArPPR_3 (often termed phospho-Wittig reagents) has been shown by Protasiewicz and co-workers and ArPPR_3 is only stable when the aryl-group is sterically demanding (Ar = Mes*, Mes*Ter, DipTer).^{70–72}

Conclusion

Even though limited in scope, we have shown that simple PEt_3 catalyses the coupling of dibromophosphanes, to give a rare example of an aryl-substituted dibromodiphosphane in **1** or the diphosphene **2**. Moreover, Mes_2PX and Ph_2PCl were coupled to give the diphosphanes **6** and **7**, respectively. Control experiments have shown that $[\text{BrPEt}_3]\text{PBr}$ is one of the oxidation products and zinc powder acts as a sacrificial reductant to regenerate PEt_3 . Diphosphene **2** has a half-life time of ca. 28 d decomposing cleanly to give $(\text{PDip})_n$ ($n = 3,4$). When irradiated at 396 nm **2** cleanly converts into $(\text{PDip})_3$. The addition of NHC IME_4 to **2** afforded the corresponding NHC phosphinidene adduct **5**. Furthermore **2** dimerizes in the presence of PdCl_2 to give the corresponding *cyclo*-tetraphosphane

$(\text{DipP})_4$ (**4**). In future studies we will look to further extend the scope of this catalytic protocol to make this an invaluable tool for E–E bond formation reactions beyond the formation of P–P bonded species.

Author contributions

A. S. discovered the catalytic reduction of TipPBr_2 and carried out first optimisation reactions. J.-E. S. optimised the catalytic reactions, carried out the reactivity studies on **2** and comprehensively analysed all materials. J.-E. S. carried out the computational work and prepared the experimental part of the manuscript. C. H.-J. designed the overall research, supervised the work, contributed to IR analysis, wrote the manuscript, proofread the experimental part and coordinated the overall project.

Conflicts of interest

There are no conflicts to declare.

Acknowledgements

This research was funded by the Leibniz Association within the scope of the Leibniz ScienceCampus Phosphorus Research Rostock (<http://www.sciencecampus-rostock.de>). We thank our technical and analytical staff for assistance, especially Dr Anke Spannberg for her support regarding X-ray analysis. We also wish to thank the ITMZ at the University of Rostock for access to the Cluster Computer and especially Malte Willert for technical support.

Notes and references

- S. Greenberg and D. W. Stephan, *Chem. Soc. Rev.*, 2008, **37**, 1482–1489.
- W. Rory, *Curr. Org. Chem.*, 2008, **12**, 1322–1339.
- D. Han, F. Anke, M. Trose and T. Beveries, *Coord. Chem. Rev.*, 2019, **380**, 260–286.
- K. Kaniewska, A. Dragulescu-Andrasi, L. Ponikiewski, J. Pikies, S. A. Stoian and R. Grubba, *Eur. J. Inorg. Chem.*, 2018, **2018**, 4298–4308.
- H. Dorn, R. A. Singh, J. A. Massey, J. M. Nelson, C. A. Jaska, A. J. Lough and I. Manners, *J. Am. Chem. Soc.*, 2000, **122**, 6669–6678.
- F. Choffat, S. Käser, P. Wolfer, D. Schmid, R. Mezzenga, P. Smith and W. Caseri, *Macromolecules*, 2007, **40**, 7878–7889.
- H. C. Johnson, E. M. Leitao, G. R. Whittell, I. Manners, G. C. Lloyd-Jones and A. S. Weller, *J. Am. Chem. Soc.*, 2014, **136**, 9078–9093.

- 8 A. Staubitz, M. E. Sloan, A. P. M. Robertson, A. Friedrich, S. Schneider, P. J. Gates, J. Schmedt auf der Günne and I. Manners, *J. Am. Chem. Soc.*, 2010, **132**, 13332–13345.
- 9 A. Kumar, H. C. Johnson, T. N. Hooper, A. S. Weller, A. G. Algarra and S. A. Macgregor, *Chem. Sci.*, 2014, **5**, 2546–2553.
- 10 U. S. D. Paul, H. Braunschweig and U. Radius, *Chem. Commun.*, 2016, **52**, 8573–8576.
- 11 A. N. Marziale, A. Friedrich, I. Klopsch, M. Drees, V. R. Celinski, J. Schmedt auf der Günne and S. Schneider, *J. Am. Chem. Soc.*, 2013, **135**, 13342–13355.
- 12 S. Burck, D. Gudat and M. Nieger, *Angew. Chem., Int. Ed.*, 2004, **43**, 4801–4804.
- 13 D. L. Dodds, M. F. Haddow, A. G. Orpen, P. G. Pringle and G. Woodward, *Organometallics*, 2006, **25**, 5937–5945.
- 14 S. Burck, K. Götz, M. Kaupp, M. Nieger, J. Weber, J. Schmedt auf der Günne and D. Gudat, *J. Am. Chem. Soc.*, 2009, **131**, 10763–10774.
- 15 N. A. Giffin, A. D. Hendsbee, T. L. Roemmele, M. D. Lumsden, C. C. Pye and J. D. Masuda, *Inorg. Chem.*, 2012, **51**, 11837–11850.
- 16 N. Szykiewicz, L. Ponikiewski and R. Grubba, *Dalton Trans.*, 2018, **47**, 16885–16894.
- 17 J. Bresien, Y. Pilopp, A. Schulz, L. S. Szych, A. Villinger and R. Wustrack, *Inorg. Chem.*, 2020, **59**, 13561–13571.
- 18 K. Issleib and W. Seidel, *Chem. Ber.*, 1959, **92**, 2681–2694.
- 19 H. Nöth and H.-J. Vetter, *Chem. Ber.*, 1961, **94**, 1505–1516.
- 20 H. Niebergall and B. Langenfeld, *Chem. Ber.*, 1962, **95**, 64–76.
- 21 W. A. Henderson, M. Epstein and F. S. Seichter, *J. Am. Chem. Soc.*, 1963, **85**, 2462–2466.
- 22 C. Dörken, *Ber. Dtsch. Chem. Ges.*, 1888, **21**, 1505–1515.
- 23 K. Issleib and K. Krech, *Chem. Ber.*, 1965, **98**, 1093–1096.
- 24 D. L. Dodds, J. Floure, M. Garland, M. F. Haddow, T. R. Leonard, C. L. McMullin, A. G. Orpen and P. G. Pringle, *Dalton Trans.*, 2011, **40**, 7137–7146.
- 25 S. Molitor, J. Becker and V. H. Gessner, *J. Am. Chem. Soc.*, 2014, **136**, 15517–15520.
- 26 H. Schneider, D. Schmidt and U. Radius, *Chem. Commun.*, 2015, **51**, 10138–10141.
- 27 K. Schwedtmann, R. Schoemaker, F. Hennersdorf, A. Bauzá, A. Frontera, R. Weiss and J. J. Weigand, *Dalton Trans.*, 2016, **45**, 11384–11396.
- 28 R. Dobrovetsky, K. Takeuchi and D. W. Stephan, *Chem. Commun.*, 2015, **51**, 2396–2398.
- 29 G. Fritz, *Adv. Inorg. Chem.*, 1987, **31**, 171–243.
- 30 K.-O. Feldmann and J. J. Weigand, *J. Am. Chem. Soc.*, 2012, **134**, 15443–15456.
- 31 J. D. Masuda, A. J. Hoskin, T. W. Graham, C. Beddie, M. C. Fermin, N. Etkin and D. W. Stephan, *Chem. – Eur. J.*, 2006, **12**, 8696–8707.
- 32 A. K. King, A. Buchard, M. F. Mahon and R. L. Webster, *Chem. – Eur. J.*, 2015, **21**, 15960–15963.
- 33 V. P. W. Böhm and M. Brookhart, *Angew. Chem., Int. Ed.*, 2001, **40**, 4694–4696.
- 34 W. Rory, *Curr. Org. Chem.*, 2012, **16**, 1313–1331.
- 35 L. Wu, V. T. Annibale, H. Jiao, A. Brookfield, D. Collison and I. Manners, *Nat. Commun.*, 2019, **10**, 2786.
- 36 M. Schaffrath, A. Villinger, D. Michalik, U. Rosenthal and A. Schulz, *Organometallics*, 2008, **27**, 1393–1398.
- 37 A. Hinke and W. Kuchen, *Chem. Ber.*, 1983, **116**, 3003–3010.
- 38 L. Weber, *Chem. Rev.*, 1992, **92**, 1839–1906.
- 39 M. Yoshifuji, I. Shima, N. Inamoto, K. Hirotsu and T. Higuchi, *J. Am. Chem. Soc.*, 1981, **103**, 4587–4589.
- 40 S. Shah, M. C. Simpson, R. C. Smith and J. D. Protasiewicz, *J. Am. Chem. Soc.*, 2001, **123**, 6925–6926.
- 41 R. C. Smith, S. Shah, E. Urnezus and J. D. Protasiewicz, *J. Am. Chem. Soc.*, 2003, **125**, 40–41.
- 42 V. J. Eilrich and E. Hey-Hawkins, *Coord. Chem. Rev.*, 2021, **437**, 213749.
- 43 T. Wellnitz and C. Hering-Junghans, *Eur. J. Inorg. Chem.*, 2021, **2021**, 8–21.
- 44 L. L. Liu, L. L. Cao, J. Zhou and D. W. Stephan, *Angew. Chem., Int. Ed.*, 2019, **58**, 273–277.
- 45 M. K. Sharma, D. Rottschäfer, S. Blomeyer, B. Neumann, H.-G. Stammer, M. van Gastel, A. Hinz and R. S. Ghadwal, *Chem. Commun.*, 2019, **55**, 10408–10411.
- 46 O. Back, B. Donnadieu, P. Parameswaran, G. Frenking and G. Bertrand, *Nat. Chem.*, 2010, **2**, 369–373.
- 47 A. Beil, R. J. Gilliard and H. Grützmacher, *Dalton Trans.*, 2016, **45**, 2044–2052.
- 48 A. Doddi, D. Bockfeld, M.-K. Zaretzke, C. Kleeberg, T. Bannenberg and M. Tamm, *Dalton Trans.*, 2017, **46**, 15859–15864.
- 49 D. Dhara, P. Kalita, S. Mondal, R. S. Narayanan, K. R. Mote, V. Huch, M. Zimmer, C. B. Yildiz, D. Scheschkewitz, V. Chandrasekhar and A. Jana, *Chem. Sci.*, 2018, **9**, 4235–4243.
- 50 D. Dhara, S. Das, S. K. Pati, D. Scheschkewitz, V. Chandrasekhar and A. Jana, *Angew. Chem., Int. Ed.*, 2019, **58**, 15367–15371.
- 51 D. Dhara, S. Das, P. Kalita, A. Maiti, S. K. Pati, D. Scheschkewitz, V. Chandrasekhar and A. Jana, *Dalton Trans.*, 2020, **49**, 993–997.
- 52 D. Dhara, D. Scheschkewitz, V. Chandrasekhar, C. B. Yildiz and A. Jana, *Chem. Commun.*, 2021, **57**, 809–812.
- 53 A. Schumann, F. Reiß, H. Jiao, J. Rabeah, J.-E. Siewert, I. Krummenacher, H. Braunschweig and C. Hering-Junghans, *Chem. Sci.*, 2019, **10**, 7859–7867.
- 54 R. Appel and H. Schöler, *Chem. Ber.*, 1977, **110**, 2382–2384.
- 55 S. E. Frazier, R. P. Nielsen and H. H. Sisler, *Inorg. Chem.*, 1964, **3**, 292–294.
- 56 S. F. Spangenberg and H. H. Sisler, *Inorg. Chem.*, 1969, **8**, 1006–1010.
- 57 J. C. Summers and H. H. Sisler, *Inorg. Chem.*, 1970, **9**, 862–869.
- 58 S. M. Godfrey, C. A. McAuliffe, I. Mushtaq, R. G. Pritchard and J. M. Sheffield, *J. Chem. Soc., Dalton Trans.*, 1998, 3815–3818.
- 59 K. Nikitin, E. V. Jennings, S. Al Sulaimi, Y. Ortin and D. G. Gilheany, *Angew. Chem., Int. Ed.*, 2018, **57**, 1480–1484.
- 60 P. Pyykkö and M. Atsumi, *Chem. – Eur. J.*, 2009, **15**, 12770–12779.

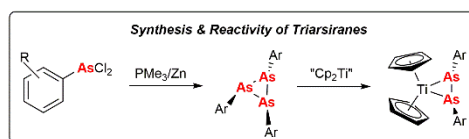
- 61 E. Niecke and R. Rüger, *Angew. Chem., Int. Ed. Engl.*, 1983, **22**, 155–156.
- 62 S. Lauk, M. Zimmer, B. Morgenstern, V. Huch, C. Müller, H. Sitzmann and A. Schäfer, *Organometallics*, 2021, **40**, 618–626.
- 63 H. Ranaivonjatovo, J. Escudié, C. Couret and J. Satgé, *Phosphorus, Su.fur Relat. Elem.*, 1987, **31**, 81–87.
- 64 A. J. Bard, A. H. Cowley, J. E. Kilduff, J. K. Leland, N. C. Norman, M. Pakulski and G. A. Heath, *J. Chem. Soc., Dalton Trans.*, 1987, 249–251.
- 65 S.-s. Asami, M. Okamoto, K. Suzuki and M. Yamashita, *Angew. Chem., Int. Ed.*, 2016, **55**, 12827–12831.
- 66 N. Hayakawa, K. Sadamori, S. Tsujimoto, M. Hatanaka, T. Wakabayashi and T. Matsuo, *Angew. Chem., Int. Ed.*, 2017, **56**, 5765–5769.
- 67 T. Krachko and J. C. Slootweg, *Eur. J. Inorg. Chem.*, 2018, **2018**, 2734–2754.
- 68 K. Oberdorf, A. Hanft, J. Ramler, I. Krummenacher, F. M. Bickelhaupt, J. Poater and C. Lichtenberg, *Angew. Chem., Int. Ed.*, 2021, **60**, 6441–6445.
- 69 S. S. Chitnis, A. P. M. Robertson, N. Burford, J. J. Weigand and R. Fischer, *Chem. Sci.*, 2015, **6**, 2559–2574.
- 70 S. Shah and J. D. Protasiewicz, *Chem. Commun.*, 1998, 1585–1586.
- 71 J. D. Protasiewicz, *Eur. J. Inorg. Chem.*, 2012, **2012**, 4539–4549.
- 72 P. Gupta, J.-E. Siewert, T. Wellnitz, M. Fischer, W. Baumann, T. Beweries and C. Hering-Junghans, *Dalton Trans.*, 2021, **50**, 1838–1844.

5.7 Aryl-substituted triarsiranes: synthesis and reactivity

A. Schumann, M. Fischer, J. Bresien, C. Hering-Junghans

Chem. Commun. **2021**, 57, 1014–1017.

DOI: 10.1039/D0CC07533G



Reprinted (adapted) with permission from *Chemical Communications*.

Copyright 2021 Royal Society of Chemistry.



Aryl-substituted triarsiranes: synthesis and reactivity†‡

Cite this: *Chem. Commun.*, 2021, 57, 1014Received 16th November 2020
Accepted 13th December 2020

DOI: 10.1039/d0cc07533g

rsc.li/chemcomm

André Schumann,^a Jonas Bresien,^b Malte Fischer^b and Christian Hering-Junghans^b*

Cyclotriarsanes are rare and described herein is a scalable synthetic protocol towards (AsAr)₃, which allowed to study their reactivity towards [Cp₂Ti(C₂(SiMe₃)₂)], affording titanocene diarsene complexes, and towards N-heterocyclic carbenes (NHCs) to give straightforward access to a variety of NHC-arsinidene adducts.

The first homoleptic cyclooligoarsane (AsPh)₆ was discovered by Michaelis and Schulte when they reduced phenyl arsenic oxide with crystalline hypophosphorous acid in refluxing ethanol, affording pale yellow crystals that were believed to be the diarsene PhAs=AsPh, the so-called arsabenzene.¹ Even though the synthesis and reactivity of the related cyclooligophosphanes (PR)_n (*n* = 3, 4, 5, 6) have been studied in detail,² the heavier oligopnictanes (PnR)_n (Pn = As, Sb, Bi; *n* = 3, 4, 5, 6) have received considerably less interest. To the best of our knowledge only eight examples of cyclotriarsanes, also referred to as triarsiranes, have been reported (Fig. 1).

In 1910 Ehrlich synthesized “Salvarsan”, as a cure for syphilis, by reduction of 3-nitro-4-hydroxyphenyl-arsonic acid with dithionite and hypophosphorous acid, originally formulated as a diarsene (Scheme 1, top).^{3,4} Recently a mass spectrometric study gave the first evidence that Salvarsan mainly consists of cyclooligoarsanes (AsR)_n (R = 3-H₂N-4-HOC₆H₃; *n* = 3, 5; Scheme 1, iii).⁵ The first cyclotriarsane derivative was 4-methyl-1,2,6-triarsatrimethyl-2.2.1.0]-heptane (Fig. 1, A), a cage-compound in which the organic substituents are forced into an all-*cis* arrangement with respect to the As₃ ring.⁶ Treatment of K₂[As₂(^tBu)₂] with submolar amounts of ^tBuAsCl₂ in non-polar solvents afforded (As^tBu)₃ (Fig. 1, B), which after

tedious workup, was obtained in ca. 10% yield.⁷ In contrast, the reduction of FcAsCl₂ (Fc = ferrocenyl) with LiAlH₄ or Zn gives (AsFc)₃ in almost quantitative yield (Fig. 1, C).⁸ 1992 West and co-workers described a rather exotic example of a cyclotriarsane within a tricyclic structure (Fig. 1, D), which was synthesized by activation of As₃ with the disilene Si₂Mes₄.⁹ In addition, a metal-carbyne-substituted triarsirane [Tp*(CO)₂M≡C-As]₃ (M = Mo, W; Tp* = HB(3,5-Me₂-pyrazolyl)₃; Fig. 1, E) was afforded, in the cyclo-trimerization of arsenediyls of the type [Tp*(CO)₂M≡C-As].¹⁰

Recently, Kilian and co-workers constructed stable arsanylidene-phosphoranes through peri-substitution of an acenaphthene-unit.¹¹ Upon exposure to oxygen, the intramolecular phosphine-stabilization is removed and the free arsindenenes oligomerize to afford the respective cyclic tri- and tetraarsanes (Fig. 1, F). Oxidation of strontium and barium diarsanyldisiloxanes afforded a unique siloxane-bridged bis-As₃ tetracyclic compound (Fig. 1, G), in which all As atoms are silyl-substituted.¹² Despite their scarce representation in the literature cyclotriarsanes are interesting synthons in inorganic chemistry as evidenced by the utilization

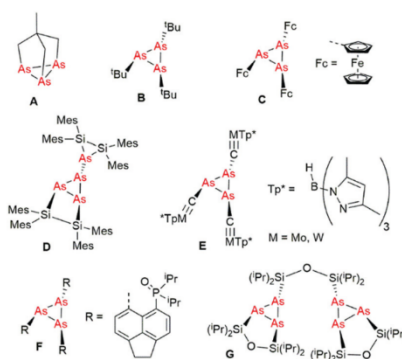


Fig. 1 Cyclotriarsanes reported in the literature A–G.

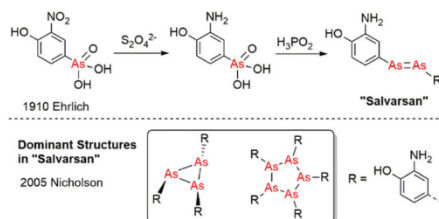
^a Leibniz Institut für Katalyse e.V. (LIKAT), A.-Einstein-Str.3a, 18059 Rostock, Germany. E-mail: christian.hering-junghans@catalysis.de

^b Anorganische Chemie, Institut für Chemie, Universität Rostock, A.-Einstein-Str.3a, 18059 Rostock, Germany

† Dedicated to Prof. Dr Uwe Rosenthal on the occasion of his 70th birthday.

‡ Electronic supplementary information (ESI) available: Detailed experimental, crystallographic and computational details. CCDC 2041965–2041971. For ESI and crystallographic data in CIF or other electronic format see DOI: 10.1039/d0cc07533g

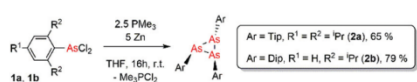
Communication



Scheme 1 Ehrlich's "Salvarsan" and dominant structures of "Salvarsan" revealed by mass spectrometry.

of (AsMe)₃ and (AsPh)₆ in organoarsenic chemistry.¹³ The reaction of (As(CF₃))₄ and [Pd(PPh₃)₄] gave the diarsene complex [(Ph₃P)₂Pd(As₂(CF₃)₂)] indicating a diarsene intermediate.¹⁴ When (As^tBu)₄ was heated in the presence of (AlCp^{*}), the polyhedral compound (Cp^{*}₃Al₃As₂) was obtained.¹⁵ Recently we outlined a methodology for the selective synthesis of aryl-substituted triphosphiranes (PAr)₃ (Ar = Mes = 2,4,6-Me₃-C₆H₂; Dip = 2,6-ⁱPr₂-C₆H₃, Tip = 2,4,6-ⁱPr₃-C₆H₂) and their fragmentation was observed in the reaction with [Cp₂Ti(C₂(SiMe₃)₂)] to give titanocene diarsene complexes selectively.¹⁶ Herein we report on the synthesis of novel cyclotriarsanes and discuss their reactivity towards [Cp₂Ti(C₂(SiMe₃)₂)], giving the first examples of titanocene diarsene complexes and towards N-heterocyclic carbenes (NHCs).

TipAsCl₃ (**1a**) was obtained in a 2-step synthesis from TipMgBr and AsCl₃ to generate the mixed dihaloarsane TipAsX₂ (with X = Cl, Br).¹⁷ Stirring TipAsX₂ with an excess of ZnCl₂ in THF, gave TipAsCl₃ as an analytically pure, highly viscous oil in 71% yield. Attempts to similarly synthesize DipAsCl₃ gave a product mixture, which could not be separated. Pure DipAsCl₃ (**1b**) was obtained in 33% yield by using Dip₂Mg (obtained from DipMgBr and an excess of 1,4-dioxane) in the transmetalation with two equivalents AsCl₃. In a next step **1a** and **1b** were reduced using a mixture of PMe₃ and Zn powder in THF at ambient temperature and after removal of the solvent, extraction with *n*-hexane and concentration to incipient crystallization, the cyclotriarsanes (AsTip)₃ (**2a**) and (AsDip)₃ (**2b**) were obtained as colorless crystalline solids in 65% and 79% yield, respectively (Scheme 2). The ¹H NMR spectra of **2a** and **2b** each show two sets of signals for two chemically inequivalent Tip and Dip substituents, with relative intensities of 1 : 2. No reduction of **1** was observed when using Zn powder in THF, indicating that PMe₃ is the active reductant.¹⁶ The Tip- and Dip-substituents have the correct steric profile to facilitate selective formation of the triarsiranes **2**. Both **2a** and **2b** show the expected *cis,trans,trans*-configuration of the substituents with respect to the central, minimally distorted As₃ ring, in which one of the As-As bonds [**2a** As2-As3 2.4767(2) Å; **2b** As1-As3 2.4769(15) Å]



Scheme 2 Synthesis of the triarsiranes **2a** and **2b**.

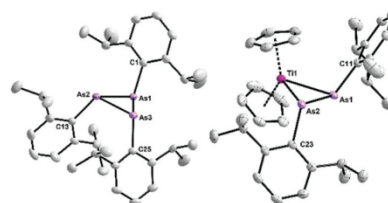
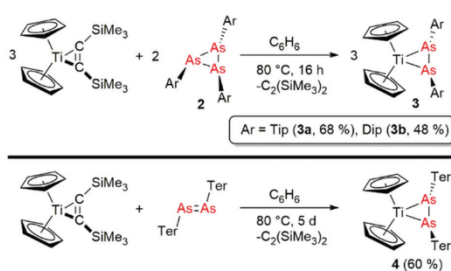


Fig. 2 ORTEP drawing of **2b** and **3b**. Ellipsoids at 50% probability at 150(2) K. Hydrogen atoms have been omitted for clarity. Selected bond lengths (Å) and angles (°): **2b** As1-As2 2.4514(2), As2-As3 2.4767(2), As1-As3 2.4530(2), As1-As2-As3 59.664(6), As2-As1-As3 60.609(7), As1-As3-As2 59.727(7); **3b** As1-As2 2.4572(3), Ti1-As1 2.6302(4), Ti1-As2 2.6428(4), As1-C11 1.9968(16), As2-C23 1.9914(17); As1-Ti1-As2 55.549(10).

is longer than the other two [**2a** 2.4514(2), 2.4530(2) Å; **2b** 2.4463(2), 2.4554(2) Å] (Fig. 2, left, for the structure of **2a** see ESI, ‡ Fig. S6).¹⁸

The observed bond lengths are longer than expected for As-As single bonds [$\sum r_{cov}(As-As) = 2.42$ Å],¹⁹ but in line with **F** [cf. Fig. 1, **F** 2.4388(8), 2.472(1), 2.502(1) Å].¹¹

Complexes of titanium with a coordinated diarsene ligand have not been reported to date. (AsFc)₃ was shown to react with [(PPh₃)₂Pt(C₂H₄)] in a 2 : 3 ratio to afford the diarsene-complex [(PPh₃)₂Pt(As₂Fc₂)].⁸ [²⁴Cp₂Zr(As₄)] was prepared from [²⁴Cp₂Zr(CO)₂] (²⁴Cp = C₅H₃^tBu₂) in the presence of As₄ and offers more insight into group 4 arsenic complexes.²⁰ In [Cp₂Ti(btmsa)] (btmsa = C₂(SiMe₃)₂) btmsa acts as a spectator ligand and its facile release under the respective reaction conditions generates the highly reactive 14-electron [Cp₂Ti] fragment *in situ*.²¹ When **2a** was combined with [Cp₂Ti(C₂(SiMe₃)₂)] in a 2 : 3 ratio in C₆D₆ (on a larger scale in C₆H₆) and the mixture was heated to 80 °C for 16 h the clean formation of a new species with a set of three septets in a 1 : 1 : 1 ratio and six doublets was detected in the ¹H NMR spectrum (Scheme 3, top). Dark red X-ray quality crystals of [Cp₂Ti(As₂Tip₂)] (**3a**) were obtained from a saturated *n*-hexane solution at -30 °C over a period of 24 h in 68% yield. In the same manner [Cp₂Ti(As₂Dip₂)] (**3b**) was obtained in 48% yield as dark red crystalline solid. UV-Vis spectroscopy revealed a broad absorption above 800 nm, which was identified by TD-DFT calculations as a LMCT-band



Scheme 3 Synthesis of the titanocene complexes **3** (top) and **4** (bottom).

originating from an As–As π^* orbital (HOMO) to a Ti-centered d-orbital (LUMO).¹⁸ Additionally, **3a** and **3b** show a characteristic absorption at 560 nm, which was identified as a HOMO–2 to LUMO transition (*cf.* ESI,† p. 51ff).¹⁸ The As–As distances in **3a** [2.4877(3) Å] and **3b** [2.4572(3) Å] are in the range of As–As single bonds ($\sum r_{\text{cov}}(\text{As–As}) = 2.42$ Å) (Fig. 2, right, for the structure of **3a** see ESI,† Fig. S11).^{19,21} The As–As distances in the three structurally characterized diarsene complexes $[\{\text{Fe}(\text{CO})_4\}\{\eta^2\text{–As}_2\text{H}_2\}]$ [2.3680(5) Å],²² $[\text{Fe}(\text{CO})_4(\eta^2\text{–C}_6\text{F}_5\text{As} = \text{AsC}_6\text{F}_5)_2]$ [2.388(7) Å],²³ and $[(\text{Ph}_3\text{P})_2\text{Pd}(\eta^2\text{–F}_3\text{CAs} = \text{AsCF}_3)]$ [2.341(1)]¹⁴ are considerably shorter and more representative of a diarsene complex, whereas in **3** a considerable charge transfer supposedly affords a Ti(IV) complex with a doubly reduced $[\text{ArAs–AsAr}]^{2-}$ ligand. The Ti–As distances are rather short [**3a** 2.6255(4); **3b** 2.6302(4), 2.6428(4) Å] when compared to the related species $[\text{Cp}_2\text{Ti}(\text{As}_3\text{Ph}_3)]$ (Ti–As 2.668(2), 2.655(2) Å)²⁴ or the Ti(IV) complex $[\text{Cl}_4\text{Ti}(\text{AsPh}_3)]$ (Ti–As 2.7465(13) Å).²⁵

To elucidate whether diarsenes are potential intermediates in the formation of **3**, the diarsene (AsTer)₂ was prepared from TerAsCl₂ using an excess PMe₃ and Zn in THF,²⁶ clearly showing that the steric profile of the aryl group is the major factor for the product distribution. Upon heating a mixture of (AsTer)₂ with $[\text{Cp}_2\text{Ti}(\text{C}_2(\text{SiMe}_3)_2)]$ in C₆D₆ for 5 days (Scheme 3, bottom), a new species showing one signal for the Cp-protons and six signals in a 1:1:1:1:1:1 ratio for the methyl groups of the *ortho*-methyl groups of the terphenyl moiety were observed in the ¹H NMR spectrum. The formation of the diarsene complex $[\text{Cp}_2\text{Ti}(\text{As}_2\text{Ter}_2)]$ (**4**) was confirmed by single crystal X-ray crystallography (Fig. 3, left). The As–As distance in **4** [2.4440(3) Å] is in the range of complexes **3** and considerably longer than in free (AsTer)₂ [2.276(3) Å],²⁷ thus more descriptive of an As–As single bond. The As–Ti–As angle [4 54.738(11) °] is narrower than in **3a** [56.558(11) °] and **3b** [55.549(10) °], while the Ti–As distances are minimally longer [4 2.6581(5), 2.6582(5) Å], in line with the decreased As–As distance in **4**. The formation of **4** shows that diarsenes are potential intermediates in the formation of **3a** and **3b**.

The electronic structures of compounds **2–4** were investigated by Density Functional Theory (DFT) and *ab initio* calculations (for a detailed description of all computations, please refer to the ESI,† p. S42ff). As expected, the As₃ systems **2**

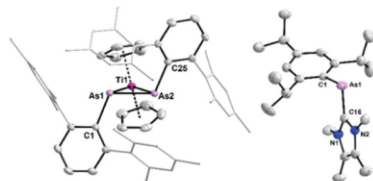


Fig. 3 ORTEP drawing of **4** (left) and **5aa** (right). Ellipsoids drawn at 50% probability at 150(2) K.²³ Hydrogen atoms have been omitted for clarity. Selected bond lengths (Å) and angles (°): **4** As1–As2 2.4440(3), Ti1–As1 2.6581(5), Ti1–As2 2.6582(5), As1–C1 2.004(2), As2–C25 2.004(2); As1–Ti1–As2 54.738(11); **5aa** As1–C16 1.909(3), As1–C1 1.989(3), N1–C16 1.361(4), N2–C16 1.360(4); C16–As1–C1 104.83(12), N2–C16–N1 105.0(2).

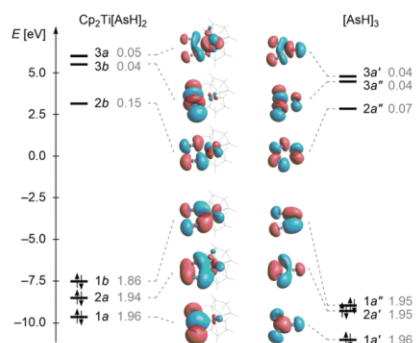
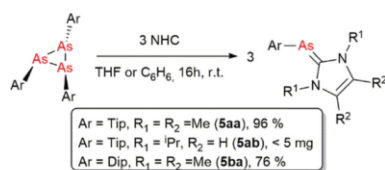


Fig. 4 Depiction of the Natural Orbitals (NOs) of the active space (CAS(6,6)/def2-TZVP) of the model systems $\text{Cp}_2\text{Ti}(\text{AsH}_2)_2$ (point group C_2) and $[\text{AsH}_3]$ (point group C_3). Results for **2b** and **3** can be found in the ESI,† p. S42ff. NO Occupation Numbers (NOONs) are given in grey, indicating no substantial multireference character of the wavefunctions. The weights of the depicted determinants are 89% and 93%, respectively.

display three covalent As–As bonds; their electronic structure is primarily interesting in comparison with the Ti complexes **3** (see below, *cf.* Fig. 4). The electronic structure of the latter was of particular interest, especially regarding the formal oxidation state of the Ti atom; that is, whether the complex is best described as a diarsene–Ti(II) complex, a diarsenediide–Ti(IV) complex, or possibly even a Ti(III) complex with a singly reduced diarsene ligand (and antiferromagnetic coupling between the unpaired electrons). To that end, Complete Active Space SCF (CASSCF) computations were performed.

The active space was chosen to include the relevant bonding and antibonding $\sigma(\text{As–As})$ and $\pi(\text{As–As})$ orbitals of the ligand, which interact with the d orbitals at the titanocene unit, resulting in 6 electrons in 6 orbitals, *i.e.* a CAS(6,6) calculation. Inspection of the Natural Orbitals (NOs) clearly implies that the three occupied orbitals are localized at the ligand to a significant extent (Fig. 4, left). The Ti–As bonding is mainly described by orbitals **2a** and **1b**, which involve the formal π and π^* orbitals of the $[\text{AsR}]_2$ moiety. As there is no significant static correlation between orbitals **1b** and **2b**, the biradical character is low ($\beta = 10\%$),^{28,29} and the complex is best described as a closed-shell Ti(IV) complex with a diarsenediide ligand. This agrees well with the observed structural parameters (see above). It is worth noting the similarities between the bonding orbitals of the TiAs₂ and As₃ ring system (Fig. 4), underlining the description of the Ti species as a metallacycle. Complementary Natural Bond Orbital (NBO) analyses (PBE-D3/def2-TZVP level of theory) resulted in a similar picture; there are two Ti–As σ bonds that are polarized towards the As atoms (NBO: As 62%, Ti 38%; see also Fig. S36–S38, ESI,†).¹⁸ The Wiberg bond indices for both Ti–As bonds amount to 0.87 (**3a**, **3b**), which is similar to the bond order of the As–As bond (0.85). This again points towards a formally doubly reduced diarsene moiety. It is worthy to note that the lone pairs (LPs) at the two arsenic atoms do not contribute significantly to the Ti–As bonding.

Scheme 4 Utilization of **3** for the synthesis of NHC arsinidene adducts **5**.

N-Heterocyclic carbene–arsinidene adducts were first reported by Arduengo *et al.* from the reaction of IMes (IMes = 1,3-dimesitylimidazol-2-ylidene) with (AsPh)₆ or (AsC₆F₅)₄, respectively.³⁰ In addition, NHC adducts of the parent arsinidene “AsH” have been recently synthesized.³¹ In contrast to NHC–phosphinidene adducts,³² the chemistry of their analogous arsenic compounds is considerably less developed.³³ To elucidate the potential as arsinidene transfer reagents **2a** and **2b** were combined with the carbenes IMe₄ (IMe₄ = 1,3,4,5-tetramethylimidazol-2-ylidene) or ⁱPr₂ (ⁱPr₂ = 1,3-diisopropylimidazol-2-ylidene) in THF or benzene at room temperature to afford TipAs = IMe₄ (**5aa**), TipAs = ⁱPr₂ (**5ab**) and DipAs = IMe₄ (**5ba**) as yellow solids (Scheme 4) and X-ray quality crystals of **5aa** and **5ab** were obtained (Fig. 3, right, for **5ab** see ESI† Fig. S19).

The As–C_{NHC} distances [**5aa** 1.909(3), **5ab** 1.9376(16) Å] are minimally shorter than expected for a single bond ($\sum r_{cov}(As-C) = 1.96$ Å),¹⁹ and in agreement with the As–C_{NHC} distance in IMes = AsPh [1.899(3) Å].³⁰ The C–As–C_{NHC} in **5ab** [94.97(7)°] is rather acute, whereas the angle for **5aa** [104.83(12)°] is wider, which is in line with the longer As–C_{NHC} in **5ab**. Lastly, NBO analyses were performed for the NHC-arsinidene adducts **5**. In accord with a Wiberg bond index of approx. 1.2 for the As–C_{NHC} bond, a polarized As–C π orbital is found, which is mainly localized at the As atom (**5aa**: As 75%, **5ab**: 67%; cf. Fig. S40 and S41, ESI†). Thus, the electronic structure is best described as an inversely polarized arsaalkene.

In summary we have outlined a straightforward route to aryl-substituted cyclotriarsanes and have shown their utility in the formation of the first diarsene complexes **3**. DFT and CASSCF calculations revealed that complexes **3** and **4** are best described as Ti(IV) complexes with a doubly reduced diarsendiide ligand. In addition, NHC arsinidene adducts **5** are conveniently prepared from the combination of **2** with NHCs. Currently studies are underway to uncover the structure of the active agents in Ehrlich's “Salvarsan”.

C. H.-J. thanks Prof. M. Beller for his support, the European Union for funding (H2020-MSCA-IF-2017 792177), and support by an Exploration Grant of the Boehringer Ingelheim Foundation (BIS) is acknowledged. We thank our technical and analytical staff, especially Dr A. Spannenberg for her support regarding X-ray analysis. J. B. wishes to thank the ITMZ at the University of Rostock for access to the Cluster Computer and especially M. Willert for technical support.

Conflicts of interest

There are no conflicts to declare.

Notes and references

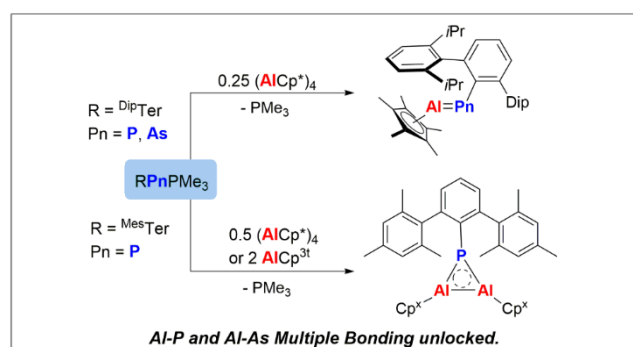
- 1 A. Michaelis and C. Schulte, *Ber. Dtsch. Chem. Ges.*, 1881, **14**, 912.
- 2 T. Wellnitz and C. Hering-Junghans, *Eur. J. Inorg. Chem.*, 2020, DOI: 10.1002/ejic.202000878, and references therein.
- 3 P. Ehrlich and A. Berthelm, *Ber. Dtsch. Chem. Ges.*, 1912, **45**, 756.
- 4 S. Riethmiller, *Bull. Hist. Chem.*, 1999, **24**, 28.
- 5 N. C. Lloyd, H. W. Morgan, B. K. Nicholson and R. S. Ronimus, *Angew. Chem., Int. Ed.*, 2005, **44**, 941.
- 6 G. Thiele, G. Zoubek, H. A. Lindner and J. Ellermann, *Angew. Chem., Int. Ed. Engl.*, 1978, **17**, 135.
- 7 M. Baudler and P. Bachmann, *Angew. Chem., Int. Ed. Engl.*, 1981, **20**, 123.
- 8 C. Spang, F. T. Edelmann, M. Noltemeyer and H. W. Roesky, *Chem. Ber.*, 1989, **122**, 1247.
- 9 R. P. Tan, N. M. Comerlato, D. R. Powell and R. West, *Angew. Chem., Int. Ed. Engl.*, 1992, **31**, 1217.
- 10 L. Weber, G. Dembeck, P. Lönneke, H.-G. Stammler and B. Neumann, *Organometallics*, 2001, **20**, 2288–2293.
- 11 B. A. Chalmers, M. Bühl, K. S. Athukorala Arachchige, A. M. Z. Slawin and P. Kilian, *J. Am. Chem. Soc.*, 2014, **136**, 6247.
- 12 C. Clobes, P. Jerabek, I. Nußbruch, G. Frenking and C. von Hänisch, *Eur. J. Inorg. Chem.*, 2015, 3264.
- 13 H. Imoto and K. Naka, *Arsenic-Containing Oligomers and Polymers*, in *Main Group Strategies towards Functional Hybrid Materials*, ed. T. Baumgartner and F. Jäkle, 2018, pp. 383–403.
- 14 J. Grobe, A. Karst, B. Krebs, M. Läge and E.-U. Würthwein, *Z. Anorg. Allg. Chem.*, 2006, **632**, 599.
- 15 C. K. F. von Hänisch, C. Uffing, M. A. Junker, A. Ecker, B. O. Kneisel and H. Schnöckel, *Angew. Chem., Int. Ed. Engl.*, 1996, **35**, 2875–2877.
- 16 A. Schumann, F. Reiß, H. Jiao, J. Rabeah, J.-E. Siewert, I. Krummenacher, H. Braunschweig and C. Hering-Junghans, *Chem. Sci.*, 2019, **10**, 7859–7867.
- 17 A. C. Behrle and J. R. Walensky, *Dalton Trans.*, 2016, **45**, 10042–10049.
- 18 Please refer to the ESI† for more information.
- 19 P. Pyykkö and M. Atsumi, *Chem. – Eur. J.*, 2009, **15**, 12770.
- 20 M. Schmidt, A. E. Seitz, M. Eckhardt, G. Balázs, E. V. Peresyphina, A. V. Virovets, F. Riedlberger, M. Bodensteiner, E. M. Zolnhofer, K. Meyer and M. Scheer, *J. Am. Chem. Soc.*, 2017, **139**, 13981.
- 21 T. Beveries, M. Haehnel and U. Rosenthal, *Catal. Sci. Technol.*, 2013, **3**, 18.
- 22 R. Rund, G. Balázs, M. Bodensteiner and M. Scheer, *Angew. Chem., Int. Ed.*, 2019, **58**, 16092.
- 23 P. S. Elmes, P. Leverett and B. O. West, *J. Chem. Soc. D*, 1971, 747b.
- 24 P. Mercado, A.-J. Dimas and A. L. Rheingold, *Angew. Chem., Int. Ed. Engl.*, 1987, **26**, 244.
- 25 T. Thomas, D. Pugh, I. P. Parkin and C. J. Carmalt, *Dalton Trans.*, 2010, **39**, 5325–5331.
- 26 R. C. Smith, P. Gantzel, A. L. Rheingold and J. D. Protasiewicz, *Organometallics*, 2004, **23**, 5124–5126.
- 27 B. Twamley, C. D. Sofield, M. M. Olmstead and P. P. Power, *J. Am. Chem. Soc.*, 1999, **121**, 3357–3367.
- 28 L. Salem and C. Rowland, *Angew. Chem., Int. Ed. Engl.*, 1972, **11**, 92.
- 29 E. Miliordos, K. Ruedenberg and S. S. Xantheas, *Angew. Chem., Int. Ed.*, 2013, **52**, 5736.
- 30 A. J. Arduengo, J. C. Calabrese, A. H. Cowley, H. V. R. Dias, J. R. Goerlich, W. J. Marshall and B. Riegel, *Inorg. Chem.*, 1997, **36**, 2151–2158.
- 31 A. Doddi, M. Weinhart, A. Hinz, D. Bockfeld, J. M. Goicoechea, M. Scheer and M. Tamm, *Chem. Commun.*, 2017, **53**, 6069–6072.
- 32 T. Krachko and J. C. Sloatweg, *Eur. J. Inorg. Chem.*, 2018, 2734.
- 33 A. Doddi, M. Peters and M. Tamm, *Chem. Rev.*, 2019, **119**, 6994–7112.

5.8 Isolable Phospha- and Arsaaluminenes

M. Fischer, S. Nees, T. Kupfer, J. T. Goettel, H. Braunschweig, C. Hering-Junghans

J. Am. Chem. Soc. **2021**, *143*, 11, 4106–4111.

DOI: 10.1021/jacs.1c00204



Reprinted (adapted) with permission from *J. Am. Chem. Soc.* **2021**, *143*, 11, 4106–4111.

Copyright 2021 American Chemical Society.

Isolable Phospha- and Arsaaluminenes

Malte Fischer,^{||} Samuel Nees,^{||} Thomas Kupfer, James T. Goettel, Holger Braunschweig,^{*} and Christian Hering-Junghans^{*}

Cite This: *J. Am. Chem. Soc.* 2021, 143, 4106–4111

Read Online

ACCESS |

Metrics & More

Article Recommendations

Supporting Information

ABSTRACT: The combination of $(\text{AlCp}^*)_4$, a source of monomeric $:\text{AlCp}^*$ at elevated temperatures, with $^{\text{Dip}}\text{TerPnPMe}_3$ (Pn = P, As), so-called pnicta-Wittig reagents, at 80 °C cleanly gives the pnictaaluminenes $^{\text{Dip}}\text{TerPnAlCp}^*$ with polarized Pn–Al double bonds and intramolecular stabilization through interactions of Al with a flanking aryl group of the terphenyl substituent on Pn. In contrast, using $^{\text{Mes}}\text{TerPPMe}_3$, the reaction with 2 equiv of $:\text{AlCp}^*$ or $:\text{AlCp}^*$ afforded the three-membered 2π -aromatic ring systems $^{\text{Mes}}\text{TerP}(\text{AlCp}^*)_2$ ($x = 3t, *$).

Heavier element–element multiple bonds had been long considered inaccessible,¹ and the so-called “double-bond rule” was formulated.^{2,3} Weaker p-orbital overlap along with increased intra- and interatomic Pauli repulsion are synthetically limiting factors,^{4,5} and in the 1980s the first species with Si=Si⁶ and P=P⁷ double bonds were reported. Heteroatomic double bonds are now well established between elements of group 14, 15, and 16⁸—recent examples include arsaaluminenes,⁹ phosphasilenes,¹⁰ or oxophosphonium cations.¹¹ The number of heteroatomic Al=E multiple bonds is still limited,^{12,13} and only recently the terminal aluminum-imides $\text{K}[\text{MesN}=\text{Al}(\text{O}(\text{SiMe}_2\text{NDip})_2)]$ ¹⁴ ($d(\text{Al}=\text{N}) = 1.7251(11)$ Å; Dip = 2,6-*i*-Pr₂C₆H₃) and $\text{K}[\text{DipN}=\text{Al}(\text{NON})]$ ¹⁵ ($d(\text{Al}=\text{N}) = 1.723(2)$ Å; NON = 4,5-bis-(NDip)-2,7-*t*-Bu₂-9,9-Me₂-xanthene) have been structurally characterized, obtained by the reaction of potassium aluminyls¹⁶ with MesN₃ or DipN₃, respectively. A neutral NHC-stabilized iminoalane with an Al–N distance of 1.705(2) Å was reported by Cui et al.¹⁷ Examples of unsupported aluminum phosphorus or arsenic multiple bonds have not been reported. Su et al. theoretically investigated compounds of the type R–P≡Al–R and concluded that “. . . sterically bulky ligands can greatly stabilize the R–P≡Al–R species”.¹⁸ Due to alternating Lewis acidic and Lewis basic centers, AlP species are prone to oligomerize. Oligomerization should be suppressed by either kinetic stabilization, acceptor stabilization of the group 15 element, or by intra- or intermolecular interaction of the Lewis acidic metal center with a donor. Lewis base stabilized variants of *cyclo*-1,3-diphospha-2,4-dialanes [RPAIH-(NMe₂)₂] (R = *Si*tBuPh₂, *i*Pr₃Si, Me₂(*i*PrMe₂C)Si) (Figure 1, A), formally the dimers of RPAIR’ have been prepared by the combination of silyl-substituted R₃Si–PH₂ with H₃Al–NMe₃.^{19,20} Attempts to generate the NHC-adducts of the corresponding phosphaaluminenes RP=Al(NHC)H afforded the bis-carbene adducts [RPAIH(NHC)]₂ (NHC = *i*Pr₂, BImY).²⁰ The base adducts of the lighter phosphaborenes are obtained when [Mes*PB(Tmp)]₂²¹ (Tmp = 2,2,6,6-tetramethylpiperidino) is heated to 100 °C in the presence of Ime₄ or DMAP (Figure 1, B1).²² Alternatively, the thermal

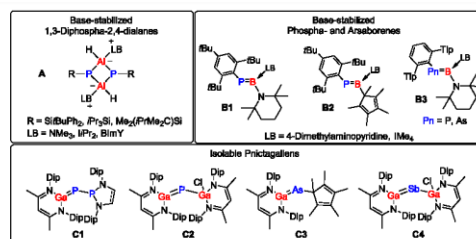


Figure 1. Examples of *cyclo*-diphosphadialanes (A), Lewis base stabilized pnictaborenes (B), and isolable pnictagallenes (C).

elimination of Me₃SiCl starting from Mes*(SiMe₃)PB(Cl)Cp* in the presence of DMAP or Ime₄ (Figure 1, B2) or treatment of $^{\text{Temp}}\text{TerPn}(\text{H})=\text{B}(\text{Br})(\text{Temp})$ (Pn = P, As; $^{\text{Temp}}\text{Ter}$ = 2,6-(2,4,6-*i*-Pr₃C₆H₂)₂-C₆H₃) with 2 equiv of DMAP afforded base-stabilized pnictaborenes (Figure 1, B3).^{23,24}

Phosphagallenes were recently reported, utilizing phosphanyl- or gallaphosphaketenes in the reaction with $(^{\text{Dip}}\text{Nacnac})\text{Ga}$ ($^{\text{Dip}}\text{Nacnac} = \text{HC}[\text{C}(\text{Me})\text{NDip}]_2$) facilitating CO cleavage and formation of $[(\text{S})\text{P}]-\text{P}=\text{Ga}(^{\text{Dip}}\text{Nacnac})$ ($[(\text{S})\text{P}] = (\text{H}_n\text{CNAr}^*)_2\text{P}$; $n = 1, 2$) or $(^{\text{Dip}}\text{Nacnac})\text{Ga}=\text{P}-\text{Ga}(\text{Cl})-(^{\text{Dip}}\text{Nacnac})$ (Figure 1, C1 and C2), respectively.^{25,26} When Cp*AsCl₂ was treated with 2 equiv $(^{\text{Dip}}\text{Nacnac})\text{Ga}$, the arsaaluminene $(^{\text{Dip}}\text{Nacnac})\text{Ga}=\text{AsCp}^*$ (Figure 1, C3) was obtained with concomitant formation of $(^{\text{Dip}}\text{Nacnac})\text{GaCl}_2$.²⁷ In contrast, $(^{\text{Dip}}\text{Nacnac})\text{Ga}=\text{Sb}-\text{Ga}(\text{Cl})(^{\text{Dip}}\text{Nacnac})$ (Figure 1, C4) was accessed by the reduction of the stable stibanyl radical $[(^{\text{Dip}}\text{Nacnac})\text{Ga}(\text{Cl})]_2\text{Sb}^\cdot$ with KC₈ at 25 °C.²⁸ In these

Received: January 7, 2021

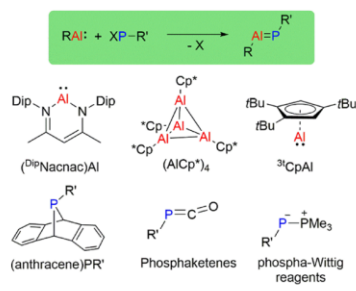
Published: March 10, 2021



systems the HOMO shows considerable π -back-donation from the pnictogen atom to a vacant p-orbital located on Ga.

One plausible strategy for the synthesis of phosphaluminenes is the combination of an Al(I) species with a phosphinidenoid compound RPX, in which X is an unreactive leaving group (Scheme 1). This is similar to the route applied by Powers and

Scheme 1. Synthetic Strategy toward Phosphaluminenes Using Al(I) Species and a Phosphinidene Precursor



Roesky in the reaction of $(D^{ip}Nacnac)E$ ($E = Al, Ga$) with $T^{ip}TerN_3$ to give the corresponding monomeric imides after N_2 -elimination.²⁹

$(AlCp^*)_4$ was first reported in 1991,^{30,31} and has been shown to dissociate into $:AlCp^*$ at elevated temperature.³² In this realm, the recently reported $:Al^{31}Cp$ ($^{31}Cp = 1,2,4-tBu_3-C_5H_2$) is noteworthy,³³ as well as the landmark monomeric β -diketiminato complex $(D^{ip}Nacnac)Al$,^{34,35} prepared in reproducibly high yields through transmetalation of $(D^{ip}Nacnac)Na$ with $(AlCp^*)_4$.³⁶ Recently, the monomeric alanediyli $(3,5-iPr-Ter)Al$ was synthesized by reduction of $(3,5-iPr-Ter)AlI_2$ with $Na/NaCl$.^{37,38} Possible phosphinidenoid compounds include $RP(anthracene)$ species, which have been shown to act as phosphinidene transfer agents,³⁹ for example in the iron- and fluoride-catalyzed phosphinidene transfer to styrenic olefins.⁴⁰ As mentioned before, phosphanylphosphaketenes R_2P-PCO are synthetic surrogates for phosphinidenes, which unlocked a pathway toward the stable singlet phosphinidene $[P]P$ ($[P] = (H_2CNAr^*)_2P$, $Ar^{**} = 2,6-bis[(4-tert-butylphenyl)methyl]-4-methylphenyl$).⁴¹ Additionally, facile ligand exchange of CO in $[SP]PCO$ for PR_3 , $CNAd$, $IiPr_2$, and $EtCAAC$ has been described.⁴² Phospho-Wittig reagents of the type $ArPPMe_3$ ($Ar = 2,4,6-tBu_3-C_6H_2$, Mes^* ; $2,6-Mes_2-C_6H_3$, Mes^*Ter ; $T^{ip}Ter$),^{43,44} have been shown to transfer the ArP -group to quinones,⁴⁵ when combined with $Cp_2Zr(PMe_3)_2$,⁴⁶ or to NHCs to give NHC phosphinidenes.⁴⁷

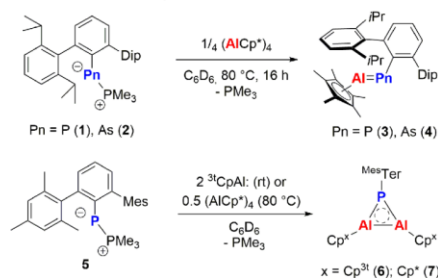
We now show the facile synthesis of the first phospho- and arsaaluminenes as stable compounds using $ArPnPM_3$ in combination with $(AlCp^*)_4$.

As a starting point the sterically crowded phospho- and arsa-Wittig reagents $D^{ip}TerPnPM_3$ ($Pn = P, 1$; $As, 2$; $D^{ip}Ter = 2,6-Dip_2C_6H_3$) were selected. In contrast to $ArPPMe_3$, there is only one arsa-Wittig reagent, $T^{ip}TerAsPM_3$.³⁸ The reduction of $D^{ip}TerAsCl_2$ with Zn/PM_3 in a 1/10/10 ratio in THF afforded **2** in 72% yield, and SC-XRD experiments showed a short $As-P$ bond [2.2224(5) Å] (Figure S5), in line with the formulation as an arsanilidene phosphorane.³⁹ When **1** or **2** was heated with 1 equiv of $^{31}CpAl$: at 80 °C in C_6D_6 ,³³ only decomposition of $^{31}CpAl$: and formation of elemental

aluminum were observed. As a second entry $(AlCp^*)_4$ was selected as an Al(I) synthon.³² DFT calculations at the PBE0-D3/def2SVP level of theory showed that the reaction between **1** or **2** and Cp^*Al : with concomitant release of PM_3 and formation of $D^{ip}TerPn=AlCp^*$ ($Pn = P, 3$; $As, 4$) is feasible ($\Delta_R G^\circ_{298} = -51.2$ (**3**); -60.9 kJ/mol (**4**)).

Combining **1** or **2** with $(AlCp^*)_4$ in a 4:1 ratio in C_6D_6 and heating to 80 °C for 2 h showed the appearance of a signal at -62.7 ppm in the ^{31}P NMR spectrum, indicating PM_3 release, and in the case of **1** at -203.9 ppm [cf. $Mes^*P(H)-Al(Cl)Mes^*$]⁴⁸ -133 ppm; $(D^{ip}Nacnac)Ga=P-Ga(Cl)-(D^{ip}Nacnac)$]²⁶ -245.8 ppm] a new P-containing species was detected along with unreacted **1** (Scheme 2, top). Heating was

Scheme 2. Synthesis of Pnictaaluminenes **3 and **4** and of the Three-Membered Ring Systems **6** and **7****



continued overnight, resulting in the full conversion of **1** and **2** and intensely purple or blue reaction mixtures, respectively. Extraction of the residue with *n*-pentane and placement in the freezer at -30 °C for 24 h afforded purple X-ray quality needles of $D^{ip}TerP=AlCp^*$ (**3**). Blue X-ray quality crystals of arsaaluminene **4** were obtained using a solvothermal approach. **3** and **4** (Figure 2) are isostructural, and the $Pn-Al$ distances [3 2.2113(6); 4 2.3084(4) Å; cf. $d(AlP)Tip_2Al-P(SiPh_3)Ad^{49}$ 2.342(2) Å; $d(AlAs)_{avg}(Mes^*Al-AsPh_3)^{50}$ 2.430 Å] are longer than the sum of the covalent radii for an $Pn=Al$ double bond ($\sum r_{cov}(P=Al) = 2.15$ Å; $(As=Al) 2.27$ Å).⁵¹

The P and As centers are dicoordinate with a narrower $C1-As1-Al1$ angle [107.64(4)°] compared to **3** [109.32(5)°]. The Al atoms show rather short contacts [3 $Al1-C7$ 2.9999(13); 4 $Al1-C19$ 3.0952(12) Å] to the *ipso*-C of the flanking Dip-groups, with an η^3 -coordinated Cp^* -group. The $C1-P1-Al1$ and $P1-Al1-Cl1$ [134.36(3)°] angles differ significantly from values predicted theoretically by Su et al. for the system $T^{ip}TerPAl^{T^{ip}Ter}[R-P-Al 121.3^\circ; P-Al-R 167.3^\circ]$, indicating the influence of the Cp^* -group in **3**. **3** and **4** can be stored in the glovebox as solids for at least one month and are thermally stable in solution at 85 °C in C_6D_6 for at least 3 days. In the 1H NMR spectra of **3** and **4**, three characteristic signals for the $D^{ip}Ter$ moieties are detected and gradually cooling a sample of **3** to -80 °C only resulted in line broadening (see Supporting Information). The Cp^* group on $Al1$ appears as a singlet signal at $\delta(^1H) = 1.49$ ppm in **3** and **4** indicating η^3 -coordination. The $Al-As$ deformation vibration in **4** at 514 cm^{-1} is red-shifted compared to the $Al-P$ stretch at 558 cm^{-1} in the IR spectrum. Investigation of the Kohn-Sham orbitals revealed rather small HOMO-LUMO gaps [3 3.564 eV; 4 3.419 eV]. The HOMOs show major contributions for polarized $Pn-Al$ π -bonds, whereas the HOMO-1 reveals $Pn-Al$ σ -bonds. The

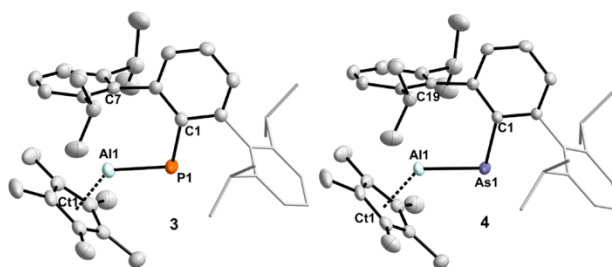


Figure 2. Molecular structures of **3** and **4**. ORTEPs drawn at 50% probability. Selected bond lengths (Å) and angles (deg) of **3**: P1–Al1 2.2113(6), Al1–C7 2.9999(13); C1–P1–Al1 109.32(5); **4**: As1–Al1 2.3084(4), Al1–C19 3.0952(12); C1–As1–Al1 107.64(4).

LUMO is best described as possessing Pn–Al σ^* character (Figures S28–29). The Wiberg Bond Index of 1.47 (**3**) and 1.46 (**4**) along with the NPA charges (Al: +1.34 (**3**), +1.31 (**4**); Pn: –0.37 (**3**), –0.31 (**4**)) further support polarized Al=Pn double bonds. NBO analyses show a polarized π -component (84.5% P, 84.9% As) in the Al=Pn bond and a lone pair of electrons at the pnictogen, which interacts with one of two lone p-type vacancies on Al. The bonding between Al and the Cp* is dominated by interactions of the Cp* π -system with the p-type vacancies at aluminum. TD-DFT calculations at the PBE0-D3/Def2SVP(benzene) level of theory show that the characteristic broad absorption in the visible region at $\lambda_{\text{max}} = 560$ nm (**3**), 590 nm (**4**) ($\lambda_{\text{max,calc}} = 525$ nm (**3**), 533 nm (**4**)) corresponds to a HOMO to LUMO (π – σ^*) transition.

Having isolated **3** and **4** we turned to $\text{M}^{\text{Mes}}\text{TerPPMe}_3$ (**5**) to elucidate the steric influence of the aryl group on P. We first combined $^3\text{CpAl}$: and **5** in a 1:1 ratio in C_6D_6 , and full conversion of $^3\text{CpAl}$: and a new species with a ^{31}P NMR signal at $\delta(^{31}\text{P}) = -79.7$ ppm was noted along with **5** in a 1:1 ratio. The reaction was repeated with **5** and $^3\text{CpAl}$: in a 1:2 ratio, which after slow evaporation of the solvent afforded yellow crystals of $\text{M}^{\text{Mes}}\text{TerP}(^3\text{CpAl})_2$ (**6**) (Scheme 2, bottom). Similarly, yellow crystalline $\text{M}^{\text{Mes}}\text{TerP}(\text{Cp}^*\text{Al})_2$ (**7**) (Figure 3),

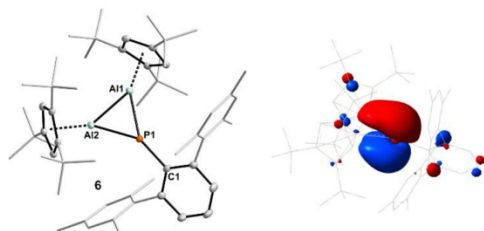


Figure 3. (Left) Molecular structure of **6**. ORTEPs drawn at 50% probability. (Right) Delocalized HOMO of **6** (isosurface plot at 0.04 au).

with a ^{31}P NMR shift of $\delta(^{31}\text{P}) = -116.4$ ppm, was obtained by heating a 2:1 mixture of **5** and $(\text{AlCp}^*)_4$ in C_6D_6 to 80 °C over a period of 36 h. LIFDI-MS studies showed fragmentation into $[\text{M}^{\text{Mes}}\text{TerPAlCp}^*]^+$ and $[\text{AlCp}^*]^+$ ($x = *$, 3t), and therefore, we believe that the formation of **6** and **7** proceeds via [2 + 1] cycloaddition reactions of transient $\text{M}^{\text{Mes}}\text{TerP}=\text{AlCp}^*$ (not observed by NMR spectroscopy) with a second equivalent of

AlCp^* . Our calculations indicated that such a [2 + 1] cycloaddition pathway is exergonic ($\Delta_{\text{R}}G_{298}^\ddagger = -80.5$ (**6**), -75.1 (**7**) kJ/mol). In the solid state, **6** (Figure 3) and **7** (Figure S23) exhibit nearly isosceles Al_2P triangles [Al1–Al2 2.5265(9) Å (**6**), 2.5016(12) Å (**7**); Al1–P1 2.3543(8) Å (**6**), 2.3249(13) Å (**7**); Al2–P1 2.3495(7) Å (**6**), 2.3304(14) Å (**7**)] with rather acute angles of ca. 60°, which agree well with the Al–Al distance [2.520(2) Å] in $\text{Na}_2[\text{M}^{\text{Mes}}\text{Ter}_3\text{Al}_3]$ with a presumably metalloaromatic Al_3 -ring.⁵² Particularly noteworthy is the presence of trigonal-planar phosphorus centers [$\Sigma = 359.7^\circ$ (**6**), 360.0° (**7**)]. True planarity is still considered a rare geometrical arrangement for P and is usually coupled to specific requirements: (i) presence of sterically demanding substituents; (ii) electronegative substituents at phosphorus; (iii) incorporation of phosphorus into (non)aromatic rings.^{53,54} The latter strategy has been exploited extensively in the chemistry of phospholes⁵⁵ and seems to be active in our Al_2P compounds as well. A direct correlation between the extent of planarization and the degree of π aromaticity of aluminum,^{56–59} and phosphorus⁶⁰ ring systems has been established. Thus, strong delocalization phenomena are presumably present in the Al_2P cores of **6** and **7**, as the HOMO of both compounds is of π symmetry spanning the Al_2P triangles (Figure 3); i.e., the two lone pair electrons of the phosphorus centers become delocalized upon interaction with the AlCp^* fragments, making **6** and **7** aromatic π systems, providing a sufficient driving force to promote its planarization. Strong aromaticity is confirmed by calculations of aromaticity descriptors. Indicators based on electronic criteria such as the multicenter indices *mc*-DI (multicenter delocalization index)⁶¹ or MCI⁶² have recently emerged as powerful tools for accurate aromaticity estimates.

With *mc*-DI values of 97.2 (**6**) and 102.6 (**7**), and MCI values of 773.1 (**6**) and 233.0 (**7**), respectively, the aromaticity of **6** and **7** outmatches that of common organic aromatics (cf. *mc*-DI: 20.5 (C_6H_6), 19.8 (NC_3H_3); MCI: 72.1 (C_6H_6), 66.0 (NC_3H_3)).⁶³ Similar findings have been reported for other all inorganic aromatics such as the Al_3^{2-} dianion (MCI: 258.3).^{64,65} We also calculated the nucleus-independent chemical shifts 1 Å above and orthogonal to the Al_2P ring plane ($\text{NICS}(1)_{\text{zz}}$)⁶⁶ and the original isotropic $\text{NICS}(0)_{\text{iso}}$ indices⁶⁷ of **6** and **7** as magnetic aromaticity descriptors. Again, moderate negative values for $\text{NICS}(1)_{\text{zz}}$ (–7.8 ppm (**6**), –7.5 ppm (**7**)) and $\text{NICS}(0)_{\text{iso}}$ (–22.1 ppm (**6**), –23.9 ppm (**7**), cf. $\text{Na}_2[(\text{GaH})_3]$ ⁶⁸ –15 ppm) verify the aromatic character of the Al_2P heterocycles, while the degree of π aromaticity is somewhat smaller than that in prototypic organic

π aromatics such as benzene (NICS(1)_{zz}: -29.5 ppm) or pyridine (NICS(1)_{zz}: -29.1 ppm). By contrast, remarkably large NICS(0)_{iso} values (cf. -8.9 ppm (C₆H₆), -7.6 ppm (NC₅H₅)) indicate significant contributions of the σ Al₂P framework in **6** and **7** to their net aromaticity (cf. HOMOs-1 and HOMOs-2).

We have shown the facile synthesis of phospho- and arsaaluminenes **3** and **4**, compounds with formal Al–Pnictogen double bonds, through combination of the Pn(I) sources ^{Dip}TerPnPMe₃ and (AlCp*)₄ in benzene at 80 °C. Using ^{Mes}TerPPMe₃ in combination with ³ⁱCpAl: or (AlCp*)₄, the π -aromatic three-membered ring systems ^{Mes}TerP(AlCp*)₂, **6** and **7** were obtained.

■ ASSOCIATED CONTENT

Supporting Information

The Supporting Information is available free of charge at <https://pubs.acs.org/doi/10.1021/jacs.1c00204>.

Experimental details for compounds ^{Dip}TerAsCl₂, **2**, **3**, **4**, **6**, and **7**, NMR and electronic spectral data, and computational details (PDF)

Accession Codes

CCDC 2054428–2054433 contain the supplementary crystallographic data for this paper. These data can be obtained free of charge via www.ccdc.cam.ac.uk/data_request/cif, or by emailing data_request@ccdc.cam.ac.uk, or by contacting The Cambridge Crystallographic Data Centre, 12 Union Road, Cambridge CB2 1EZ, UK; fax: +44 1223 336033.

■ AUTHOR INFORMATION

Corresponding Authors

Holger Braunschweig – Institut für Anorganische Chemie and Institute for Sustainable Chemistry & Catalysis with Boron, Julius-Maximilians-Universität Würzburg, Am Hubland 97074, Würzburg, Germany; orcid.org/0000-0001-9264-1726; Email: h.braunschweig@uni-wuerzburg.de

Christian Hering-Junghans – Leibniz Institut für Katalyse e.V. (LIKAT), 18059 Rostock, Germany; orcid.org/0000-0003-4937-2625; Email: christian.hering-junghans@katalyse.de

Authors

Malte Fischer – Leibniz Institut für Katalyse e.V. (LIKAT), 18059 Rostock, Germany; orcid.org/0000-0002-2806-1302

Samuel Nees – Institut für Anorganische Chemie and Institute for Sustainable Chemistry & Catalysis with Boron, Julius-Maximilians-Universität Würzburg, Am Hubland 97074, Würzburg, Germany

Thomas Kupfer – Institut für Anorganische Chemie and Institute for Sustainable Chemistry & Catalysis with Boron, Julius-Maximilians-Universität Würzburg, Am Hubland 97074, Würzburg, Germany

James T. Goettel – Institut für Anorganische Chemie and Institute for Sustainable Chemistry & Catalysis with Boron, Julius-Maximilians-Universität Würzburg, Am Hubland 97074, Würzburg, Germany; orcid.org/0000-0001-8120-3771

Complete contact information is available at: <https://pubs.acs.org/doi/10.1021/jacs.1c00204>

Author Contributions

^{||}M.F. and S.N. contributed equally.

Notes

The authors declare no competing financial interest.

■ ACKNOWLEDGMENTS

C.H.-J. thanks Prof. M. Beller for his support, and support by an Exploration Grant of the Boehringer Ingelheim Foundation (BIS) is acknowledged. We thank our technical and analytical staff for assistance, especially Dr. Anke Spannenberg for her support regarding X-ray analysis. We thank Lilyan Szych for her assistance with UV–vis measurements. C.H.-J. wishes to thank the ITMZ at the University of Rostock for access to the Cluster Computer and especially Malte Willert for technical support and Dr. Jonas Bresien for helpful discussions. J.T.G. thanks the Government of Canada for a Banting Fellowship and the Alexander von Humboldt Foundation for financial support. H.B. wishes to acknowledge financial support by the Deutsche Forschungsgemeinschaft, DFG. Dedicated to Rüdiger Beckhaus on the occasion of his 65th birthday.

■ REFERENCES

- (1) Dasent, W. E. Non-existent compounds. *J. Chem. Educ.* **1963**, *40* (3), 130.
- (2) Pitzer, K. S. Repulsive Forces in Relation to Bond Energies, Distances and Other Properties. *J. Am. Chem. Soc.* **1948**, *70* (6), 2140–2145.
- (3) Mulliken, R. S. Overlap Integrals and Chemical Binding. *J. Am. Chem. Soc.* **1950**, *72* (10), 4493–4503.
- (4) Kutzelnigg, W. Chemical Bonding in Higher Main Group Elements. *Angew. Chem., Int. Ed. Engl.* **1984**, *23* (4), 272–295.
- (5) Jacobsen, H.; Ziegler, T. Nonclassical double bonds in ethylene analogs: influence of Pauli repulsion on trans bending and pi-bond strength. A density functional study. *J. Am. Chem. Soc.* **1994**, *116* (9), 3667–3679.
- (6) West, R.; Fink, M. J.; Michl, J. Tetramesityldisilene, a Stable Compound Containing a Silicon-Silicon Double Bond. *Science* **1981**, *214* (4527), 1343.
- (7) Yoshifuji, M.; Shima, I.; Inamoto, N.; Hirotsu, K.; Higuchi, T. Synthesis and structure of bis(2,4,6-tri-tert-butylphenyl)diphosphene: isolation of a true phosphobenzene. *J. Am. Chem. Soc.* **1981**, *103* (15), 4587–4589.
- (8) Fischer, R. C.; Power, P. P. π -Bonding and the Lone Pair Effect in Multiple Bonds Involving Heavier Main Group Elements: Developments in the New Millennium. *Chem. Rev.* **2010**, *110* (7), 3877–3923.
- (9) Lee, V. Y.; Kawai, M.; Gapurenko, O. A.; Minkin, V. I.; Gornitzka, H.; Sekiguchi, A. Arsagermene, a compound with an -As = Ge < double bond. *Chem. Commun.* **2018**, *54* (78), 10947–10949.
- (10) Heider, Y.; Willmes, P.; Mühlhausen, D.; Klemmer, L.; Zimmer, M.; Huch, V.; Scheschke, D. A Three-Membered Cyclic Phosphasilene. *Angew. Chem., Int. Ed.* **2019**, *58* (7), 1939–1944.
- (11) Wünsche, M. A.; Witteler, T.; Dielmann, F. Lewis Base Free Oxophosphonium Ions: Tunable, Trigonal-Planar Lewis Acids. *Angew. Chem., Int. Ed.* **2018**, *57* (24), 7234–7239.
- (12) Franz, D.; Inoue, S. Advances in the development of complexes that contain a group 13 element chalcogen multiple bond. *Dalton Trans.* **2016**, *45* (23), 9385–9397.
- (13) Bag, P.; Weetman, C.; Inoue, S. Experimental Realisation of Elusive Multiple-Bonded Aluminium Compounds: A New Horizon in Aluminium Chemistry. *Angew. Chem., Int. Ed.* **2018**, *57* (44), 14394–14413.
- (14) Anker, M. D.; Schwamm, R. J.; Coles, M. P. Synthesis and reactivity of a terminal aluminium-imide bond. *Chem. Commun.* **2020**, *56* (15), 2288–2291.

- (15) Heilmann, A.; Hicks, J.; Vasko, P.; Goicoechea, J. M.; Aldridge, S. Carbon Monoxide Activation by a Molecular Aluminium Imide: C–O Bond Cleavage and C–C Bond Formation. *Angew. Chem., Int. Ed.* **2020**, *59* (12), 4897–4901.
- (16) Hicks, J.; Vasko, P.; Goicoechea, J. M.; Aldridge, S. The Alumanyl Anion: A New Generation of Aluminium Nucleophile. *Angew. Chem., Int. Ed.* **2021**, *60* (4), 1702–1713.
- (17) Li, J.; Li, X.; Huang, W.; Hu, H.; Zhang, J.; Cui, C. Synthesis, Structure, and Reactivity of a Monomeric Iminoalane. *Chem. - Eur. J.* **2012**, *18* (48), 15263–15266.
- (18) Lu, J.-S.; Yang, M.-C.; Su, M.-D. Aluminum-phosphorus triple bonds: Do substituents make AlP synthetically accessible? *Chem. Phys. Lett.* **2017**, *686*, 60–67.
- (19) Driess, M.; Kuntz, S.; Merz, K.; Pritzkow, H. Novel Molecular Clusters Having Aluminum-Phosphorus, Aluminum-Arsenic, and Gallium-Arsenic Skeletons, and Synthesis of an $Al_4As_4Li_4$ Rhombododecahedron. *Chem. - Eur. J.* **1998**, *4* (9), 1628–1632.
- (20) Kapitein, M.; Balmer, M.; Niemeier, L.; von Hänisch, C. Cyclic NHC-stabilized silylphosphinoalanes and -gallanes. *Dalton Trans.* **2016**, *45* (14), 6275–6281.
- (21) Arif, A. M.; Boggs, J. E.; Cowley, A. H.; Lee, J. G.; Pakulski, M.; Power, J. M. Production of a boraphosphene (RB:PR') in the vapor phase by thermolysis of a sterically encumbered diphosphadiboretane. *J. Am. Chem. Soc.* **1986**, *108* (19), 6083–6084.
- (22) Price, A. N.; Nichol, G. S.; Cowley, M. J. Phosphaborenes: Accessible Reagents for the Synthesis of C–C/P–B Isosteres. *Angew. Chem., Int. Ed.* **2017**, *56* (33), 9953–9957.
- (23) Price, A. N.; Cowley, M. J. Base-Stabilized Phosphinidene Boranes by Silylium-Ion Abstraction. *Chem. - Eur. J.* **2016**, *22* (18), 6248–6252.
- (24) Rivard, E.; Merrill, W. A.; Fettingter, J. C.; Power, P. P. A donor-stabilization strategy for the preparation of compounds featuring P = B and As = B double bonds. *Chem. Commun.* **2006**, No. 36, 3800–3802.
- (25) Wilson, D. W. N.; Feld, J.; Goicoechea, J. M. A Phosphanyl-Phosphagallene that Functions as a Frustrated Lewis Pair. *Angew. Chem., Int. Ed.* **2020**, *59* (47), 20914–20918.
- (26) Sharma, M. K.; Wölper, C.; Haberhauer, G.; Schulz, S., Multi-Talented Gallaphosphene for Ga–P–Ga Heteroallyl Cation Generation, CO₂ Storage, and C(sp³)–H Bond Activation. *Angew. Chem., Int. Ed.* **2020**, DOI: 10.1002/anie.202014381.
- (27) Helling, C.; Wölper, C.; Schulz, S. Synthesis of a Gallarsene {HC[C(Me)N-2,6-*i*-Pr₂-C₆H₃]₂}GaAsCp* Containing a Ga=As Double Bond. *J. Am. Chem. Soc.* **2018**, *140* (15), 5053–5056.
- (28) Ganesamoorthy, C.; Helling, C.; Wölper, C.; Frank, W.; Bill, E.; Cutsail, G. E.; Schulz, S. From stable Sb- and Bi-centered radicals to a compound with a Ga=Sb double bond. *Nat. Commun.* **2018**, *9* (1), 87.
- (29) Hardman, N. J.; Cui, C.; Roesky, H. W.; Fink, W. H.; Power, P. P. Stable, Monomeric Imides of Aluminum and Gallium: Synthesis and Characterization of [{HC(MeCDippN)₂}Mn-2,6-Trip₂C₆H₃] (M = Al or Ga; Dipp = 2,6-*i*-Pr₂C₆H₃; Trip = 2,4,6-*i*-Pr₃C₆H₃). *Angew. Chem., Int. Ed.* **2001**, *40* (11), 2172–2174.
- (30) Dohmeier, C.; Robl, C.; Tacke, M.; Schnöckel, H. The Tetrameric Aluminum(I) Compound [(Al(η^5 -C₅Me₅))₄]. *Angew. Chem., Int. Ed.* **1991**, *30* (5), 564–565.
- (31) Ganesamoorthy, C.; Loerke, S.; Gemel, C.; Jerabek, P.; Winter, M.; Frenking, G.; Fischer, R. A. Reductive elimination: a pathway to low-valent aluminium species. *Chem. Commun.* **2013**, *49* (28), 2858–2860.
- (32) Sitzmann, H.; Lappert, M. F.; Dohmeier, C.; Üffing, C.; Schnöckel, H. Cyclopentadienyl-derivate von Aluminium(I). *J. Organomet. Chem.* **1998**, *561* (1), 203–208.
- (33) Hofmann, A.; Tröster, T.; Kupfer, T.; Braunschweig, H. Monomeric Cp³Al(i): synthesis, reactivity, and the concept of valence isomerism. *Chem. Sci.* **2019**, *10* (11), 3421–3428.
- (34) Cui, C.; Roesky, H. W.; Schmidt, H.-G.; Noltemeyer, M.; Hao, H.; Cimpoesu, F. Synthesis and Structure of a Monomeric Aluminum(I) Compound [{HC(CMeNAr)₂}Al] (Ar = 2,6-*i*Pr₂C₆H₃): A Stable Aluminum Analogue of a Carbene. *Angew. Chem., Int. Ed.* **2000**, *39* (23), 4274–4276.
- (35) Li, X.; Cheng, X.; Song, H.; Cui, C. Synthesis of HC[(CBut)(NAr)]₂Al (Ar = 2,6-Pr₂C₆H₃) and Its Reaction with Isocyanides, a Bulky Azide, and H₂O. *Organometallics* **2007**, *26* (4), 1039–1043.
- (36) Kysliak, O.; Görls, H.; Kretschmer, R. Salt metathesis as an alternative approach to access aluminium(I) and gallium(I) β -diketiminates. *Dalton Trans.* **2020**, *49* (19), 6377–6383.
- (37) Queen, J. D.; Lehmann, A.; Fettingter, J. C.; Tuononen, H. M.; Power, P. P. The Monomeric Alanyl:AlAr^{Pr³} (Ar^{Pr³} = C₆H-2,6-(C₆H₂-2,4,6-Pr₃)₂-3,5-Pr₂): An Organoaluminum(I) Compound with a One-Coordinate Aluminum Atom. *J. Am. Chem. Soc.* **2020**, *142* (49), 20554–20559.
- (38) Hicks, J.; Juckel, M.; Paparo, A.; Dange, D.; Jones, C. Multigram Syntheses of Magnesium(I) Compounds Using Alkali Metal Halide Supported Alkali Metals as Dispersible Reducing Agents. *Organometallics* **2018**, *37* (24), 4810–4813.
- (39) Transue, W. J.; Velian, A.; Nava, M.; Garcia-Iriepa, C.; Temprado, M.; Cummins, C. C. Mechanism and Scope of Phosphinidene Transfer from Dibenzo-7-phosphanorbornadiene Compounds. *J. Am. Chem. Soc.* **2017**, *139* (31), 10822–10831.
- (40) Geeson, M. B.; Transue, W. J.; Cummins, C. C. Organoiron- and Fluoride-Catalyzed Phosphinidene Transfer to Styrenic Olefins in a Stereoselective Synthesis of Unprotected Phosphiranes. *J. Am. Chem. Soc.* **2019**, *141* (34), 13336–13340.
- (41) Liu, L.; Ruiz, D. A.; Munz, D.; Bertrand, G. A Singlet Phosphinidene Stable at Room Temperature. *Chem.* **2016**, *1* (1), 147–153.
- (42) Hansmann, M. M.; Bertrand, G. Transition-Metal-like Behavior of Main Group Elements: Ligand Exchange at a Phosphinidene. *J. Am. Chem. Soc.* **2016**, *138* (49), 15885–15888.
- (43) Shah, S. D.; Protasiewicz, J. 'Phospha-Wittig' reactions using isolable phosphoranylidene phosphines ArP = PR₃ (Ar = 2,6-Mes₂C₆H₃ or 2,4,6-*t*-Bu₃C₆H₂). *Chem. Commun.* **1998**, No. 15, 1585–1586.
- (44) Protasiewicz, J. D. Coordination-Like Chemistry of Phosphinidenes by Phosphanes. *Eur. J. Inorg. Chem.* **2012**, *2012* (29), 4539–4549.
- (45) Chen, X.; Smith, R. C.; Protasiewicz, J. D. Cycloaddition of phosphanylidene- σ -4-phosphoranes ArP = PMe₃ and quinones to yield 1,3,2-dioxophospholanes. *Chem. Commun.* **2004**, No. 2, 146–147.
- (46) Kilgore, U. J.; Fan, H.; Pink, M.; Urnezis, E.; Protasiewicz, J. D.; Mindiola, D. J. Phosphinidene group-transfer with a phospho-Wittig reagent: a new entry to transition metal phosphorus multiple bonds. *Chem. Commun.* **2009**, No. 30, 4521–4523.
- (47) Gupta, P.; Siewert, J.-E.; Wellnitz, T.; Fischer, M.; Baumann, W.; Beweries, T.; Hering-Junghans, C. Reactivity of Phospha-Wittig Reagents towards NHCs and NHOs. *Dalton Trans.* **2021**, *50*, 1838–1844.
- (48) Agou, T.; Ikeda, S.; Sasamori, T.; Tokitoh, N. Synthesis and Structure of Lewis-Base-Free Phosphinoalumane Derivatives. *Eur. J. Inorg. Chem.* **2016**, *2016* (5), 623–627.
- (49) Wehmschulte, R. J.; Ruhlandt-Senge, K.; Power, P. P. Synthesis and Characterization of Unassociated Aluminum Monophosphides. *Inorg. Chem.* **1994**, *33* (15), 3205–3207.
- (50) Wehmschulte, R. J.; Power, P. P. Reactions of (H₂AlMes*)₂ (Mes* = 2,4,6-*t*-Bu₃C₆H₂) with H₂EAr (E = N, P, or As; Ar = aryl): Characterization of the Ring Compounds (Mes*AlNPh)₂ and (Mes*AlEPh)₃ (E = P or As). *J. Am. Chem. Soc.* **1996**, *118* (4), 791–797.
- (51) Pyykkö, P.; Atsumi, M. Molecular Double-Bond Covalent Radii for Elements Li–E112. *Chem. - Eur. J.* **2009**, *15* (46), 12770–12779.
- (52) Wright, R. J.; Brynda, M.; Power, P. P. Synthesis and Structure of the "Dialuminyne" Na₂[Ar'AlAlAr'] and Na₂[(Ar'Al)₂]: Al–Al Bonding in Al₂Na₂ and Al₃Na₂ Clusters. *Angew. Chem., Int. Ed.* **2006**, *45* (36), 5953–5956.
- (53) Bouhadir, G.; Bourissou, D. Unusual geometries in main group chemistry. *Chem. Soc. Rev.* **2004**, *33* (4), 210–217.

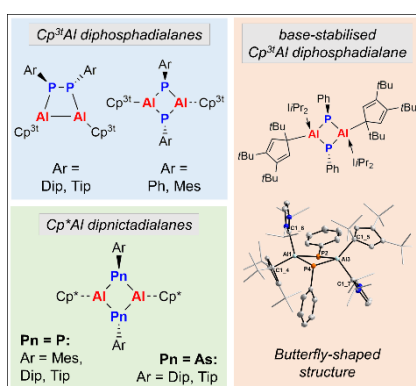
- (54) Izod, K.; Rayner, D. G.; El-Hamruni, S. M.; Harrington, R. W.; Baisch, U. Stabilization of a Diphosphagermylene through $p\pi-p\pi$ Interactions with a Trigonal-Planar Phosphorus Center. *Angew. Chem., Int. Ed.* **2014**, *53* (14), 3636–3640.
- (55) Zagidullin, A. A.; Bezishko, I. A.; Miluykov, V. A.; Sinyashin, O. G. Phospholes - Development and Recent Advances. *Mendeleev Commun.* **2013**, *23* (3), 117–130.
- (56) Yoshida, K.; Furuyama, T.; Wang, C.; Muranaka, A.; Hashizume, D.; Yasuike, S.; Uchiyama, M. Aluminepin: Aluminum Analogues of Borepin and Gallepin. *J. Org. Chem.* **2012**, *77* (1), 729–732.
- (57) Nakamura, T.; Suzuki, K.; Yamashita, M. An Anionic Aluminabenzene Bearing Aromatic and Ambiphilic Contributions. *J. Am. Chem. Soc.* **2014**, *136* (26), 9276–9279.
- (58) Thompson, E. J.; Myers, T. W.; Berben, L. A. Synthesis of Square-Planar Aluminum(III) Complexes. *Angew. Chem., Int. Ed.* **2014**, *53* (51), 14132–14134.
- (59) Bass, T. M.; Carr, C. R.; Sherbow, T. J.; Fettinger, J. C.; Berben, L. A. Syntheses of Square Planar Gallium Complexes and a Proton NMR Correlation Probing Metalloaromaticity. *Inorg. Chem.* **2020**, *59* (18), 13517–13523.
- (60) Keglevich, G.; Böcskei, Z.; Keserü, G. M.; Újszászy, K.; Quin, L. D. 1-(2,4,6-Tri-*tert*-butylphenyl)-3-methylphosphole: A Phosphole with a Significantly Flattened Phosphorus Pyramid Having Pronounced Characteristics of Aromaticity. *J. Am. Chem. Soc.* **1997**, *119* (22), 5095–5099.
- (61) Giambiagi, M.; de Giambiagi, M. S.; Mundim, K. C. Definition of a multicenter bond index. *Struct. Chem.* **1990**, *1* (5), 423–427.
- (62) Giambiagi, M.; de Giambiagi, M. S.; dos Santos Silva, C. D.; de Figueiredo, A. P. Multicenter bond indices as a measure of aromaticity. *Phys. Chem. Chem. Phys.* **2000**, *2* (15), 3381–3392.
- (63) Nees, S.; Kupfer, T.; Hofmann, A.; Braunschweig, H. Planar Cyclopenten-4-yl Cations: Highly Delocalized π Aromatics Stabilized by Hyperconjugation. *Angew. Chem., Int. Ed.* **2020**, *59* (42), 18809–18815.
- (64) Feixas, F.; Matito, E.; Duran, M.; Poater, J.; Solà, M. Aromaticity and electronic delocalization in all-metal clusters with single, double, and triple aromatic character. *Theor. Chem. Acc.* **2011**, *128* (4), 419–431.
- (65) Feixas, F.; Matito, E.; Poater, J.; Solà, M. Quantifying aromaticity with electron delocalisation measures. *Chem. Soc. Rev.* **2015**, *44* (18), 6434–6451.
- (66) Fallah-Bagher-Shaidaei, H.; Wannere, C. S.; Corminboeuf, C.; Puchta, R.; Schleyer, P. V. R. Which NICS Aromaticity Index for Planar π Rings Is Best? *Org. Lett.* **2006**, *8* (5), 863–866.
- (67) Schleyer, P. V. R.; Maerker, C.; Dransfeld, A.; Jiao, H.; van Eikema Hommes, N. J. R. Nucleus-Independent Chemical Shifts: A Simple and Efficient Aromaticity Probe. *J. Am. Chem. Soc.* **1996**, *118* (26), 6317–6318.
- (68) Xie, Y.; Schreiner, P. R.; Schaefer, H. F.; Li, X.-W.; Robinson, G. H. Are Cyclogallenes $[M_2(GaH)_2]$ ($M = Li, Na, K$) Aromatic? *J. Am. Chem. Soc.* **1996**, *118* (43), 10635–10639.

5.9 Cyclo-Dipnictadialanes

S. Nees, F. Fantuzzi, T. Wellnitz, M. Fischer, J.-E. Siewert, J. T. Goettel, A. Hofmann, M. Härterich, H. Braunschweig, C. Hering-Junghans

Angew. Chem. Int. Ed. **2021**, *60*, 24318–24325.

DOI: 10.1002/anie.202111121



Reprinted (adapted) with permission from *Angewandte Chemie International Edition*.

Copyright 2021 John Wiley and Sons. License number 5247730950384.

Main Group Chemistry

Cyclo-Dipnictadialanes

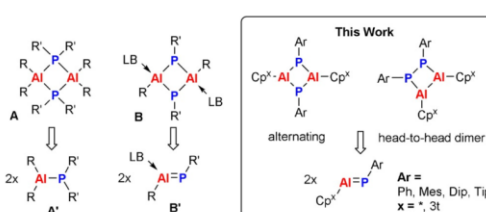
Samuel Nees[†], Felipe Fantuzzi[†], Tim Wellnitz, Malte Fischer, Jan-Erik Siewert, James T. Goettel, Alexander Hofmann, Marcel Härterich, Holger Braunschweig,* and Christian Hering-Junghans*

Dedicated to Professor Hansgeorg Schnöckel on the occasion of his 80th birthday

Abstract: Using the Al^I precursor Cp^xAl in conjunction with triphosphiranes (PAr)₃ (Ar = Mes, Dip, Tip) we have succeeded in preparing Lewis base-free cyclic diphosphadialanes with both the Al and P atoms bearing three substituents. Using the sterically more demanding Dip and Tip substituents the first 1,2-diphospha-3,4-dialuminacyclobutanes were obtained, whereas with Mes substituents [Cp^xAl(μ-PMes)]₂ is formed. This divergent reactivity was corroborated by DFT studies, which indicated the thermodynamic preference for the 1,2-diphospha-3,4-dialuminacyclobutane form for sterically more demanding groups on phosphorus. Using Cp^xAl we could extend this concept to the corresponding cyclic diarsadialanes [Cp^xAl(μ-AsAr)]₂ (Ar = Dip, Tip) and additionally add the phosphorus variants [Cp^xAl(μ-PAr)]₂ (P = Mes, Dip, Tip). The reactivity of one variant [Cp^{3t}Al(μ-PPh)]₂ towards NHCs was tested and resulted in double NHC-stabilised [Cp^{3t}-(LiPr₂)Al(μ-PPh)]₂.

Introduction

Heterocycles composed of phosphorus and the group 13 elements have been first reported by Davidson and Brown, who accidentally synthesised the trimer of Me₂Al–PMe₂ (Type A', Scheme 1), [Me₂AlPMe₂]₃.^[1] A growing interest in the use of single-source precursors for metalorganic chemical vapor deposition (MOVCD), for making group 13/15 semiconducting materials, sparked the development of cyclic heteroatomic group 13/15 compounds. Among the early examples, Cowley and Jones reported the aluminium and gallium cycles [iBu₂AlP(H)SiPh₃]₂ (Type A, Scheme 1)^[2] and [Me₂GaPzBu₂]₂,^[3] respectively. In these systems both phosphorus and the group 13 element are four-coordinate, and these are therefore the dimers of the respective phosphinoalanes and -gallanes. Pioneering work by Scheer et al. has



Scheme 1. Known Al/P ring systems (A and B) and their respective monomers (A' and B') (left). Two potential dimers of phosphoaluminanes investigated in this study (right).


revealed that the parent phosphinoalane H₂Al–PH₂ can be intercepted by using Lewis bases (LB) and Lewis acids (LA) on aluminium and phosphorus, respectively.^[4] Dehydrogenative trimerisation in CH₂Cl₂ solution afforded the six-membered species [(CO₂W)P(H)–Al(H)NMe₂]₃, which transforms into a bicyclic species upon further loss of H₂.^[5] By judicious choice of a sterically demanding (kinetically stabilising) LB, e.g., IDip₂ (IDip₂ = (HCNDip)₂C, Dip = 2,6-iPr₂C₆H₃), the first only LB-stabilised parent compounds IDip₂H₂EPnH₂ (E = Al, Ga; Pn = P,^[6] As^[7]) have recently been realised. In general, dimeric species of the type [R₂Al–PR'₂]₂ (A, Scheme 1) are obtained by condensation reactions. The driving force in these reactions is the formation of volatile by-products with thermodynamically stable bonds (e.g., H₂, alkanes, silanes, halosilanes).^[8] In particular, the extrusion of H₂ takes advantage of the protic and hydridic nature of the P–H^{δ+} and Al–H^{δ-} bonds, respectively.^[9]


In contrast, the formally doubly bonded pnictatrielenes RE=PnR' (E = Al, Ga; Pn = P, As, Sb) have eluded facile synthesis until recently. Phospha- and arsaaluminenes were

^[*] M. Sc. S. Nees,^[†] Dr. F. Fantuzzi,^[†] Dr. J. T. Goettel, Dr. A. Hofmann, M. Sc. M. Härterich, Prof. Dr. H. Braunschweig
 Institut für Anorganische Chemie
 Julius-Maximilians-Universität Würzburg
 Am Hubland, 97074 Würzburg (Germany)
 and
 Institute for Sustainable Chemistry & Catalysis with Boron
 Julius-Maximilians-Universität Würzburg
 Am Hubland, 97074 Würzburg (Germany)
 E-mail: h.braunschweig@uni-wuerzburg.de
 Dr. F. Fantuzzi^[†]
 Institut für Physikalische und Theoretische Chemie
 Julius-Maximilians-Universität Würzburg
 Emil-Fischer-Strasse 42, 97074 Würzburg (Germany)

T. Wellnitz, Dr. M. Fischer, M. Sc. J.-E. Siewert,
 Dr. C. Hering-Junghans
 Leibniz Institut für Katalyse e.V. (LIKAT)
 A.-Einstein-Strasse 3a, 18059 Rostock (Germany)
 E-mail: christian.hering-junghans@catalysis.de

^[†] These authors contributed equally to this work.

 Supporting information and the ORCID identification number(s) for the author(s) of this article can be found under:
<https://doi.org/10.1002/anie.202111121>.

 © 2021 The Authors. Angewandte Chemie International Edition published by Wiley-VCH GmbH. This is an open access article under the terms of the Creative Commons Attribution Non-Commercial License, which permits use, distribution and reproduction in any medium, provided the original work is properly cited and is not used for commercial purposes.

prepared using a Cp*Al for PMe₃ exchange starting from the pnicta-Wittig reagents ^{Dip}TerPnPMe₃ (^{Dip}Ter = 2,6-Dip₂C₆H₃, Pn = P, As) and (Cp*Al)₄ to give ^{Dip}TerPnPAlCp* (Pn = P (C1), As (C2), Scheme 2) as base-free monomeric compounds.^[10] The corresponding phosphagallenes were synthesised using phosphanyl- or gallaphosphaketenes in the reaction with (^{Dip}Nacnac)Ga (^{Dip}Nacnac = HC[C(Me)NDip]₂) facilitating CO cleavage and formation of [(S)P]–P–Ga(^{Dip}Nacnac) ([[(S)P] = (H,CNDip)₂P; n = 1, 2) (C3, Scheme 2)^[11] or (^{Dip}Nacnac)Ga=P–Ga(Cl)(^{Dip}Nacnac) (C4, Scheme 2)^[12] respectively. The arsgallene (^{Dip}Nacnac)Ga=AsCp* (C6, Scheme 2) was obtained when Cp*AsCl₂ was reacted with two equiv of (^{Dip}Nacnac)Ga.^[13] Moreover, the stibagallene (^{Dip}Nacnac)Ga=Sb–Ga(Cl)(^{Dip}Nacnac) (C5, Scheme 2) has been reported.^[14] In all these doubly bonded species the E–Pn (E = Al, Ga; Pn = P, As, Sb) multiple bond is highly polarised towards the group 15 element.

Due to their Lewis-acidic group 13 centre and electron-rich pnictogen centre, E–Pn multiple bonds are prone to oligomerisation. LB-stabilised variants of cyclo-1,3-diphospha-2,4-dialanes (**B**, Scheme 1), formally the dimers of LB-coordinated RP=AlR' (**B'**, Scheme 1), are known and were synthesised from silyl-substituted phosphanes R₃Si–PH₂ and H₂AlNMe₃, giving after dehydrocoupling the four-membered heterocycle [RPAIH(NMe₃)₂] (R = Si*t*BuPh₂, *i*Pr₂Si, Me₂–(*i*PrMe₂C)Si). Attempts to generate the NHC-adduct of the corresponding phosphaalumene (RP=Al(NHC)H) by addition of a free carbene to the four-membered ring resulted in base-exchange and formation of the respective bis-carbene adducts [RPAIH(NHC)]₂ (NHC = (HCN*t*Pr)₂C, *i*Pr₂).^[15] The reaction of Mes*AlH₂ (Mes* = 2,4,6-*t*Bu₃C₆H₃) with H₂EPh (E = P, As) in a 1:1 ratio at 160 °C afforded under H₂-elimination the trimers of Mes*Al=EPh (Mes*AlPPh₃) and (Mes*AlAsPh)₃,^[16] respectively, which are formal heavier analogues of borazine. Four-membered 1,3-diphospha-2,4-diboretanes, the boron congeners of **B** (Scheme 1), have been reported,^[17] mostly originating from unsuccessful attempts to access monomeric RP=BR species.^[18] These phosphorus–boron heterocycles contain pyramidalised phosphorus atoms, making them potential ligands for transition metals.^[17a,19] The related ring systems [RE(μ-PR'₂)₂] (E = B,^[20] R = *t*Bu, R' = *i*Pr; E = Al,^[21] R = Pr*t*Bu₂, R' = *t*Bu) with formally three

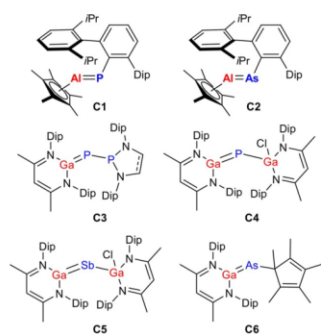
coordinate B and Al centres, respectively, have been shown to be biradicals. The cyclo-1,3-dipnicta-2,4-dialanes in which the group 13 centre is not stabilised by a Lewis-base have eluded facile synthesis to date. Herein, we close this gap and show that using cyclo-tripnictanes of the type Pn₃Ar₃ (Pn = P,^[22] As,^[23] Ar = 2,4,6-Me₃C₆H₂, Mes; Dip; 2,4,6-*i*Pr₃C₆H₂, Tip) in conjunction with the Al^I synthons (Cp*Al),^[24] and Cp^{3t}Al (Cp^{3t} = 1,2,4-*t*Bu₃C₅H₂),^[25] four-membered heterocycles with group 13 and 15 centres bearing three substituents, respectively, become synthetically feasible. Interestingly, two distinct forms were obtained, for example, the expected cyclo-1,3-dipnicta-2,4-dialanes [Cp*Al(μ-PnAr)]₂ (x = *, 3t) and the head-to-head dimers 1,2-diphospha-3,4-dialuminacyclobutanes. The experimental findings were corroborated by DFT-studies shedding light on the divergent reactivity of differently substituted precursors.

Results and Discussion

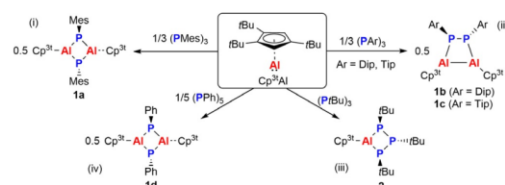
Diphosphadialanes from Cp^{3t}Al and (PR)₃/(PAr)₃

Triphosphiranes (PR)₃ and cyclo-oligophosphanes are, in general, the formal oligomers of phosphinidenes.^[26] Especially (PhP)₃ has been shown to react with NHCs to give NHC phosphinidene adducts of the type NHC=PPh₃,^[27] by formal phosphinidene transfer. We thus hypothesised that the combination of three equiv of Cp^{3t}Al with (ArP)₃ (Ar = Mes, Dip, Tip) would facilitate formation of Cp^{3t}Al=PAR, which might exist either in its monomer form or as a dimeric cyclo-diphosphadialane (Scheme 3).

At first, we monitored the reaction of (MesP)₃ with three equiv of Cp^{3t}Al in C₆D₆ at room temperature.^[28] This resulted in an initial colour change to orange and after a few minutes a yellow solution was obtained, which showed one signal in the ³¹P NMR spectrum at δ(³¹P) = –174.3 ppm and full consumption of (MesP)₃ was noted. In the ¹H NMR spectrum four characteristic signals were detected in the alky region, indicative of a Mes to Cp^{3t} ratio of 1:1. X-ray quality crystals of this compound were grown from a saturated toluene solution at –30 °C and confirmed the formation of [Cp^{3t}Al(μ-PMes)]₂ (**1a**). It needs to be pointed out that **1a** precipitates from C₆D₆ solutions after 30 minutes, therefore precluding collection of satisfactory ¹³C NMR data. We therefore switched to more polar NMR solvents, but even using C₆D₃Br the compound could not be redissolved. We next turned to (DipP)₃ and (TipP)₃, with bulkier aryl groups. When



Scheme 2. Known base-free pnictatrielenes (C1–C6).



Scheme 3. Reactivity of the alanediyli Cp^{3t}Al towards triphosphiranes (reactions i, ii, and iv) and a cyclo-pentaphosphane (ii).

combining the respective triphosphirane with three equiv of $\text{Cp}^{\text{3}}\text{Al}$, a gradual colour change of the reaction mixture to orange was observed, accompanied by the precipitation of a microcrystalline red solid. In both cases broad, unresolved multiplet resonances at ca. -117 ppm were detected in the ^{31}P NMR spectrum. Recrystallisation of the red microcrystalline solid from C_6H_6 ($\text{Ar} = \text{Dip}$) or slow evaporation of a saturated toluene solution ($\text{Ar} = \text{Tip}$) afforded X-ray quality crystals, which showed that $[\text{Cp}^{\text{3}}\text{AlPAR}]_2$ ($\text{Ar} = \text{Dip}$ (**1b**), Tip (**1c**)) had formed, although in this case the first 1,2-diphospha-3,4-dialuminacyclobutanes were obtained. This is reminiscent of the reactivity of two equiv of $^{\text{Dip}}\text{TerGa}$ with $\text{ToIN}=\text{NTol}$ ($\text{Tol} = 4\text{-Me-C}_6\text{H}_4$), giving the corresponding 1,2-diaza-3,4-digallacyclobutanes $[\text{Dip}^{\text{TerGaNTol}}]_2$.^[29] This was rationalised by initial addition of ArGa to give a three-membered N_2Ga ring system followed by insertion of a second ArGa , which then affords $[\text{Dip}^{\text{TerGaNTol}}]_2$. Consequently, diphosphenes were considered to be potential intermediates in the formation of **1b** and **1c**. In a related study we have shown that $(\text{TipP})_2$ reacted with $\text{Cp}_2\text{Ti}(\text{btmsa})$ to give the corresponding formal diphosphene complexes $[\text{Cp}_2\text{Ti}(\text{P}_2\text{Tip}_2)]$ selectively.^[22] Moreover, we have recently shown that the diphosphene $\text{DipP}=\text{PDip}$ can be obtained in the PEt_3 -catalysed reductive coupling reaction of DipPBr_2 using Zn as a sacrificial reductant.^[30] We therefore treated $(\text{DipP})_2$ with two equiv of $\text{Cp}^{\text{3}}\text{Al}$ and noted an immediate colour change of the reaction mixture to deep orange, and the formation of **1b** was ascertained by detection of the broad ^{31}P NMR resonance at $\delta(^{31}\text{P}) = -117$ ppm, as well as by cell determination of X-ray quality crystals precipitating from the reaction mixture. Similarly to **1a**, comprehensive characterisation of **1b** and **1c** by multi-nuclear NMR spectroscopy is hampered by its poor solubility in common NMR solvents, such as C_6D_6 , C_7D_8 , thf-d_8 or even $\text{C}_6\text{D}_5\text{Br}$. LIFDI-MS studies showed the expected molecular ion peaks. **1a-c** crystallise in the triclinic space group $P\bar{1}$ with two molecules in the unit cell (Figure 1).^[28] **1a** is situated on a crystallographically imposed

centre of inversion, resulting in a central Al_2P_2 rectangle with alternating P and Al atoms and P–Al distances of 2.3176(7) and 2.3317(7) Å, respectively, which agrees well with the six-membered species $(\text{Mes}^*\text{AlPPh})_3$ [cf. $d_{\text{avg}}(\text{Al-P}) = 2.328(3)$ Å].^[16] The angles at aluminium [$90.11(2)^\circ$] and phosphorus [$89.89(2)^\circ$] are nearly identical and the Mes groups on P are *trans*-oriented with respect to the Al_2P_2 plane. The Al–C_{Cp3} distances range from 2.2455(17) to 2.3584(18) Å, which renders the Cp^{3} group η^5 -coordinated. In contrast to **1a**, **1b** and **1c** show a puckered 1,2-P₂-3,4-Al₂ four-membered ring which is folded along the $\text{Al1}\cdots\text{P2}$ axis by ca. 17° . The P–P [**1b** 2.1677(9) Å; **1c** 2.1676(4) Å] bonds are contracted and closer to a single bond [cf. $(\text{DipP})_2$ 2.0293(7); $(\text{TipPBr})_2$ 2.2402(8)]. In contrast the Al–Al distances [**1b** 2.6947(11) Å; **1c** 2.6933(5) Å] are rather long [cf. $[\text{Al}(\text{CH}(\text{SiMe}_3)_2)_2]_2$ 2.660(1) Å;^[31] $(\text{Cp}^{\text{3}}\text{AlBr})_2$ 2.586(3) Å, $(^{\text{Dip}}\text{TerAl})_2(\text{CSiMe}_3)_2$ 2.4946(9) Å] and almost equidistant P1–Al1 and P2–Al2 bonds [**1b** 2.4057(9), 2.4090(9) Å; **1c** 2.4090(5), 2.3977(5) Å] are detected within the ring. The Dip and Tip substituents are *trans*-oriented with respect to the P₂-unit [$\chi(\text{C}_{\text{Ar}}\text{-P-P-C}_{\text{Ar}})$ **1b** 94.31° ; **1c** 93.73°], which agrees well with the structure of $[\text{Dip}^{\text{TerGaNTol}}]_2$ [$\chi(\text{C}_{\text{ToI}}\text{-N-N-C}_{\text{ToI}})$ 77.5°].^[29] The angles at P within the four-membered ring are larger than 90° [**1b** $94.96(3)$, $94.66(3)$; **1c** $93.617(13)$, $96.732(13)^\circ$], while the angles at Al are rather acute [**1b** $82.58(3)$, $82.47(3)$; **1c** $81.798(13)$, $83.846(13)^\circ$].

In order to investigate the bonding situation of these distinct three-coordinate phosphorus–aluminium heterocycles, we conducted DFT calculations for **1a** and **1b** at the PBE0-D3(BJ)/def2-SVP level of theory.^[34] For **1a**, the Mayer bond orders of the P–Al bonds are ca. 0.88,^[35] indicating that no double bond character is found for these bonds, in agreement with the X-ray data. Charge analyses reveal that the phosphorus atoms are partially negative, whereas the aluminium centres are positive. Accordingly, natural bond orbital (NBO)^[36] and intrinsic bond orbital (IBO)^[37] calculations indicate that the Al–P bonds are polarised to

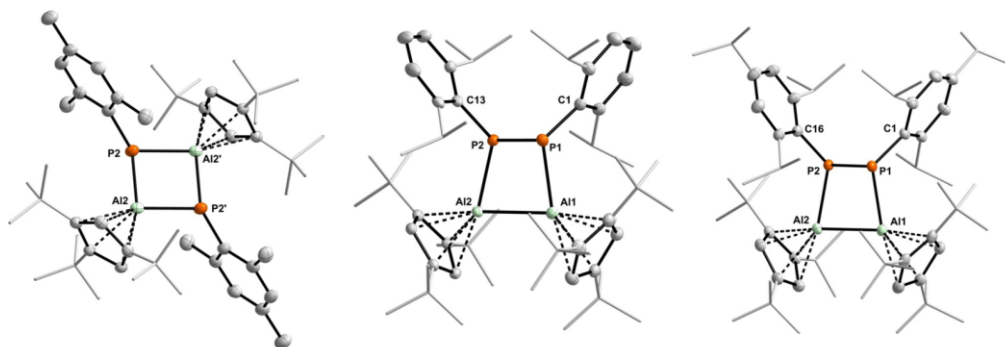


Figure 1. Molecular structures of **1a**, **1b**, and **1c**. ORTEPs drawn at 50% probability. For clarity, all H atoms have been omitted and the alkyl groups on the Cp^{3} , Dip, and Tip substituents have been rendered as wireframe. Selected bond lengths (Å) and angles ($^\circ$) of **1a**: P2–Al2 2.3176(7), P2–Al2' 2.3317(7); Al2–P2–Al2' $90.11(2)$, P2–Al2–P2' $89.89(2)$; **1b**: P1–P1 2.1677(9), Al1–P1 2.4057(9), Al2–P2 2.4090(9), Al1–Al2 2.6947(11); P2–P1–Al1 $94.66(3)$, P1–P2–Al2 $94.96(3)$, P1–Al1–Al2 $82.58(3)$, P2–Al2–Al1 $82.47(3)$; **1c**: P1–P1 2.1676(4), Al1–P1 2.4090(5), Al2–P2 2.3977(5), Al1–Al2 2.6933(5); P2–P1–Al1 $93.617(13)$, P1–P2–Al2 $96.732(13)$, P1–Al1–Al2 $83.846(13)$, P2–Al2–Al1 $81.798(13)$.

phosphorus (see Figure S41). The HOMO of **1a** is composed majorly by contributions at the phosphorus centres, while the LUMO is located mainly on the π system of the Mes substituents (Figure 2, left). At the PBE0-D3(BJ)/def2-SVP level of theory, the HOMO–LUMO gap of **1a** is 4.50 eV.

According to the Mayer bond order calculations, P–P (1.06) and Al–Al (0.86) single bonds are found in **1b**, supporting the attribution based on the crystal structures. The HOMO of **1b** is composed of a linear combination of the phosphorus lone pairs, while the LUMO is located at the π space of the Al–Al motif (Figure 2, right). The HOMO of **1b** is destabilised by ca. 0.7 eV in comparison to that of **1a**, while the LUMO is stabilised by ca. 0.5 eV. As a consequence, the HOMO–LUMO gap of **1b** (3.25 eV) is significantly smaller than that of **1a**. This indicates that the alternating Al_2P_2 heterocycle is more stable than its head-to-head counterpart if steric hindrance caused by the substituents is negligible, which is confirmed by further calculations (see below).

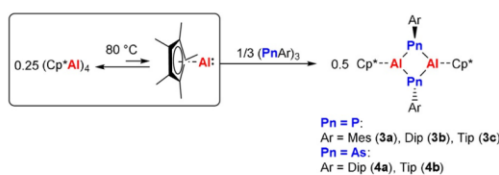
We then set out to test alkyl-substituted cyclo-oligophosphanes as phosphinidene source to determine the influence of the P substituent. When $(\text{PrBu})_3$ ^[38] was treated with three equiv of Cp^*Al (Scheme 3, reaction iii), a new species with an AX_2 spin system was detected in the ^{31}P NMR spectrum ($\delta(^{31}\text{P}) = 76.1, -60.6$ ppm; $J_{\text{PP}} = 210.6$ Hz) and in the ^1H NMR spectrum unreacted Cp^*Al was detected as well, indicating the formation of the four-membered ring $[\text{Cp}^*\text{Al}(\text{PrBu})_3]$ (**2**). This is in analogy to the formation of $[\text{Cp}^*\text{Al}(\text{PrBu})_3]$ ^[39] and $[(\text{SiMe}_3)_2\text{CGa}(\text{PrBu})_3]$ ^[40] which are formed in a ring-expansion reaction starting from $(\text{PrBu})_3$ and the respective E(L) source. Using cyclo-pentaphosphane $(\text{PPh})_5$, the reaction with five equiv of Cp^*Al gave rise to the formation of a new species with a ^{31}P NMR signal at $\delta(^{31}\text{P}) = -130.6$ ppm and a Ph to Cp^* ratio of 1:1 according to ^1H NMR spectroscopy (Scheme 3, reaction iv). The formulation as the 1,3-diphospha-2,4-dialane $[\text{Cp}^*\text{Al}(\mu\text{-PPh})_2]$ (**1d**) was corroborated by X-ray analysis of crystals grown by slow

evaporation of a saturated C_6H_6 solution of **1d**. The metrical parameters of **1d** are nearly identical with **1a** and the Ph rings are *trans*-oriented with respect to the Al_2P_2 plane. The AlP_3 ring in **2** is minimally folded along the P1–P3 axis by ca. 10.7° with an all-*trans* orientation of the *t*Bu groups at phosphorus and an η^5 -coordinated Cp^* ring on aluminium. The P–Al distances [P1–Al1 2.3764(11), P3–Al1 2.3829(12)] are minimally longer than in $[\text{Cp}^*\text{Al}(\text{PrBu})_3]$ [2.359(1), 2.360(1) Å]^[39] indicating the influence of the sterically more demanding Cp^* group. Consequently, the fold angle in **1d** is smaller than in $\text{Cp}^*\text{Al}(\text{PrBu})_3$ [18.7°]^[39]

Dipnictadialanes from Cp^*Al and $(\text{PAr})_3$

We next investigated whether Cp^*Al , generated from $(\text{Cp}^*\text{Al})_4$ at 80°C ,^[24a,41] would show a reactivity like Cp^*Al . Firstly, $(\text{PAr})_3$ was combined with 0.75 equiv of $(\text{Cp}^*\text{Al})_4$ in C_6D_6 and the mixtures were heated to 80°C overnight resulting in colourless solutions (Scheme 4). Analysis by ^{31}P NMR spectroscopy revealed full conversion of the starting triphosphiranes and species with a singlet at $\delta(^{31}\text{P}) = -208.2$ (Ar = Mes), -230.6 (Ar = Dip) and -231.6 ppm (Ar = Tip) were detected. In the ^1H NMR spectrum one sharp signal for the Cp^* group, indicating η^5 -coordination, and signals for the aryl groups were detected in a 1:1 ratio. It needs to be noted that for **3a–c** the aryl groups can rotate freely on the NMR time-scale, as evident from a minimal set of signals in the ^1H NMR spectrum (e.g., no splitting observed for the *o*-Me groups (**3a**) or the *o*-*i*Pr groups (**3b–c**)). After evaporation of the solvent and extraction with *n*-hexane, X-ray quality crystals were obtained from concentrated filtrate solutions at -30°C . In all three cases the base-free 1,3-diphospha-2,4-dialanes $[\text{Cp}^*\text{Al}(\mu\text{-PAr})_2]$ (Ar = Mes **3a**, Dip **3b**, Tip **3c**; Figure 3, left; Table 1) had formed. **3a–c** crystallise in the triclinic spacegroup $P\bar{1}$ with one molecule in the unit cell, with the Al_2P_2 ring being situated on a centre of inversion. In agreement with **1a** and **1d**, the central planar Al_2P_2 ring is a parallelogram with two distinct Al–P distances [**3a** 2.3218(16), 2.3226(15); **3b** 2.3068(11), 2.3448(12); **3c** 2.3099(6), 2.3395(6) Å] and the angles at P [**3a** 86.06(4); **3b** 89.00(3); **3c** 91.205(18)] and Al [**3a** 93.94(4); **3b** 91.00(3); **3c** 88.796(19)] deviate minimally from 90° . The phosphorus atoms are trigonal pyramidally coordinated, even though a considerable degree of planarisation is observed according to the sum of angles at P [**3a** 326.01; **3b** 334.60; **3c** 332.816°].

Four-membered Al_2As_2 heterocycles are rare and, for example, the butterfly-shaped cyclic species $[(\text{Et}_3\text{N})\text{ClAl}(\mu\text{-AsSi}(\text{CMe}_2\text{iPr})\text{Me}_2)_2]$ ^[42] and $[(\text{Me}_3\text{N})\text{HAl}(\mu\text{-AsR})_2]$ (R =



Scheme 4. Reactivity of Cp^*Al towards aryl-substituted cyclotriphosphiranes giving $[\text{Cp}^*\text{Al}(\mu\text{-PnAr})_2]$ (Pn = P, **3a–c**; Pn = As, **4a–b**).

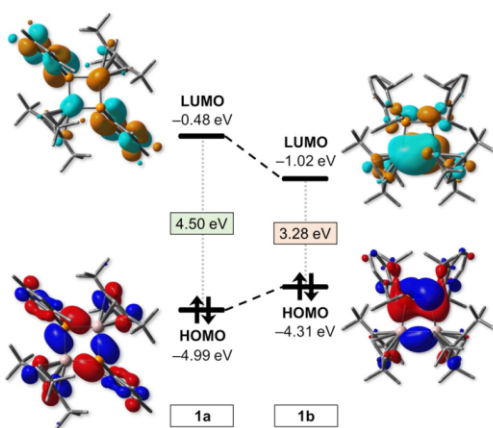


Figure 2. Canonical Kohn–Sham molecular orbitals of **1a** and **1b** at the PBE0-D3(BJ)/def2-SVP level of theory. Isovalues: 0.03 a.u.

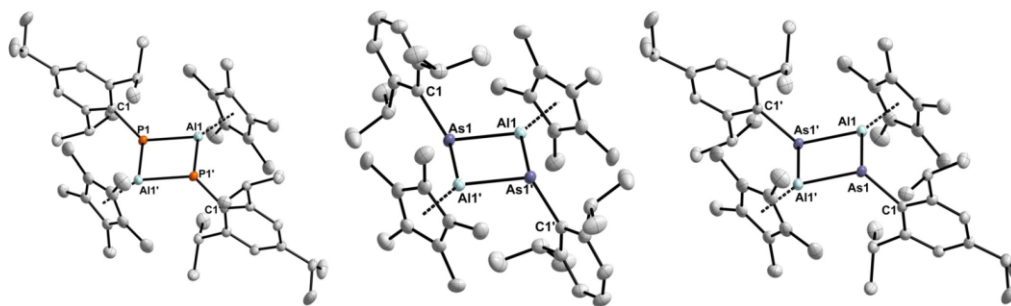


Figure 3. Molecular structures of **3c** (left), **4a** (middle), and **4b** (right). ORTEPs drawn at 50% probability. All H atoms have been omitted and the η^5 -coordination mode of Cp* is indicated by a dotted line from Al to the centroids of the Cp ring. Selected bond lengths (Å) and angles ($^\circ$) are summarised in Table 1.

Table 1: Selected bond lengths and angles of the Cp*-substituted ring systems **3a–c**, **4a**, and **4b**.

	3a	3b	3c	4a	4b
Pn1–Al1 [Å]	2.3218(16)	2.3068(11)	2.3099(6)	2.4106(8)	2.4160(5)
Pn1–Al1' [Å]	2.3226(15)	2.3448(12)	2.3395(6)	2.4462(16)	2.4445(5)
Al1–Pn1–Al1 [$^\circ$]	86.06(4)	89.00(3)	91.205(18)	87.27(5)	86.990(15)
Pn1–Al1–Pn1' [$^\circ$]	93.94(4)	91.00(3)	88.796(19)	92.73(5)	93.009(15)
$\Sigma(\chi, \text{Pn})$ [$^\circ$]	326.01	334.60	332.816	328.51	324.49

Si^iPr_3 , $\text{SiMe}_2(\text{CMe}_2\text{iPr})$ ^[43] have been described in which the arsenic centre is three-coordinate and the aluminium centre is four-coordinate due to Lewis-base adduct formation. Other examples with four-coordinate Al and As centres have been synthesised by the Power group through the combination of the kinetically stabilised primary alane $\text{Me}^{\text{es}}\text{TerAlH}_2$ with liquid PhAsH_2 in the bulk phase, giving $[\text{Me}^{\text{es}}\text{Ter}(\text{H})\text{Al}(\text{H})\text{As}(\text{H})\text{Ph}]_2$.^[44] In analogy to the synthesis of **3a–c** we reasoned that aryl-substituted cyclo-triarsanes (AsAr_3) (Ar = Dip, Tip)^[23] would give base-free cyclo-diarsadialanes in the reaction with $(\text{Cp}^*\text{Al})_4$ and combination of both in a 4:3 ratio in C_6D_6 and heating to 80 °C overnight afforded colourless solutions that showed ^1H NMR spectra, which are similar to those of **3b** and **3c**. X-ray quality crystals grown from saturated *n*-hexane solutions at –30 °C showed that $[\text{Cp}^*\text{Al}(\mu\text{-AsAr})_2]$ (Ar = Dip **4a**, Tip **4b**) had indeed formed. **4a** and **4b** are colourless solids, which crystallise in the triclinic space group $P\bar{1}$, with one molecule on a crystallographically imposed centre of inversion in the unit cell (Figure 3, middle, right; Table 1). Again, the central $[\text{Al}(\mu\text{-As})_2]$ ring is best described as a parallelogram with different As–Al distances [**4a** 2.4106(8), 2.4462(16); **4b** 2.4160(5), 2.4445(5)] and intra-ring angles at arsenic smaller than 90° [**4a** 87.27(5); **4b** 86.990(15) $^\circ$] and wider angles on aluminium [**4a** 92.73(5); **4b** 93.009(15) $^\circ$], with the arsenic atoms being considerably planarised [$\Sigma(\chi, \text{As})$ **4a** 328.51; **4b** 324.49 $^\circ$]. This agrees well with the six-membered species $(\text{Mes}^*\text{AlAsPh})_3$ reported by Power and co-workers [cf. $d_{\text{avg}}(\text{Al}(\text{As})) = 2.430(5)$ Å; $\Sigma(\chi, \text{As}) = 319.7(3.0)^\circ$].^[16]

Stability of Diposphadialanes from DFT Calculations

In this section, we analyse the steric and electronic factors dictating the preferential formation of Al_2P_2 (alternating or head-to-head) and AlP_3 heterocycles based on thermodynamic arguments. All calculations were performed at the SMD(solvent = benzene)^[45]/PBE0-D3(BJ)/def2-TZVP^[34] level of theory from gas-phase-optimised structures at the PBE0-D3(BJ)/def2-SVP level (see SI for more details).

Our experiments revealed that, while an alternating Al_2P_2 ring is formed from Cp^*Al and $(\text{PAR})_3$ (Ar = Mes), a head-to-head Al_2P_2 structure is achieved if sterically more demanding Ar groups (Dip, Tip) are used. The relative free energies of **1a**, **1b**, and their unobserved isomers, $[\text{Cp}^*\text{Al}(\text{PMe})_2]$ and $[\text{Cp}^*\text{Al}(\mu\text{-PDip})_2]$, respectively, are shown in Figure 4a. The head-to-head compound **1b** (Ar = Dip) is 27.7 kcal mol^{–1} more stable than its alternating isomer $[\text{Cp}^*\text{Al}(\mu\text{-PDip})_2]$. This indicates that for sterically more demanding substituents, the thermodynamic reaction product is the head-to-head isomer, and its isomerization to the alternating structure is thermodynamically unfavoured. However, if sterically less demanding substituents at the phosphorus atoms are used, such as Mes, the alternating isomer becomes the thermodynamic product (for Ar = Mes, a free energy of 18.6 kcal mol^{–1} favouring the alternating isomer is found). These results are in excellent agreement with the experimental findings, revealing that thermodynamic reasoning is already enough to predict the preference of head-to-head or alternating isomers during the course of the reaction. Another important experimental finding is that the reaction of Cp^*Al with $(\text{PR})_3$ (R = *t*Bu) leads to an AlP_3 heterocycle, while an alternating Al_2P_2 system is formed if R = Mes. In order to explain this distinct reactivity profile, in Figure 4b we compare the free energy of reaction leading to compounds $[\text{Cp}^*\text{Al}(\mu\text{-PMes})_2]$ (**1a**, Scheme 3, reaction i), $[\text{Cp}^*\text{Al}(\text{PrBu})_3]$ (**2**, Scheme 3, reaction iii), and to the corresponding species $[\text{Cp}^*\text{Al}(\text{PMes})_3]$ and $[\text{Cp}^*\text{Al}(\mu\text{-PrBu})_2]$. Our results show that for both R groups,

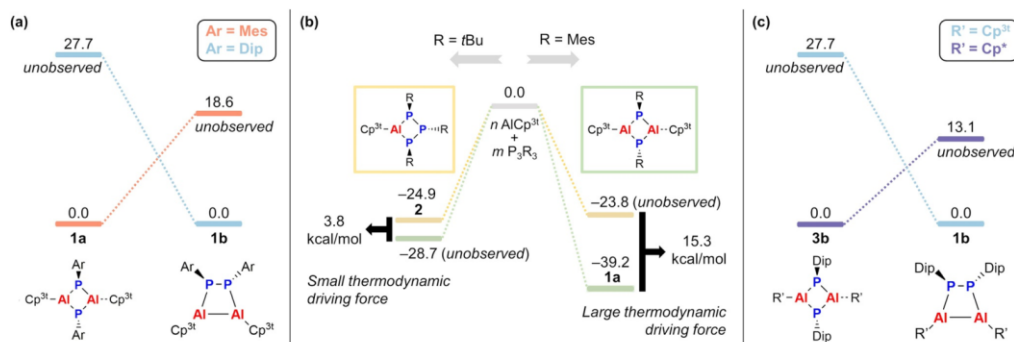


Figure 4. Thermodynamic profiles of the distinct phosphorus–aluminum heterocycles depicted in this work. a) Comparison of the alternating $[\text{Cp}^* \text{ Al}(\mu\text{-PAr})_2]$ and head-to-head $[\text{Cp}^* \text{ Al}(\mu\text{-PR})_2]$ structures for $\text{Ar} = \text{Mes}$, Dip . b) Comparison of the free energies of reaction forming the $[\text{Cp}^* \text{ Al}(\text{PR})_2]$ and $[\text{Cp}^* \text{ Al}(\mu\text{-PR})_2]$ ($\text{R} = \text{tBu}$, Mes) heterocycles. c) Comparison of the alternating $[\text{R}' \text{ Al}(\mu\text{-PDip})_2]$ and head-to-head $[\text{R}' \text{ Al}(\mu\text{-PDiP})_2]$ structures for $\text{R}' = \text{Cp}^*$, Cp^* . All energies are in kcal mol^{-1} .

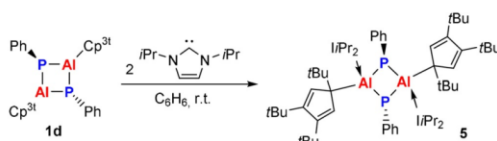
the alternating Al_2P_2 heterocycle is the thermodynamic product. However, in the case of $\text{R} = \text{Mes}$, a larger thermodynamic driving force for forming the alternating Al_2P_2 system is found, as the free energy difference between the two reactions is ca. 15 kcal mol^{-1} . Conversely, the free energy difference for $\text{R} = \text{tBu}$ is merely 4 kcal mol^{-1} . These results indicate that steric factors are responsible for the distinct reactivity patterns observed for different R groups, with the sterically demanding tBu groups precluding the formation of alternating Al_2P_2 heterocycles by decreasing their stabilities in comparison to the AlP_3 system, presumably the first intermediate formed after interaction of $\text{Cp}^* \text{ Al}$ and $(\text{PR})_3$.

Finally, we also performed DFT calculations to investigate the reactivity trends observed in our experiments if the $\text{Cp}^* \text{ Al}$ species is considered. As shown in Scheme 4, if $\text{Cp}^* \text{ Al}$ is used, the alternating $[\text{Cp}^* \text{ Al}(\mu\text{-PR})_2]$ isomer is found for $\text{R} = \text{Mes}$, Dip , Tip , whereas for $\text{Cp}^* \text{ Al}$ the head-to-head $[\text{Cp}^* \text{ Al}(\mu\text{-PDip})_2]$ isomer is found for $\text{R} = \text{Dip}$, Tip . The relative free energies of the diphosphadialane systems with $\text{R} = \text{Dip}$ and $\text{Cp}^* \text{ Al}$ and $\text{Cp}^* \text{ Al}$ fragments are shown in Figure 4c. Our results indicate that while **1b** is preferred over its alternating isomer if $\text{R} = \text{Dip}$, reduction of the steric demands in the Al substituents inverts the free energy trends, with the head-to-head $[\text{Cp}^* \text{ Al}(\mu\text{-PDip})_2]$ isomer lying $13.1 \text{ kcal mol}^{-1}$ above **3b**. Similarly to the previous cases, steric demands on the substituents drastically influence the free energy trends of the corresponding heterocycles, ultimately dictating the reactivity profile of the diphosphadialane systems studied herein. The preferred products from the reactions depicted in this work are effectively predicted by thermodynamic reasoning.

Reactivity of Diphosphadialanes with Lewis Bases

Lewis-base-stabilised dipnictadialanes have been described,^[15,43] and as an entry, **1d**, with a rather small Ph group on the phosphorus atoms, was combined with two equiv of the

NHC IiPr_2 ($\text{IiPr}_2 = (\text{HCN}(\text{tBu})_2)_2\text{C}$). The ^{31}P NMR spectrum showed one new species at $\delta(^{31}\text{P}) = -123.3 \text{ ppm}$, which is minimally deshielded compared to **1d** and indicates formation of the bis-NHC adduct $[\text{Cp}^* \text{ Al}(\text{IiPr}_2)_2(\mu\text{-PPh})_2]$ (**5**, Scheme 5), which was corroborated by X-ray analysis of crystals grown from slow evaporation of a C_6H_6 solution (Figure 5). The molecular structure revealed that IiPr_2 is coordinated to Al and in *trans*-arrangement with respect to the Al_2P_2 ring resulting in a haptotropic shift from η^5 to η^1 of the Cp^* group.^[46] This is reminiscent of the cluster compound $[(\text{Cp}^* \text{ Al}(\text{IME}_4))(\mu, \eta^3\text{-}\eta^4\text{-P}_3)\text{FeCp}^*]$ with an η^1 Cp^* group on aluminium, which displays an $\text{Al}\cdots\text{C}_{\text{NHC}}$ distance $[2.017(6) \text{ \AA}]$ shorter than those of **5** $[2.100(2), 2.083(2)]$.^[47] In the related compound $[(\text{IiPr}_2)\text{HAl}(\mu\text{-PSiPh}_2\text{tBu})_2]$ the NHCs are in a *cis*-arrangement.^[15] Surprisingly, one of the ring phosphorus atoms is now in a nearly planar coordination environment ($\Sigma(\angle\text{P}2) = 347.87^\circ$), whereas the other is now closer to an ideal trigonal pyramidal coordination environment ($\Sigma(\angle\text{P}1) = 299.83^\circ$). This is accompanied by deformation of the formerly planar near-rectangular Al_2P_2 ring, which is now folded by ca. 16° along the $\text{P}1\cdots\text{P}2$ axis giving a butterfly structure, in accord with $[(\text{IiPr}_2)\text{HAl}(\mu\text{-PSiPh}_2\text{tBu})_2]$. The $\text{Al}\cdots\text{P}$ bonds show a pair of longer $[\text{Al}3\cdots\text{P}4 \text{ 2.4206(6)}, \text{Al}1\cdots\text{P}4 \text{ 2.4009(5) \AA}]$ and shorter $[\text{P}2\cdots\text{Al}1 \text{ 2.3371(7)}, \text{P}2\cdots\text{Al}3 \text{ 2.3335(5) \AA}]$ bonds, with the shorter distances to the more planar phosphorus atom. The molecular structure would imply two chemically and magnetically distinct phosphorus atoms and, consequently, a set of two doublets in the ^{31}P NMR spectrum.



Scheme 5. Reaction of **1d** with the NHC IiPr_2 , giving rise to the formation of the bis-NHC adduct **5**.

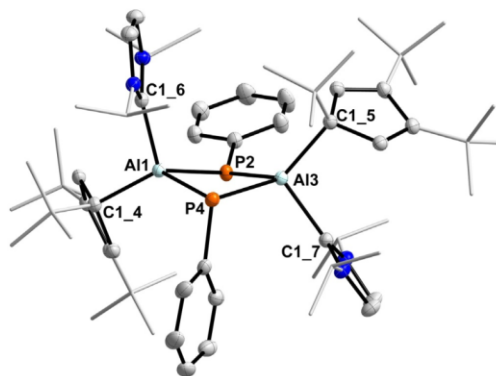


Figure 5. Molecular structure of **5**. ORTEPs drawn at 50% probability, all H atoms omitted and alkyl substituents on Cp* and *i*Pr₂ rendered as wireframe. Selected bond lengths (Å) and angles (°) of **5**: P2–Al1 2.3371(7), P2–Al3 2.3335(5), Al3–P4 2.4206(6), Al1–P4 2.4009(5), P2–C1 1.825(2), P4–C1 1.846(2), Al1–C1_4 2.084(1), Al3–C1_5 2.092(1), Al1–C1_6 2.100(2), Al3–C1_7 2.083(2); Al1–P2–Al3 91.49(2), P2–Al3–P4 87.98(2), Al3–P4–Al1 87.87(2), P4–Al1–P2 88.37(2), Al1–P2–C1 128.61(6), Al1–P4–C1 104.08(5).

Thus, a solution of **5** in [D₈]toluene was cooled to -80°C , which resulted in splitting of the singlet resonance at room temperature into two doublets at $\delta(^{31}\text{P}) = -122.6$ and -129.7 ppm ($J_{\text{HP}} = 67.1$ Hz). This indicates rapid exchange in solution between the phosphorus positions at room temperature, but even at lower temperatures, as a significant deshielding of the planarised P atom would be expected.

Conclusion

Pnictaalumenes are characterised by alternating Lewis acidic group 13 and electron-rich group 15 atoms, which results in a propensity to oligomerise. To date the corresponding cyclo-dipnictadialanes have only been synthesised as their Lewis base adducts. Herein, we show that using cyclo-tripnictanes ($(\text{ArPn})_3$ (Ar = Mes, Dip, Tip; Pn = P, As)) in conjunction with Cp*Al ($x = *, 3t$) afforded the first examples of base-free cyclo-dipnictadialanes. With small aryl substituents on the pnictogen, Cp*Al (**1a**, **1d**) and with Cp*Al (**3a–c**, **4a–b**) in all cases the rings with alternating P and Al atoms [Cp*Al(μ -PnAr)]₂ are thermodynamically favoured. Interestingly, the head-to-head-connected 1,2-diphospha-3,4-dialuminacyclobutanes, **1b** and **1c**, are preferred when both the substituents on phosphorus and aluminium are sterically demanding. This study clearly demonstrates (i) the potential of cyclo-tripnictanes as building blocks to implement PnAr units into unusual small molecules and (ii) that base-free cyclo-dipnictadialanes are synthetically feasible by judicious choice of the substituents on aluminium and the pnictogen. Studies on the reactivity of the ring systems presented in here with respect to their potential to act as a source of the monomeric pnictaalumenes are currently underway.

Acknowledgements

C.H.-J. thanks Prof. M. Beller for his continuous support, and support by an Exploration Grant of the Boehringer Ingelheim Foundation (BIS) and the GSO for a Klaus-Tschira Boost fund is acknowledged. We thank our technical and analytical staff for assistance, especially Dr. Anke Spannenberg for her support regarding X-ray analysis. F.F. thanks the Coordenação de Aperfeiçoamento de Pessoal de Nível Superior (CAPES) and the Alexander von Humboldt (AvH) Foundation for a Capes–Humboldt postdoctoral fellowship. J.T.G. thanks the AvH Foundation for financial support and the Government of Canada for a Banting Fellowship. H.B. wishes to acknowledge financial support by the Deutsche Forschungsgemeinschaft, DFG. Open Access funding enabled and organized by Projekt DEAL.

Conflict of Interest

The authors declare no conflict of interest.

Keywords: aluminium · carbene ligands · main group elements · phosphorus · small ring systems

- [1] N. Davidson, H. C. Brown, *J. Am. Chem. Soc.* **1942**, *64*, 316–324.
- [2] A. M. Arif, B. L. Benac, A. H. Cowley, R. Geerts, R. A. Jones, K. B. Kidd, J. M. Power, S. T. Schwab, *J. Chem. Soc. Chem. Commun.* **1986**, 1543–1545.
- [3] A. H. Cowley, R. A. Jones, M. A. Mardones, J. Ruiz, J. L. Atwood, S. G. Bott, *Angew. Chem. Int. Ed. Engl.* **1990**, *29*, 1150–1151; *Angew. Chem.* **1990**, *102*, 1169–1171.
- [4] U. Vogel, A. Y. Timoshkin, M. Scheer, *Angew. Chem. Int. Ed.* **2001**, *40*, 4409–4412; *Angew. Chem.* **2001**, *113*, 4541–4544.
- [5] M. Bodensteiner, U. Vogel, A. Y. Timoshkin, M. Scheer, *Angew. Chem. Int. Ed.* **2009**, *48*, 4629–4633; *Angew. Chem.* **2009**, *121*, 4700–4704.
- [6] M. A. K. Weinhart, A. S. Lisoenko, A. Y. Timoshkin, M. Scheer, *Angew. Chem. Int. Ed.* **2020**, *59*, 5541–5545; *Angew. Chem.* **2020**, *132*, 5586–5590.
- [7] M. A. K. Weinhart, M. Seidl, A. Y. Timoshkin, M. Scheer, *Angew. Chem. Int. Ed.* **2021**, *60*, 3806–3811; *Angew. Chem.* **2021**, *133*, 3850–3855.
- [8] S. Schulz, *Coord. Chem. Rev.* **2001**, *215*, 1–37.
- [9] L. K. Krannich, C. L. Watkins, S. J. Schauer, C. H. Lake, *Organometallics* **1996**, *15*, 3980–3984.
- [10] M. Fischer, S. Nees, T. Kupfer, J. T. Goettel, H. Braunschweig, C. Hering-Junghans, *J. Am. Chem. Soc.* **2021**, *143*, 4106–4111.
- [11] a) D. W. N. Wilson, J. Feld, J. M. Goicoechea, *Angew. Chem. Int. Ed.* **2020**, *59*, 20914–20918; *Angew. Chem.* **2020**, *132*, 21100–21104; b) D. W. N. Wilson, J. Feld, J. M. Goicoechea, *Angew. Chem. Int. Ed.* **2021**, *60*, 22057–22061; *Angew. Chem.* **2021**, *133*, 22228–22232.
- [12] a) M. K. Sharma, C. Wölper, G. Haberhauer, S. Schulz, *Angew. Chem. Int. Ed.* **2021**, *60*, 6784–6790; *Angew. Chem.* **2021**, *133*, 6859–6865; b) M. K. Sharma, C. Wölper, G. Haberhauer, S. Schulz, *Angew. Chem. Int. Ed.* **2021**, *60*, 21784–21788; *Angew. Chem.* **2021**, *133*, 21953–21957.
- [13] C. Helling, C. Wölper, S. Schulz, *J. Am. Chem. Soc.* **2018**, *140*, 5053–5056.
- [14] C. Ganesamoorthy, C. Helling, C. Wölper, W. Frank, E. Bill, G. E. Cutsail, S. Schulz, *Nat. Commun.* **2018**, *9*, 87.

- [15] M. Kapitein, M. Balmer, L. Niemeier, C. von Hänisch, *Dalton Trans.* **2016**, 45, 6275–6281.
- [16] R. J. Wehmschulte, P. P. Power, *J. Am. Chem. Soc.* **1996**, *118*, 791–797.
- [17] a) G. E. Coates, J. G. Livingstone, *J. Chem. Soc.* **1961**, 1000–1008; b) G. Fritz, W. Hölderich, *Z. Anorg. Allg. Chem.* **1977**, *431*, 61–75; c) P. Kölle, G. Linti, H. Nöth, K. Polborn, *J. Organomet. Chem.* **1988**, *355*, 7–18; d) P. Kölle, G. Linti, H. Nöth, G. L. Wood, C. K. Narula, R. T. Paine, *Chem. Ber.* **1988**, *121*, 871–879; e) D. Dou, G. W. Linti, T. Chen, E. N. Duesler, R. T. Paine, H. Nöth, *Inorg. Chem.* **1996**, *35*, 3626–3634; f) G. He, O. Shynkaruk, M. W. Lui, E. Rivard, *Chem. Rev.* **2014**, *114*, 7815–7880.
- [18] a) K. Knabel, T. M. Klapötke, H. Nöth, R. T. Paine, I. Schwab, *Eur. J. Inorg. Chem.* **2005**, 1099–1108; b) A. N. Price, G. S. Nichol, M. J. Cowley, *Angew. Chem. Int. Ed.* **2017**, *56*, 9953–9957; *Angew. Chem.* **2017**, *129*, 10085–10089.
- [19] B. Kaufmann, H. Nöth, R. T. Paine, K. Polborn, M. Thomann, *Angew. Chem. Int. Ed. Engl.* **1993**, *32*, 1446–1448; *Angew. Chem.* **1993**, *105*, 1534–1536.
- [20] D. Scheschkewitz, H. Amii, H. Gornitzka, W. W. Schoeller, D. Bourissou, G. Bertrand, *Science* **2002**, *295*, 1880–1881.
- [21] P. Henke, T. Pankewitz, W. Klopper, F. Breher, H. Schnöckel, *Angew. Chem. Int. Ed.* **2009**, *48*, 8141–8145; *Angew. Chem.* **2009**, *121*, 8285–8290.
- [22] A. Schumann, F. Reiß, H. Jiao, J. Rabeah, J.-E. Siewert, I. Krummenacher, H. Braunschweig, C. Hering-Junghans, *Chem. Sci.* **2019**, *10*, 7859–7867.
- [23] A. Schumann, J. Bresien, M. Fischer, C. Hering-Junghans, *Chem. Commun.* **2021**, 57, 1014–1017.
- [24] a) C. Dohmeier, C. Robl, M. Tacke, H. Schnöckel, *Angew. Chem. Int. Ed. Engl.* **1991**, *30*, 564–565; *Angew. Chem.* **1991**, *103*, 594–595; b) O. Kysliak, H. Görls, R. Kretschmer, *Dalton Trans.* **2020**, 49, 6377–6383.
- [25] A. Hofmann, T. Tröster, T. Kupfer, H. Braunschweig, *Chem. Sci.* **2019**, *10*, 3421–3428.
- [26] a) V. J. Eilrich, E. Hey-Hawkins, *Coord. Chem. Rev.* **2021**, *437*, 213749; b) T. Wellnitz, C. Hering-Junghans, *Eur. J. Inorg. Chem.* **2021**, 8–21.
- [27] T. Krachko, J. C. Slootweg, *Eur. J. Inorg. Chem.* **2018**, 2734–2754.
- [28] See Supporting Information for all experimental details. Deposition numbers 2102648, 2102649, 2102650, 2102651, 2102652, 2102653, 2102654, 2102655, 2102656, 2102657 and 2102658 contain the supplementary crystallographic data for this paper. These data are provided free of charge by the joint Cambridge Crystallographic Data Centre and Fachinformationszentrum Karlsruhe Access Structures service.
- [29] R. J. Wright, M. Brynda, J. C. Fettinger, A. R. Betzer, P. P. Power, *J. Am. Chem. Soc.* **2006**, *128*, 12498–12509.
- [30] J.-E. Siewert, A. Schumann, C. Hering-Junghans, *Dalton Trans.* **2021**, <https://doi.org/10.1039/D1DT03095G>.
- [31] W. Uhl, *Z. Naturforsch. B* **1988**, *43*, 1113–1118.
- [32] A. Hofmann, A. Lamprecht, O. F. González-Belman, R. D. Dewhurst, J. O. C. Jiménez-Halla, S. Kachel, H. Braunschweig, *Chem. Commun.* **2018**, *54*, 1639–1642.
- [33] C. Cui, X. Li, C. Wang, J. Zhang, J. Cheng, X. Zhu, *Angew. Chem. Int. Ed.* **2006**, *45*, 2245–2247; *Angew. Chem.* **2006**, *118*, 2303–2305.
- [34] a) C. Adamo, V. Barone, *J. Chem. Phys.* **1999**, *110*, 6158–6170; b) M. Ernzerhof, G. E. Scuseria, *J. Chem. Phys.* **1999**, *110*, 5029–5036; c) F. Weigend, R. Ahlrichs, *Phys. Chem. Chem. Phys.* **2005**, *7*, 3297–3305; d) S. Grimme, J. Antony, S. Ehrlich, H. Krieg, *J. Chem. Phys.* **2010**, *132*, 154104; e) S. Grimme, S. Ehrlich, L. Goerigk, *J. Comput. Chem.* **2011**, *32*, 1456–1465.
- [35] a) I. Mayer, *Chem. Phys. Lett.* **1983**, *97*, 270–274; b) I. Mayer, *Int. J. Quantum Chem.* **1984**, *26*, 151–154.
- [36] F. Weinhold, C. R. Landis, E. D. Glendening, *Int. Rev. Phys. Chem.* **2016**, *35*, 399–440.
- [37] G. Knizia, *J. Chem. Theory Comput.* **2013**, *9*, 4834–4843.
- [38] a) M. Baudler, C. Gruner, *Z. Naturforsch. B* **1976**, *31*, 1311–1312; b) M. Baudler, J. Hahn, H. Dietsch, G. Fürstenberg, *Z. Naturforsch. B* **1976**, *31*, 1305–1310.
- [39] C. Üffing, C. v. Hänisch, H. Schnöckel, *Z. Anorg. Allg. Chem.* **2000**, *626*, 1557–1560.
- [40] W. Uhl, M. Benter, *J. Chem. Soc. Dalton Trans.* **2000**, 3133–3135.
- [41] H. Sitzmann, M. F. Lappert, C. Dohmeier, C. Üffing, H. Schnöckel, *J. Organomet. Chem.* **1998**, *561*, 203–208.
- [42] C. von Hänisch, *Z. Anorg. Allg. Chem.* **2003**, *629*, 1496–1500.
- [43] M. Driess, S. Kuntz, K. Merz, H. Pritzkow, *Chem. Eur. J.* **1998**, *4*, 1628–1632.
- [44] R. J. Wehmschulte, P. P. Power, *New J. Chem.* **1998**, *22*, 1125–1130.
- [45] A. V. Marenich, C. J. Cramer, D. G. Truhlar, *J. Phys. Chem. B* **2009**, *113*, 6378–6396.
- [46] J. M. O'Connor, C. P. Casey, *Chem. Rev.* **1987**, *87*, 307–318.
- [47] R. Yadav, T. Simler, B. Goswami, C. Schoo, R. Köppe, S. Dey, P. W. Roesky, *Angew. Chem. Int. Ed.* **2020**, *59*, 9443–9447; *Angew. Chem.* **2020**, *132*, 9530–9534.

Manuscript received: August 18, 2021

Accepted manuscript online: September 3, 2021

Version of record online: October 5, 2021